



THÈSE

EN VUE DE L'OBTENTION DU DIPLOME DE DOCTORANT

Domaine : Science de la Matière

Filière : Chimie

Spécialité : Analyse Chimique et Chimie des Matériaux

Présentée par :

TAOURI Lydia

Thème :

**Electrochemical micro-sensors based on carbon
nanomaterials for environmental and food monitoring**

Soutenu le 15 septembre 2021.

Devant le Jury composé de :

Mr. BEZZI Nacer	Professeur	Univ. Bejaia	Président
Mr. BOUROUINA Mustapha	Professeur	Univ. Bejaia	Rapporteur
Mr. HAUCHARD Didier	MC-HDR	ENSCR, France	Co-rapporteur
Mme. SENHADJI Ounissa	Professeur	Univ. Bejaia	Examineur
Mme. BELKACEMI Hayet	Professeur	Univ. Bejaia	Examineur
Mr. AMINE Aziz	Professeur	Univ. Casablanca, Maroc	Examineur
Mr. ADDALA Abderezak	MCA	Univ. Setif	Invité

2020-2021



Faculty of Exact Sciences
Department of Chemistry

THESIS

PRESENTED TO OBTAIN A DIPLOMA OF DOCTORATE

Field: Material Sciences

Branch: Chemistry

Specialty: Chemical Analysis and Chemistry of Materials

Presented by

TAOURI Lydia

Theme

**Electrochemical micro-sensors based on carbon
nanomaterials for environmental and food monitoring**

Public defense on 15th September 2021.

Members of jury:

M. BEZZI Nacer	Professor	Univ. Bejaia	President
M. BOUROUINA Mustapha	Professor	Univ. Bejaia	Rapporteur
M. HAUCHARD Didier	MC-HDR	ENSCR, France	Co-rapporteur
Mrs. SENHADJI Ounissa	Professor	Univ. Bejaia	Reviewer
Mrs. BELKACEMI Hayet	Professor	Univ. Bejaia	Reviewer
M. AMINE Aziz	Professor	Univ. Casablanca, Morocco	Reviewer
M. ADDALA Abderezak	MCA	Univ. Setif	Invited Reviewer

Session 2020-2021

Acknowledgment

*Foremost, I would like to thank **ALLAH**, for giving me the courage, patience, blessing, chance and power to accomplish this thesis on time and in just four years with good results.*

*I express my gratefully acknowledgements to the Algerian Ministry of Education and Scientific Research and Campus France program under grant agreement **PROFAS B+** to theirs financial support.*

*I would like to express my deep gratitude to Professor **BOUROUINA Mustapha** for supervising my PhD thesis, for having offered me a fascinating research topic, for his guidance during all this years. I would like to thank him especially for having faith in me, for his constant availability, for his all advices in the professional field and generally in life. I am very proud for all his kind help, confidence, gentleness and generosity to me. In addition, to his time, generous guidance, patience and encouragement. He was a veritable source of motivation and help for me, to be successful and to raise rapidly.*

*The experimental part of this presented LMD Doctorate thesis is carried out at the CIP laboratory of the National Superior School of Chemistry of Rennes (France) under the supervision of Doctor **HAUCHARD Didier**.*

*Doctor **HAUCHARD Didier**, special thanks for his accepting to supervise my doctoral thesis, for welcoming me to his laboratory and for integrating me into his team. I would like to thank him especially for his guidance, his constant availability, his advices and the daily attention he paid to my work. Without him, this PhD thesis could never have been completed in the time and with the brilliant results. I would think him for have offering me the opportunity to work in his laboratory, to learn a lot beside him and to allow me*

to achieve the goal and especially for his kindness, generosity and good humorous.

*I address also my thanks to Doctor **ADJAOUT Rachid**, MCA at Amazigh language and culture department in Bejaia University, for translating the abstract section into the National Amazigh language.*

*I would also like to thank members of jury for the thesis defense Professor **BEZZI Nacer**, Professor **SENHADJI Ounissa**, Professor **BELKACEMI Hayet**, and Doctor **ADDALA Abderezak** for taking time out of their busy schedules to evaluate my research work. Their suggestions and critical opinions will help me to improve quality of this work.*

*I would particularly like to thank Professor **AMINE Aziz**, in Hassan II University (Morocco) and Editor in Biosensors & Bioelectronics (Elsevier), who honored me by accepting to evaluate my research work.*

*My special thanks and gratitude are for **my parents** and **my sister**, I could not have finished this Doctoral thesis without him full support. I would like to thanks them for their patience, daily encouragements, for being with me in each step and for him continuous prayers that have make me stronger each and every day on completing this study. Even though thanks is a too simple word to express my gratitude to them, I pray to **ALLAH** that I may always be your pride and may one day give you more than what you give me.*

Table of contents

Acknowledgment

Table of contents

Preface

Agzul (Abstract with National Amazigh language)

Abbreviation

Figures list

Tables list

General introduction.....	1
References	5
Chapter I: Literature review.....	6
Introduction	7
I.1. Electrochemistry sensing	7
I.2. Types of electrochemical sensors	8
I.2.1. Conductometric sensors	8
I.2.2. Potentiometric sensors.....	9
I.2.3. Amperometric sensors.....	9
I.3. Characteristics of an electrochemical sensor	10
I.4. Types of electrodes	11
I.4.1. Carbon paste electrode (CPE)	12
a. Brief historic.....	12
b. Description of the CPE	12
c. Advantages and disadvantages of the CPE	13
I.4.2. Cavity microelectrode (CME).....	14
a. Brief historic.....	14
b. Description of the CME	15
c. Packing and cleaning of the CME.....	16
d. Advantages and disadvantages of CME	16
I.5. Electrodes fabrication procedures.....	17
I.6. Modification of carbon paste electrode.....	18
I.7. Carbon nanomaterials for the electrochemical sensing	20
I.7.1. Introduction	20
I.7.2. What are carbon nanomaterials (CMs)?	20
I.7.3. What are CMs proprieties and advantages?	22
I.7.4. Why CMs are received a great attention?	22

I.7.5. Different carbon nanomaterials using in electrochemical sensing.....	23
a. Graphite.....	23
b. Diamond.....	24
c. Graphene	25
d. Carbon Nanotubes (CNTs)	25
e. Fullerene.....	26
f. Carbon Dots (CDs)	27
g. Carbon black (CB)	29
Conclusion.....	30
References	31
Chapter II: Experimental section	42
II.1. Chemical reagents.....	43
II.2. Electrochemical apparatus	44
II.3. Electrochemical methods.....	44
II.3.1. Cyclic voltammetry (CV)	44
II.3.2. Square wave voltammetry (SWV)	45
II.3.3. Chronamperometry (CA)	46
II.3.4. Electrochemical impedance spectroscopy (EIS).....	46
II.3.5. Electrochemical preconcentration (EP)	47
II.4. Other methods.....	47
II.4.1. Scanning electron microscopy (SEM)	47
II.4.2. Fourier transform infrared (FTIR) spectroscopy	48
II.4.3. Ultra performance liquid chromatography coupled with UV spectrophotometry (UPLC/UV)	48
II.4.4. Standard addition method	49
II.5. Preparation of electrodes modifiers	51
II.5.1. Preparation of the functionalized multi-walled carbon nanotubes (f-MWCNTs)	51
II.5.2. Preparation of the functionalized carbon black (CBf)	51
II.5.3. Preparation of the activated carbon (AC)	51
II.6. Fabrication of modified electrodes	51
II.6.1. Fabrication of the modified f-MWCNTs-FNTs/ CPE	51
II.6.2. Preparation of modified cavity microelectrodes (CME).....	52
II.6.2.1. Fabrication of modified CBf-AC/ CME.....	52
II.6.2.2. Fabrication of the modified CB/ CME	52
II.7. Preparation of solution.....	53
II.7.1. Preparation of electrolyte support	53

II.7.2. Preparation of analyte solutions	53
II.8. Preparation of real samples for validation analysis	53
II.8.1. Commercial sugar vanilla samples	53
II.8.2. Artificial urine samples	54
II.8.3. Water samples	54
References	55
Chapter III: Carbon paste electrode based on fullerene and MWCNT for the detection of vanillin as additive	57
Introduction	58
Part III.1: Vanillin.....	59
III.1.1. Introduction	60
III.1.2. Vanillin generality	61
III.1.3. Uses	61
III.1.4. Side effects	62
III.1.5. Norms	62
Part III.2: Electrochemical detection of vanillin at carbon paste electrode modified with fullerene and MWCNT.....	63
III.2.1. Introduction	64
III.2.2. Characterization of the f-MWCNTs-FNTs/ CPE.....	64
a. Characterization of the modified electrode by scanning electron microscopy (SEM)..	64
b. Characterization of the modified electrode by chronoamperometry method (CA).....	66
c. Characterization of the modified electrode by electrochemical impedance spectroscopy (EIS).....	66
III.2.3. Electrochemical behavior of the f-MWCNTs-FNTs/ CPE	67
III.2.4. Effect of pH	68
III.2.5. Effect of scan rate.....	69
III.2.6. Effect of accumulation time	69
III.2.7. Quantitative analysis of vanillin.....	70
III.2.8. Repeatability and reproducibility of f-MWCNTs-FNTs/ CPE	73
III.2.9. Selectivity of f-MWCNTs-FNTs/ CPE	73
III.2.10. Stability of f-MWCNTs-FNTs/ CPE.....	75
III.2.11. Validation of the proposed sensor in sugar vanilla samples	75
Conclusion.....	78
References	80

Chapter IV: Cavity microelectrode based on carbon black and activated carbon for the simultaneous detection of 4-aminophenol, paracetamol and ciprofloxacin in water and urine..... 83

Introduction	84
Part IV.1: Pharmaceutical products	86
IV.1.1. Introduction	87
IV.1.2. Pharmaceutical products generality	87
IV.1.3. Source of pharmaceutical contaminants in environment	88
IV.1.4. Pharmaceutical substances in the aquatic environment	89
IV.1.5. Risk of the presence of pharmaceuticals in environment.....	90
IV.1.6. Aminophenol.....	90
IV.1.6.1. Generality	90
IV.1.6.2. Uses	91
IV.1.6.3. Side effects	91
IV.1.6.4. Norms	91
IV.1.7. Paracetamol	92
IV.1.7.1. Generality	92
IV.1.7.2. Uses	92
IV.1.7.3. Side effects	92
IV.1.7.4. Norms	93
IV.1.8. Ciprofloxacin.....	93
IV.1.8.1. Generality	93
IV.1.8.2. Uses	94
IV.1.8.3. Side effects	94
IV.1.8.4. Norms	95
IV.1.9. Pharmaceuticals interactions	95
Part IV.2: Electrochemical detection of ciprofloxacin, paracetamol and 4-aminophenol at cavity microelectrode modified with carbon black and activated carbon	96
IV.2.1. Introduction	97
IV.2.2. Characterization of the CBf-AC/ CME.....	98
a. Characterization of the modified electrode by scanning electron microscopy (SEM)..	98
b. Characterization of the modified electrode by Fourier transform infrared (FTIR) spectroscopy.....	98
c. Characterization of the modified electrode by electrochemical impedance spectroscopy (EIS).....	101
IV.2.3. Electrochemical behavior of the CBf-AC/ CME	102
IV.2.4. Effect of pH.....	103

IV.2.5. Effect of scan rate.....	105
IV.2.6. Effect of accumulation time	106
IV.2.7. Individual analysis of 4-aminophenol.....	107
IV.2.8. Individual analysis of paracetamol	108
IV.2.9. Individual analysis of ciprofloxacin.....	109
IV.2.10. Simultaneous analysis of 4-aminophenol, paracetamol and ciprofloxacin.....	110
IV.2.11. Repeatability and reproducibility of CBf-AC/ CME	113
IV.2.12. Selectivity of CBf-AC/ CME	114
IV.2.13. Validation of the proposed sensor in water samples.....	115
IV.2.13. Validation of the proposed sensor in urine samples	116
Conclusion.....	117
References	118
Chapter V: Ultra-traces analysis of paracetamol in water by electrochemical preconcentration on the carbon black cavity microelectrode.....	128
Introduction	129
V.1. Characterization of electrode materials	130
V.1.1. Characterization of the modified electrode by scanning electron microscopy.....	130
V.1.2. Characterization of the modified electrode by electrochemical impedance spectroscopy (EIS).....	130
V.1.3. Determination of the electrochemical active area	131
V.2. Optimization of the electrochemical detection method	132
V.2.1. Effect of scan rate.....	132
V.2.4. Effect of pH.....	134
V.2.2. Effect of preconcentration potential	135
V.2.3. Effect of preconcentration time	136
V.3. Electrochemical behavior of PAR on the CB/ CME.....	136
V.4. Determination of PAR on the CB/ CME.....	137
V.5. Repeatability and reproducibility.....	140
V.6. Selectivity of the modified cavity microelectrode.....	141
V.7. Real simple analysis.....	142
Conclusion.....	143
References	144
General Conclusion, perspectives and originality of the thesis.....	147
General Conclusion	148
Perspectives	150
Originality of the thesis.....	150

Preface

The presented LMD Doctorate thesis is carried out mainly in the chemistry laboratory of the University of Bejaia (Algeria) and in the National Superior School of Chemistry of Rennes (France). This thesis is presented as a compendium of publications.

All the scientific articles produced are presented below:

Accepted publication

1. L. Taouri, M. Bourouina, S. Bourouina-Bacha, D. Hauchard, Fullerene-MWCNT nanostructured-based electrochemical sensor for the detection of Vanillin as food additive, *Journal of Food Composition and Analysis (Impact Factor = 3.721)* Volume 100, **2021**, 103811, <https://doi.org/10.1016/j.jfca.2021.103811>.

Submitted publication

1. L. Taouri, M. Bourouina, S. Bourouina, D. Hauchard, Ultra-traces analysis of paracetamol in water by electrochemical preconcentration on the carbon black cavity microelectrode, in the process of submission.
2. L. Taouri, M. Bourouina, S. Bourouina, D. Hauchard, Low-cost cavity microelectrode for the simultaneous detection of ciprofloxacin, paracetamol and 4-aminophenol in urine.

International communication

1. L. Taouri, M. Bourouina, D. Hauchard ; Nanostructured micro-cavity electrode for trace analysis of ciprofloxacin in urine ; 9^{ème} Symposium on Electrochemistry in Nanoscience, ELECNANO9; November 23-24, 2020; Paris, France. (oral communication)
2. L. Taouri, M. Bourouina, D. Hauchard ; Electrochemical sensor nanostructured with carbon material for the determination of vanillin additive in food samples; 3rd International Symposium On Material, Electrochemistry & Environment, CIMEE20, September 17-19, 2020; CCIAT, Tripoli, Lebanon. (oral communication)

National communication

1. L. Taouri ; Capteurs chimiques à détection de traces de polluants : construction et optimisation ; Journées doctoriales d'innovation et de transfert technologiques, Juillet 15-16, 2019 ; Université A. Mira de Bejaia, Algérie. (oral communication)
2. L. Taouri, M. Bourouina ; Electrochemical determination of pyrogallol at aluminum oxide modified paste carbon electrodes ; 8^{ème} journées de chimie ; Mars 26-27, 2019 ; Ecole Militaire Polytechniques, Bordj El-Bahri, Algérie. (poster communication)

Agzul

(Abstract with National Amazigh language)

Tazrawt-a treṣṣa yef wemhaz n yimaṭṭafen d wamzi-yimaṭṭafen izefikruranen yersen yef wamzi-icermaḍ n lkarbun d tesnast deg wennar deg teessast tawennaṭant d usadduran i wakken ad yili useḥbiber yef lemḥadra n tezmart n yemdanen.

Taddra n usenfar-a tcudd ar wamzi-ayessan n yimaṭṭafen yettumehzen akked tuddsiwin n wamzi-icermaḍ n lkarbun yemgaraden, d ayen ara yawin ar tizmirin tizefikruranin d tselḍanin yufraren. Rnu aseḡdec n wamzi-ilikrubert yellan tatiṭṭuct s tuddsa-s akked wamzi-icermaḍ n lkarbun d-yettaken tufrarin n tqaεett taweseant, s uḥulfu ameqqran d tlisa n usebgen rehfont.

Kraḍ n yimaṭṭafen izefakruranen d-yettuxedmen i usebgen n lavallin am umernu asadduran deg sker asenzan n vanille, askan n dindin n siprofloksasin, n parasitmul d laminufinul deg yibeccan d-yettuxedmen seg laburatwar akked ttmersiwt n yizefakruran n limarat n parasitamul deg waman n tbernint d waman n diri.

Amzi-imaṭṭafen d iḥerfiyen run d idamsanen d-yettusumren ttgensisen aḥulfu d wefran ameqqran, ma d tilisa n usebgen-n sen turahfont (amezwar-n sent seg nM). Anect-a, yezmer ad s-yefk tisellit d tesyufit s uwalem n tesleḡt tillawit (in-situ) s war aheggi uzzig n tubbirt.

Abbreviation

<u>Acronym</u>	<u>Definition</u>
AC	Activated carbon
ADI	Acceptable daily intake
AMP	4-Aminophenol
ANSM	National Medicines Safety Agency
BDD	Boron-doped diamonds
BDDEs	Boron-doped diamond electrodes
BRS	Britton Robinson Solution
C₆₀	Fullerene
C₆₀NWs	Fullerene nanowhiskers
CA	Chronoamperometric measurement
CB	Carbon black
CBf	Functionalized carbon black
CDs	Carbon dots
CE	Counter electrode
CIP	Ciprofloxacin
CME	Cavity microelectrode
CMs	Carbon nanomaterials
CNTs	Carbon nanotubes
CPDs	Carbonized polymer dots
CPE	Carbon paste electrode
CQDs	Carbon quantum dots
CV	Cyclic voltammetry
DNA	Deoxyribonucleic acid
EIS	Electrochemical impedance spectroscopy
EP	Electrochemical preconcentration
FDA	Food and Drug Administration
FNFs	Fullerene nanofibers
FNTs	Fullerene nanotubes
FAO	Food and Agriculture Organization of the United Nations
GQDs	Graphene quantum dots
GPE	Graphite paste electrode

JECFA	FAO/WHO Expert Committee on Food Additives
K_{ow}	Octanol / water partition coefficient
LOD	Limit of detection
LOQ	Limit of quantification
LR	Linear range
MWCNTs	Multi-walled carbon nanotubes
NSAIDs	Non-Steroidal Anti-Inflammatory Drugs
PAR	Paracetamol
PGEs	Pencil graphite electrodes
pH	Potential hydrogen
pK_a	Constant acidity
RE	Reference electrode
RSD	Relative standard deviation
S/N	Signal to noise ratio
SEM	Scanning electron microscopy
SPE	Screen-printed electrodes
SWCNTs	Single-walled carbon nanotubes
SWV	Square wave voltammetry
UN	United Nations
UPLC/UV	Ultra performance liquid chromatography coupled with UV detection
US	United States
USP	United States Pharmacopeia
VAN	Vanillin
WE	Working electrode
WHO	World Health Organization
WWTPs	Wastewater treatment plants

Figures list

Figure I.1. Chemical sensor classification	8
Figure I.2. Schematic representation of the carbon paste electrode.....	13
Figure I.3. Schematic representation of the cavity microelectrode.....	15
Figure I.4. Schematic representation of SPE.....	18
Figure I.5. The different procedures for manufacturing CMs based electrodes	19
Figure I.6. The different dimensional carbon nanomaterials	21
Figure I.7. Classification of CDs and their main preparation approaches	28
Figure I.8. Schematic representation of CB morphology	29
Figure II.1. Schematic representation of the conventional three electrodes system.....	44
Figure II.2. Typical cyclic voltammogram of a reversible redox reaction	45
Figure II.3. Representation of a standard addition method.....	50
Figure II.4. Graphical presentation of f-MWCNTs-FNTs/CPE sensor fabrication.....	52
Figure III.1. SEM images for (A) graphite (x10.000), (B) f-MWCNTs-FNTs/ CPE (x10.000), (C) FNTs (x10.000), (D) FNTs (x50.000), (E) MWCNT (x30.000) and (F) f-MWCNT (x30.000).	65
Figure III.2. Nyquist diagrams for EIS of CPE (●) and f-MWCNT-FNTs/CPE (●) in 1mM Fe(CN)_6^{3-} and BRS 0.04 M at pH=7	67
Figure III.3. Cyclic voltammograms at (1) CPE without VAN, and with 10^{-5}mol.L^{-1} VAN at (2) CPE, (3) f-MWCNTs/ CPE and (4) f-MWCNTs-FNTs/CPE in BRS 0.04 M (pH = 7)	67
Figure III.4. (A) Effect of pH on the peak oxidation current of VAN with different pH values (5 to 9) at the f-MWCNTs-FNTs/ CPE in BRS 0.04 M (pH = 7) at 20 mV.s^{-1} . (B) Corresponding plot of the oxidation peak potential of VAN versus pH.....	68
Figure III.5. The effect of different scan rates (5 to 80 mV.s^{-1}) on the oxidation peak current of $10^{-6}\text{ mol.L}^{-1}$ VAN at the f-MWCNTs-FNTs/ CPE in BRS 0.04M (pH = 7).	69
Figure III.6. Effect of accumulation time on the oxidation peak current of $10^{-6}\text{ mol.L}^{-1}$ VAN at the f-MWCNTs-FNTs/ CPE in BRS 0.04M (pH = 7).....	70
Figure III.7. (A) Cyclic voltammograms of VAN from 5×10^{-8} to $1 \times 10^{-4}\text{ mol L}^{-1}$ at f- MWCNTs-FNTs/ CPE in BRS 0.04M (pH = 7), Insert: from 5×10^{-8} to $9 \times 10^{-6}\text{ mol L}^{-1}$. (B, C) Calibration curves of VAN concentrations against peak current from 5×10^{-8} to $9 \times 10^{-6}\text{ mol L}^{-1}$ and from 1×10^{-5} to $1 \times 10^{-4}\text{ mol L}^{-1}$, respectively.....	71
Figure III.8. The relative peak current response of $1\text{ }\mu\text{M}$ VAN in the presence of some potential interfering substances at the f-MWCNTs-FNTs/ CPE in BRS 0.04 M (pH = 7).....	74

Figure III.9. The study of stability of the f-MWCNTs-FNTs/ CPE of the relative peak current response of 1 μM VAN in 10 days of storage.....	75
Figure III.10. Calibration curve of the VAN standard solutions	76
Figure IV.1. Major source of pharmaceutical contaminants in environment.....	88
Figure IV.2. Country survey on the number of pharmaceutical substances detected in surface waters, groundwater, or tap/drinking water [33].....	89
Figure IV.3. SEM images for (A) graphite (x10.000), (B) AC (x10.000), (C) CB (x50.000), (D) CBf (x50.000), (E) CBf-AC (x5.000) and (F) CBf-AC (x50.000)	99
Figure IV.4. Fourier transform infrared spectrograms of (A) CB and (B) CBf	100
Figure IV.5. Nyquist diagrams for EIS of AC/CME (•), CBf/CME (•) and CBf-AC/CME(•) in 1mM $\text{Fe}(\text{CN})_6^{3-/4-}$ at BRS 0.04 M (pH=5).....	101
Figure IV.6. (A) Cyclic voltammograms of the AC/CME,CBf/CME and CBf-AC/ CME in the presence of 5 μM AMP, PAR and CIP in BRS 0.04 M (pH = 5); 20 mV.s^{-1} (B) The corresponding sensitivity of the CMEs.	102
Figure IV.7. Cyclic voltammograms of 5 μM AMP, PAR and CIP in BRS 0.04 M at different pH value (3 to 6) at the CBf-AC/CME	103
Figure IV.8. A, B and C: Effect of pH on the peaks current oxidation of AMP, PAR and CIP, respectively. E, F and G: Corresponding plots of the oxidation peaks potential of AMP, PAR and CIP versus pH, respectively at the CBf-AC/CME.....	104
Figure IV.9. Cyclic voltammograms of 5 μM AMP, PAR and CIP in BRS 0.04 M (pH=5) with different scan rate values (25 to 275 mV.s^{-1}) at the CBf-AC/CME	105
Figure IV.10. Plot of the peaks current oxidation of AMP, PAR and CIP versus scan rates at the CBf-AC/CME in BRS 0.04 M (pH=5).....	106
Figure IV.11. A, B and C: The effect of accumulation time on the oxidation peak current of 5 μM AMP, PAR and CIP, respectively at the CBf-AC/CME in BRS 0.04 M (pH = 5).	106
Figure IV.12. (A) Square wave voltammograms of the determination of AMP from 0.1 to 3 μM at CBf-AC/CME in BRS 0.04 M (pH = 5). (B) Calibration curves of AMP concentrations against peak current.....	107
Figure IV.13. Mechanism of the electrochemical reaction of 4-aminophenol.....	107
Figure IV.14. (A) Square wave voltammograms of the determination of PAR from 0.05 to 2 μM at CBf-AC/CME in BRS 0.04 M (pH = 5). (B) Calibration curves of PAR concentrations against peak current.....	108
Figure IV.15. Mechanism of the electrochemical reaction of paracetamol	108

Figure IV.16. (A) Square wave voltammograms of the determination of CIP from 0.1 to 3 μM at CBf-AC/CME in BRS 0.04 M (pH = 5). (B) Calibration curves of CIP concentrations against peak current.....	109
Figure IV.17. Mechanism of the electrochemical reaction of ciprofloxacin	109
Figure IV.18. (A) Square wave voltammograms of the simultaneous determination of AMP, PAR and CIP from 0.1 to 3 μM ; 0.025 to 3 μM and 0.05 to 3 μM , respectively, at CBf-AC/CME in BRS 0.04 M (pH = 5).....	110
Figure IV.19. A, B and C: Calibration curves of AMP, PAR and CIP concentrations against peak current, respectively in the simultaneous determination at CBf-AC/CME in BRS 0.04 M (pH = 5).	112
Figure IV.20. The relative peak current response of AMP, PAR and CIP in the presence of some potential interfering substances at the CBf-AC/CME in BRS 0.04M (pH = 5).	114
Figure V.1. SEM images for CB (A) (x 5.000), (B) (x 50.000).....	130
Figure V.2. Nyquist diagrams for EIS at CB/ CME in 1 mM $\text{Fe}(\text{CN})_6^{3-/4-}$ at BRS 0.04 M (pH=7) with and without EP.....	131
Figure V.3. (A) Cyclic voltammograms of 1 mM of $\text{K}_3\text{Fe}(\text{CN})_6$ in BRS 0.04 M (pH=7) at different scan rate values (5 to 300 mV.s^{-1}) at the CB/CME (B) Plot of the peaks current oxidation of PAR versus scan rate.....	132
Figure V.4. (A) Cyclic voltammograms of 1 μM PAR in BRS 0.04 M (pH=7) at different scan rate values (25 to 250 mV.s^{-1}) at the CB/CME (B) Plot of the peaks current oxidation of PAR versus scan rate for 1 μM PAR (C) Plot of the peaks current oxidation of PAR versus scan rate for 0.05 μM PAR.....	133
Figure V.5. (A) Cyclic voltammograms of 1 μM PAR in BRS 0.04 M at different pH value (3 to 9) at the CB/CME (B) Effect of pH on the peaks current oxidation of PAR in BRS 0.04 M with different pH value (3 to 9) at the CB/CME. (C) Corresponding plots of the oxidation peaks potential of PAR versus pH.....	134
Figure V.6. Effect of the preconcentration potential on the oxidation peak current of 0.1 μM PAR at the CB/CME in BRS 0.04 M (pH=7).....	136
Figure V.7. Effect of the preconcentration time on the oxidation peak current of 0.1 μM PAR at the CB/CME in BRS 0.04 M (pH = 7).....	136
Figure V.8. (A) Cyclic voltammogram of CB/CME in a presence of 1 μM PAR in BRS 0.04 M (pH = 7) at 25 mV.s^{-1} (B) SW voltammograms of 30 μM PAR (a) before and (b) after EP at 0 V for 900 s on CB/ CME.....	137

Figure V.9. (A) SW voltammograms of PAR from 5×10^{-9} to 1×10^{-6} without EP (B) SW voltammograms of PAR from 5×10^{-10} to 1×10^{-6} with EP at 0 V for 900 s on CB/ CME in BRS 0.04 M (pH = 7). (C& D) Calibration curves of [PAR] vs peak currents from 5×10^{-9} to 9×10^{-8} and from 1×10^{-7} to 1×10^{-6} , respectively.....138

Figure V.10. Effect of the preconcentration time on the oxidation peak current of 0.1 μ M PAR at the CB/CME in BRS 0.04 M (pH =7).....139

Figure V.11. The relative peak current response of PAR in the presence of some potential interfering substances at the CB/CME in BRS 0.04M (pH = 7).141

Tables list

Table I.1. Comparison of sensing materials used in chemical sensors	23
Table II.1. List of chemicals	43
Table III.1. Main physicochemical properties of vanillin.....	62
Table III.2. Comparison of this work with the previously reported VAN analysis with electrochemical sensor	72
Table III.3. Study of repeatability and reproducibility of the f-MWCNTs-FNTs/ CPE for different VAN concentrations in BRS 0.04M (pH = 7); pre-concentration time under stirring 300 s; 20 mV.s ⁻¹	73
Table III.4. Values of pKa and Log Kow for some interfering compounds	74
Table III.5. Results of UPLC/UV analysis of the VAN standard solutions	76
Table III.6. Results of UPLC/UV analysis of the different samples of sugar vanilla.....	77
Table III.7. Determination of VAN mass fraction indifferent real commercial sugar vanilla samples with electrochemical and UPLC/UV methods	77
Table IV.1. Main physicochemical properties of 4-aminophenol.....	90
Table IV.2. Main physicochemical properties of paracetamol.	92
Table IV.3. Main physicochemical properties of ciprofloxacin.....	94
Table IV.4. Comparison of this work with those previously reported for the simultaneous analysis of AMP, PAR and CIP with electrochemical sensor.....	113
Table IV.5. Study of the repeatability and reproducibility of the simultaneous detection for different concentrations at CBf-AC/CME in BRS 0.04 M (pH = 5). *n = 3	113
Table IV.6. Validation of the CBf-AC/CME in the determination of AMP, PAR and CIP wastewater samples.	115
Table IV.7. Validation of the CBf-AC/CME in the determination of AMP, PAR and CIP inartificial urine.	116
Table V.1. Parameters and characteristics of the calibration curves for the analysis of PAR without and with electrochemical preconcentrationat CB/ CME at 0 V for 900 s in BRS 0.04M (pH = 7).....	139
Table V.2. Comparison of this work with a previously reported for the simultaneous analysis of AMP, PAR and CIP with electrochemical sensor.....	140
Table V.3. Study of the repeatability and reproducibility of detection of PAR concentrations at CB/CME in BRS 0.04 M (pH = 7).....	140

Table V.4. Validation of the CB/CME in the determination of PAR directly intap and wastewater samples.....	142
---	-----

General Introduction

General Introduction

Human health is the most central human happiness and well-being, which contributes significantly to prosperity, wealth, and even economic progress. Health can be defined as the complete state of physical, emotional, spiritual, and social well-being, and not only the absence of illness and infirmity [1]. However, human health is constantly affected by a multitude of factors, whether positive or negative, which are referred to as the determinants of health, which can be classified into nutrition, lifestyle, environment, genetics and pharmaceutical care determinants [2]. Among those factors that have a significant influence on health are the environment, food and pharmaceutical products.

In one hand, food has a vital significance, it is necessary for the body development and essential nutriment that maintain the human life. However, it can also be the reason of his illness or even death when it is either consumed in overdose or contaminated by environmental contaminants, food processing contaminants, food additives and migrants from packaging materials [3]. Especially with the increase of population and the change of life style that promote considerably the consumption of the industries food, which involve the incorporation of food additives with incontrollable amount in order to have attractive taste food. However, as food additive affect considerably the quality of food, it also, can affect indirectly the human health. Consequently, the increased consumption of food additives induces various side effects that endanger human health in case they are not controlled in the food production process phase or are not taken in acceptable amounts. Therefore, the monitoring of food additive concentrations and generally food quality is primordial to ensure and to preserve the human life. Thus, in addition to food additive, water and food are contaminated primarily by environmental contaminates, particularly chemical contaminates that are generally classified as emerging contaminates.

In another hand, pharmaceutical products are essential and indispensable compounds that treat diseases and improve health. Nevertheless, it is important to know that all pharmaceuticals have risks as well as benefits. The main known and direct risk is the taking of medicines in overdose, an action that leads to poisoning and risk of mortality [4]. Monitoring the composition of medicines at the production stage is very important to avoid any risk. Secondly, drug monitoring is still necessary in different areas such as medical diagnostics to determine the levels of antibiotics or anti-cancer drugs in patients' body fluids [5]. However, another indirect risk is the presence of pharmaceuticals in the environment after their discharge by various ways. The accumulation and persistence of these substances, even at low concentration, in the

environment, can affect not only human life by the contamination of foods, wastewater and drinking water, but also the aquatic life and the environment in general. Therefore, pharmaceuticals and their metabolites are recognized as emerging contaminants for the environment [6]. Consequently, emerging contaminants consist a major problem for the environment and the human health; they are chemical substances with properties such as low degradation potential and environmental persistence, including pharmaceuticals, plasticizers and pesticides that are frequently detected in environment media [7].

In this context, it is crucial to pay greater attention to develop new methodologies as tools for human biological diagnostics and for monitoring the emerging contaminants, medicines and food qualities to improve quality of industrials products, prevent diseases, protect the environment and assure a safety human health. For this purpose, several analytical methods have been developed such as chromatography, spectroscopy, chemiluminescence and capillary electrophoresis. However, these conventional techniques, despite their reliability and precision, are not recommended for rapid in situ analysis. In addition to the fact that they require complicated instrumentation, are very expensive, require fastidious sample preparation, and qualified personnel. Contrariwise, electrochemical sensors are alternative solutions for environmental analysis, industrial monitoring and body diagnostics owing to their greater selectivity, sensitivity and above all allow simplicity, ease of use, rapidity of analysis, portability and applicability for in-situ analysis [8].

The field electrochemical sensing began with the conventional solid electrode, whose surfaces were based on gold, platinum and other noble metals. These reported electrodes are suitable for electrochemical analyzes, but their applications are limited due to: (1) they are applicable only in the cathode region because that is rather limited by a low hydrogen overvoltage, which has limited their potential window; (2) formation of oxide layers or dissolution of metals; (3) the possibility of interaction of the electrode metal with analytes [9]. Over the years, electrochemical techniques have undergone significant developments, including the introduction of new kinds of electrodes (carbon paste electrode, cavity microelectrode and screen-printed electrode) in addition to their modification by various materials that make electrochemical sensing a very attractive topic. Several studies have reported on the development of sensors, which are currently being applied to analyze different types of samples in various fields.

Therefore, in order to achieve a lower detection limit and higher sensitivity, nanomaterials have started to emerge and be integrated into the electrode matrix. These nanomaterials have received particular attention due to their exceptional proprieties that improve considerably the performances of the sensors. In particular, carbon nanomaterials are environmental-friendly and renewable materials, which have exceptional electrochemical properties and a high adsorption capacity that enhance the sensitivity with chemical stability in different analytical media [10]. In fact, nanostructuring with carbon nanomaterials allows developing rapid, sensitive, inexpensive and transportable devices for the in situ detection of different (bio) analytes.

This thesis focuses on the development of amperometric electrochemical sensors and micro-sensors based on carbon nanomaterials for the analysis of some targets in food and waters. The overall aim of this project is, in one hand, to design low-cost, reliable, stable and precise devices for food and environmental monitoring that have superior sensing characteristics toward selective targets that can enable analysis of real samples by anyone, anywhere and at any time. On the other hand, to highlight the importance of nanostructured carbon nanomaterials in improving the characteristics of the developed sensors. The designed sensors and micro-sensors were applied after optimisation of several parameters that affect their performance, and then evaluated by scanning electron microscopy, chronoamperometry, electrochemical impedance spectroscopy and voltamperometry techniques. Also, the fabricated electrodes were validated for the determination of the selected targets on real samples (food and water). This manuscript is organized in five chapters briefly presented below:

The ***First Chapter*** will report, in the first part, on the literature review of electrochemical sensors, their different types and characteristics. The natures of working electrodes used in the conception of proposed sensors and micro-sensors will also be described and their advantages and disadvantages will be numerated to explain their use in this thesis. In a second part, an introduction to the carbon materials used in the structuring of electrodes and their properties will be presented, in addition to the description of the different carbon materials commonly used in electrochemical sensing.

The ***Second Chapter*** presents the experimental part and describes in detail the preparation of the modified electrodes and the samples used for the validation analysis. It will include all techniques and experimental protocols used in the following chapters.

The ***Third Chapter*** will present a carbon paste electrode modified with fullerene and multi-walled carbon nanotubes for the monitoring of vanillin additive. The first part will give some

general information on vanillin, its uses and the interest of its detection and monitoring. The second part, will describe the optimization, the experimental conditions of the conception and the validation of the proposed modified carbon paste electrode in real samples of commercial vanilla sugar.

The ***Fourth Chapter*** will present a micro-sensor fabricated using a modified cavity microelectrode with functionalized carbon black and activated carbon for the simultaneous detection of ciprofloxacin, paracetamol and 4-aminophenol. This chapter will also be divided in two parts. The first one will focus on presenting some general information on pharmaceuticals, how they contaminate the environment and the risk of their presence in the aquatic media. Generalities about the pharmaceutical products studied in this thesis and the relevance of their detection and monitoring will be presented. The second part will present the optimization of the different operating conditions for the designed micro-sensor, the experimental conditions of the conception and validation of the proposed modified cavity microelectrode for the simultaneous detection of the three targets in artificial urine samples.

The ***Last Chapter*** will present a simple cavity microelectrode modified with carbon black for the electrochemical preconcentration and detection of paracetamol traces directly in water. It will present the optimization of the different experimental conditions. Next, the relevance of electrochemical preconcentration will be demonstrated and modified microelectrodes will be compared before and after preconcentration. Finally, a trace analysis of paracetamol with the proposed method will be applied to tap water and local wastewater.

Finally, the manuscript will end with a ***General Conclusion*** that summarizes all the important results obtained during this research work followed by perspectives that seem interesting for the continuity of the development of new sensors for food and environment applications.

References

- [1] Li A. M. (2017). Ecological determinants of health: food and environment on human health, *Environmental science and pollution research international*, 24(10), 9002.
- [2] Patwardhan, B., Mutalik, G. & Tillu, G. (2015). Chapter 3 - Concepts of Health and Disease, Editor(s): Patwardhan, B., Mutalik, G. & Tillu, G. Integrative Approaches for Health, *Academic Press*, 53.
- [3] Rather, I.A., Koh, W.Y., Paek, W.K. & Lim, J. (2017). The Sources of Chemical Contaminants in Food and Their Health Implications, *Frontiers in Pharmacology*, 8, 830.
- [4] Daly, C., Griffin, E., Corcoran, P., Webb, R. T., Ashcroft, D. M., Perry, I. J., & Arensman, E. (2020). A national case fatality study of drugs taken in intentional overdose. *The International journal on drug policy*, 76, 102609.
- [5] Frosch, T., Knebl, A. & Frosch, T. (2020). Recent advances in nano-photonic techniques for pharmaceutical drug monitoring with emphasis on Raman spectroscopy, *Nanophotonics*, 9(1), 19.
- [6] Valdez-Carrillo, M., Abrell, L., Ramírez-Hernández, J., Reyes-López, J. A., & Carreón-Díazconti, C. (2020). Pharmaceuticals as emerging contaminants in the aquatic environment of Latin America: a review. *Environmental science and pollution research international*, 27(36), 44863.
- [7] Pereira, L. C., de Souza, A. O., Franco Bernardes, M. F., Pazin, M., Tasso, M. J., Pereira, P. H., & Dorta, D. J. (2015). A perspective on the potential risks of emerging contaminants to human and environmental health. *Environmental science and pollution research international*, 22(18), 13800.
- [8] Lu, Y., Liang, X., Niyungeko, C., Zhou, J., Xu, J. & Tian, G. (2018). A review of the identification and detection of heavy metal ions in the environment by voltammetry, *Talanta*, 178, 324.
- [9] Uslu, B. & Ozkan, S.A. (2007). Solid Electrodes in Electroanalytical Chemistry: Present Applications and Prospects for High Throughput Screening of Drug Compounds, *Combinatorial Chemistry & High Throughput Screening*, 10, 495.
- [10] Tajik, S., Beitollahi, H., Nejad, F.G., Safaei, M., Zhang, K., Le, Q.V., Varma, R. S., Jang, H. W. & Shokouhimehr, M. (2020). Developments and applications of nanomaterial-based carbon paste electrodes, *RSC Advances*, 10, 21561.

Chapter I
Literature review

Introduction

This chapter is organized in two parts. The first one presents generalities about electrochemical sensing, types of electrochemical sensors and the description of the different procedures adopted in the fabrication of electrodes. We will focus on the description of the nature of the working electrodes used in the design of the sensors and micro-sensors proposed in our study. The second part presents a brief review of the literature related to carbon nanomaterials, their proprieties and their performance in the detection of different targets molecules.

I.1. Electrochemical sensing

Electrochemistry is a domain of science that studies the interrelation between electrical and chemical changes caused by the passage of current [1]. In the recent decade, the scientists and researchers have focused on the electrochemical sensing, due to their unique advantages, namely ease of preparation, low instrumentation costs, miniaturization, fast response and high sensitivity [2]. In addition, to the possibility of the on-site analysis of environmental pollutants, the monitoring of industrial products (drugs or foods) and the analysis of biological fluids [3].

So, what is an electrochemical sensor?

In general, a sensor is a device that transforms a physical quantity into a signal that can be read by an electronic instrument [4]. Especially, the chemical sensor converts chemical information (such as concentration, moisture, activity) into an analytically useful signal [5]. It consists of two fundamental elements: receptor and transducer. The receptor is a molecular recognition that is in direct contact with a selective substance or a group of substances, and the transducer is the element that transforms the interaction between receptor and analyte into measurable electric quantity (voltage, current, or resistivity) [6]. Chemical sensors are classified according to the properties used for the molecular detection as conductivity, potential, capacitance, heat, concentration or optical constants (Fig. I.1). The most attractive chemical sensors are electrochemical sensors due to their experimental simplicity, low-cost and ability to selective and sensitive detection. There are three main types of electrochemical sensors: conductometric, potentiometric and amperometric [5].

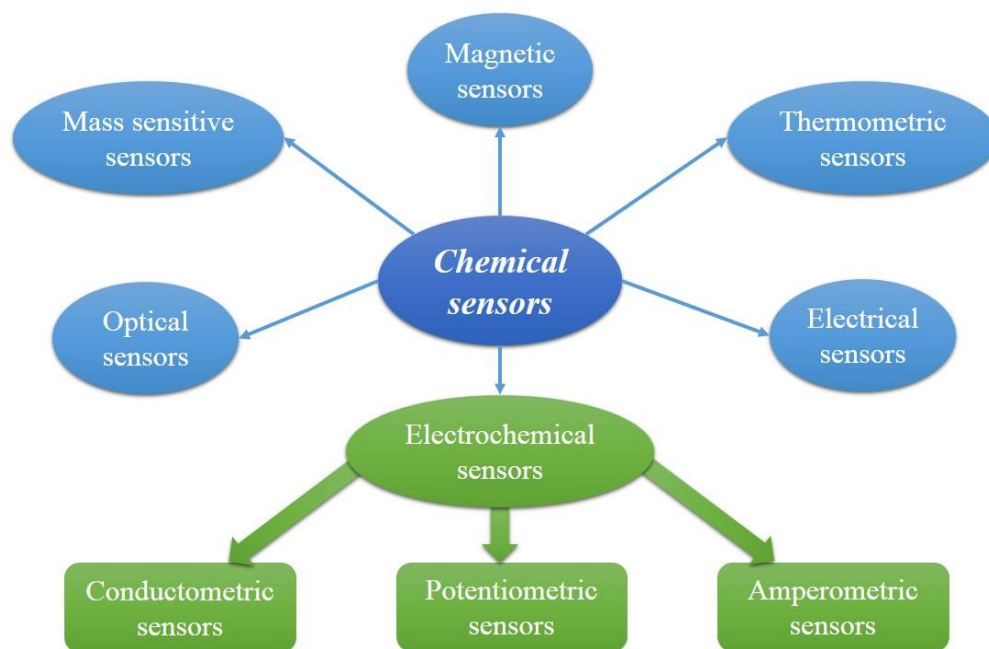


Figure I.1. Chemical sensor classification

I.2. Types of electrochemical sensors

I.2.1. Conductometric sensors

Conductimetry measures the consumption or production of charged species generated during a molecular reaction at the receptor. Thus, conductometric sensor is based on measuring the electrical conductivity of an electrolytic solution containing mobile electrical charges [7]. They present various advantages such as simplicity, low cost compared to the other electrochemical sensors because they do not require reference electrode to operate and suitable for miniaturization in the form of planar interdigitated electrodes, in addition to its insensitive to light [8]. Conductimetry sensing have a limited use, it is often used for conductivity measurements and gas detection. For example in the development of a sensitive and selective conductometric sensor based on Sm_2O_3 nanoparticles for the monitoring of important volatile organic compounds (VOCs) such as ethanol and acetone in air [9]. In the same field, another study investigated the fabrication of a ZnO nanotetrapod (NTP) based conductometric sensor for the detection of VOCs such as formaldehyde, ethanol, methanol and acetone [10]. In addition to that, some recent work has reported the use of this kind of sensor for the detection of potassium in whole blood [8] and for monitoring degradation of automotive engine oils [11].

I.2.2. Potentiometric sensors

Potentiometric sensors measure the potential variation between the working and reference electrodes at generally zero current [12]. This potential difference is a function of the concentration of ions present in the electrolyte in which the sensor is immersed and are related by the Nernst equation [13]: $E_{eq}(Ox/Red) = E^{\circ}(Ox/Red) + \frac{RT}{nF} \ln \frac{a_{Ox}}{a_{Red}}$, **Eq. 1.1**

with:

E° : standard potential of a half-reaction;

R : universal gas constant ($R = 8,314 \text{ J. (mol.K)}^{-1}$) ;

F : Faraday constant ($F = 96500 \text{ C.mol}^{-1}$) ;

T : temperature in Kelvin degree ;

n : number of electrons (eq. mol^{-1}) involved in the half-reaction;

a_{Ox} (a_{Red}): activity of the oxidized (reduced) species.

This type of sensor has several advantages including simplicity, inexpensive, rapidity, in-situ analysis and they do not require auxiliary electrode to operate [14]. However, potentiometric sensors have some drawbacks; their responses are strictly temperature dependent, require frequent calibration, have low sensitivity, the reference electrode is unstable and the working electrode can be contaminated by adsorption of solution components [15].

The potentiometry sensing have found some applications in the clinical and environmental analysis, the best known potentiometric sensor being the pH-meter. Various reviews have reported on their performances in several fields such as the determination of VOCs contaminated air [16], monitoring the antioxidant activity of food and herbal extracts [17], detection of pharmaceuticals in biological samples [14] and biosensing of metal ions, DNA, proteins, bacteria and small molecules including cholesterol, galactose and uric acid [18].

I.2.3. Amperometric sensors

Amperometric sensor measures the intensity of the current through an electrochemical cell as a function of time by controlling the potential of the working electrode with a potentiostat. The current measured is a function of the concentration of the electroactive species. When the potential is kept at a constant value, it is called potentiostatic sensing, and when it is scanned between two values, it is called potentiodynamic sensing. A conventional electrochemical cell with three electrodes (working, reference and auxiliary) connected to a potentiostat are the basic

instruments for amperometric analysis [5]. Amperometric sensing presents multiple advantages such as a high sensitivity and selectivity, low limit of detection, wide linear range, simplicity, low cost, possibility of miniaturization, modification for target specific analysis, rapid and on-site analysis of analytes. The most common inconvenience for this kind of sensors is their dependence on the pH of the electrolyte support, the possibility of detecting interfering species and the need of to modify the electrode surface to achieve better selectivity [19]. This sensing method is most commonly used in biosensors and chemical sensors for environmental monitoring, health, food and industry controls.

In our study, we focused on the design of amperometric sensors for the electrochemical detection of food additives and pharmaceuticals. The choice of this type of sensor over other electrochemical sensors is based on the advantages and characteristics already mentioned for sensing targets. They are species selective and allow the target species to be quantified with good accuracy and for low detection amounts.

I.3. Characteristics of an electrochemical sensor

The performance of a sensor is evaluated in terms of its effectiveness for a particular application in a specific field. The validation of the final developed sensor requires at least the evaluation of the following technical and functional characteristics:

Linear range (LR): corresponds to the concentration range determined by upper and lower values, where the sensitivity of the sensor remains constant as the concentration of the analyte increases;

Limit of detection (LOD): corresponds to the lowest concentration that a sensor can detect, it is expressed as three times the signal to noise (3 S/N) ratio;

Limit of quantification (LOQ): corresponds to the lowest concentration that a sensor can measure, provided with an acceptable level of reliability and known uncertainty, it is expressed as ten times the signal to noise (10 S/N) ratio;

Sensitivity: corresponds to the lowest value that a sensor can detect an analyte; it is expressed by the ratio between the variation of the output and the input values. In the majority of sensors, it is indicated by the slope of the calibration curve;

Selectivity: corresponds to the specificity of the sensor to detect a specific analyte with avoiding false response attribute to the presence of interfering species, which may enhance the sensor signal. It is the capacity of the sensor to discriminate between the target analyte and other substances;

Stability: is the ability of the sensor to provide same response when used in the same conditions to measure the same target over a period of time;

Response time: is the time the device needs to respond on the abrupt variation of the measured;

Repeatability: corresponds to the ability of a sensing system to give identical response under the same operating conditions over some period of time;

Reproducibility: corresponds to the ability of a sensor to give identical output under changing measurement conditions [5, 20].

I.4. Types of electrodes

Over the past decades, scientists have been improving or discovering several analytical and electrochemical methods in order to develop efficient devices for the quantitative and qualitative analysis in medical, industrial and environment applications. With the aim to have a simple and economical instrument that provides sensitivity in short time with wide electroanalytical applications, researchers have manufactured several new electrochemical measurement devices. The most known and used in the latest years are: carbon paste electrodes, glassy carbon electrodes, cavity microelectrodes, screen printed electrodes, boron doped diamond electrode, pyrolytic carbon nanoglass electrodes, sub-millimeter electrode, carbon felt electrode, rotating disk electrode, graphite electrode, pencil graphite electrode and 3D-printed electrode.

In the following paragraphs, we will focus to the detailed presentation of the electrodes used in our studies, namely the carbon paste electrode and the cavity microelectrode. Then, we will discuss briefly the different procedure of electrodes fabrication.

II.4.1. Carbon paste electrode (CPE)

a. Brief historic

In 1958, R. N. Adams introduced a new kind of electrode, “the carbon paste electrode”, which was originally designed as an alternative to the dropping mercury electrode [21]. Early work with this electrode focused on the characteristics of the CPE and its applicability in anodic [22] and cathodic [23] voltammetry. Since then, CPE has been studied in electroactive redox mechanism and qualitative studies, and some papers propose the use of the carbon paste electrode as a sensor in electrochemical detection.

For example, in 1963, Jacobs use a CPE as an analytical sensor for the determination of gold and silver ions [24]. After 1964, many scientists became interested in CPE and reported different modifiers for carbon paste in order to improve their sensitivity and selectivity [25-28]. Since then, several scientists have suggested this kind of electrodes in electrochemical studies, which have already been summarized in several reviews [29, 30]. Today, the application of the carbon paste electrodes as electrochemical sensors is considered as a suitable and mainly used device in the analysis of foods, biological fluids and environment waters. The latest review on the CPE applications as powerful sensors approach for the determination of food contaminants, drug ingredients and environmental pollutants was published in 2019 [31].

b. Description of the CPE

The carbon paste electrode (CPE) is a cylindrical electrode support made of glass, plastic or Teflon (an inert material) with a length of 10 to 12 centimeter. Through it passes a conductive wire (usually copper wire) with a diameter of few millimeter. The extremity part of the support is a cavity of 1.4 to 3 millimeters in diameter and approximately 3 millimeters in depth (Fig. I.2). Inside this cylindrical cavity, a paste is introduced and compacted. It is then smoothed on a clean paper until a uniform surface is obtained. The paste used in the CPE is consisted generally by a conductor material such as graphite or carbon black with appropriate ration of binder, just to assure a good mechanical strength of the whole, without reducing the proprieties of the electrode. Indeed, the binder has insulating properties which can affect the sensitivity of the sensor when used in higher proportions, but its incorporation into the paste used in the CPE is necessary to agglomerate the powders and obtain a consist paste.

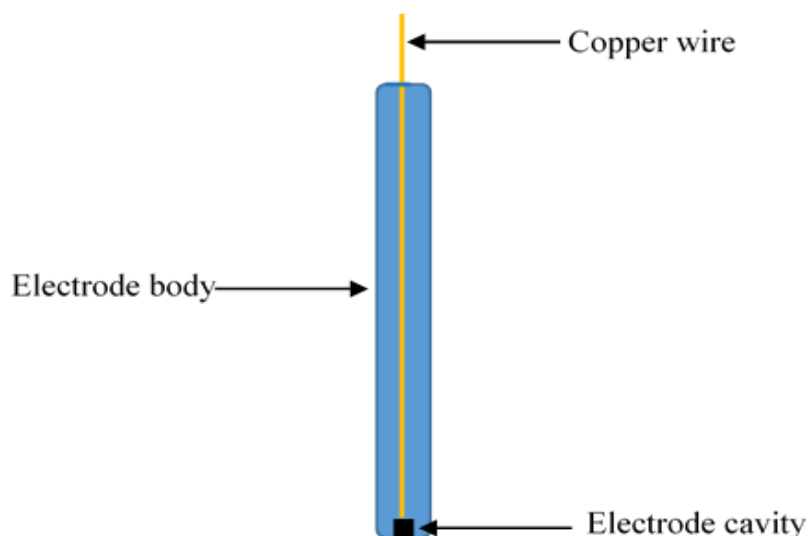


Figure I.2. Schematic representation of the carbon paste electrode

c. Advantages and disadvantages of the CPE

The use of carbon paste electrode has special benefits compared to some usually electrodes, such as Au electrode, platinum electrode, mercury electrode or glassy carbon electrode. The most of these advantages are:

- Low background currents;
- A large potential window;
- Possibility of the use in various interactions (electrolysis, catalysis, adsorption, extraction, ion-pairing, and their combination);
- Simple preparation procedure;
- Low cost method;
- Easy of conditioning and regenerating of the electrode surface and;
- Easy of packing and cleaning [29, 32].

However, carbon paste electrodes also exhibit some disadvantages such as:

- Relative weaker fabrication reproducibility;
- Mechanical stability;
- Weakness in the electrochemical response of the sensor due to the use of the binder, which has a no conducting proprieties;
- High double layer capacitance and a non-negligible contribution of the ohmic drop due to the large dimensions of the electrode;
- low scanning rates that can allow to long experimentation period;
- Slower kinetic of electron transfer [33, 34].

I.4.2. Cavity microelectrodes (CME)

a. Brief historic

In 1994, at Wuhan University, Cha and its team laboratory have developed the powder microelectrode or a cavity microelectrode (CME). The main aim of their research was to find techniques that offer the possibility to study the electrochemical kinetic and cyclic behavior of various powders. In addition, to minimize the side effects induced by large electrode dimension, which destroy the cyclic voltammetry and reduce then the reaction volume, due to both large ohmic drop and capacitive current [35]. Initial research with the CME focused on the study of the electrochemical behaviour of several materials such as carbon [36], conducting polymers [37], battery materials [38, 39] and electrocatalysts [40-43]. This device was also used for the quantitative determination of the number of the active site of a mixed $\text{IrO}_2\text{-SnO}_2$ powders [44], in the study of an electrolytic manganese dioxide powder used in alkaline batteries in order to determine its potentialities as a pH sensor [45]. Moreover, the powder microelectrode have found application in various field of electrochemistry, in electrochemical sensing, energy storage and energy production [46, 47], electrocatalysis [43, 48], polymers with its derivatives [49, 50].

In the electrochemical sensing, the use of CME as a sensor for target reagents determination is still recent and some articles report its use in this application such as for the detection of hydrazine [51], dopamine [52], cholesterol [53], glucose oxidase [54] or alkylphenol [55]. For example, in our team, D. Hauchard with Ayman Chmayssem, have developed a new method based on a microelectrode sensor for the simultaneous electrochemical detection of three alkylphenol micropollutants in water. They compared the results obtained with both CME and a classical electrode and successfully demonstrated that the small cavity dimension reduce considerably the electrochemical interface by especially reducing the ohmic drop and the double layer capacitance allowing measurements of alkylphenol concentrations in water without any electrolyte addition [55]. Some others reports show the role of the CME devise in improving the signal response and enhancing the detection sensitivity allowing to lower detection limits. For instance, carbon black packed CME was employed in the detection of ultra-low concentration of dopamine with very high sensitivity. In the recent work done in 2017, H. Bao-Shan and coll used the powder microelectrode embedded with carboxyl MWCNTs in the rapid detection of ascorbic acid. In comparison with conventional microelectrodes, this CME has a larger specific surface area and more active sites that lead to high sensitivity and

lower detection and quantitative limits [56]. Another paper published in 2018 by this same team, reported the use of the same technique (CME embedded with carboxyl MWCNTs) for the sensitive detection of nitrofurazone and semicarbazide with short detection time in real samples of pork [57].

b. Description of the CME

The cavity microelectrode (CME) is a glassy cylindrical body with a diameter of about 8 millimeters and a length of 10 to 15 centimeters (Fig. I.3). Through it passes a platinum wire of 25 to 50 micrometers and about one millimeter length. A graphite powder intermediary connects this last one to a copper wire. In the extremity part of the electrode support, a microcavity was formed either by chemical attack in aqua regia on the platinum wire or by laser digging [58]. The use of this CME has the advantage in the reduction of the electrochemical interface compared to the classical carbon paste electrode, improves the electrical properties of the micro-sensor, enriching conductivity and reducing resistance that was often observed with the use of binder and allows them to be applied in poorly conductive media, directly in situ [40].

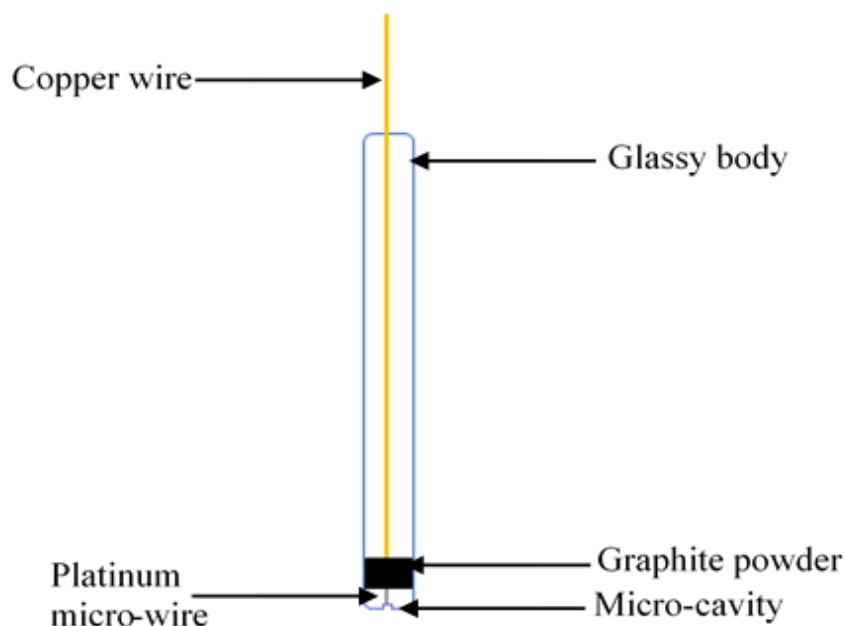


Figure I.3. Schematic representation of the cavity microelectrode

c. Packing and cleaning of the CME

Packing of the CME: A sufficient amount of the prepared powders was transferred to a glass slide. Then, pressed and packed into the cavity microelectrode body using it as a pestle, in order to compact the past inside the cavity. These steps were repeated several times to ensure that the CME is completely filled.

Cleaning of the CME: The cleaning of the CME can be carried out in ultrasonic cleaner for 5 minutes in the successive following solutions: HNO_3 0.1 M, H_2O_2 0.1 M and finally in deionized water. In the literature, it is stated that the cleaning of the CME can be also achieved by applying several cycles of cyclic voltammetry on the potential range of water electro-activity to form gas bubbles at the bottom of the cavity that will help expel the material from the cavity. However, whatever the cleaning method used, a check must be carried out to verify that the cavity has been free of powder material. For this, cyclic voltammetry is plotted in a sulfuric acid solution (0.5 M) can be applied. The resulting voltammogram must be similar to the typical platinum electrode voltammogram response showing the adsorption and desorption peak systems of hydrogen as well as the peaks of formation and reduction of platinum oxide system [58].

d. Advantages and disadvantages of the CME

The cavity microelectrode has various advantages; it solves all the problems encountered with the use of the CPE in addition to some beneficiaries attributed to the small dimension of the microelectrode. The most of these attractive benefits are:

- Higher specific surface area;
- Use small amount of pure electroactive materials;
- Rapid scanning rates that can allow to short experimentation period;
- Faster kinetic of electron transfer;
- Low double layer capacitance and a negligible contribution of the ohmic drop due to the miniaturization of the electrode dimensions;
- Very low currents value;
- Simple preparation procedure and;
- Low cost method.

Therefore, the only drawback of the CME is the packing of their micro-cavity, it is very difficult to know the amount of the materials inserted in the cavity and assure the reproducibility of the packing. In addition, this can affect directly the response of the microelectrode and its reproducibility in term of current value [34].

I.5. Electrodes fabrication procedures

There are multiple ways to manufacture or modify an electrode depending on the materials used, the suitable analytical requirements and economic opportunities. In general, the fabrication of any electrode type uses one of these three procedures, illustrated in the [Fig. I.5](#).

1. Paste mixing: In agate mortar with pestle, appropriate amounts of powder materials are mixed with or without a binder to obtain a homogeneous paste mixture that is introduced into the electrode cavity. This method is used in the fabrication of carbon paste electrode and cavity microelectrodes. The drawback of this method is the difficulty to know whether the materials are homogenous and the reducing of the paste materials conductivity, in the case of using the binder.

2. Drop casting: This method first requires mixing the materials in an adequate solvent at a concentration of 1 mg.mL^{-1} by ultrasonication, after stabilization of the suspension it is dripped onto the surface of the electrode body. It is then ready for use after the solvent has been vaporized. The disadvantage of this method is the thickness and the uniformity of coating film. The application of this method requires very high precision.

3. Screen-printing: This technique usually applied in the manufacture of screen-printed electrodes (SPE), represented in to be emerging portable tools ([Fig. I.4](#)). They consist of a chemically inert and non-conductive substrate (generally plastic supports) onto which screen-printing technology is applied to produce the necessary electrode for suitable analysis. The greatest benefice of this electrode kind that the three conventional electrodes are involved in the same miniaturized device, which has proved to be a compact transducer and portable apparatus with a fast response [\[59\]](#).

The following steps describe the fabrication of screen-printed electrodes:

- First, the solder paste is formed by mixing solder powder and flux into a paste with adhesiveness;
- Then, the solder paste is placed flat onto stencils and the opening holes of the stencil are aligned with the corresponding printed circuit board locations;
- Next, a squeegee is used to move horizontally on the stencil to apply the solder paste onto the printed circuit board via the stencil opening holes;
- Finally, the stencil is separated from the substrate, and an appropriate amount of the solder paste is applied onto the bonding pad [\[60\]](#).

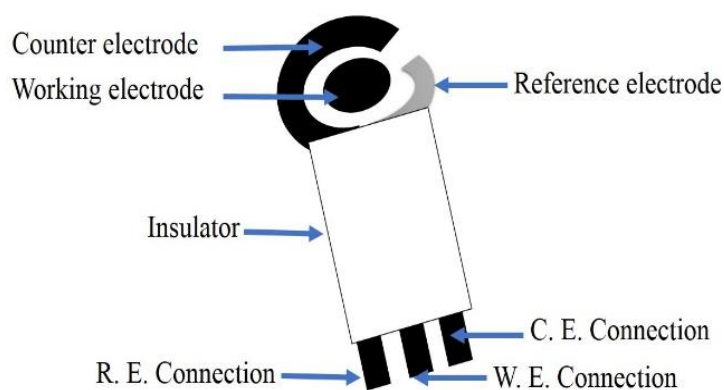


Figure I.4. Schematic representation of SPE

I.6. Modification of carbon paste electrode

The performance of an electrochemical sensor depends on the surface properties of the electrode and the type materials used in its conception. The modification of the electrode surface provides interesting properties with improved sensitivity and selectivity, which can lead to a specific detection and/or a pre-concentration of the analytes. The modified electrode is the best approach to achieve high charge transfer, improve the specific redox process, avoid electrode fouling and control electrochemical reaction rates [61].

Recently, the introduction of nanotechnology in the field of sensors has allowed the incorporation of nanomaterials into the electrode matrix in order to improve its performance. Several nanomaterials have been used in the fabrication of many sensors such as metal nanoparticles, metal oxide nanoparticles, polymers, molecular imprinted polymers, carbon nanomaterials and inorganic nanomaterials. The main advantages of using nanoparticle-modified electrodes are as follows:

- Enhancing of the electrochemically active surface area;
- Better accessibility of the analyte to the electrode surface;
- Increasing the charge transfer and acceleration the electrochemical reaction
- Improving the adsorption of targets on the electrode surface
- Catalytic effect of certain nanoparticles toward specific targets [62].

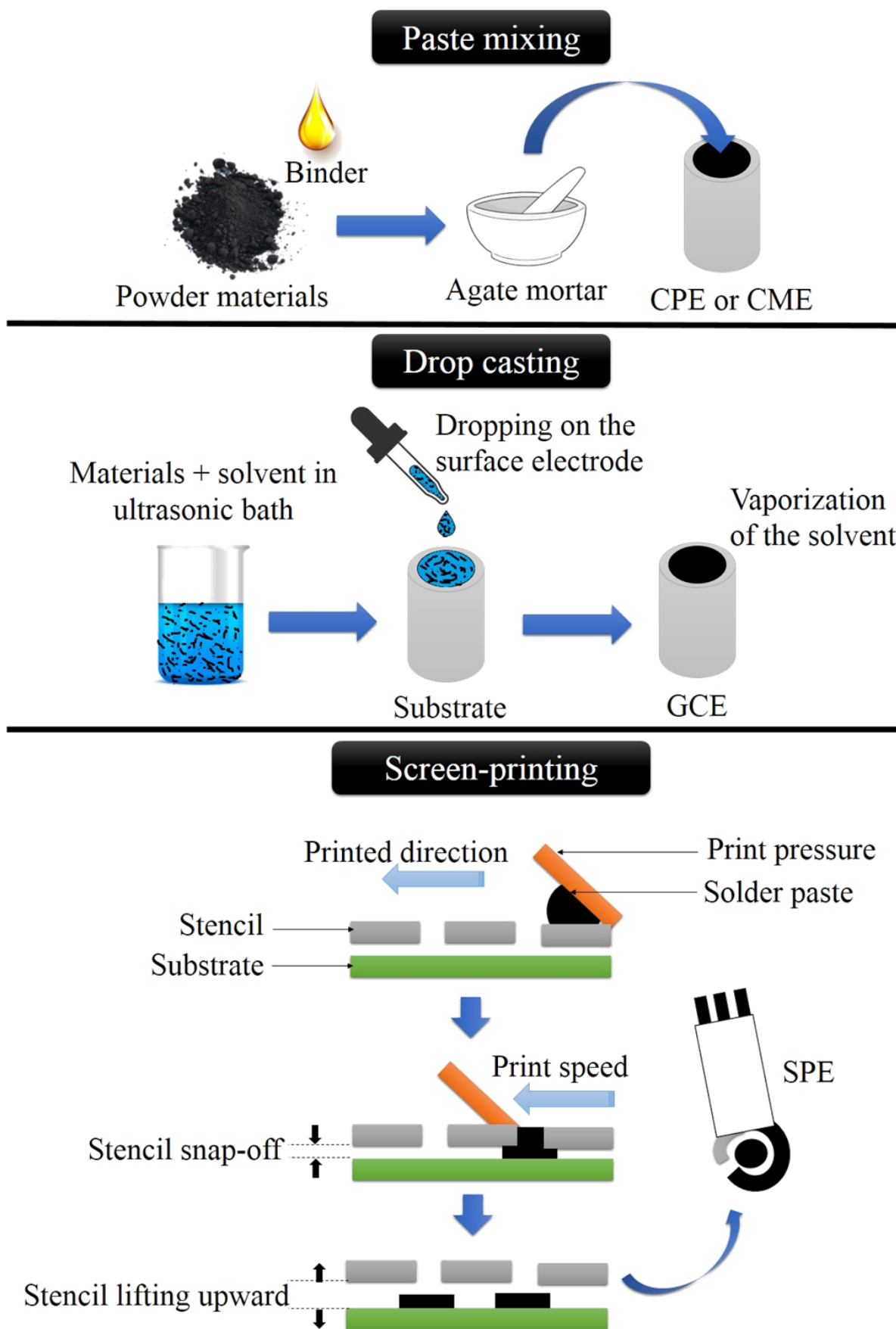


Figure I.5. The different procedures for manufacturing CMs based electrodes

I.7. Carbon nanomaterials for the electrochemical sensing

I.7.1. Introduction

In the recent years, researchers pay attention to the investigation of a new electrode materials with some specific characteristics, which offers suitable and performant sensor. Most of these characteristics required in the conception of an electrochemical device are a broader potential window, low background noise, mechanical stability, and possibility of the in situ analysis with resistance toward passivation [63]. In this context, it appears that carbon nanomaterials have attracted a lot of attention due to their outstanding structural, physiochemical and electrochemical properties that make them potential candidates for electrochemical applications, in particular sensing [64]. So, what are carbon nanomaterials? What are their proprieties? Why they are received these attention?

In the following section, we will present a review of recent carbon nanomaterials used in the design and construction of electrochemical sensors. We will discuss their specific properties, the general procedure of their pretreatments with a brief overview of the proposed sensor platforms based on carbon nanomaterials reported in recent years.

I.7.2. What are carbon nanomaterials (CMs)?

Carbon, as one of the most abundant elements in the earth, is capable to form a wide range of allotropes due to its ability to undergo single, double and triple covalent bonds with each other or with other elements, expressed by the sp , sp^2 and sp^3 hybridization states, respectively [64]. Furthermore, carbon atoms can undergo polarization and form a long chain of atoms. Due to the previous abilities, carbon can possess different physical structures with distinct physical properties despite of the same chemical composition [65]. With the emergence of nanotechnology, carbon nanomaterials have been the subject of intense investigation with a broad range of structures from zero to three dimensional (D) structures (Fig. I.6). In general, carbon nanomaterials are materials with a carbon size smaller than 100 nm, with a high surface area per unit weight, which have remarkable electronic, optical, mechanical, chemical and thermal properties. CMs have already been applied in various fields such as electronics, foods, cosmetics, electronics, drug development and sensing devices [66].

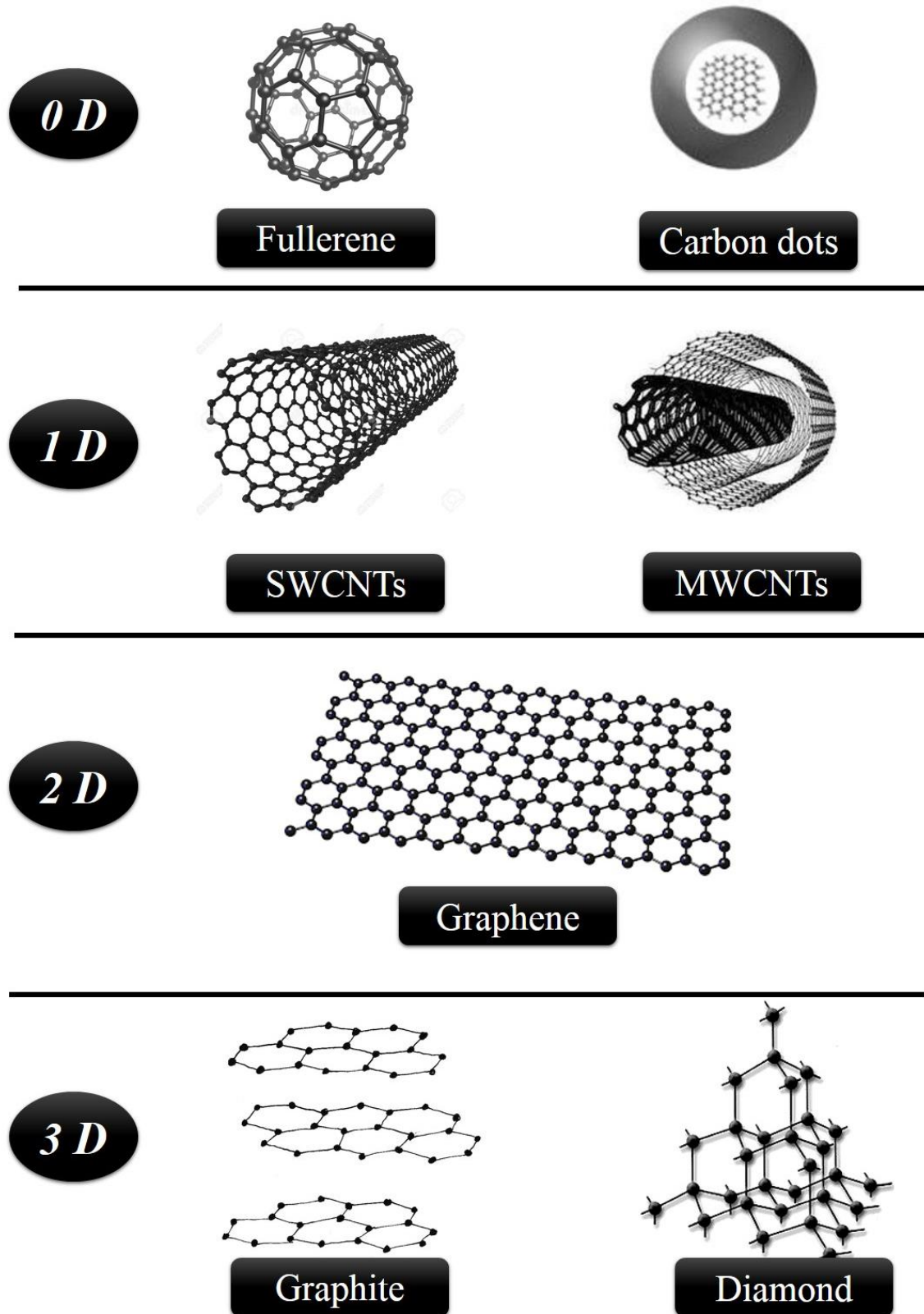


Figure I.6. The different dimensional carbon nanomaterials

I.7.3. What are CMs proprieties and advantages?

Carbon nanomaterials possess several proprieties that can depend highly on their structuration (atom arrangement, bonds, hybridation, dimension, etc.). However, CMs present generally the following proprieties:

- high surface area;
- high porosity;
- excellent electrical conductivity;
- electrocatalytic activity;
- adsorption capability;
- wide potential range;
- chemical inertness;
- Optical inertness;
- non-toxicity;
- biocompatibility;
- simple;
- economical;
- long-term stability;
- good electrochemical activity for a wide range of compounds;
- Ecofriendliness.

Among all these diverse properties, CM has a special place in the field of electrochemistry and has found applications in several areas of bioimaging, nanomedicine, photo/electro-catalysis, and bio/chemical sensing [8, 63].

I.7.4. Why CMs are received a great attention?

Several nanomaterials have been used in the electrochemical sensing, including magnetic (possessing a core of Fe_3O_4), metallic (Ag, Au, Pd are often used) and polymeric nanoparticles modifier materials that have intrinsic properties, which contribute to their use in specific applications. However, the most of them have some drawbacks that limit their uses, such as the availability, expansiveness, stability, complicated synthesis procedure and limited application fields [16, 66]. The comparison of the mentioned sensing nanomaterials with carbon nanomaterials is provided in Table I.1. Carbon nanomaterials possess many advantages over other nanomaterials mentioned. They are cheap alternatives with varied properties and good electrochemical activity for a wide range of compounds after suitable functionalization methods, which enhance their electrochemical sensing capabilities. In addition, the CMs can act simultaneously as adsorbent agents and transducer platforms [10, 67]. Thus, CMs have attracted considerable attention for their use as electrodes modifier with appropriate characteristics and are considered indispensable in electrochemistry and electroanalysis.

Table I.1. Comparison of sensing materials used in chemical sensors.

<i>Modifier</i>	<i>Carbon nanomaterials</i>	<i>Metallic nanomaterials</i>	<i>Polymeric nanomaterials</i>
<i>Characteristics</i>			
<i>Conductivity</i>	Very good	Good	Poor
<i>Surface area</i>	Very high	High	Poor
<i>Electrocatalytic activity</i>	Poor	Very high	Medium
<i>adsorption capability</i>	Very high	Medium	Poor
<i>Inertness</i>	Inert	Inert	Inert
<i>Toxicity</i>	Non toxic	Toxic	Toxic
<i>Stability</i>	Very good	Poor	Very poor
<i>Sensitivity</i>	High	High to some specific analytes	High to humidity
<i>Selectivity</i>	Good after nanostructuration	Good for specific analytes	Good
<i>Cost</i>	Low cost	Cost effective	Cost effective
<i>Preparation</i>	Simple	Difficult	Very difficult

I.7.5. Different carbon nanomaterials using in electrochemical sensing

a. Graphite

Graphite a black, greasy, electrically conductive substance, is a form of coal and a crystalline allotrope of carbon, considered one of the pure forms of carbon and one of the most versatile non-metallic minerals [68, 69]. Graphite consists of layers of graphene sheets (2D), which are bound with each other by non-covalent Van Der Waals forces to form a three dimensional network [70, 71]. Graphite has not only a specific structure, but also characteristics which differentiate it from others carbon materials. It is the most thermodynamically stable form of carbon under standard conditions. It has a free electron that moves along the planar layers making this material highly conducting [69]. This delocalized electron can absorb all the radiation in the optical region and thus gives a black appearance to this material [72]. Graphite is chemically inert and known to have properties of both metals and non-metals [73], usefully used as basic electrode material in several electrodes arrays. For example, graphite has been used in the conception of a $\text{Sb}_2\text{O}_3/\text{MWCNTs}$ modified CPE for the simultaneous electrochemical detection of cadmium and lead ions with a high sensitivity [74].

On the other hand, since a being long time, graphite has been well known in the production of pencils, prepared by mixing natural graphite (~65 %), clay (~30 %) with organic binder. It is widely used by everyone on a daily basis for writing purposes. In recent years and since 1997,

pencil graphite has been identified as a cheap, available and renewable electrode material, currently named pencil graphite electrodes (PGEs) [75]. PGEs have gained considerable attention due to their numerous features such as low cost, high sensitivity, superior stability, good conductivity and ease of preparation and modification. In addition, the most important benefits of PGEs compared to other electrodes employed are their availability, renewable surface area, strong adsorption properties, lower background currents and wide potential window [76, 77]. Pencil graphite electrodes have often been used as voltammetric sensors in order to quantify a variety of analytes with good signal reproducibility, well defined voltammetric peaks and excellent sensitivity [78]. Research using this advantageous tool includes the work of Purushothama H. T. et al., [76], in the development of a selective, simple and sensitive electrochemical sensor using pencil graphite electrode for the detection of chlorpromazine (CPZ) in a pharmaceutical sample. PGE showed a well high peak current and a good electrocatalytic activity towards the determination of CPZ with a simpler and less time consuming method [76]. In another investigation, a treated PGE was previously used as an electrochemical sensor for the determination of paracetamol in the presence of ascorbic acid and caffeine. The prepared electrode offered benefits such as low cost, disposability, abundance, ease of manufacture and reduced analysis time [79].

b. Diamond

Diamond, a three dimensional crystalline carbon material with a cubic structure, is the hardest known transparent mineral. The absence of a free electron in its chemical structure leads to many extreme proprieties making the diamond an excellent electrical insulator with very high thermal conductivity and extremely high electrical resistivity with a very wide band gap semiconductor, which makes diamond at first sight useless in electrochemistry fields [80].

However, doping impurities can be introduced into diamond in order to enhance its conductivity and electron-transfer reactivity. This insertion is achieved by p-type doping, which consist to incorporate Boron as a charge acceptor into diamond. Thus, boron-doped diamonds (BDD) decrease the resistivity of a diamond and allow the possibility to use BDD as electrode materials for various electrochemical applications [81]. Boron-doped diamond electrodes (BDDEs) present several notable features such as mechanical robustness, reduced fouling, high stability, large electrochemical potential window, low and stable background current resulting in higher sensitivity and improved detection limits. BDDEs are suitable electrode tools for many applications including electrochemistry, analytical chemistry, electrocatalysis, biomedical or

biological science, and other related trends [82]. For instance, BDDEs were used in the development of a simple and accurate methodology for the analysis of a carbamate pesticide (formetanate) in fruits. The attained data showed satisfactory linearity, lower limits of detection and quantification as well as good sensitivity, repeatability, reproducibility and accuracy [83]. Recently, an overview has been reported on the recent developments and advances of boron-doped diamond electrodes as electrochemical drug sensors. It provides a presentation of the electrochemical properties of the BDD film electrode, its fundamental research, electrochemical pretreatment process and summarizes the available data in the field of drug electro-sensing between 2015 and 2020 [84].

c. Graphene

Graphene, a two dimensional hexagonal lattice form, is a single atomic layer of graphite. It presents the same intrinsic physicochemical characteristics as graphite and CNTs, with higher specific surface area, multiple functional site, fast electron transfer and unparalleled electrical conductivity [85]. However, the major problem encountered with the use of graphene is its low dispersion in aqueous media; it has a low throughput and hydrophobicity. A problem that can be solved by modifying its surface by hydrophilic functional groups and achieving to extraordinary electrical conductivity and easy adsorption of targets [86]. Graphene has received considerable attention in various areas of electrochemical sensing platforms. Graphene-based electrochemical sensors have been widely reported and many reviews have been published for this purpose [87-91].

d. Carbon nanotubes (CNTs)

Carbon nanotubes, a one-dimensional crystal lattice, are cylindrical/tubular structures formed by graphene sheets rolled up into cylindrical shapes. Based on the number of the consist layers structure, CNTs can be divide in two types: SWCNTs which are consist of only a one single layer and MWCNTs which are made up of multiple layers. Generally, SWCNTs have a diameter around 1–3 nm and a length of few micrometers whereas MWCNTs have a diameter of 5–25 nm and a length around 10 μm . CNTs have excellent optical, mechanical, electrical and thermal properties. Exceptionally, they are characterized by high stability, large surface area, good conductivity, small size and easy functionalization [65]. These distinguished properties have driven researchers to explore CNTs in sensing methodologies. In this context, several papers have reported the use of CNTs in the modification of electrodes and have proven their

excellent adsorbing properties of various metal ions [92]. For example, Wu W. et al. [93] constructed an electrochemical sensor base on a composite of Fe_3O_4 and MWCNTs for simultaneous detection of several heavy metals. The developed method proved the increase in current intensity in the presence of MWCNTs, which considerably improve the sensitivity and exhibits excellent performances [93]. In another concept, CNTs have also been used in the manufacture of electrochemical device for the monitoring of pharmaceuticals and clinical medicine. A sensitive sensing platform was developed for the analysis of acetaminophen using platinum and MWCNTs modified glassy carbon electrode. The modified electrode showed a good linear response over a range from 0.5 to 100 mM acetaminophen concentration with a detection limit of 0.13 μM [94].

e. Fullerenes

Fullerene (C_{60}), a zero dimensional carbon allotropes, was discovered in 1985 by Kroto and his team [95]. It can be derived from stitching together a segment of graphene into a spherical shape or by a formation of clusters of carbon atoms greater than 20 atoms [65, 86]. Fullerene has a high electroactive surface area, good electronic conductivity, high chemical stability, have multiple redox states and the ability to accept and transport easily electrons, leading to the possibility of functionalization, signal mediation and others remarkable characteristics [96-98]. In recent years and with the emergence of nanotechnology, scientists are focusing on arranging atoms and molecules into different shapes and patterns by self-assembly in order to recognize their properties. In this context, novel various form of fullerene have been investigated such as fullerene nanowhiskers (C_{60}NWs), fullerene nanofibers (FNFs) and fullerene nanotubes (FNTs). The FNFs are thin fibers made up of C_{60} , C_{70} , endohedral fullerenes, or other functionalized fullerene molecules. They can have single crystalline, polycrystalline, amorphous or polymer structures. C_{60}NWs are the crystalline FNFs and are usually single crystalline. However, FNTs are fullerenes that grow spontaneously in the form of tubes with a single crystalline, polycrystalline or amorphous structures [99, 100]. Fullerene received enormous attention from physicists, chemists and material designers due to its unique nanostructure, remarkable electrochemical, electrocatalysis and photocatalysis properties, which have enabled their use in a variety of fields [65]. The applications of fullerene in electrochemical sensors have recently been explored in the determination of different analytes. For instance, Zhu and al [101] constructed a selective electrochemical sensor based on platinum nanoparticles and fullerene composite for the determination of catechol and hydroquinone. For example, Zhu and his team [101] constructed a selective electrochemical sensor based on

platinum nanoparticles and a fullerene composite for the determination of catechol and hydroquinone. The modified electrode exhibited excellent distinguishing capacity for the oxidation of these two phenolic compounds isomers, showed a strong oxidation current and improved catalytic activity [101]. Furthermore, a modified electrode using C₆₀-functionalized CNTs and ionic liquid was applied for the quantitative detection of diazepam in serum, urine, and tablets. The results indicate that C₆₀ deposited onto CNTs could effectively increase the electron transfer rate between electrode surface and the target due to the good conductivity of the composite allowed a higher electrocatalytic current over a large concentration linear range from 0.3 to 700 μ M with a low LOD of 87 nM [102].

f. Carbon dots (CDs)

Carbon dots are zero dimensional fluorescent carbon nanomaterials, consisted of carbon atoms with a size below 10 nm. They accidentally discovered in 2004 by Xu et al during purification of single-walled carbon nanotubes [103]. CDs are classified into 03 categories (Fig. I.7) according to the type of carbon material used in their fabrication, the procedure followed and their different formation mechanisms:

- Graphene quantum dots (GQDs), exhibit mini smithereens of graphite or graphene structures attached to multiple functional groups (e.g., amino, hydroxyl, carboxyl) on the surface/edge or inside the interlayer defect. Usually synthesized by “top-down” methods that are consisted on cutting graphite or graphene materials into small pieces. The lateral dimensions of GQDs are greater than their height, making them anisotropic;
- Carbon quantum dots (CQDs) possess multiple-layer graphite structures connected to surface groups. Their photoluminescence mechanism is presented by the intrinsic state luminescence and the quantum size confinement effect;
- Carbonized polymer dots (CPDs) represent aggregated/cross-linked and carbonized polymer hybrid nanostructures. They have unique “core shell” nanostructures which are made up of carbon cores less than 20 nm in diameter with strongly dehydrated cross-linking polymer frames or slight graphitization, and shells made up of functional groups and polymer chains in abundance.

CQDs and CPDs are usually spherical and are created by combining, polymerizing, cross-linking, and carbonizing small molecules, polymers, or biomass using "bottom-up" methods (e.g., combustion, thermal treatment) [104].

Generally, carbon dots have several distinct merits owing to their appreciable properties such as small size, strong absorption, bright photoluminescence, excellent photostability, good biocompatibility, low toxicity, chemical inertness, green and simple synthesis, providing important applications in various fields including biomedicine, catalysis and optoelectronic devices [105]. Moreover, due to these desirable properties, they have been used as CMs based electrochemical sensors. For example, GQDs were incorporated in MWCNTs for the development of a rapid, simple, and sensitive voltammetric sensor for the dopamine detection with low LOD (95 nM) and large linear range 0.25-250 μM [106]. The role of CQDs in increasing the kinetic of electrochemical reaction with improving the sensitivity and electrical conductivity of electrodes was provide in the work reported by C. Ramalechume et al. [107] on the development of a glassy carbon electrode modified with CQDs doped with metal oxides as Bismuth oxide for the electrochemical detection of heavy metal ions [107]. In another work, Won H. J. et al. [108] developed a novel wireless electrochemical biosensor based on polymer dot-manganese oxide complexes (PD/MnO₂) for the detection of cancer cells on a coated surface. The proposed sensor provided not only a fluorescence-based approach but also an electrochemical response with low limit of detection, high sensitivity and real time cancer detection directly using a smart phone [108].

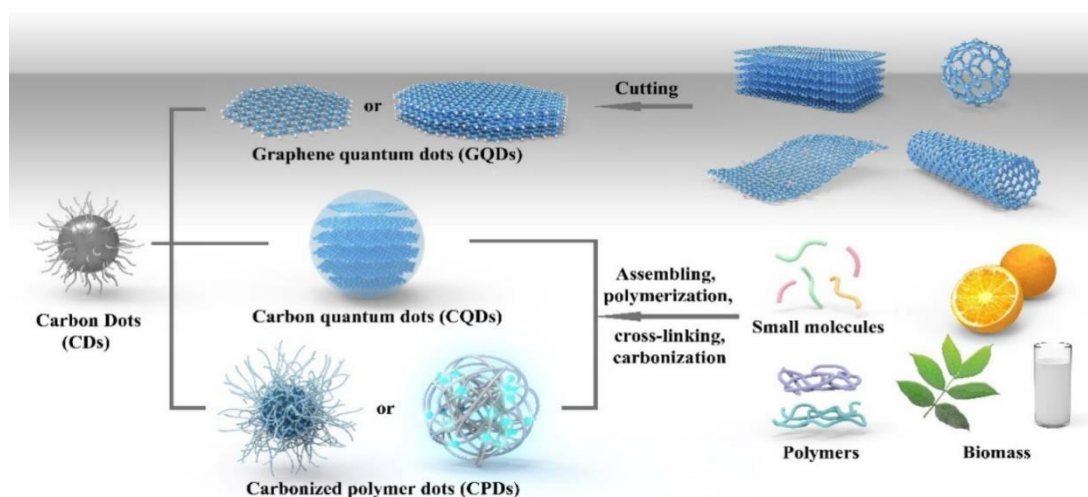


Figure I.7. Classification of CDs and their main preparation approaches [104]

g. Carbon black (CB)

Carbon black is an amorphous three-dimensional form of carbon, which is composed of spherical carbon particles strongly bonded together by covalent bonds to form aggregates with a distinctly long dimension that can form agglomerates (Fig. I.8) [109]. Their surface has usually oxygen and hydrogen group functions, depending on the conditions of manufacture [110]. It is produced from the combustion or thermal decomposition of petroleum products [111]. CB has a large specific surface area, high conductivity, strong chemical stability, a large pore size, and a high number of defective sites, making it capable to attach molecules on their surface and ideal for electrochemical applications [112]. It has been widely used for different applications either for polymers reinforcement [113], catalysis [114], enzyme immobilization [115]. Recently, it has become an attractive candidate for the development of electrochemical sensors and biosensors, due to its high electroactive surface area and rapid charge transfer, comparable to carbon nanotubes and graphene [116]. According to recent research, modified electrodes based only on nanostructured CB was employed for the simultaneous electrochemical determination of Pb (II) and Cd (II) traces. The CB-modified electrode has special pore structures with remarkable surface chemical functional groups, endow CB excellent catalytic and adsorption properties [117]. In another work, an eco-friendly electrochemical sensor based on carbon black (CB) and gold sononanoparticles was developed for bisphenol A detection, it showed high surface area that lead to a higher electroactivity, with a higher sensitivity, and a rather low limit of detection [118, 119].

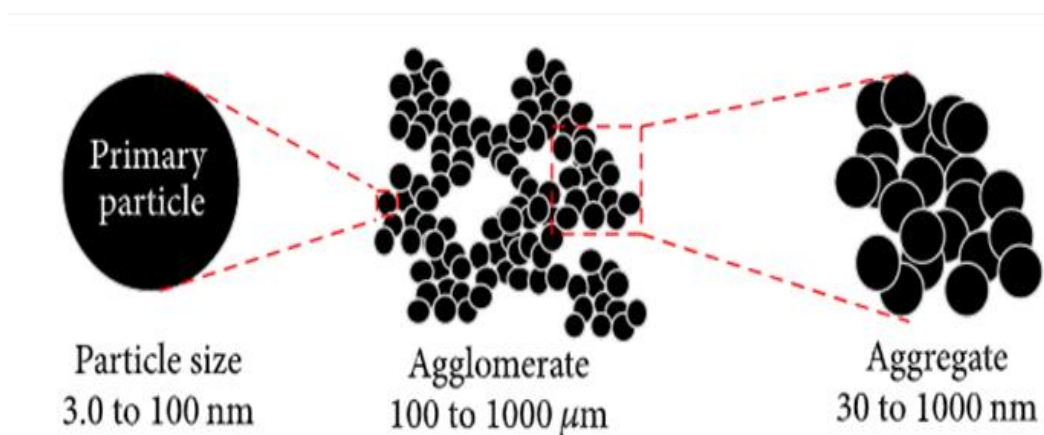


Figure I.8. Schematic representation of CB morphology [116].

Conclusion

Based on the literature review, amperometric sensors were selected for the conception of the developed electrodes owing to their unique characteristics that allow to multiple advantages among them the possibility of modification for specific analysis of a various target species with a good selectivity, accuracy, low detection limits for on-site analysis in the environment, human body, food and industry controls.

Moreover, we have chosen to manufacture our electrodes from carbon nanomaterials (graphite, activated carbon, carbon black, fullerene and MWCNTs) owing to their availability, inexpensiveness, ecofriendliness and as well as their various properties and good electrochemical activity for a wide range of compounds.

In our study, we chose to work with two kinds of working electrodes: carbon paste electrode (CPE) and cavity microelectrode (CME). This choice was based on their several advantages. The CPE was chosen for its simplicity, easy of use, low background current and large potential window. It was used in the *Chapter III* for the elaboration of a sensor, in the framework of quality control, for the quantitative analysis of vanillin as additive in commercial products.

Therefore, in the framework of environmental monitoring and health diagnostics, our choice was directed to discover CME in the electrochemical sensing. This device was recently introduced in the field of electrochemical sensing and was selected, in this study, in order to have a very miniaturized tool that requires only small amounts of materials and allow to lower detection limit, higher sensitivity and faster response. This sensor has the advantage to incorporate in the microcavity materials of micro and nano seize without binder addition and to present a 3 D structured electrode surface. Moreover, the small seize of the microcavity diameter provides the proprieties of the microelectrode, such as a stationary disfusion which established quickly, a high flow of electroactive species, a low current in the nanoampere range allowed measurements in poorly conductive media. *Chapter IV* presents the use of this microelectrode in the conception of micro-sensor for the simultaneous analysis of three pharmaceuticals products (ciprofloxacin, paracetamol and 4-aminophenol) in urine samples. *Chapter V* demonstrates the performance of the electrochemical preconcentration of paracetamol on modified CME in the traces analysis of this target in environmental water monitoring. The choice of the analytes studied will be shown in the followings chapters.

References

- [1] Bhattacharyya, B. (2015). Chapter 2 - Electrochemical Machining: Macro to Micro, Editor(s): Bhattacharyya, B. In Micro and Nano Technologies, Electrochemical Micromachining for Nanofabrication, MEMS and Nanotechnology, *William Andrew Publishing*, 25.
- [2] Zhu, C., Yang, G., Li, H., Du, D., & Lin, Y. (2014). Electrochemical Sensors and Biosensors Based on Nanomaterials and Nanostructures. *Analytical Chemistry*, 87(1), 230.
- [3] Beitollahi, H., Mohammadi, S. Z., Safaei, M., & Tajik, S. (2020). Applications of electrochemical sensors and biosensors based on modified screen-printed electrodes: A review. *Analytical Methods*, 12, 1547.
- [4] Raj, M. A. & John, S. A. (2019). Chapter 1 - Graphene-Modified Electrochemical Sensors, Editor(s): Pandikumar, A. & Rameshkumar, P. in Micro and Nano Technologies, Graphene-Based Electrochemical Sensors for Biomolecules, *Elsevier*, 2019, 1.
- [5] Abdul, S., Judit, T., Ilona, F. & Nikoletta, M. (2018). Chapter 16 - Functional thin films and nanostructures for sensors, Editor(s): Barhoum, A., Salam, A. & Makhoul, H. In Micro and Nano Technologies, Fundamentals of Nanoparticles, *Elsevier*, 485.
- [6] Gründler, P. (2017). Chemical sensors, *ChemTexts* 3, 16.
- [7] Zhu, X. & Shi, L. (2019). Chapter 9 - Electrochemistry, Editor(s): Li G., Nano-Inspired Biosensors for Protein Assay with Clinical Applications, *Elsevier*, 209.
- [8] Braiek, M., Djebbi, M. A., Chateaux, J.-F. & Jaffrezic-Renault, N. (2016). A conductometric sensor for potassium detection in whole blood, *Sensors and Actuators B: Chemical*, 235, 27.
- [9] Jamnani, S. R., Moghaddam, H. M., Leonardi, S.G. & Neri, G. (2018). A novel conductometric sensor based on hierarchical self-assembly nanoparticles Sm_2O_3 for VOCs monitoring, *Ceramics International*, 44 (14), 16953.
- [10] Xu, F., Zhou, C. & Ho, H.-P. (2021). A rule for operation temperature selection of a conductometric VOC gas sensor based on ZnO nanotetrapods, *Journal of Alloys and Compounds*, 858, 158294.
- [11] Latif, U. & Dickert, F. L. (2011). Conductometric sensors for monitoring degradation of automotive engine oil, *Sensors*, 11(9), 8611.
- [12] Bi, H. and X. (2019). 10 - Chemical sensors for environmental pollutant determination, Editor(s): Mitsubayashi, K., Niwa, O. & Ueno, Y. Chemical, Gas, and Biosensors for Internet of Things and Related Applications, *Elsevier*, 147.

- [13] Simões, F.R. & Xavier, M.G. (2017). 6 - Electrochemical Sensors, Editor(s): Da Róz, A.L., Ferreira, M., de Lima Leite, F. & Oliveira, O.N. In Micro and Nano Technologies, Nanoscience and its Applications, *William Andrew Publishing*, 155.
- [14] Özbek, O., Berkel, C. & Isildak, Ö. (2020). Applications of Potentiometric Sensors for the Determination of Drug Molecules in Biological Samples, *Critical Reviews in Analytical Chemistry*, 1.
- [15] Cosio, M.S., Scampicchio, M. & Benedetti, S. (2012). Chapter 8 - Electronic Noses and Tongues, Editor(s): Picó, Y. *Chemical Analysis of Food: Techniques and Applications, Academic Press*, 219.
- [16] Itagaki, Y., Mori, M. & Sadaoka, Y. (2018). EMF response of the YSZ based potentiometric sensors in VOC contaminated air, *Current Opinion in Electrochemistry*, 11, 72.
- [17] Brainina, K. Z., Ivanova, A. V., Sharafutdinova, E. N. & Saraeva, S. Y. (2007). Procedure 40 Potentiometric determination of antioxidant activity of food and herbal extracts, Editor(s): Alegret, S. & Merkoçi, A. *Comprehensive Analytical Chemistry, Elsevier*, 49, e277.
- [18] Ding, J. & Qin, W. (2020). Recent advances in potentiometric biosensors, *Trends in Analytical Chemistry*, 124, 115803.
- [19] Luka, G., Ahmadi, A., Najjaran, H., Alocilja, E., DeRosa, M., Wolthers, K., Malki, A., Aziz, H., Althani, A. & Hoorfar, M. (2015). Microfluidics Integrated Biosensors: A Leading Technology towards Lab-on-a-Chip and Sensing Applications. *Sensors*, 15(12), 30011.
- [20] Ensafi, A. A. (2019). Chapter 1 - An introduction to sensors and biosensors, Editor(s): Ensafi, A. A. *Electrochemical Biosensors, Elsevier*, 1.
- [21] Adams, R. N. (1958). Carbon paste electrodes, *Analytical Chemistry*, 30, 1576.
- [22] Olson, C. & Adams, R. N. (1960). Carbon paste electrodes: Application to anodic voltammetry, *Analytical Chemistry*, 22, 582.
- [23] Olson, C. & Adams, R. N. (1963). Carbon paste electrodes: Application to cathodic reductions and anodic stripping voltammetry, *Analytical Chemistry*, 29, 358-363.
- [24] Jacobs, E.S. (1963). Anodic stripping voltammetry of gold and silver with carbon paste electrodes. *Analytical Chemistry*, 35, 2112.
- [25] Karimi, F., Fallah-Shojaei, A., Tabatabaeian, K. & Shakeri, S. (2017). CoFe₂O₄ nanoparticle/ionic liquid modified carbon paste electrode as an amplified sensor for epirubicin analysis as an anticancer drug. *Journal of Molecular Liquids*, 242, 685.

- [26] Fekry, A.M. (2017). A new simple electrochemical moxifloxacin Hydrochloride sensor built on carbon paste modified with silver nanoparticles. *Biosens Bioelectron*, 87, 1065.
- [27] Ganesh, P.S., Swamy, B.E.K. & Harisha, K.V. (2017). Electropolymerisation of DL-methionine at carbon paste electrode and its application to the determination of catechol and hydroquinone. *Analytical and Bioanalytical Electrochemistry*, 9, 74.
- [28] Gheibi, S., Gharibi, G., Khalilzadeh, M.A. & Pourfarzad, A. (2017). Electrochemical analysis of ascorbic acid in food and drug samples using a biosynthesized Ag nanoparticle as a mediator in carbon paste matrix. *Analytical Bioanalytical Electrochemistry*, 9, 365.
- [29] Švancara, I., Vytřas, K., Barek, J. & Zima, J. (2001). Carbon Paste Electrodes in Modern Electroanalysis, *Critical Reviews in Analytical Chemistry*, 3(4), 311.
- [30] Švancara, I., Walcarius, A., Kalcher, K. & Vytřas, K. (2009). Carbon paste electrodes in the new millennium. *Central European Journal of Chemistry*, 7, 598.
- [31] Karimi-Maleh, H., Karimi, F., Rezapour, M., Bijad, M., Farsi, M., Beheshti A. & Shahidi, S.-A. (2019). Carbon Paste Modified Electrode as Powerful Sensor Approach Determination of Food Contaminants, Drug Ingredients, and Environmental Pollutants: A Review, *Current Analytical Chemistry*, 15, 410.
- [32] Bojdi, M. K., Behbahani, M., Omid F. & Hesam, G. (2016). Application of a novel electrochemical sensor based on modified siliceous mesocellular foam for electrochemical detection of ultra-trace amounts of mercury ions, *New Journal of Chemistry*, 40, 4519.
- [33] Canbay, E., Türkmen, H. & Akyilmaz, E. (2014). Ionic liquid modified carbon paste electrode and investigation of its electrocatalytic activity to hydrogen peroxide. *Bulletin of Materials Science*, 37, 617.
- [34] Cachet-Vivier, C., Keddah, M., Vivier, V. & Yu, L.T. (2013). Development of cavity microelectrode devices and their uses in various research fields, *Journal of Electroanalytical Chemistry*, 688, 12.
- [35] Cha, C.S., Li, C.M., Yang, H.X. & Liu, P.F. (1994). Powder microelectrodes, *Journal of Electroanalytical Chemistry*, 368, 47.
- [36] Cachet-Vivier, C., Vivier, V., Cha, C. S., Nedelec, J.-Y. & Yu, L. T. (2001). Electrochemistry of powder material studied by means of the cavity microelectrode (CME), *Electrochimica Acta*, 47, 181.
- [37] Vivier, V., Cachet-Vivier, C., Cha, C.S., Nedelec, J.-Y. & Yu, L.T. (2000). Cavity microelectrode for studying battery materials: application to polyaniline powder, *Electrochemistry Communications*, 2 (3), 180.

- [38] Vivier, V., Belair, S., Cachet-Vivier, C., Nedelec, J.-Y. & Yu, L.T. (2001). A rapid evaluation of vanadium oxide and manganese oxide as battery materials with a micro-electrochemistry technique, *Journal of Power Sources*, 103 (1), 61.
- [39] Merzouki, A., Cachet-Vivier, C., Vivier, V., Nédélec, J.-Y., Yu, L.T., Haddaoui, N., Joubert, J.-M. & Percheron-Guégan, A. (2002). Microelectrochemistry study of metal-hydride battery materials: Cycling behavior of $\text{LaNi}_{3.55}\text{Mn}_{0.4}\text{Al}_{0.3}\text{Co}_{0.75}$ compared with LaNi_5 and its mono-substituted derivatives, *Journal of Power Sources*, 109 (2), 281.
- [40] Vivier, V., Cachet-Vivier, C., Mezaille, S., Wu, B. L., Cha, C. S., Nedelec, J.-Y., Fedoroff, M., Michel, D. & Y, L. T. (2000). Electrochemical Study of Bi_2O_3 and $\text{Bi}_2\text{O}_2\text{CO}_3$ by Means of a Cavity Microelectrode. I. Observed Phenomena and Direct Analysis of Results, *Journal of the Electrochemical Society*, 147 (11), 4252.
- [41] Vivier, V., Régis, A., Sagon, G., Nedelec, J.-Y., Yu, L.T. & Cachet-Vivier, C. (2001). Cyclic voltammetry study of bismuth oxide Bi_2O_3 powder by means of a cavity microelectrode coupled with Raman microspectrometry, *Electrochimica Acta*, 46 (6), 907.
- [42] Guilminot, E., Corcella, A., Chatenet, M. & Maillard, F. (2007). Comparing the thin-film rotating disk electrode and the ultramicroelectrode with cavity techniques to study carbon-supported platinum for proton exchange membrane fuel cell applications, *Journal of Electroanalytical Chemistry*, 599 (1), 2007, 111.
- [43] Vertova, A., Barhdadi, R., Cachet-Vivier, C., Locatelli, C., Minguzzi, A., Nedelec, J.-Y. & Rondinini, S. (2008). Cavity microelectrodes for the voltammetric investigation of electrocatalysts: the electroreduction of volatile organic halides on micro-sized silver powders, *Journal of Applied Electrochemistry*, 38, 965.
- [44] Locatelli, C., Minguzzi, A., Vertova, A., Cava, P., & Rondinini, S. (2011). Quantitative studies on electrode material properties by means of the cavity microelectrode, *Analytical chemistry*, 83(7), 2819.
- [45] Cachet-Vivier, C., Tribollet, B. & Vivier, V. (2010). Cavity microelectrode for studying manganese dioxide powder as pH sensor, *Talanta*, 82 (2), 555.
- [46] Come, J., Taberna, P.-L., Hamelet, S., Masquelier C., & Simon, P. (2011). Electrochemical Kinetic Study of LiFePO_4 Using Cavity Microelectrode citation, *Journal of Electrochemical Society*, 158, A1090.
- [47] Wang, Y., Zheng, D., Yang, X.-Q. & Qu, D. (2011). High rate oxygen reduction in non-aqueous electrolytes with the addition of perfluorinated additives, *Energy & Environmental Science*, 4, 3697.

- [48] Sakai, T., Shironita, S., Inoue, M. & Umeda, M. (2011). Current-Potential Curves at Powder Catalyst-Packed Porous Microelectrode in the Presence of Both Methanol and Oxygen, *Electrochemistry*, 79, 349.
- [49] Benabdellah, A., Ilikti, H., Belarbi, H., Fettouhi, B., Ait, A.A. & Hatti, M. (2011). Effects of The Synthesis Temperature on Electrical Properties of Polyaniline and their Electrochemical Characteristics onto Silver Cavity Microelectrode Ag/C-EM, *International Journal of Electrochemical Science*, 6, 1747.
- [50] Bouazza, S., Alonzo, V. & Hauchard, D. (2009). Synthesis and characterization of Ag nanoparticles–polyaniline composite powder material, *Synthetic Metals*, 159, 1612.
- [51] Zhao, Y.-D., Zhang, W.-D., Chen, H. & Luo, Q.-M. (2002). Anodic oxidation of hydrazine at carbon nanotube powder microelectrode and its detection, *Talanta*, 58, 529.
- [52] Chen, J. & Cha, C.-S. (1999). Detection of dopamine in the presence of a large excess of ascorbic acid by using the powder microelectrode technique, *Journal of Electroanalytical Chemistry*, 463 (1), 93.
- [53] Fang, D.-J., Jiang, D.-C., Lu, H., Chiel, H.J., Kelley T. J. & Burgess, J.D. (2009). Observation of Cellular Cholesterol Efflux at Microcavity Electrodes, *Journal of the American Chemical Society*, 131, 12038.
- [54] Sun, W., Guo, C.X., Zhu, Z. & Li, C.M. (2009). Ionic liquid/mesoporous carbon/protein composite microelectrode and its biosensing application, *Electrochemistry Communication*, 11, 2105.
- [55] Chmayssem, A. & Hauchard, D. (2017). Direct ultra-trace detection of alkylphenols in water using a cavity carbon-paste microelectrode sensor, *Desalination and Water Treatment*, 1.
- [56] He, B.-S. & Zhang, J.-X. (2017). Rapid Detection of Ascorbic Acid Based on a Dual-Electrode Sensor System Using a Powder Microelectrode Embedded with Carboxyl Multi-Walled Carbon Nanotubes, *Sensors* 17 (7), 1549.
- [57] He, B.-S. & Zhang, J.-X. (2018). Powder microelectrode embedded with carboxyl multi-walled carbon nanotubes for sensitive and quantitative detection of nitrofurans residues, *Analytical Methods*, 10, 1372.
- [58] Vivier, V. & Mottin, S. (2009). Microélectrode à cavité: Principe, développement et applications pour l'étude de la réactivité de matériaux insolubles, *PU Saint-Etienne*, 15.
- [59] Felismina, T.C., Moreira, M. Judite, M.S., Ferreira, J.R.T., Puga, M. & Goreti F. S. (2016). Screen-printed electrode produced by printed-circuit board technology.

- Application to cancer biomarker detection by means of plastic antibody as sensing material, *Sensors and Actuators B: Chemical*, 223, 927.
- [60] Huang, C.-Y. (2018). Applying the Taguchi parametric design to optimize the solder paste printing process and the quality loss function to define the specifications, *Soldering & Surface Mount Technology*, 30 (4), 217.
- [61] Adarakatti, P.S. & Kempahanumakkagari, S.K. (2019). Modified electrodes for sensing, *Electrochemistry*, 15, 58.
- [62] Tonelli, D., Scavetta, E., & Gualandi, I. (2019). Electrochemical Deposition of Nanomaterials for Electrochemical Sensing, *Sensors*, 19 (5), 1186.
- [63] Tajik, S., Beitollahi, H., Garkani Nejad, F., Safaei, M., Zhang, K., Le, Q.V., Varma, R.S., Jang H.W. & Shokouhimehr, M. (2020). Developments and applications of nanomaterial-based carbon paste electrodes, *RCS Advances*, 10, 21561.
- [64] Asadian, E., Ghalkhani, M. & Shahrokhian, S. (2019). Electrochemical sensing based on carbon nanoparticles: A review, *Sensors and Actuators B: Chemical*, 293, 183.
- [65] Kour R., Arya, S., Young, S.-J., Gupta, V., Bandhoria, P. & Khosla A. (2020). Review—Recent Advances in Carbon Nanomaterials as Electrochemical Biosensors; *Journal of The Electrochemical Society*, 176 (3), 037555.
- [66] Săndulescu, R., Tertiș, M., Cristea, C. & Bodoki, E. (2015). New Materials for the Construction of Electrochemical Biosensors, *Biosensors- Micro and Nanoscale Applications*.
- [67] Yang, N., Swain, G.M. & Jiang, X. (2016). Nanocarbon Electrochemistry and Electroanalysis: Current Status and Future Perspectives, *Electroanalysis*, 28, 27.
- [68] Sattler, K. D. (2016). Carbon Nanomaterials Sourcebook Volume II: Nanoparticles, Nanocapsules, Nanofibers, Nanoporous Structures, and Nanocomposites, *CRC Press*.
- [69] Thakur, V. K. & Thakur, M. K. (2015). Chemical functionalization of carbon nanomaterials: Chemistry and applications. *CRC Press*.
- [70] Kharisov, B.I. & Kharissova, O.V. (2019). Carbon Allotropes: Metal-Complex Chemistry, Properties and Applications, *Springer International publishing, CRC Press*.
- [71] Hui, Y.Y., Chang, H.-C., Dong, H. & Zhang, X. (2019). Carbon Nanomaterials for Bioimaging, Bioanalysis, and Therapy, *Wiley*.
- [72] Mathur, R. B., Singh, B. P., & Pande, S. (2016). Carbon nanomaterials: synthesis, structure, properties and applications. *CRC Press*.

- [73] Nasir, S., Hussein, M. Z., Zainal, Z., & Yusof, N. A. (2018). Carbon-Based Nanomaterials/Allotropes: A Glimpse of Their Synthesis, Properties and Some Applications, *Materials*, 11(2), 295.
- [74] Hai, T.L. Hung, L.C., Phuong, T.T.B., Ha, B.T.T., Nguyen, B.-S., Hai, T.D. & Nguyen, V.-H. (2020). Multiwall carbon nanotube modified by antimony oxide ($\text{Sb}_2\text{O}_3/\text{MWCNTs}$) paste electrode for the simultaneous electrochemical detection of cadmium and lead ions, *Microchemical Journal*, 153, 104456.
- [75] Sharma, A.S., Jain, R., & Raja, A. N. (2020). Review—Pencil Graphite Electrode: An Emerging Sensing Material. *Journal of The Electrochemical Society*, 167(3), 037501.
- [76] Purushothama, H.T., Arthoba Nayaka, Y., Vinay, M.M., Manjunatha, P., Yathisha, R.O. & Basavarajappa, K.V. (2018). Pencil graphite electrode as an electrochemical sensor for the voltammetric determination of chlorpromazine, *Journal of Science: Advanced Materials and Devices*, 3 (2), 161.
- [77] Kawde, A.-N., Baig, N. & Sajid, M. (2016). Graphite pencil electrodes as electrochemical sensors for environmental analysis: a review of features, developments, and applications, *RSC Advances*, 6, 91325.
- [78] David, I.G., Popa, D.-E. & Buleandr, M. (2017). Pencil Graphite Electrodes: A Versatile Tool in Electroanalysis, *Journal of Analytical Methods in Chemistry*, 2017, 22.
- [79] Koyun, O., Gorduk, S., Arvas, M.B. & Sahin, Y. (2018). Electrochemically Treated Pencil Graphite Electrodes Prepared in One Step for the Electrochemical Determination of Paracetamol, *Russian Journal of Electrochemistry*, 54, 796.
- [80] Macpherson, J. V. (2015). A practical guide to using boron-doped diamond in electrochemical research, *Physical Chemistry Chemical Physics*, 17, 2935.
- [81] Muzyka, K., Sun, J., Fereja, T.H., Lan, Y., Zhang W. & Xu, G. (2019). Boron-doped diamond: current progress and challenges in view of electroanalytical applications, *Analytical Methods*, 11, 397.
- [82] Freitas, J. M., Oliveira, T., Munoz, R., & Richter, E. M. (2019). Boron Doped Diamond Electrodes in Flow-Based Systems, *Frontiers in chemistry*, 7, 190.
- [83] Ribeiro, F.W.P., Sousa, C.P., Morais, S., de Lima-Neto, P. & Correia, A.N. (2018). Sensing of formetanate pesticide in fruits with a boron-doped diamond electrode, *Microchemical Journal*, 142, 2018, 24.
- [84] Yence, M., Cetinkaya, A., Ozcelikay, G., Kaya, S. I. & Ozkan, S. A. (2021). Boron-Doped Diamond Electrodes: Recent Developments and Advances in View of Electrochemical Drug Sensors, *Critical Reviews in Analytical Chemistry*.

- [85] Tiwari, S.K., Sahoo, S., Wang, N. & Huczko, A. (2020). Graphene research and their outputs: Status and prospect, *Journal of Science: Advanced Materials and Devices*, 5, (1), 10.
- [86] Badenhorst, H. (2019). A review of the application of carbon materials in solar thermal energy storage, *Solar Energy*, 192, 35,
- [87] Yu, H., Guo, W., Lu, X., Xu, H., Yang, Q., Tana, J. & Zhang, W. (2021). Reduced graphene oxide nanocomposite based electrochemical biosensors for monitoring foodborne pathogenic bacteria: A review, *Food Control*, 127, 108117.
- [88] Raghavan, V.S., O'Driscoll B., Bloor, J.M., Li, B., Katare, P., Sethi, J., Gorthi, S.S. & Jenkins, D. (2021). Emerging graphene-based sensors for the detection of food adulterants and toxicants – A review, *Food Chemistry*, 355, 129547.
- [89] Liua, G., Xiong, Z., Yang, L., Shi, H., Fang, D., Wang, M., Shao, P. & Luo, X. (2021). Electrochemical approach toward reduced graphene oxide-based electrodes for environmental applications: A review, *Science of The Total Environment*, 778, 146301.
- [90] Baig, N., Waheed, A., Sajid, M., Khan, I., Kawde, A.-N. & Sohail, M. (2021). Porous graphene-based electrodes: Advances in electrochemical sensing of environmental contaminants, *Trends in Environmental Analytical Chemistry*, 30, e00120.
- [91] Hou, X., Xu, H., Zhen, T. & Wu, W. (2020). Recent developments in three-dimensional graphene-based electrochemical sensors for food analysis, *Trends in Food Science & Technology*, 105, 76.
- [92] Rasheed, T., Nabeel, F., Adeel, M., Rizwan, K., Bilal, M. & Iqbal, H.M.N. (2019). Carbon nanotubes-based cues: A pathway to future sensing and detection of hazardous pollutants, *Journal of Molecular Liquids*, 292, 111425.
- [93] Wu, W., Jia, M., Zhang, Z., Chen, X., Zhang, Q., Zhang, W., Li, P. & Chen, L. (2019). Sensitive, selective and simultaneous electrochemical detection of multiple heavy metals in environment and food using a low cost Fe₃O₄ nanoparticles/fluorinated multi-walled carbon nanotubes sensor, *Ecotoxicology and Environmental Safety*, 175, 243.
- [94] Wu, Y., Wu, Y., Lv, X., Lei, W., Ding, Y., Chen, C., Lv, J., Feng, S., Chen, S.-M. & Hao, Q. (2020). A sensitive sensing platform for acetaminophen based on palladium and multi-walled carbon nanotube composites and electrochemical detection mechanism, *Materials Chemistry and Physics*, 239, 121977.
- [95] Kroto, H. W. (1987). The stability of the fullerenes C_n, with n = 24, 28, 32, 36, 50, 60 and 70, *nature*, 329, 529.
- [96] Sherigara, B. S., Kutner, W. & Souza, F. D. (2003). Electrocatalytic Properties and Sensor Applications of Fullerenes and Carbon Nanotubes, *Electroanalysis*, 15 (9), 753.

- [97] Pan, Y., Liu, X., Zhang, W., Liu, Z., Zeng, G., Shao, B., Liang, Q., He, Q., Yuan, X., Huang, D. & Chen, M. (2020). Advances in photocatalysis based on fullerene C₆₀ and its derivatives: Properties, mechanism, synthesis, and applications, *Applied Catalysis B: Environmental*, 265, 118579.
- [98] Pilehvar, S. & Wael, K. D. (2015). Recent Advances in Electrochemical Biosensors Based on Fullerene-C60 Nano-Structured Platforms, *Biosensors*, 5 (4), 712.
- [99] Miyazawa K. (2009). Synthesis and properties of fullerene nanowhiskers and fullerene nanotubes. *Journal of nanoscience and nanotechnology*, 9 (1), 41.
- [100] Rao, R. V. K., Karthik, P. S., Abhinav, V. K., Lin, Z., Myint, M. T. Z., Nishikawa, T., Hada, M., Yamashita, Y., Hayashi, Y., & Singh, S. P. (2016). Self-assembled C60 fullerene cylindrical nanotubes by LLIP method. In *16th International Conference on Nanotechnology - IEEE NANO, Institute of Electrical and Electronics Engineers*, [7751386], 303.
- [101] Zhu, Y., Huai, S., Jiao, J., Xu, Q., Wu, H. & Zhang, H. (2020). Fullerene and platinum composite-based electrochemical sensor for the selective determination of catechol and hydroquinone, *Journal of Electroanalytical Chemistry*, 878, 114726.
- [102] Rahimi-Nasrabadi, M., Khoshroo, A. & Mazloum-Ardakani, M. (2017). Electrochemical determination of diazepam in real samples based on fullerene-functionalized carbon nanotubes/ionic liquid nanocomposite, *Sensors and Actuators B: Chemical*, 240, 125.
- [103] Sagbas, S. & Sahiner, N. (2019). 22 - Carbon dots: preparation, properties, and application, Editor(s): Khan, A., Jawaid, M., Inamuddin & Asiri, A.M. In Woodhead Publishing Series in Composites Science and Engineering, Nanocarbon and its Composites, Woodhead Publishing, 651.
- [104] Liu, J., Li, R. & Yang, B. (2020). Carbon Dots: A New Type of Carbon-Based Nanomaterial with Wide Applications, *ACS Central Science*, 6 (12), 2179.
- [105] Xia, C., Zhu, S., Feng, T., Yang, M. & Yang, B. (2019). Evolution and Synthesis of Carbon Dots: From Carbon Dots to Carbonized Polymer Dots, *Advanced Science*, 1901316.
- [106] Arumugasamy, S.K., Govindaraju, S. & Yun, K. (2020). Electrochemical sensor for detecting dopamine using graphene quantum dots incorporated with multiwall carbon nanotubes, *Applied Surface Science*, 508, 145294.
- [107] Ramalechume, C., Keerthana, S., Mercy, C. & Swamidoss, A. (2020). Electrochemical detection of heavy metals using carbon quantum dots modified with metal oxides, *Materials Today: Proceedings*.

- [108] Won, H.J., Robby, A., Jhon, H.S. Insik (2020). In, Ryu, J.H. & Park, S.Y. Wireless label-free electrochemical detection of cancer cells by MnO₂-Decorated polymer dots, *Sensors and Actuators B: Chemical*, 320, 128391.
- [109] Long, C.M., Nascarella, M.A. & Valberg, P.A. (2013). Carbon black vs. black carbon and other airborne materials containing elemental carbon: Physical and chemical distinctions, *Environmental Pollution*, 181, 271.
- [110] Wang, H., Xu, H., Jia, W. & Ren, S. (2018). Functionalized carbon black nanoparticles used for separation of emulsified oil from oily wastewater, *Journal of Dispersion Science and Technology*, 39 (4), 497.
- [111] Ibáñez-Redín, G., Silva, T.A., Vicentini, F.C. & Fatibello-Filho, O. (2018). Effect of carbon black functionalization on the analytical performance of a tyrosinase biosensor based on glassy carbon electrode modified with dihexadecylphosphate film, *Enzyme and Microbial Technology*, 116, 41.
- [112] Kutty, M., Settu, R., Chen, S.-M., Chen, T.-W., Tseng, T.-W., Hatamleh, A.A., Yu, J., Yu, R. & Huang, C.-C. (2019). An Electrochemical Detection of Vanillin Based on Carbon Black Nanoparticles Modified Screen Printed Carbon Electrode, *International Journal of Electrochemistry Science*, 14, 5972.
- [113] Naik, P., Pradhan, S., Sahoo, P. & Acharya, S.K. (2020). Effect of filler loading on mechanical properties of natural carbon black reinforced polymer composites, *Materials Today: Proceedings*, 26 (2), 1892.
- [114] Watanabe M. & Tryk D.A. (2019). The Role of Carbon Blacks as Catalyst Supports and Structural Elements in Polymer Electrolyte Fuel Cells. In: Nakashima N. Nanocarbons for Energy Conversion: Supramolecular Approaches. Nanostructure Science and Technology. Springer, Cham.
- [115] Nadifiyine, S., Haddam, M., Mandli, J., Chadel, S., Blanchard, C.C., Marty, J.L. & Amine, A. (2013). Amperometric Biosensor Based on Tyrosinase Immobilized on to a Carbon Black Paste Electrode for Phenol Determination in Olive Oil, *Analytical Letters*, 46(17), 2705.
- [116] Silva, T.A., Moraes, F.C., Janegitz, B.C. & Fatibello-Filho, O. (2017). Electrochemical Biosensors Based on Nanostructured Carbon Black: A Review, *Journal of Nanomaterials*, 2017, 14.
- [117] Xie, R., Zhou, L., Lan, C., Fan, F., Xie, R., Tan, H., Xie, T. & Zhao, L. (2018). Nanostructured carbon black for simultaneous electrochemical determination of trace lead and cadmium by differential pulse stripping voltammetry. *Royal Society open science*, 5, 180282.

- [118] Jebril, S., Cubillana-Aguilera, L., Palacios-Santander, J.M. & Dridi, C. (2021). A novel electrochemical sensor modified with green gold sononanoparticles and carbon black nanocomposite for bisphenol A detection, *Materials Science and Engineering: B*, 264, 114951.
- [119] Attar, A., Amine, A., Achi, F., Bourouina Bacha, S., Bourouina, M, Cubillana-Aguilera, L., Palacios-Santander, J.M., Baraket, A. & Errachid, A. (2016). A novel amperometric inhibition biosensor based on HRP and gold sononanoparticles immobilised onto Sonogel-Carbon electrode for the determination of sulphides. *International Journal of Environmental Analytical Chemistry*, 2016, 96 (6), 515.

Chapter II

Experimental section

Chapter II: Experimental section

This chapter brings details about chemical compounds, devices and electrochemical methods used to carry out the present work. The procedures for preparing the different electrodes as well as the actual samples for validation analysis are clearly described.

II.1. Chemical reagents

All chemical reagents used in this study are summarized in the [Table II.1](#).

Table II.1. List of chemicals

<i>Carbon materials</i>			
<i>Name</i>	<i>Characteristics</i>	<i>Purity (%)</i>	<i>Provider</i>
Graphite	4 μm	99.5	ProGraphite GmbH
Graphite	20 μm	Not mentioned	
Carbon black	Average 100 nm	Not mentioned	Vulcan XC-72 Cabot Corporation
Fullerenemulti-walled nanotubes	20 nm, 5- 20 μm	95	Fluka Chemika
Multi-walled carbon nanotubes	1.5 μm	90	GoodFellow (NC006090)
<i>Chemical target</i>			
<i>Name</i>	<i>Formula</i>	<i>Purity (%)</i>	<i>Provider</i>
Vanillin	$\text{C}_3\text{H}_8\text{O}_3$	98	Fluka Chemika
4-Aminophenol	$\text{C}_6\text{H}_7\text{NO}$	97	Acros Organics
Paracetamol	$\text{C}_8\text{H}_9\text{NO}_2$	98	Sigma-Aldrich
Ciprofloxacin	$\text{C}_{17}\text{H}_{18}\text{FN}_3\text{O}_3$	98	Acros Organics
<i>Electrolytes</i>			
<i>Name</i>	<i>Formula</i>	<i>Purity (%)</i>	<i>Provider</i>
Acetic acid	CH_3COOH	≥ 99	Fulka Chemika
Phosphoric acid	H_3PO_4	85	Acros Organics
Boric acid	H_3BO_3	99.5	Acros Organics
Sodium hydroxide	NaOH	≥ 98	Sigma-Aldrich
<i>Modification of carbon materials</i>			
<i>Name</i>	<i>Formula</i>	<i>Purity (%)</i>	<i>Provider</i>
Nitric acid	HNO_3	70	Sigma-Aldrich
Sulfuric acid	H_2SO_4	98	Sigma-Aldrich
Hydrochloric acid	HCl	37	Sigma-Aldrich
<i>Others chemicals</i>			
<i>Name</i>	<i>Formula</i>	<i>Purity (%)</i>	<i>Provider</i>
Paraffin oil	Not mentioned		Fulka Chemika
Potassium hexacyanoferrate (III)	$\text{C}_6\text{N}_6\text{FeK}_3$	≥ 99	Sigma-Aldrich

II.2. Electrochemical apparatus

Electrochemical experiments were performed using a PGSTAT20 Metrohm Autolab electrochemical analyzer (Netherlands), connected to a computer using NOVA 2.1.2 software to control the analysis and data processing. This potentiostat / galvanostat was connected to a conventional electrochemical cell containing three electrodes:

- Reference electrode (RE): Ag/AgCl (3 M KCl) electrode, which is used as a point of reference for potential control and measurements, it has a stable and defined potential;
- Auxiliary (or counter) electrode (CE): Platinum wire electrode, an inert electrode, which is used to close the current circuit in an electrochemical cell;
- Working electrode (WE): In the present work two types of modified electrodes have been used as working electrode; carbon paste electrode and cavity microelectrode.

More details will be given in the [sections II.6](#).

All measurements were carried out at room temperature inside the Faraday cage to reduce the noise and all disturbances that can affect the response of the electrodes.

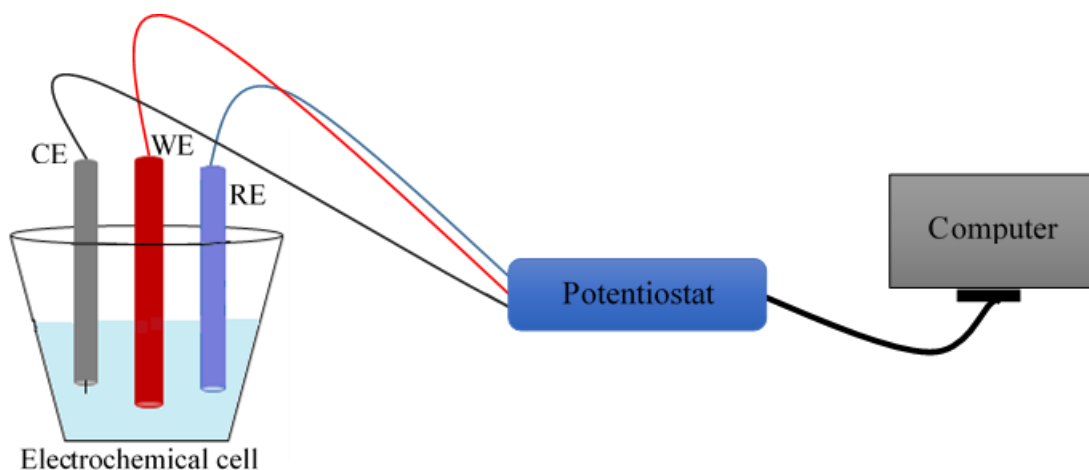


Figure II.1. Schematic representation of the conventional three electrodes system

II.3. Electrochemical methods

The electrochemical measurements of the different electrodes were investigated in an electrochemical cell at three electrodes as described in the [section II.2](#). The three electrodes were immersed in 20 mL BR solution (0.04 mol. L^{-1}) at a specific pH. Then, an appropriate micro-volume of the reagent solution was added into the cell.

II.3.1. Cyclic voltammetry (CV)

Cyclic voltammetry (CV) is the most popular basic technique, commonly used to acquire information about the electrochemical processes of molecular species, such as the

thermodynamics of redox processes and the kinetics of heterogeneous electron-transfer reactions, as well as the process control, reversibility and mechanism of redox process. CV is the first analysis that is recommended to assess the possibility of selective detection. However, it is not appropriate for the trace analysis as the detection limits cannot be very low [1]. This technique consists of scanning linearly the potential of a stationary WE using a triangular potential waveform, applying a potential to a WE and changing it with time at a certain rate. This applied potential is swept from the initial potential (E_i) to inversion potential (E_v) followed by a sweep back to the E_i , providing current vs applied potential the curves during the oxidation and reduction of a compound (Fig. II.2). Generally, the value of the measured peak current depends on several factors, including the concentration of the analyte, the kinetics of electron transfer and the mass transport of the analyte [2].

In our study, cyclic voltammetry was performed for the study of the electrochemical behavior of the reagents by applying the i - E curves. It is also used to optimize the experimental conditions, for the electrochemical characterization of the CB/ CME using a solution of $[\text{Fe}(\text{CN})_6]^{3-/4-}$ and to exploit the electro-analytical properties of the f-MWCNTs-FNTs modified electrode for the quantification of vanillin.

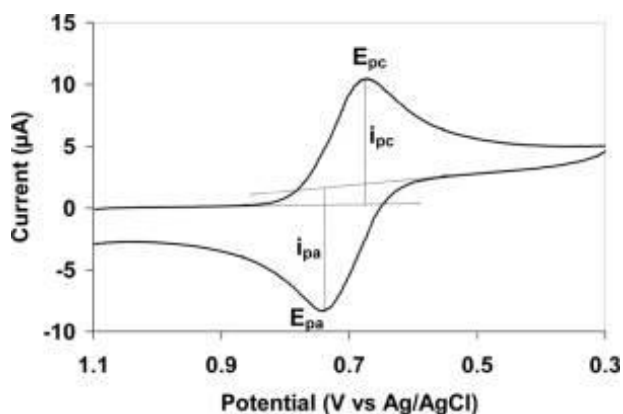


Figure II.2. Typical cyclic voltammogram of a reversible redox reaction.

II.3.2. Square wave voltammetry (SWV)

Square wave voltammetry (SWV) is widely used in the electrochemical sensing and mechanistic study of electrode kinetic processes due to its high sensitivity and lower detection limits. Typically, it consists on the superimposition of a square wave on each staircase potential ramp which will correspond to a single potential cycle; it will be obtained after the imposition of two potential pulses equal in height and opposite in direction [2]. In SWV technique, the time depend of the imposed frequency; it decreases when the frequency

increase accompanied with an increase in the measured current, making the voltammogram peaks more defined and sharp [1]. The step corresponds to the jump of the pulse and it defined the scan rate of scanning. In addition, the modulation amplitude (ΔE) corresponds to the height of the pulse; it should preferably be in the range of 5 to 100 mV, but as the ΔE increases, the peak becomes large, leading to lower resolution.

In our study, the square wave voltammetry was recorded to study the electro-analytical properties of the CBf-AC/ CME toward the simultaneous detection of AMP, PAR and CIP and the CB/ CME toward the PAR analysis, at step of 5 mV, modulation amplitude of 25 mV and frequency of 10 Hz.

II.3.3. Chronoamperometry (CA)

The chronoamperometric method is carried out for the detection of analytes in flowing systems, to find the value of the diffusion coefficient of the electroactive species and the surface area of the working electrode. Amperometry consists to apply a constant potential to the WE and measure the response current as a function of time [3].

In our study, chronoamperometric measurement was applied to determine active surface area of the f-MWCNTs-FNTs modified electrode.

II.3.4. Electrochemical impedance spectroscopy (EIS)

Electrochemical impedance spectroscopy is a sensitive electrochemical technique, used in the characterization of the electrode/electrolyte interface, giving information on the change in conductance or impedance [4]. EIS consists to apply a small-amplitude sinusoidal alternative current with a known frequency to a system, the frequency is varied and the overall impedance of the cell is recorded as a function of frequency [5]. The applications of EIS include the study of interfacial processes of reactions in solution combined with redox processes, the determination of solution and materials resistance. In addition to its application in power sources systems such as in batteries, fuel cells, membranes, corrosion studies, electrocatalytic reactions, self-assembly monolayers and sensors. Complex plane (Nyquist) and Bode plots are the most commonly used methods for interpreting EIS results. Nyquist plots are the most commonly used in electrochemical literature as they provide easy prediction of circuit elements and allow easy relation to electrical model. The EIS diagram named Nyquist plot have a semicircle part at higher frequencies corresponding to the limiting

by electron transfer process and a linear part at lower frequencies correlating with the diffusional controlled region [6].

In our work, electrochemical impedance spectroscopy was applied to characterize the electrical impedance of the interface between the presented electrodes and the electrolyte solution containing 10^{-3} mol.L⁻¹ of potassium hexacyanoferrate (III) in the frequency range from 10^{-3} to 10^{+5} Hz by using a sinusoidal excitation signal (sine signal) with an amplitude of 0.01 V.

II.3.5. Electrochemical preconcentration (EP)

The electrochemical preconcentration at fixed potential is one of the most frequently discussed preconcentration techniques. It have various advantages like simplicity, high sensitivity and effective preconcentration of the target at the surface of the sensor without any contamination risk [7]. This technique is based on accumulation of the target on the surface of the electrode, which is a crucial step that results in the exceptional selectivity that can be accomplished via the specific interaction between the analyte of interest with the electrode surface functionalities. In order to have a lower detection limit, the preconcentration step can be coupled with a sensitive and selective detection technique (differential pulse voltammetry or square wave voltammetry). Moreover, a longer accumulation time or a stirring up the solution can improve considerably the preconcentration efficiency [8].

In our study, this technique was carried out for the electrochemical preconcentration of paracetamol traces amounts on the surface of CB/ CME at 0 V for 900 s. The procedure is applied with SWV by maintaining the potential at 0 V during 900 s with stirring the solution. During this time the analyte is adsorbed on the microelectrode.

II.4. Other methods

II.4.1. Scanning electron microscopy (SEM)

Scanning electron microscopy is a technique based on electron-matter interactions, allows a qualitative analysis of the morphology of deposits. A fine beam of electrons whose energy can vary from a few hundred eV to 40 keV is focused on the surface of the sample, which it scans in a grid of parallel lines. Under the impact of this electron beam, the various electron-matter interactions result in the emission of different signals. These are collected to form an image of the surface of the object under study, or to make a chemical analysis of the same surface [9].

In the presented work, the surface morphology of the prepared sensors (f-MWCNTs-FNTs/CPE) and CBf-AC/ CME, CB/CME micro-sensors was characterized by scanning electron microscopy (SEM) (JEOL JSM-7100F, Detector EDS (Energy Dispersive Spectrometry) Oxford Instrument 50 mm²) from CMEBA center of ISCR-CNRS6226 at Rennes, France.

II.4.2. Fourier transform infrared (FTIR) spectroscopy

The FTIR spectroscopy is the most effective techniques to determine of functional group present in a compound. This method consist to apply the absorption spectrum for a compound using a spectrophotometer, which produces a beam of IR irradiation. The sample absorbs specific frequencies of energy, which are uniquely characteristic of the sample from the interferogram. Then, the detector measures the special interferogram signal in energy versus time for all frequencies simultaneously. Finally, depending on the infrared absorption frequency range 600-4000 cm⁻¹, the specific molecular groups presenting in the sample will be determined through spectrum data in the automated software of spectroscopy [10].

The FTIR analysis was investigated for the comparison of the carbon black material with the functionalized one. It was recorder using a Thermo Scientific Nicolet iS5 FT-IR spectrometer with iD7 ATR accessory. Spectra were obtained using 32 scans at 4 cm⁻¹ resolution using OMNIC software.

II.4.3. Ultra performance liquid chromatography coupled with UV spectrophotometry (UPLC/UV)

UPLC is a physico-chemical analysis technique used to identify, quantify and separate the compounds of a mixture. Its principle is based on the concentration equilibrium of the compounds present between two phases in contact; the stationary phase and mobile phase. The mobile phase moves through the column carrying the compounds with it. This method is characterized by the small size of a column and particles that require high pump pressures and lead to provide rapid analysis with better separation [11]. In UPLC/UV, the separated compounds enter the UV detector just after leaving the column. This detector is used to determine the concentration of the compound by measuring the light absorbed by the compounds at specific wavelengths.

The chromatograph used, in our study, is from ACQUITY HClass Waters model equipped with an Acquity UPLC R BEH type C18 column, with dimensions of 2.1 x 100 mm and a

particle size of 1.7 μm thermostated at 30 $^{\circ}\text{C}$ and equipped with Photodiode Array (PDA $\text{e}\lambda$) detector. An elution gradient was used by using two mobile phases (A: ultra-pure water, 10 % Acetonitrile and 0.1 % formic acid; B: acetonitrile) with 0.1 % in a flow rate of 0.4 $\text{mL}\cdot\text{min}^{-1}$. The injected volume was 10 μL and the UV detection was performed at a wavelength of 230 nm. This technique was used to quantify vanillin in commercial vanilla sugar samples. The results found were compared with those obtained by the electrochemical method using the designed f-MWCNTs-FNTs/ CPE sensor in order to validate them.

II.4.4. Standard addition method

The most commune method used to determine an unknown concentration of the analyte of interest is a conventional curve. However, this method has some limitations, namely the use of substantial sample dilution, in order to nullify matrix interference. Nevertheless, this dilution is not always possible because some matrix effects may even be involved and it would be preferable to limit sample dilution to keep analyte concentrations within the assay detection range when allowing for matrix interference on a case-by-case. In addition, this matrix affect are often complex, not completely known, and probably differ from sample to sample. Thus, it would be impossible to replicate these matrix effects in an external standard [12].

For this raison, the standard addition method has been introduced. This one is commonly used to determine a very low concentration of an analyte in a complex matrix such as biological fluids, soil samples, etc. A standard addition method consist in to directly add or spike a sample containing an unknown concentration, with successive additions of known concentrations of the target analyte, followed by measuring the increasing responses of the spiked analyte. Then, a standard curve is generated in the same matrix in which the analysis is performed. After that, the unknown concentration can be founded by the extrapolation of the regression line to the x-intercept. The y-axis corresponds to the response, while the x-axis corresponds to the unknown amount of the analyte [13].

The Fig. II.3. show the relative response as a function of the added concentrations. Using the equation for a straight line: $Y_i = a C_i + b$

Eq. 2.1

Where: Y_i is the response of the added analyte, X_i is the concentration of the analyte, a is the plot of the calibration curve and b is the intercept.

Chapter II: Experimental section

The following equation demonstrate how to find the unknown concentration of the analyte C_x in the solution without any add, with a relative response of Y_x :

The begin solution contain the analyte after the successive added, so a response Y_x will be registered even when the $C_i=0$, it correspond to $Y_i=Y_x$ **Eq. 2.2**

Known from the Eq. 2.1 that when $C_i=0$ the $Y_i=b$ **Eq. 2.3**

Thus, from Eq. 2.2. and 2.3 : $Y_x=b$ when $C_i=0$ so $Y_i=a C_i + Y_x$ **Eq. 2.4**

In addition, the concentration C of the solution is $C=C_x+C_i$

When $C=0$, $C_x+C_i=0$ thus $C_i=-C_x$

And when $Y_i=0$, $aC_i + Y_x=0$

Thus, $-aC_x+Y_x=0$ and $C_x=Y_x/a$ **Eq. 2.5**

This final equation is used to determine the unknown concentration of the analyte in the sample.

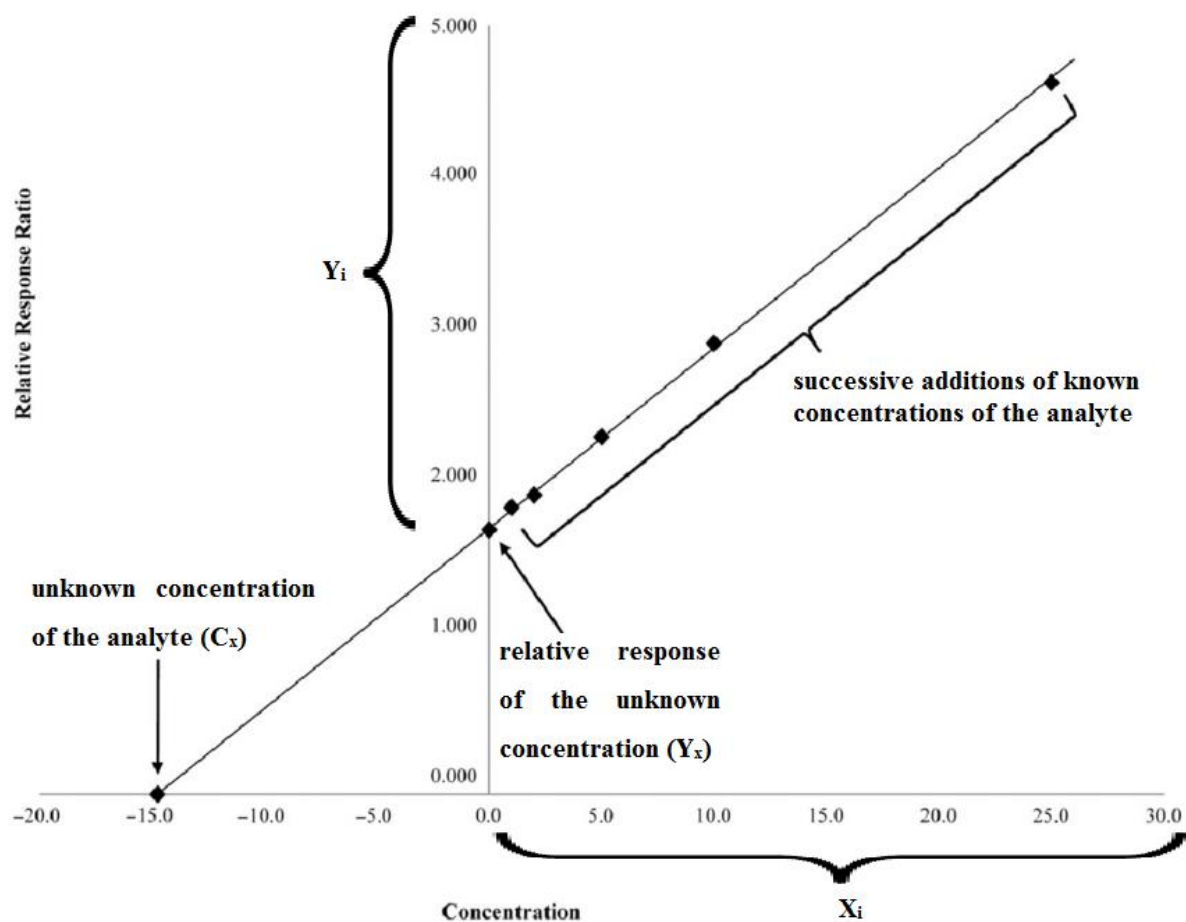


Figure II.3. Representation of a standard addition method

II.5. Preparation of electrode modifiers

II.5.1. Preparation of functionalized multi-walled carbon nanotubes (f-MWCNTs)

The f-MWCNTs were prepared according to the method reported by Baykal and al., [14] with minor modification in the procedure: 0.5 g of MWCNTs was added in a mixture of concentrated sulfuric acid (15 mL) and nitric acid (5 mL) then stirred vigorously for 24 hours. After that, 100 mL of distilled water was added to the prepared solution and stirred for another hour. The final suspension was filtered and washed 2 times with distilled water and dried at room temperature for 12 hours. Afterwards, the product was washed again with distilled water for 3 times. At the end, the f-MWCNTs were dried at 70 °C for 18 hours.

II.5.2. Preparation of functionalized carbon black (CBf)

3 g of carbon black was immersed in a uniform dispersion of acid mixture (nitric acid and sulfuric acid) in a ratio 1:1 and was kept under vigorous stirring for 21 hours, at ambient temperature to get the oxidized CB. Afterward, the resulting black suspension was diluted with 100 mL distilled water and stirred for a further 3 hours. Then washed several times with distilled water, until the pH was about 7. Finally, the functionalized CB (CBf) was oven dried for 16 h at 80 °C.

II.5.3. Preparation of activated carbon (AC)

The activated carbon was prepared according to the procedure followed by D. Moscone group [15] with some modifications: after cleaning 2 g of graphite with acetone and distilled water, it was activated with aqua regia (mixture of hydrochloric acid and nitric acid at 1:3 v/v) for 30 min. The obtained suspension was washed with distilled water until a pH of about 7 was reached, then dried at 400 °C for one hour.

II.6. Fabrication of modified electrodes

II.6.1. Fabrication of modified f-MWCNTs-FNTs/ CPE

The following pastes were prepared in an agate mortar with a pestle, by mixing and homogenizing the specified compounds to obtain well dispersed paste, which then was introduced into the cylindrical cavity (1.6 mm diameter and 3 mm depth).

- f-MWCNTs-FNTs/CPE: graphite, f-MWCNTs and FNTs at ratio (55 %; 20 %; 10 %), respectively.
- f-MWCNTs/ CPE: graphite and f-MWCNTs at ratio (55 %; 30 %), respectively.

➤ CPE: 85 % of graphite.

The ratio of the binder (paraffin oil) was maintained at 15 % for all the pastes prepared. This was chosen to have a paste with good mechanical strength, good consistency, which does not crumble and having good conductivity. The preparation steps for f-MWCNTs-FNT / CPE are illustrated in [Figure II.4](#).

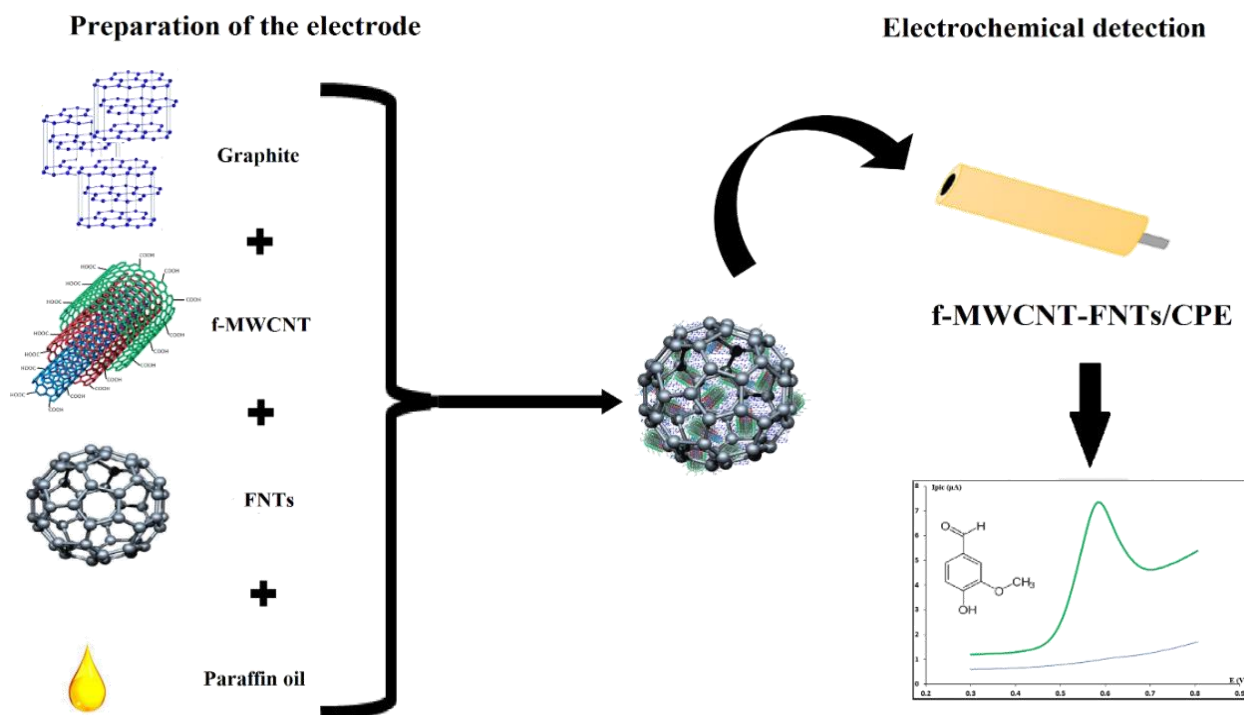


Figure II.4. Graphical presentation of f-MWCNTs-FNTs/CPE sensor fabrication.

II.6.2. Preparation of modified cavity microelectrodes (CME)

II.6.2.1. Fabrication of modified CBf-AC/ CME

4.5 mg of CBf and 1.5 mg of AC, in a proportion of 75 to 25 %, respectively, were well mixed and homogenized in an agate mortar. Then, transferred to a glass slide to be introduced into the microelectrode cavity (diameter $\varnothing = 25 \mu\text{m}$ and depth $h = 10 \pm 1 \mu\text{m}$) following the steps of packing described in the [section I.4.2](#).

II.6.2.2. Fabrication of modified CB/ CME

The preparation of the CB/ CME is very simple and easy procedure. It enough to take a quantity of CB with any modification and to introduce it into the microelectrode cavity following the steps of packing described in the [section I.4.2](#).

II.7. Preparation of solution

II.7.1. Preparation of electrolyte support

An electrolyte support is an ionic conductive substance, which is added to the solution in order to improve its conductivity and reduce the capacitive current. Generally, the electrolyte support concentration is higher than that of the analyte, to maintain a constant high ionic level despite small variations in analyte concentration during the electrochemical reaction. It is important to choose an electrolyte that does not interfere with the measurement. In our case, the measurements were performed in Britton–Robinson Solution (BRS) with different pH.

The Britton–Robinson Solution was prepared by dissolving in 1 L of pure water: 0.04 M H_3BO_3 (2.47 g/L), 0.04 M H_3PO_4 (2.74 mL of H_3PO_4 85 % / 1 L) and 0.04 M CH_3COOH (2.32 M CH_3COOH 99 % / 1L). After that, the prepared BRS is adjusted at the desired pH with 0.2 M NaOH (4 g in 500 mL of pure water).

II.7.2. Preparation of analyte species solutions

Solutions of vanillin and pharmaceuticals at 10^{-2} M concentration were prepared in volumetric flasks in pure water with the exception of ciprofloxacin that is prepared in 0.1 M HCl (because this compound is lowly soluble in water). Then, they were well agitated to ensure their dissolution. The latter prepared solutions were diluted in order to prepare daughter solutions at concentrations of 10^{-3} , 10^{-4} , 10^{-5} and 10^{-6} M. Finally, stored in tightly stoppered bottles in the dark and at 4 °C.

II.8. Preparation of real samples for validation analysis

II.8.1. Commercial sugar vanilla samples

Four different commercial brands of sugar vanilla samples were purchased from a local supermarket. The ingredients indicated in their packaging do not give precision about their specific quantities: sugar, cornstarch, VAN and exhausted vanilla pods. The sample solutions were prepared by the following procedure: In 100 mL of ultra-pure water, about 5 mg of each sample was dispersed after to be sonicated for 30 min in ultrasonic bath. Then, the resulted solution was filtered with syringe filter (0.45 μm) and 1 mL of each sample was transferred in the voltammetric cell containing 19 mL of the supporting electrolyte (BR Solution, pH = 7), for the validation of the proposed f-MWCNTs-FNTs/CPE by following the same procedure

developed for the synthetic solution. In the same time, the filtrated solutions of sugar samples were analyzed by UPLC/UV as control method after the realization of a calibration curve (0.5 to 15 mg.L⁻¹) by integrating the chromatographic peak at $t_r=2.03$ min (at $\lambda_{\max} = 230$ nm).

II.8.2. Artificial urine samples

The synthetic urine was prepared by following the procedure reported by Laube et al., [16], and in a way to contain the majority constituents of the real urine, by dissolving: 60 mg KCl, 20 mg NaCl, 80 mg KH₂PO₄, 44 mg CaCl₂, 38.4 mg NH₄Cl and 43.2 mg urea in 100 ml double-distilled water under magnetic stirring. The prepared artificial urine was diluted twice by the supporting electrolyte (10 ml of urine in 10 ml of BR Solution, pH = 5) and 1 μ M of each reagent AMP, PAR and CIP were dissolved there in. The above solution was transferred into electrochemical cell for the test of the validity of the sensor CBf-AC/ CME proposed in this work for the simultaneous detection of AMP, PAR and CIP.

II.8.3. Water samples

The local tap water and wastewater collected from the station of the wastewater treatment in Betton (Rennes,France) were simply filtered with syringe filter (0.45 μ m) to remove possible impurity and spiked with appropriate concentration of PAR, without any dilution or using supporting electrolyte. The prepared solutions were transferred directly into the electrochemical cell for the validation of the proposed CB/ CME.

References

- [1] Batista Deroco, P., Giarola, J. de F., Wachholz Júnior, D., Arantes Lorga, G. & Tatsuo Kubota, L. (2020). Editor(s): Merkoçi, A. In Chapter Four - Paper-based electrochemical sensing devices, *Comprehensive Analytical Chemistry, Elsevier*, 89, 91.
- [2] Hoyos-Arbeláez, J., Vázquez, M. & Contreras-Calderón, J. (2017). Electrochemical methods as a tool for determining the antioxidant capacity of food and beverages: A review, *Food Chemistry*, 221, 1371.
- [3] Choudhary, Y.S., Jothi, L. & Nageswaran, G. (2017). Chapter 2 - Electrochemical Characterization, Editor(s): Thomas, S., Thomas, R., Zachariah, A.K. & Mishra, R.K. In Micro and Nano Technologies, Spectroscopic Methods for Nanomaterials Characterization, *Elsevier*, 19.
- [4] Randviir, E. P. & Banks, C. E. (2013). Electrochemical impedance spectroscopy: an overview of bioanalytical applications, *Analytical Methods*, 5, 1098.
- [5] Nnamchi, P.S. & Obayi, C.S. (2018). Chapter 4 - Electrochemical Characterization of Nanomaterials, Editor(s): Bhagyaraj, S.M., Oluwafemi, O.S., Kalarikkal, N. & Thomas, S. In Micro and Nano Technologies, Characterization of Nanomaterials, Woodhead Publishing, 103.
- [6] Pajkossy, T. & Jurczakowski, R. (2017). Electrochemical impedance spectroscopy in interfacial studies, *Current Opinion in Electrochemistry*, 1 (1), 53.
- [7] Samandari, L., Bahrami, A., Shamsipur, M., Farzin, L. & Hashemi, B. (2019): Electrochemical preconcentration of ultra-trace Cd^{2+} from environmental and biological samples prior to its determination using carbon paste electrode impregnated with ion imprinted polymer nanoparticles, *International Journal of Environmental Analytical Chemistry*, 99 (2), 172.
- [8] Shiu, K.-K. & Shi, K. (1998). Preconcentration and Electroanalysis of Copper Species at Electrochemically Activated Glassy Carbon Electrodes, *Electroanalysis*, 10(4), 959.
- [9] Pinto, A.M.F.R., Oliveira, V.B. & Falcão, D.S. (2018). 4 - Experimental methods of characterization, Editor(s): Pinto, A.M.F.R., Oliveira, V.B. & Falcão, D.S. In Direct Alcohol Fuel Cells for Portable Applications, *Academic Press*, 113.
- [10] Mohamed, M.A., Jaafar, J., Ismail, A.F., Othman, M.H.D. & Rahman, M.A. (2017). Chapter 1 - Fourier Transform Infrared (FTIR) Spectroscopy, Editor(s): Hilal, N., Ismail, A.F., Matsuura, T. & Oatley-Radcliffe, D. In Membrane Characterization, *Elsevier*, 3.

- [11] Batool, A. & Mena, F. (2020). Chapter 13 - Concentration and purification of seaweed components by chromatography methods, Editor(s): Torres, M.D., Kraan, S. & Dominguez, H. In *Advances in Green Chemistry, Sustainable Seaweed Technologies*, Elsevier, 315.
- [12] Pang, S. & Cowen, S. (2017). A generic standard additions based method to determine endogenous analyte concentrations by immunoassays to overcome complex biological matrix interference, *Scientific Reports*, 7, 17542.
- [13] Mohammed, Y., Pan, J., Zhang, S., Han, J. & Borchers, C.H. (2018). ExSTA: External Standard Addition Method for Accurate High-Throughput Quantitation in Targeted Proteomics Experiments, *Clinical Proteomics for Precision Medicine*, 12 (2), 1600180.
- [14] Baykal, A., Senel, M., Unal, B., Karaoğlu, E., Sözeri H. & Toprak, M. S. (2013). Acid Functionalized Multiwall Carbon Nanotube/Magnetite (MWCNT)-COOH/Fe₃O₄ Hybrid: Synthesis, Characterization and Conductivity Evaluation, *Journal of Inorganic and Organometallic Polymers*, 23, 726.
- [15] Moscone, D., D'Ottavi, D., Compagnone, D. & Palleschi, G. (2001). Construction and analytical characterization of prussian blue-based carbon paste electrodes and their assembly as oxidase enzyme sensors, *Analytical Chemistry*, 73, 2529.
- [16] Laube, N., Mohr, B. & Hesse, A. (2001). Laser-probe-based investigation of the evolution of particle size distributions of calcium oxalate particles formed in artificial urines, *Journal of Crystal Growth*, 233 (1–2), 367.

Chapter III

***Carbon paste electrode based on fullerene
and MWCNT for the detection of vanillin as
additive***

Introduction

Food is an essential nutriment that maintains the human life. However, it can also be the reason of his illness or even death. When it is not controlled, it can become toxic and pathogenic. Especially with the increase of population and the change of life style that promote considerably the consumption of the industries food, which involve the incorporation of food additives. Various additional food ingredients are employed and one of the most frequently flavoring agent used in over the whole world is vanillin. Its flavor affects considerably the quality of food, but also, can affect indirectly the human health. Thus, monitoring the amount of vanillin in the foods is necessary.

In the aim to have a simple and economical device allowing a sensitive and easy analysis of vanillin concentration in commercial products, we developed a first nanostructured sensor based on fullerene and multi-walled carbon nanotubes.

The newly fabricated electrode offers several advantages over other techniques used for the determination of vanillin, including the simplicity of the sensor preparation, low cost, rapidity and very good analytical characteristics as selectivity, high sensitivity and low detection limit. Moreover, the most important advantage is the feasibility to determine the vanillin concentration in real matrices, without any pretreatment following an easy procedure.

In this chapter, we present in the first part generalities about vanillin. Then in the second part, we describe the optimization, conception and validation of the proposed modified carbon paste electrode.

The results presented in this chapter are published in Journal of Food Composition and Analysis, 2021, 103811.

Part III.1: Vanillin

In this part, we present a general bibliographic studies about vanillin and there different uses. A discussion about its side effect toward the human life and the norms, which must be respected during its incorporation in the food products and its consumption will be presented.

III.1.1. Introduction

The food additives are natural or synthetic substances added to the food during its processing or preparation. The purpose of their use is to increase the shelf life and/or to maintain or to improve the physicochemical, sensorial and microbiological properties of the commercial foods [1]. In the food industries, there are several varieties of food additives, which are classified by the World Health Organization (WHO) with agreement of Food and Agriculture Organization of the United Nations (FAO) into three broad categories based on their function (flavoring agents, enzyme preparations and other additives) [2].

The flavoring agents are substances added in food to enhance their taste or aroma. They are classified in two categories: natural flavors extracted directly from plants, herbs, animals, or microbial fermentations; and chemical or synthetic flavors that are more easily available and less expensive but they are not an exact copy of the natural flavorings, they just imitate their taste or aroma [3].

Vanilla is one of the most popular flavoring additives widely used in foods, beverages, fragrance, and pharmaceutical products. The natural vanillin flavor is extracted from vanilla bean that is difficult to grow and harvest that is why its price is very expensive. According to food business news published in 2019, the price for first-grade extraction of vanilla beans hit \$600 per kilogram [4]. Vanilla extract contains more than 200 compounds, including vanillin, and represents 1 to 2 % of the global extract. Vanillin is considered like the key compound of vanilla extract because it is the most characteristic compound that offers sweet and intense aroma for vanilla flavor. The production of natural vanillin by isolation from vanilla beans is a laborious and costly process (from 500 Kg of vanilla pods just 1 Kg of vanillin extracted) [5]. For this reason, the need of an artificial flavoring that imitates the vanillin natural flavor is necessary, especially with the cross demand of vanillin in the global market, which reaches 37.286 tons in 2018 and is estimated to reach 59.458 tons by 2024 [6].

Nowadays, the majority of the global production of vanillin is produced synthetically. However, this increase in the production and the consumption of vanillin induce various side effects that risk human health in the case where it is not controlled in the phase of food production process or not taken in acceptable quantities. Therefore, the monitoring of the vanillin concentration is primordial to ensure the quality product and to preserve human life.

III.1.2. Vanillin generality

Vanillin is chemically 4-hydroxy-3-methoxybenzaldehyde, an organic polyfunctional compound with an aromatic ring bonded to an aldehyde group, -OH phenolic, and a methoxy group [7]. This aromatic compound is a white crystalline powder with a sweet smell and pleasant taste like vanilla [8]. The principal physicochemical proprieties of vanillin at ambient conditions are summarized in Table III.1. Apart from these properties, vanillin has beneficial proprieties, when it is used in low concentrations, offered by their biological and therapeutic activities such as antioxidant, antimicrobial, antimutagenic, hypolipidemic, antisickling and others activities [9]. Vanillin is the world's most popular flavor; it can be found in the market as a natural or synthetic vanillin.

➤ *Natural Vanillin flavor*, can be extracted from 110 different species of tropical vanilla plants that belongs to the family Orchidaceous. Generally, it obtained from the cured beans of vanilla planifolia and vanilla tahitensus. The first cited specie (vanilla planifolia) is widely recommended due to its highest vanillin content comparatively with the second specie. Vanilla extract bean is richer and more beneficent that the artificial vanillin, it contains Vitamin B and minerals such as thiamin, riboflavin, calcium, potassium and iron. However, vanilla is very difficult to cultivate, the processing of the beans need a very long time to inspect their quality and aroma. In addition, the isolation process of vanillin is laborious and expansive. Consequently, to meet the growing demand in the food markets, the synthetic vanillin is introduced.

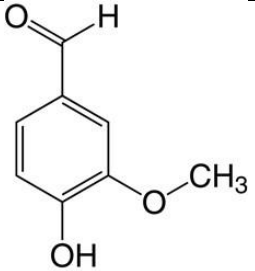
➤ *Synthetic vanillin flavor*, is a chemical alternative of a natural vanillin, made from industries. It only contains the main flavor vanillin and its derivatives, compared to natural vanilla that is richer. This artificial vanillin is commonly used due to its low cost, availability and ability to satisfy the demand of the vanillin consumers. The most synthetics vanillin flavorings are ethyl vanillin and vanillin. However, like any synthetic compound the artificial vanillin flavor can contain impurities that can affect the quality of the final product and the human health. Thus, artificial vanilla tends to be cheaper, but the health impact is to be considered [10].

III.1.3. Uses

Vanillin has widely used in various areas. It is used like flavoring agent in foods, beverages and pharmaceuticals products [11]. It is also employed in the production of some deodorant, herbicides and house fold products [12]. In addition to their biological and therapeutic

properties, VAN is used to cure some health problems such as anxiety, digestive problems, stomach pain, stress [13] and to inhibit harmful bacteria and cancer cells [14]. However, these beneficial applications are only possible with natural vanillin and in low acceptable amounts.

Table III.1. Main physicochemical properties of vanillin [8].

Vanillin		
<i>N° CAS</i>	121-33-5	
<i>Molecular weight</i>	152.15 g.mol ⁻¹	
<i>Solubility in water (at 25 °C)</i>	1.102 × 10 ⁻⁴ mg.L ⁻¹	
<i>pKa</i>	7.4	
<i>Log Kow</i>	1.37	
<i>Boiling Point</i>	285 °C	
<i>Melting Point</i>	81.5 °C	

III.1.4. Side effects

Excessive ingestion of VAN have side effects toward the human health, it can cause potential health problems and aggravate the condition of migraine sufferers, headaches, insomnia, nausea, vomiting, and even liver and kidney problems. Apart from the fact that the enticing smell of VAN may cause addiction to such food or beverages [14]. Synthetics vanillin flavorings can contains impurities and neurotoxins that can kill the brain cells even at negligible amounts. In addition, the synthesized ethyl vanillin can lead to allergic reactions and irritate eyes and skin [10]. In high concentrations (mM range), VAN has been described as a cytotoxic agent against many cell lines [15]. Due to all these side effects observed with the excessive intake of VAN, the monitoring of its level is necessary not only to control the quality of the product but also to ensure the protection of the human health.

III.1.5. Norms

An acceptable daily intake (ADI) of 10 mg/Kg for VAN has been set by the Joint FAO/WHO Expert Committee on Food Additive (JECFA) in 1967 and later confirmed in its 2001 re-evolution as flavoring. An ADI value that has been also agreed by the European Union [16]. For a person with a weight of 70 kg, the ADI is 700 mg VAN [10]. Toxic effects are observed when the intake exceeds 75 mg/Kg [17]. According to Food and Drug Administration (FDA) rules in the United States, declare that dairy products must get its flavor from natural vanilla and in the case where it is get its flavor through some other source, the company should label “vanilla flavored” or “artificial vanilla” on the package [10].

Part III.2: Electrochemical detection of vanillin at carbon paste electrode modified with fullerene and MWCNT

In this second part of chapter III, we describe the experimental conditions of the conception of a new electrochemical sensor for the quantification of vanillin, from the carbon materials to the final modified carbon paste electrode. The surface of the proposed sensor was characterized by scanning electron microscopy technique, chronoamperometric measurement and electrochemical impedance spectroscopy method. A study of the electrochemical behavior of vanillin and the optimization of operating conditions, such as supporting electrolytes, pH values and accumulation time are also discussed. The electrochemical characteristics (linear range, detection limit, stability, repeatability and reproducibility) of the modified carbon paste electrode was evaluated by cyclic voltammetry method. Then, validated in real samples of commercial vanilla sugar with a comparison to UPLC/UV as control method.

III.2.1. Introduction

Recent work revealed that the fullerene has multiple redox states and an ability to accept and transport easily electrons. In addition to that, fullerene have high electroactive surface area, good electronic conductivity, and high chemical stability that leads to the possibility of functionalization, signal mediation and others remarkable characteristics [18-20]. These new discovered carbon is considered as new and attractive element in the development of sensors and biosensors and the use of fullerene as electrode modifier material is still recent.

Various form of fullerene have been investigated. In our study, we have interested to the use of fullerene nanotubes (FNTs) as material in the conception of a nanostructured sensor, which are fullerene that grow spontaneously into the form of tubes with a single crystalline, polycrystalline or amorphous structures [21]. This material is used for the first time as an electrode modifier to the best of our knowledge.

Carbon nanotubes received a great attention due to its exceptional optical, mechanical, electronic and thermal properties that driven the researchers to explore these nanomaterials in electrochemical sensing [22].

Therefore, the combination of FNTs with multi-walled carbon nanotubes (MWCNTs) were more effective in facilitating the electrons transfer, enhancing the surface area and improving the electroanalytical proprieties of the modified sensor.

III.2.2. Characterization of f-MWCNTs-FNTs/ CPE

a. Characterization of modified electrode by scanning electron microscopy (SEM)

The SEM method is used in order to study the surface morphology and the materials composition of the proposed sensor.

Fig. III.1 shows a corresponding SEM images for the components of f-MWCNTs-FNTs modified electrode. In the Fig. III.1-A, the graphite surface appears as particles with flake shaped structure ranging in size from lower than 1 μm thick and lower than 4 μm diameter. While fullerene wires showed their nanometrical size in diameter (estimated from 15 to 20 nm) they have a tube shaped structure and are wound into a ball and appear as balls of wood with a diameter lower than 50 μm (Fig.III.1-C & D). The multi-walled carbon nanotubes (MWCNTs) have a spaghetti shaped structure less compacted than FNTs and with a diameter slightly weaker 10-15 nm (Fig. III.1-E). The functionalization of MWCNTs as done in section II.5.1 provided a more disperse structure with lower length of the nanotubes in comparison with the non-functionalized ones (Fig. III.1-F). For the CPE modified electrode, in the (Fig. III.1-B), it can

be seen that in the mixture of f-MWCNTs, FNTs and graphite are linked in a way to avoid the stacking of graphite platelet and to promote the accessibility to the analyte in their surfaces and improve the charge transfer in the paste. Globally, the f-MWCNTs-FNTs electrode showed a uniform and nanostructured surface which could yield to large surface area and improve the characteristics of the previous fabricated sensor.

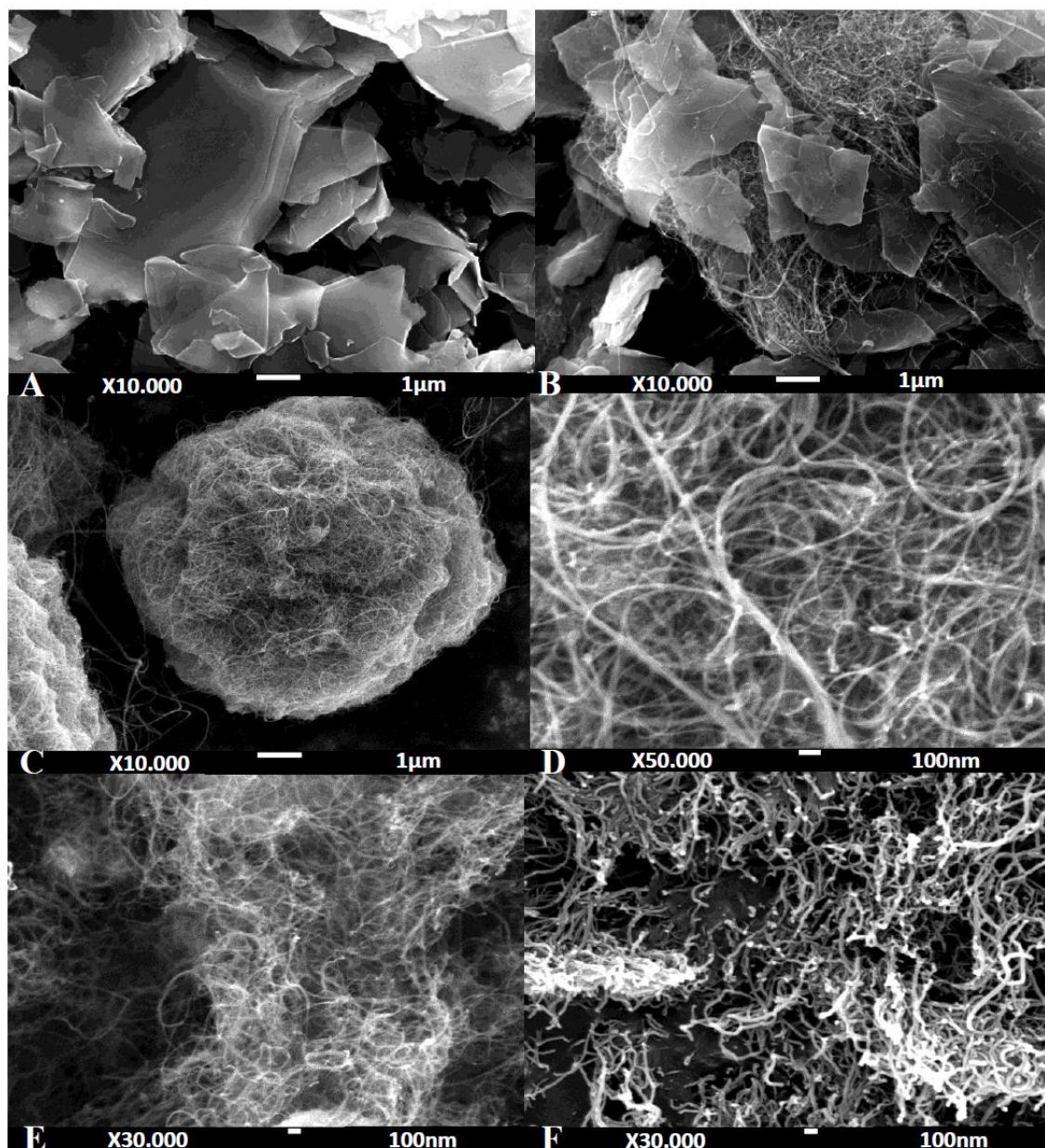


Figure III.1. SEM images for (A) graphite (x10.000), (B) f-MWCNTs-FNTs/ CPE (x10.000), (C) FNTs (x10.000), (D) FNTs (x50.000), (E) MWCNT (x30.000) and (F) f-MWCNT (x30.000).

b. Characterization of the modified electrode by chronoamperometry method (CA)

In order to determine the active surface area of the modified electrode, we have used the chronoamperometric method in the presence of 10^{-3} mol.L $^{-1}$ potassium hexacyanoferrate (III) as the redox probe. In the condition of diffusion control for the current obtained in CA, the current-time response is described by the Cottrell equation [23]:

$$i = \frac{nFAD^{1/2}C^*}{\pi^{1/2}t^{1/2}} \quad \text{Eq. 3.1}$$

Where A is the active area of the electrode, C^* is the initial concentration of ferrocyanide, D the diffusion coefficient of ferrocyanide which is well known to be 6.22×10^{-6} cm 2 .s $^{-1}$ [24] in aqueous electrolyte and the other parameters have their typical significances.

The electrochemical active area of the sensor was estimate to be 0.14 cm 2 from the slope of the linear regression line of current density versus square root of time. While, the geometric surface of the 1.6 mm diameter electrode was calculated to be 0.02 cm 2 considering the cross section of the cavity. Thus, the nanostructuration of the carbon paste sensor gives a greater specific surface than the geometric one and enables the access of the cell solution to a larger surface of graphite particles by avoiding their stacking.

c. Characterization of modified electrode by electrochemical impedance spectroscopy (EIS)

The impedance spectra were recorded for CPE and f-MWCNTs-FNTs/CPE in electrolyte solution containing 10^{-3} mol.L $^{-1}$ of potassium hexacyanoferrate (III) in the frequency range from 10^{-3} to 10^{+5} Hz by using a sinusoidal excitation signal (sine signal) with amplitude of 0.01 V (Fig. III.2).

A Nyquist plot showed a semicircle with a large diameter for the CPE that indicate a higher charge transfer resistance (16.7 K Ω) and when CPE modified the diameter of the semicircle decrease at 6.81 K Ω indicated a lower charge transfer resistance (reduction by a factor of 2.5). This is ascribed to the incorporation of f-MWCNT and FNTs, which stimulating electron transfer, increasing conductivity and reducing charge transfer resistance. The linear parts for the lowest frequencies at a Nyquist plot are not depending on the composition of the carbon paste electrode (same slope). This is consistent with an identical diffusion controlled process identical in both cases.

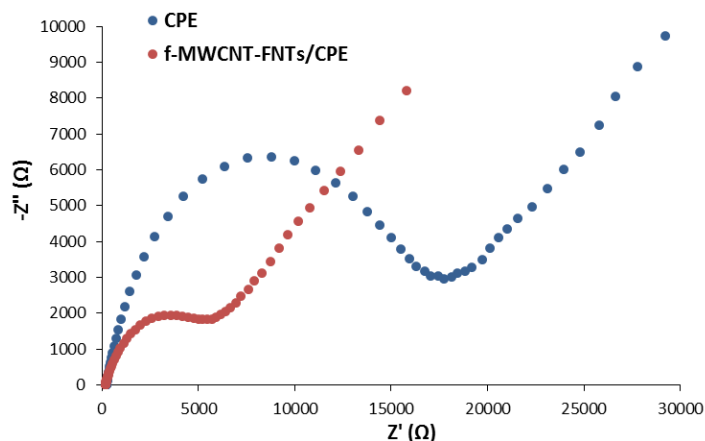


Figure III.2. Nyquist diagrams for EIS of CPE (●) and f-MWCNT-FNTs/CPE (●) in 1mM $\text{Fe}(\text{CN})_6^{3-}$ and BRS 0.04 M at pH=7

III.2.3. Electrochemical behavior of the f-MWCNTs-FNTs/ CPE

The electrochemical behavior of f-MWCNTs-FNTs modified CPE was investigated by CV in presence of $10^{-5} \text{ mol.L}^{-1}$ VAN at scan rate of 20 mV.s^{-1} in BR buffer at pH=7 as the supporting electrolyte. As it can be seen from Fig. III.3, the CV of CPE, in the presence of VAN shows an ill-defined (or a poorly defined) anodic peak ($2.3 \mu\text{A}$) at around +0.6 V. The incorporation of f-MWCNTs in the paste (30 %) leads to enhance the peak current of VAN oxidation ($6.3 \mu\text{A}$). The addition of FNTs (10 %, by replacing a part of MWCNTs and maintaining all the carbon nanotubes to 30 %), improves notably the peak intensity. Therefore, the anodic peak current obtained with the nanostructured modified electrode ($9.2 \mu\text{A}$) is 4 times higher than with CPE. The combination of FNTs and f-MWCNTs facilitate the accessibility of VAN to graphite particles and the electron transfer at the electrode material.

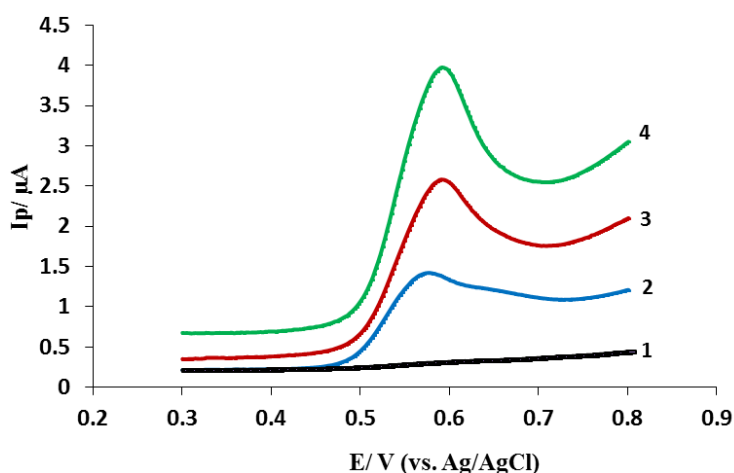


Figure III.3. Cyclic voltammograms at (1) CPE without VAN, and with $10^{-5} \text{ mol.L}^{-1}$ VAN at (2) CPE, (3) f-MWCNTs/ CPE and (4) f-MWCNTs-FNTs/CPE in BRS 0.04 M (pH = 7)

III.2.4. Effect of pH

The dependence of the peak oxidation of VAN on the pH value of the electrolyte was carried out using CV measurements in the BR solution in the pH range from 5 to 9 at 18 °C in the presence of 10^{-6} mol.L⁻¹ VAN.

As shown in Fig. III.4-A, the peak oxidation current of the VAN is depending on the pH value and increases with increasing pH until it reaches the maximum at pH = 7, then decreases with higher pH values. The optimized pH corresponding to the higher peak current was 7, indicating that protons are involved in the reaction of VAN oxidation. Moreover, as the pKa of VAN was equal to 7.4 at 25 °C [25], this result indicated that the analyte was preferentially adsorbed in the neutral form.

In addition, it is found that the values of peak potential shift to lower values with the increase of pH values, as can one be seen on Fig. III.4-B. Thus, the peak potential is linearly depended on the pH according to the following equation:

$$E_p(\text{V}) = -0.0542 \text{ pH} + 1.01 \quad (R^2 = 0.993) \quad \text{Eq. 3.2}$$

A shift of typically 54.2 mV per pH unit is approximately close to the theoretical value of 57.6 mV per pH unit at 18 °C [23]. This demonstrates that the electron-transfer process during the oxidation of VAN involved an equal number of protons and electrons (two electrons and two protons take part in the oxidation process). This result is in agreement with those previously reported by other authors [26-28].

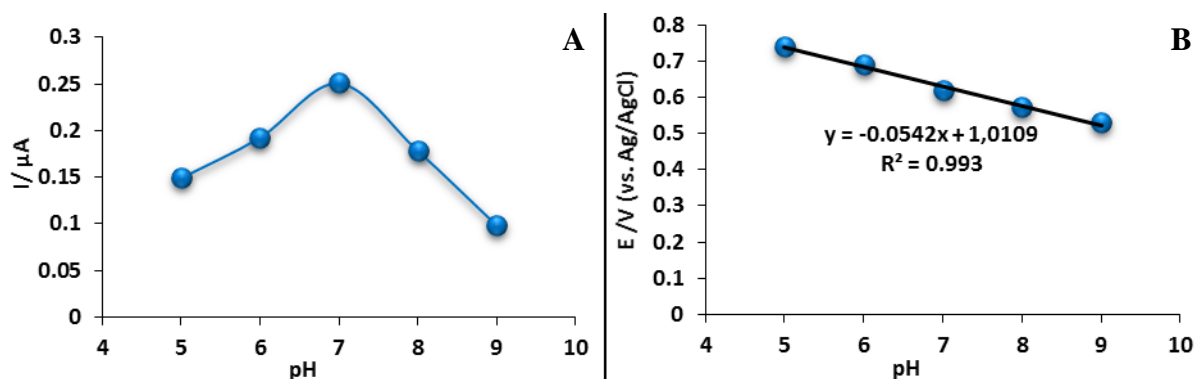


Figure III.4. (A) Effect of pH on the peak oxidation current of VAN with different pH values (5 to 9) at the f-MWCNTs-FNTs/ CPE in BRS 0.04 M (pH = 7) at 20 mV.s⁻¹. (B) Corresponding plot of the oxidation peak potential of VAN versus pH

III.2.5. Effect of potential scan rate

In order to establish the electrochemical behavior of VAN on the surface of the modified paste electrode, a study of the effect of scan rate was carried out by cyclic voltammetry. The measurements were recorded for 10^{-6} mol.L⁻¹ of VAN at f-MWCNTs-FNTs/CPE for different potential scan rates in the range of 5 to 80 mV.s⁻¹ in BR solution at pH = 7. The variation of the peak current in function of the scan rate is presented in Fig. III.5. It can be seen that the oxidation peak current of VAN increases linearly with the increasing of the scan rate, with a linear relationship:

$$I_p = 1.28 U + 0.168 \quad (R^2=0.998) \quad \text{Eq. 3.3}$$

This indicates that the oxidation of the VAN is controlled by an adsorption process of the VAN to the electrode. This adsorption step will provide sensibility for the developed sensor and lead to a low detection limit.

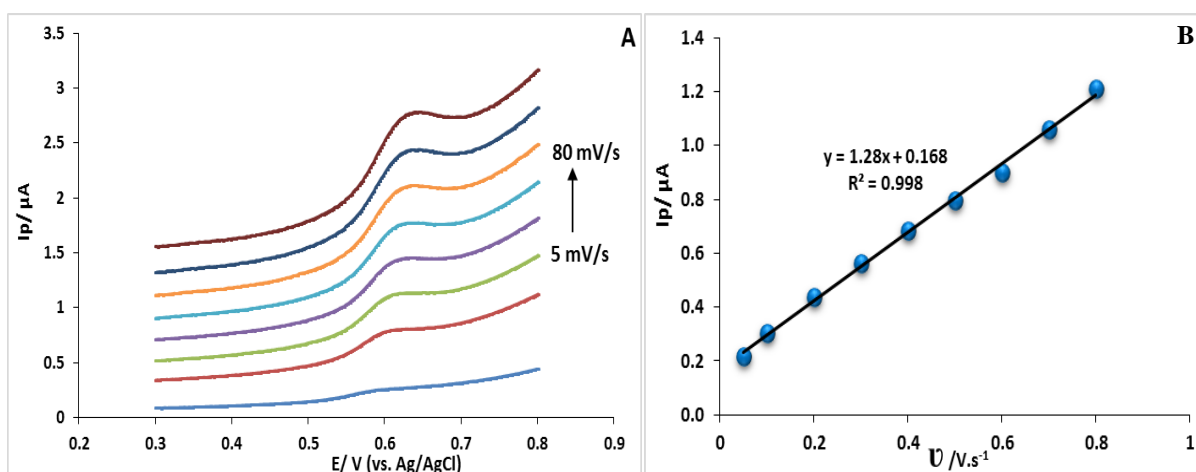


Figure III.5. The effect of different scan rates (5 to 80 mV.s⁻¹) on the oxidation peak current of 10^{-6} mol.L⁻¹ VAN at the f-MWCNTs-FNTs/ CPE in BRS 0.04M (pH = 7).

III.2.6. Effect of accumulation time

As vanillin oxidation is limited by an adsorption step, the accumulation time will allow the CPE to be saturated with the analyte and ensure an optimal response.

This accumulation was done by stirring the solution in the electrochemical cell with a magnetic bar. The dependence of the VAN intensity peak was studied with CV method for 10^{-6} mol.L⁻¹ VAN at f-MWCNTs-FNTs/ CPE in BR buffer at pH = 7 (Fig. III.6). As seen, the oxidation peak current of VAN gradually increased with increasing accumulation time from 30 to 360 s, and reached the maximum current response at 300 s then remains almost constant at longer

accumulation times. For practical purposes, a 300 s (5 min) accumulation time is sufficient and used for the determination of VAN.

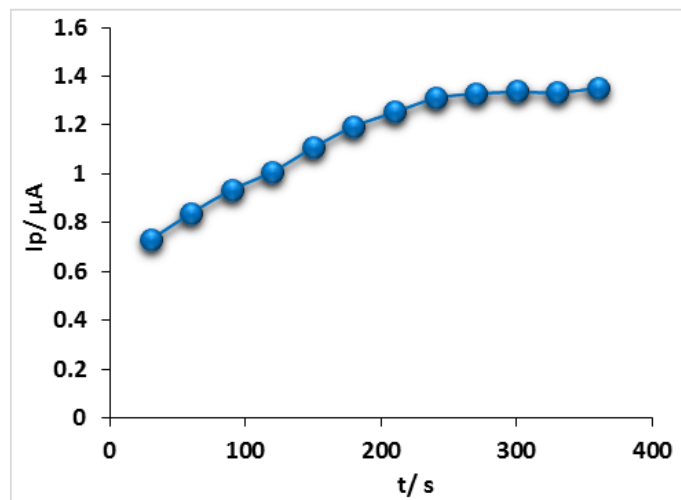


Figure III.6. Effect of accumulation time on the oxidation peak current of 10^{-6} mol.L $^{-1}$ VAN at the f-MWCNTs-FNTs/ CPE in BRS 0.04M (pH = 7).

III.2.7. Quantitative analysis of vanillin

In order to evaluate the linear concentration range and the detection limit of the f-MWCNTs-FNTs/CPE, the quantitative analysis of VAN concentration using the developed sensor was performed by cyclic voltammetry under the optimized conditions in SBR (0.04 M) at pH = 7 and scan rate of 20 mV.s $^{-1}$ after stirring for 5 min (Fig. III.7-A).

The calibration curves for the oxidation peak current (I_p) as a function of the concentration of [VAN] have been plotted and shown in Fig. III.7. As can be seen the intensity of the oxidation peak currents increases with the concentrations of the VAN (Fig. III.7-B & C) and presents two clearly defined linear ranges.

- from 5×10^{-8} to 9×10^{-6} mol.L $^{-1}$, the linear regression equation is:

$$I_p = 3.89 \times 10^5 [\text{VAN}] + 0.522, \quad (R^2 = 0.999) \quad \text{Eq. 3.4}$$

- from 10^{-5} to 10^{-4} mol.L $^{-1}$, the linear regression equation is:

$$I_p = 7.80 \times 10^4 [\text{VAN}] + 5.35, \quad (R^2 = 0.995) \quad \text{Eq. 3.5}$$

These two concentration ranges indicate that the VAN oxidation is not controlled by the same process. For the lowest concentrations (below 10^{-5} mol.L $^{-1}$), the peak current is controlled by an adsorption step of VAN at the electrode surface (as seen in the section III.2.6) which provides

an interesting sensibility. For highest concentration ($> 10^{-5} \text{ mol.L}^{-1}$) the peak current is controlled by the diffusion of VAN.

The detection limit of the proposed method is found to be $3.4 \times 10^{-8} \text{ mol.L}^{-1}$, calculated from the formula:

$$\text{LOD} = 3.3 \times \text{SD}/b \quad \text{Eq. 3.6}$$

Where, SD is the standard deviation of the linear regression solution and b is the slope of the linear regression [29].

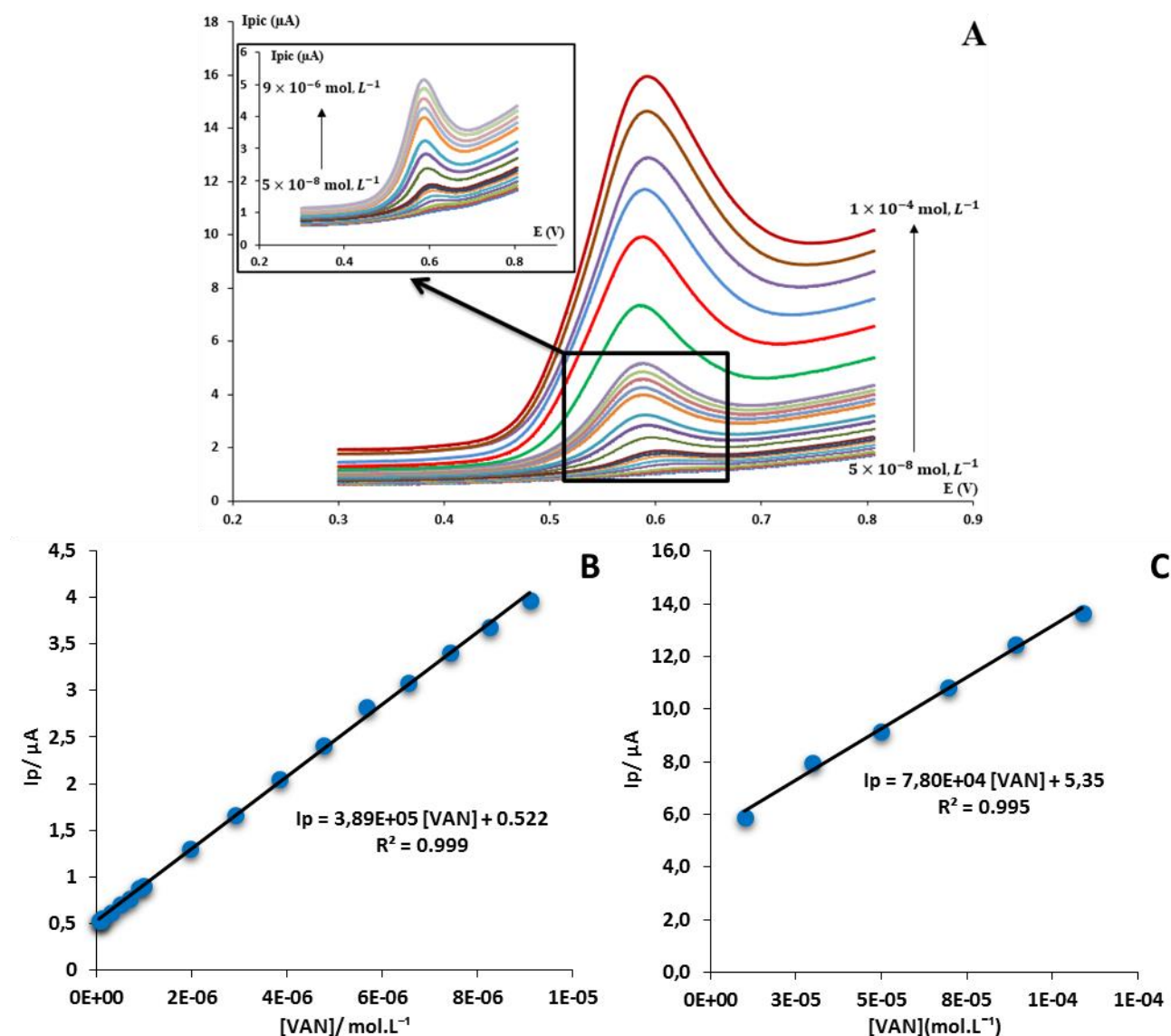


Figure III.7. (A) Cyclic voltammograms of VAN from 5×10^{-8} to $1 \times 10^{-4} \text{ mol.L}^{-1}$ at f-MWCNTs-FNTs/ CPE in BRS 0.04M (pH = 7), Insert: from 5×10^{-8} to $9 \times 10^{-6} \text{ mol.L}^{-1}$. (B, C) Calibration curves of VAN concentrations against peak current from 5×10^{-8} to $9 \times 10^{-6} \text{ mol.L}^{-1}$ and from 1×10^{-5} to $1 \times 10^{-4} \text{ mol.L}^{-1}$, respectively.

As can be seen on Table III.2, the f-MWCNTs-FNTs/CPE prepared sensor shows a low detection limit and a large linear concentration range compared to those reported in the literature.

Thus, the proposed electrochemical sensor show very good performances by just using a few cost electrodes materials in comparison with some reports that give practically similar analytical characteristics. It is also distinguished by the simplicity and the quick modification step of the electrode, which make it an attractive sensor for the monitoring of the quality analysis of food products containing VAN as additive [10, 13, 26, 30-34].

Table III.2. Comparison of this work with the previously reported VAN analysis with electrochemical sensor

Electrode	LR (mol.L ⁻¹)	LOD (mol.L ⁻¹)	Ref.
CB/SPCE ¹	5×10 ⁻⁵ to 4.5×10 ⁻⁴	3.9×10 ⁻⁸	[10]
CNT-SPE ²	2.5×10 ⁻⁶ to 7.5×10 ⁻⁴	1.03×10 ⁻⁶	[13]
Au-MWCNTs/GCE ³	7×10 ⁻⁸ to 6.5×10 ⁻⁶ and 7×10 ⁻⁶ to 7.5×10 ⁻⁵	3.8×10 ⁻⁸	[26]
p-PGE ⁴	5×10 ⁻⁷ to 1×10 ⁻⁵	1.6×10 ⁻⁷	[29]
C ₃ N ₄ /GCE ⁵	2×10 ⁻⁸ to 1×10 ⁻⁵ and 1.5×10 ⁻⁵ to 2×10 ⁻⁴	7×10 ⁻⁹	[30]
BGPE ⁶	4×10 ⁻⁶ to 1.5×10 ⁻⁵ and 2×10 ⁻⁵ to 7×10 ⁻⁵	1.29×10 ⁻⁶	[31]
T3T-Au electrode ⁷	1×10 ⁻⁷ to 1.13×10 ⁻⁵	4×10 ⁻⁸	[32]
CPE/NiO-SWCNTs/BPrPF ₆ ⁸	1×10 ⁻⁸ to 3.5×10 ⁻⁴	4×10 ⁻⁹	[33]
f-MWCNTs-FNTs/ CPE	5×10 ⁻⁸ to 9×10 ⁻⁶ and 1×10 ⁻⁵ to 1×10 ⁻⁴	3.5×10 ⁻⁸	This work

¹Carbon Black Nanoparticles Modified Screen Printed Carbon Electrode, ²Multi-walled carbon nanotube screen-printed electrode, ³Gold nanoparticles modified multi-walled carbon nanotubes glassy carbon electrode, ⁴Pre-oxidized Pencil Graphite Electrode, ⁵Pyrolyzed graphitic carbon nitride electrode, ⁶Bare graphene paste electrode, ⁷1H-1,2,4-triazole-3-thiol polymer film modified gold electrode, ⁸Carbon Paste Electrode modified with NiO decorated single wall carbon nanotubes and 1-butylpyridinium hexafluorophosphate.

III.2.8. Repeatability and reproducibility of f-MWCNTs-FNTs/ CPE

The repeatability of the nanostructured carbon paste electrode is carried for three different concentrations (10^{-7} , 10^{-6} and 10^{-5} mol.L⁻¹) in order to cover the two control processes; adsorption and diffusion. Three successive measurements were carried out for each concentration using the same sensor. The resulting values of relative standard deviation (RSD) presented in Table III.3 indicate acceptable repeatability (RSD < 7 %). Furthermore, reproducibility is checked by recording the current response of the three concentrations at two independent sensor prepared with the same procedure and paste composition. As we can see in Table III.3, the obtained values of RSD are lower than 6 % and good accuracy could be achieved especially for the lowest concentration (10^{-7} mol.L⁻¹) with RSD value of 2.1 %.

Table III.3. Study of repeatability and reproducibility of the f-MWCNTs-FNTs/ CPE for different VAN concentrations in BRS 0.04 M (pH = 7); pre-concentration time under stirring 300 s; 20 mV.s⁻¹.

VAN concentration (μM)	Determination of repeatability & reproducibility	
	Repeatability of I_p RSD % *	Reproducibility of I_p RSD % **
0.1	2.1	2.1
1	6.7	5.8
10	2.9	1.1

*n=3, **n=2

III.2.9. Selectivity of f-MWCNTs-FNTs/ CPE

The selectivity of the f-MWCNTs-FNTs/CPE was tested using the CV technique in adsorption control process by recording the response of 10^{-6} mol.L⁻¹ of VAN in the presence of some potential interfering substances at similar concentrations (Fig. III.8).

The presence of sugars such as glucose and saccharose has no noticeable effect on peak intensity (variation < 5 %). This indicates that it is unlikely to have matrix effects for the analysis of vanilla sugars. The greatest effects were observed for caffeine and uric acid with a variation not exceeding 22 %. These low variations in the oxidation current response of VAN are likely due to the presence of similar electroactive functional group. In order to preserve the selectivity of VAN for samples containing these interferents, it is preferable to dilute them to minimize their concentrations and to analyze low concentrations of VAN with an adsorption step to guarantee the specificity of the response. Indeed, for any target molecules to be selectively absorbed on the electrode surface, they must have sufficient affinity for the sensor material to be detected. This affinity can be governed by an adsorption equilibrium constant, which can be sufficiently

different to specifically detect a particular analyte, depending on the properties of the electrolyte (pH in our case), the surface properties of the carbon paste and the hydrophobic/hydrophilic character of the molecule.

Even if we did not test all the molecules that could be present in the same matrix as vanillin, we chose to study only some of the molecules that may interfere in the vanilla sugar samples (the sample chosen to do the validation). As shown in the following table (Table III.4), vanillin has a hydrophobic character ($\log Kow = 1.37$) compared to rather hydrophilic molecules ($\log Kow < 0$). This is probably not the own reason that could explain this selectivity. Indeed, the possibility of the charge on the molecule, in relation with pKa value and the pH of the electrolyte, could influence molecule adsorption on carbon paste. For vanillin ($pKa = 7.4$), it adsorbs in neutral form whereas other molecules studied such as uric acid and ascorbic acid ($pKa < 5.5$) negatively charged in the BR solution ($pH = 7$), their adsorption could be unfavorable.

Table III.4. Values of pKa and Log Kow for some interfering compounds

	Vanillin	Saccharose	Glucose	Caffeine	Uric acid	Ascorbic acid
pKa	7.4	12.62	12.92	14	5.4	4.7
Log Kow	1.37	-3.7	-3.0	-0.07	Not founded	-1.85

Other interferents such sulfate, chloride, Fe(III), oxalate and acetate ions show negligible impact on current responses. Therefore, the results demonstrate the possibility to obtain high selectivity of f-MWCNTs-FNTs/CPE toward VAN and permit the feasibility for real food sample analysis of VAN.

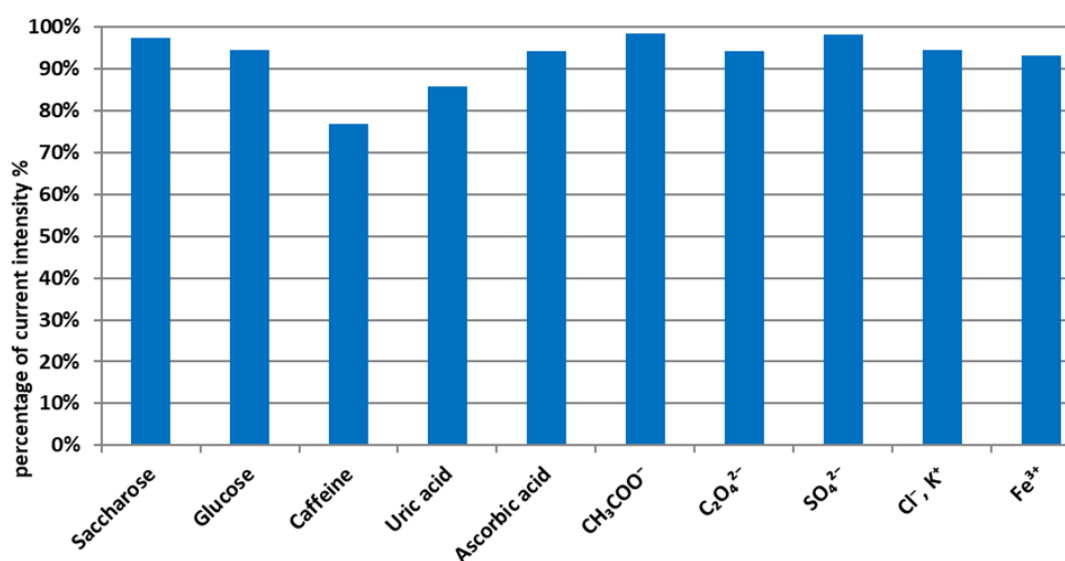


Figure III.8. The relative peak current response of 1 μ M VAN in the presence of some potential interfering substances at the f-MWCNTs-FNTs/ CPE in BRS 0.04 M ($pH = 7$).

III.2.10. Stability of f-MWCNTs-FNTs/ CPE

The stability of a sensor is an important parameter that leads to a practical and usable device for long time. The study of this parameter for the f-MWCNTs-FNTs modified carbon paste electrode is evaluated using CV for 10^{-5} mol.L⁻¹ VAN in BRS (pH = 7) at 20 mV.s⁻¹. Then, the CV current responses were tested before and after storage at 25 °C during 10 days without following a specific procedure and the results are shown in Fig III.9. It appears that the electrode remains stable during 7 days storage, with a slight decreasing of peak current lower than 5%. The variation does not exceed 10 % after 10 days indicating a good stability of the sensor.

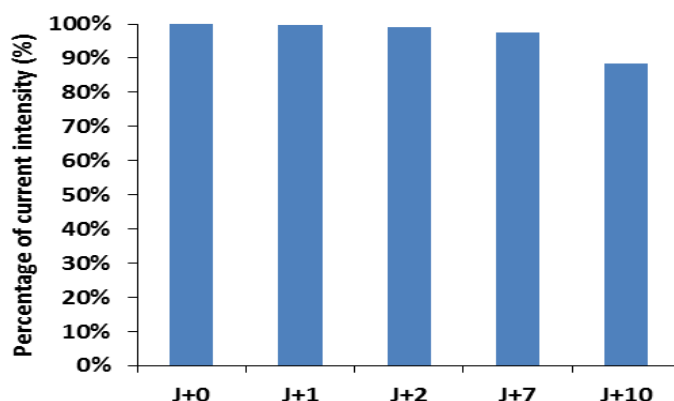


Figure III.9. The study of stability of the f-MWCNTs-FNTs/ CPE of the relative peak current response of 1 μ M VAN in 10 days of storage.

III.2.11. Validation of the proposed sensor in sugar vanilla samples

The performance and the feasibility of the f-MWCNTs-FNTs developed sensor to quantify VAN was evaluated for four real sugar vanilla samples from different commercial brands for which the manufacturers do not indicate the VAN proportion in composition. The concentration of VAN in the samples was determined by standard addition method by successively adding known amounts of VAN (2×10^{-6} , 4×10^{-6} and 6×10^{-6} mol.L⁻¹) to the electrochemical cell containing the electrolyte in which the sugar sample was dissolved (as described in section II.8.1). This operation was achieved in triplicate for each sugar sample.

In order to validate the results, UPLC/UV was used as a control method to determine the content of VAN in the four sugar vanilla samples. Each sample of the different brands of commercial sugar vanilla was analyzed by UPLC/UV method, after making a calibration curve using a standard VAN solution prepared with a synthetic vanillin in the range of 0.5 to 15 mg.L⁻¹. The retention time and peak area of each VAN concentration are shown in Table III.5 and Fig. III.10 shows the corresponding calibration curve.

Table III.5. Results of UPLC/UV analysis of the VAN standard solutions

Concentration (mg.L ⁻¹)	Surface (μV.sec)	tr (min)
0.5	38049	2.029
1	76958	2.033
2	157776	2.033
5	374727	2.03
10	759452	2.03
15	1199321	2.032

An excellent linearity ($R^2 > 0.999$) in the concentration range of 0.5 to 15 mg.L⁻¹ for UPLC/UV was found for the standard solution. This calibration curve was used for the determination of the VAN concentration in the different brands of commercial sugar vanilla. Then the concentration of the analyzed samples is calculated from the calibration line (results showed in Table III.6).

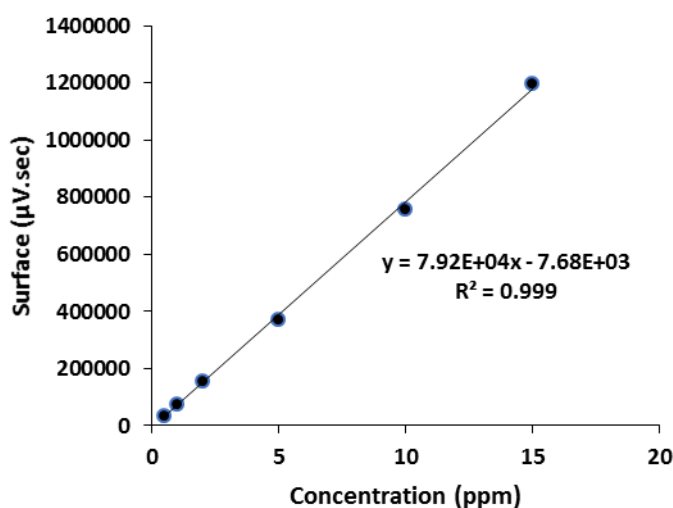


Figure III.10. Calibration curve of the VAN standard solutions

Table III.6. Results of UPLC/UV analysis of the different samples of sugar vanilla

Samples (S)		Surface ($\mu\text{V}.\text{sec}$)	Concentration (ppm)	Mean (ppm)	RSD (%)
S1	Injection 1	282801	3.67	3.68	0.29
	Injection 2	285118	3.70		
	Injection 3	284268	3.69		
S2	Injection 1	360572	4.65	4.65	0.13
	Injection 2	361312	4.66		
	Injection 3	359829	4.64		
S3	Injection 1	275756	3.58	3.58	0.11
	Injection 2	275969	3.58		
	Injection 3	275160	3.57		
S4	Injection 1	213468	2.79	2.78	0.68
	Injection 2	214194	2.80		
	Injection 3	210437	2.75		

The results obtained with the proposed method and the control analytical method are compiled in Table III.7. The VAN contents of the different samples ranged from 0.19 to 0.32 $\mu\text{mol.L}^{-1}$ VAN per g sugar (less than 0.5 %), which is on accuracy with the vanillin amount in sugar vanilla stipulated by the expert vanilla, with a repeatability comparable to that previously observed in synthetic solutions (see section III.2.8).

The results obtained with the developed sensor are in accordance with those obtained by the UPLC/UV control method (recovery values between 100-107 % for the different samples). We can conclude that the constituents of vanilla sugar do not interfere in the VAN analysis.

Therefore, the proposed nanostructured composite modified carbon paste electrode (f-MWCNTs-FNTs/CPE) is able to control the VAN as ingredient after simple dissolution of vanilla sugar samples without extraction procedure. This proposed electroanalytical method demonstrates good accuracy of the proposed sensor and its feasibility in food sample analysis.

Table III.7. Determination of VAN mass fraction indifferent real commercial sugar vanilla samples with electrochemical and UPLC/UV methods

Sugar samples	Determination of VAN mass fraction mg.g ⁻¹				Recovery (%)
	Electrochemical method (n=3)		UPLC Analytical method (n=3)		
	Mean± confidence interval***	RSD %	Mean± confidence interval***	RSD %	
E1	3.91± 0.22	3.0	3.67± 0.02	0.3	106.5
E2	4.79± 0.92	10.4	4.61± 0.02	0.2	103.9
E3	3.64± 0.23	3.3	3.61± 0.01	0.1	100.8
E4	2.88± 0.34	6.5	2.76± 0.02	0.7	104.3

Conclusion

In this chapter, was fabricated a sensitive sensor for the quantification of the vanillin using a modified carbon paste electrode with fullerene and functionalized multi-walled carbon nanotubes. The both optimization of operating conditions and the study of the performances of the sensor was investigated by cyclic voltammetry. The results show a large linear responses from 5×10^{-8} to 9×10^{-6} mol.L⁻¹ for VAN trace concentrations and from 10^{-5} to 10^{-4} mol.L⁻¹ for higher levels, with a low detection limit of 3.4×10^{-8} mol.L⁻¹, in BR solution (0.04 M) at pH = 7, after a previous stirring step (300 s).

The optimized conditions indicate that the electron-transfer process of the reaction of VAN oxidation involved an equal number of protons and electrons and it is not control by the same controlled process: the peak current is controlled by an adsorption step of VAN at the electrode surface for [VAN] < 10^{-5} mol.L⁻¹ and for highest concentration (> 10^{-5} mol.L⁻¹) the peak current is controlled by the diffusion of VAN.

The results of morphology characterization of f-MWCNTs-FNTs electrode surface demonstrate that the combination of f-MWCNTs, FNTs and graphite are linked in a way that avoid the stacking of graphite platelet and promote the accessibility to VAN in their surfaces and improve the charge transfer in the paste. This uniform and nanostructured modified electrode gives a greater specific surface with a reduced charge transfer resistance and an increase in the electron transfer kinetic. The selectivity of this sensor toward the detection of VAN is assured by its affinity to be adsorbed selectively on the surface of the electrode and its molecule charge in relation with pKa value and pH of electrolyte, it was previously demonstrated that VAN is adsorbed preferentially in neutral form.

The proposed modified electrode was successfully applied to the determination of vanillin in commercial sugar vanilla samples with a satisfactory recovery in comparison of the control UPLC/UV analytical method and without any specific preparation of the samples, just by dissolving the sample in the BRS electrolyte.

Hence, the so-designed f-MWCNTs-FNTs modified CPE is a suitable, promising and preferential sensor to quantify and monitor vanillin as ingredient in commercial food compared to those founded in the literature, because it offers more advantages in the simplicity and feasibility to the determination of the real vanillin concentration in real matrices, with any pretreatment by following a clearer procedure. Moreover, in our study, to have a very lower LOD is not our objective, because we aim to quantify and monitor the concentration of vanillin

in real food samples. Furthermore, our sensor use very simple materials, economical and show a very good characteristics and very selective for the detection of vanillin.

References

- [1] Martins, F.C.O., Sentanin, M.A. & de Souza, D. (2018). Analytical methods in food additives determination: compounds with functional applications, *Food Chemistry*, 272, 732.
- [2] World Health Organisation, Food additives. (2018). From <https://www.who.int/news-room/fact-sheets/detail/food-additives> 11-2-2021. Accessed 11 February 2021.
- [3] Food Safety Helpline.com. (2015). What are Flavouring Agents? What do FSSAI Regulations say? From <https://foodsafetyhelpline.com/what-are-flavouring-agents-what-do-fssai-regulations-say/>. Accessed 11 February 2021.
- [4] Gelski, J. (2019). Vanilla prices slowly drop as crop quality improves, Food Business News. From <https://www.foodbusinessnews.net/articles/13570-vanilla-prices-slowly-drop-as-crop-quality-improves>. Accessed 11 February 2021.
- [5] Gallage, N. J. & Møller, B. L. (2015). Vanillin–Bioconversion and Bioengineering of the Most Popular Plant Flavor and Its De Novo Biosynthesis in the Vanilla Orchid, *Molecular Plant*, 8 (1), 40.
- [6] Research and Markets, The World's Largest Market Research Store (2019). Vanilla and Vanillin Market: Global Industry Trends, Share, Size, Growth, Opportunity and Forecast 2019-2024, IMARC Group, Report ID: 4752325.
- [7] Isac-García, J., Dobado, J. A., Calvo-Flores, F. G. & Martínez-García, H. (2016). Chapter 11 - Microscale Experiments. Editors: Isac-García, J., Dobado, J. A., Calvo-Flores, F. G. & Martínez-García, H. In *Experimental Organic Chemistry*, Academic press, 371.
- [8] National Center for Biotechnology Information (2021). PubChem Compound Summary for CID 1183, Vanillin. From <https://pubchem.ncbi.nlm.nih.gov/compound/Vanillin>. Accessed 14 February 2021.
- [9] Sinha, A.K., Sharma, U.K. & Sharma, N. (2008). A comprehensive review on vanilla flavor: Extraction, isolation and quantification of vanillin and others constituents, *International Journal of Food Sciences and Nutrition*, 59 (4), 299.
- [10] Vijayalakshmi, S., Disalva, X., Srivastava, C. & Arun A. (2019). Vanilla- Natural Vs Artificial: A Review. *Research Journal of Pharmacy and Technology*, 12 (6), 3068.
- [11] Kutty, M., Settu, R. I., Chen, S. M., Chen, T. W., Tseng, T. W., Hatamleh, A. A., Yu, J., Yu, R. & Huang, C. C. (2019). An Electrochemical Detection of Vanillin Based on Carbon Black Nanoparticles Modified Screen Printed Carbon Electrode, *International Journal of Electrochemical Science*, 14, 5972.

- [12] Zhao, J., Xia, H., Yu, T., Jin, L., Li, X., Zhang, Y., Shu, L., Zeng L. & He, Z. (2018). A colorimetric assay for vanillin detection by determination of the luminescence of o-toluidine condensates, *PLoS One*, 13 (4), e0194010.
- [13] Chen, L., Chaisiwamongkhol, K., Chen Y. & Compton, R.G. (2019). Rapid Electrochemical Detection of Vanillin in Natural Vanilla, *Electroanalysis*, 31 (6), 1067.
- [14] Sivakumar, M., Sakthivel, M. & Chen, S.-M. (2017). Simple synthesis of cobalt sulfide nanorods for efficient electrocatalytic oxidation of vanillin in food samples, *Journal of Colloid Interface Science*, 490, 719.
- [15] Bezerra, D.P., Soares, A. K.N. & De Sousa, D.P. (2016). Overview of the role of vanillin on redox status and cancer development, *Oxidative Medicine and Cellular Longevity*, 9.
- [16] Younes, M., Aggett, P, Aguilar, F., Crebelli, R., Dusemund, B., Filipic, M., Jose Frutos, M., Galtier, P., Gundert-Remy, U., Georg Kuhnle, G., Lambre, C., Leblanc, J. C., Therese Lillegaard, I., Moldeus, P., Mortensen, A., Oskarsson, A., Stankovic, I., Waalkens-Berendsen, I., Woutersen, R. A., Wright, M., Tobback, P., Smeraldi, C. & Gott, D. (2018). Safety of orthosilicic acid-vanillin complex (OSA-VC) as a novel food ingredient to be used in food supplements as a source of silicon and bioavailability of silicon from the source, *EFSA Journal*, 16 (1), 5086.
- [17] Ramesh, M. & Muthuraman, A. (2018). Flavoring and Coloring Agents: Health Risks and Potential Problems, *Natural and Artificial Flavoring Agents and Food Dyes, Handbook of Food Bioengineering*, 1.
- [18] Sherigara, B. S., Kutner, W. & Souza, F. D. (2003). Electrocatalytic Properties and Sensor Applications of fullerenes and Carbon Nanotubes, *Electroanalysis*, 15 (9), 753.
- [19] Pan, Y., Liu, X., Zhang, W., Liu, Z., Zeng, G., Shao, B., Liang, Q., He, Q., Yuan, X., Huang, D. & Chen, M. (2020). Advances in photocatalysis based on fullerene C60 and its derivatives: Properties, mechanism, synthesis, and applications, *Applied Catalysis B: Environmental*, 265, 118579.
- [20] Pilehvar, S. & Wael, K. D. (2015). Recent Advances in Electrochemical Biosensors Based on FNTserene-C60 Nano-Structured Platforms, *Biosensors*, 5 (4), 712.
- [21] Miyazawa K. (2009). Synthesis and properties of fullerene nanowhiskers and fullerene nanotubes. *Journal of nanoscience and nanotechnology*, 9 (1), 41.
- [22] D'Souza, O. J., Mascarenhas, R. J., Satpati, A. K., Mane, V. & Mekhalif Z. (2017). Application of a Nanosensor Based on MWCNT-Sodium Dodecyl Sulphate Modified Electrode for the Analysis of a Novel Drug, Alpha-Hydrazinonitroalkene in Human Blood Serum, *Electroanalysis* 29 (7), 1794.

- [23] Bard, A. J. & Faulkner, L. R. (2001). *Electrochemical Methods: Fundamentals Applications*, (2nd Eds), New York: Wiley, 87.
- [24] Denuault, G., Mirkin, M. V. & Brad, A. J. (1991). Direct determination of diffusion coefficients by chronoamperometry at microdisk electrodes, *Journal of Electroanalytical Chemistry* 308, 27.
- [25] Serjeant, E.P. & Dempsey B. (1979). Ionisation constants of organic acids in aqueous solution, *International union of pure and applied chemistry, IUPAC Chemical Data Serie*, 23, 989.
- [26] Ceylan Koçak, Ç. & Ulubay Karabiberoğlu, Ş. (2018). Electrochemical Vanillin Determination on Gold Nanoparticles Modified Multiwalled Carbon Nanotube Electrode, *Journal of Science and Engineering*, 20 (59), 461.
- [27] Abbasghorbani, M. (2017). Electrochemical Determination of Vanillin in Food Samples Using MgO/SWCNTs-ionic Liquid Modified Electrode, *International Journal of Electrochemical Science*, 12 (12), 11656 .
- [28] Kalaiyarasi, J., Meenakshi, S., Pandian, K. & Gopinath, Subash C. B. (2017). Simultaneous voltammetric determination of vanillin and guaiacol in food products on defect free graphene nanoflakes modified glassy carbon electrode, *Microchim Acta*, 184, 2131.
- [29] Shrivastava, A. & Gupta, V. B. (2011). Method for the determination of limit of detection and limit of quantification of the analytical methods, *Chronicles of Young Scientists*, 2 (1), 21.
- [30] Dilgin, D. G. (2019). Voltammetric Determination of Vanillin Using a Pretreated Pencil Graphite Electrode, *Akademik Gıda*, 17 (1), 1.
- [31] Fu, L., Xie, K., Wu, D., Wang, A., Zhang, H. & Ji, Z. (2020). Electrochemical determination of vanillin in food samples by using pyrolyzed graphitic carbon nitride, *Materials Chemistry and Physics*, 242, 122462.
- [32] Raril, C. & Manjunatha, J.G. (2020). A simple approach for the electrochemical determination of vanillin at ionic surfactant modified graphene paste electrode, *Microchemical journal*, 154, 104575.
- [33] Tabanlıgil Calam, T. (2020). Voltammetric determination and electrochemical behavior of vanillin based on 1H-1,2,4-triazole-3-thiol polymer film modified gold electrode, *Food Chemistry*, 328, 127098.
- [34] Gupta, V. K., Karimi-Maleh, H., Agarwal, S., Karimi, F., Bijad, M., Farsi, M., Shahidi, S. A. (2018). Fabrication of a Food Nano-Platform Sensor for Determination of Vanillin in Food Samples, *Sensors*, 18, 2817.

Chapter IV

***Cavity microelectrode based on carbon black
and activated carbon for the simultaneous
detection of 4-aminophenol, paracetamol and
ciprofloxacin in water and urine***

Introduction

Pharmaceuticals products are essential and indispensable compounds around the globe, more than 3000 products are used to prevent or treat diseases for human and animals [1]. Global pharmaceutical uses were estimated to be in the range of 166 million to 373 million people worldwide in 2018 [2]. However, these drugs have not only beneficial effects. Indeed, their uncontrollable increase consumption leads to a risk for humans, animals and environment. Drug overdoses contribute to the raise in mortality worldwide, for example, in US, 67 367 people died from drug overdoses in 2018 [3]. Moreover, pharmaceuticals are excreted daily in environment via urine. A person produces approximately 1.2 L urine per day, which may contain, in addition to nutrients (nitrogen and phosphorus), hormones and pharmaceuticals. The presence of drug compounds in urine can be indicative of disease in the human body when present in high concentration, but it is also a source of environment pollution, even at low amounts, as these substances can be transferred into the food chain by seepage into groundwater [4]. Therefore, analysis of urine samples is essential to monitor human health and prevent the contamination of wastewater.

In this chapter of the thesis, we focused on two of the most widely used pharmaceuticals and emerging pollutants in the aquatic environment, namely paracetamol and ciprofloxacin. In addition to 4-aminophenol, an intermediate drug involved in the synthesis of paracetamol and in various pharmaceutical formulations.

In the recent decade, research has focused on the detection of these three drugs with the development of methods that offer simple, economical, fast and in situ analysis. Various studies report the analytical determination of the mentioned products such as chromatography [5-7], fluorescence spectroscopy [8-10] and capillary electrophoresis detection [11-13]. However, as it is known, the conventional methods are complicated; require expansive and specific equipment and their response is often slow. Nevertheless, the electrochemical methods are a promising alternative that combine performance, reliability, low-cost, high sensitivity and allow in situ and real-time analyzes. In this context, several papers report the electrochemical analysis of ciprofloxacin, paracetamol and 4-aminophenol separately [14, 16]. Other studies have reported the simultaneous electrochemical detection of both aminophenol and paracetamol [17], ciprofloxacin and paracetamol [18]. However, to our knowledge, no work has been reported on the simultaneous electrochemical detection of these three pharmaceuticals products.

Chapter IV: Simultaneous detection of 4-aminophenol, paracetamol and ciprofloxacin

Thus, in order to simultaneously analyze ciprofloxacin, paracetamol and 4-aminophenol with a single sensitive device, we propose a first nanostructured sensor for the detection of these three analytes.

In this chapter, we first present some general information on pharmaceuticals. Then, in the second part, we describe the optimization, design and validation of the proposed modified cavity microelectrode for the simultaneous detection of ciprofloxacin, paracetamol and 4-aminophenol.

Part IV.1: Pharmaceutical products

In this part, we present general information about pharmaceuticals, how they contaminate the environment and the risk of their presence in aquatic environment. We also present the three drugs (ciprofloxacin, paracetamol and 4-aminophenol); discuss their proprieties, uses, side effects and standards for each.

IV.1.1. Introduction

Pharmaceuticals are very important substances for the human and animal body. However, the industrial revolution, increase in living standards and huge population explosion have led to a large and uncontrollable use of these substances [19]. Extensive medicines ingestion leads to overdose poisoning and risk of mortality [20]. Moreover, most used antibiotics are discharged by various ways in the environment and are detected in aquatic ecosystems in the ng/L to mg/L concentration range [21]. In addition, their accumulation, even at low concentrations, constitutes serious problems for the aquatic organism without forgetting the risk of contamination of foods, wastewater and drinking water. Pharmaceuticals and their metabolites are recognized as emerging contaminants for the environment [22]. Among the most common used drugs in the world are paracetamol and ciprofloxacin, in addition to the 4-aminophenol that is used as drug intermediate in various pharmaceutical formulations. These pharmaceuticals present a risk for human health when they are taken on overdose and a risk for environmental water, aquatic life and a risk of bacteria resistance after accumulation in foods and water.

IV.1.2. Pharmaceutical products generality

Pharmaceutical products, also known as Medicines or Drugs, are a combination of active substances with additional materials (excipients), which are selected to control dosage delivery, enhance performance and facilitate manufacturing [23]. These medicines have several proprieties to prevent or to treat a disease and to restore the health of the organism [24]. For this reasons, the use of drugs is increasingly used worldwide in human and veterinary therapy [25].

In order to assure a drug safety use and achieve the utmost benefits, the medicines are generally classified on various pharmacologic classes, basing to their:

- chemical structure;
- mechanism of action: is the specific biochemical reaction that can be at the receptor, membrane or tissue level;
- and, physiologic effect: that mean the specific way in which the organ, system, or whole body respond to the drug [26].

According to the United States Pharmacopeia (USP), the drug compounds are classified under one of 49 different therapeutic classes, such as antibiotics, antipyretics, analgesics, anti-inflammatories, antidepressants and hormones [27].

IV.1.3. Source of pharmaceutical contaminants in environment

Pharmaceutical compounds attain the environment via several ways. After ingestion by human and animals, the drugs are excreted with urine either in their native form or in metabolites forms, and are introduced into the sewage system. In addition, antibiotics and hormones are often used in livestock, which can contaminate the soil and water [28]. The pharmaceutical industry, hospitals and domestic discharge contribute in the introduction of pharmaceuticals in municipal wastewater [29]. Despite the wastewater treatment plants (WWTPs), the pharmaceuticals products stay suspended in water after WWTPs, because this procedure have a limited removal efficiency for this kind of organic micropollutants, which are often no biodegradable and have a high solubility that favor their environmental persistence. Therefore, the resulting effluents lead to the contamination of surface water, groundwater and drinking water [30]. Furthermore, these microsubstances remain in ecosystem in different links of the food chain either in water or in food [31].

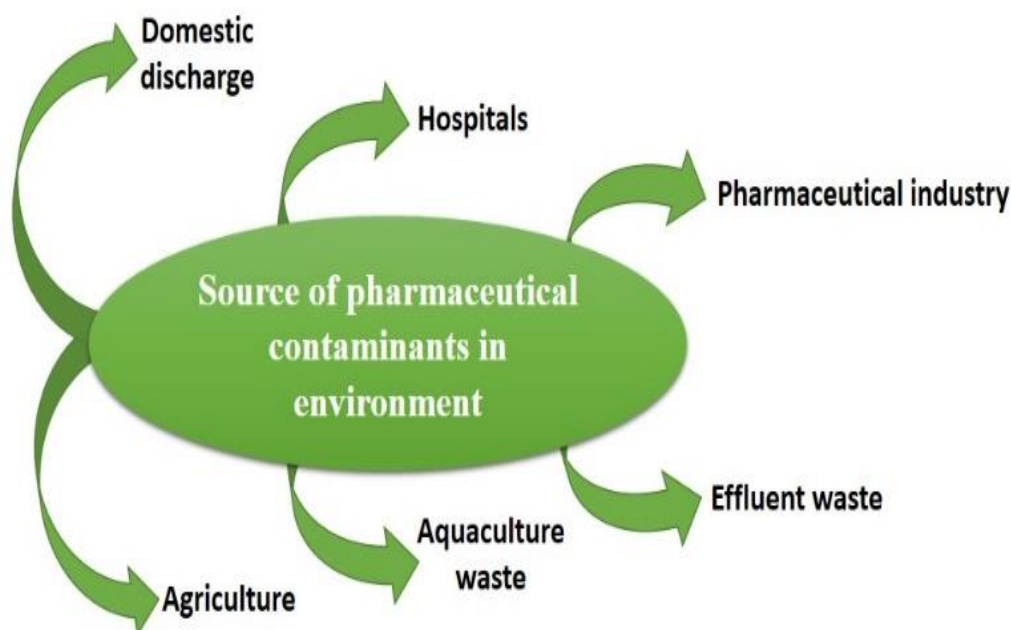


Figure IV.1. Major source of pharmaceutical contaminants in environment

IV.1.4. Pharmaceutical substances in the aquatic environment

According to the database reviewed in the literature, the most frequently identified pharmaceuticals in water belong to the beta-blocker group, non steroidal anti inflammatory drugs, drugs affecting nervous system, hormones, lipid regulators and antibiotics [32].

The studies on occurrence of pharmaceuticals in aquatic environment in each UN regional group have been reported in Fig. IV.2. It was noticed that more than 100 different pharmaceutical substances have been found in several European countries and the United States Followed Asia-Pacific, Latin American and Caribbean States countries. For the Africa Group, 30 different pharmaceutical substances or fewer have been detected but no data is available for the major region of this group [33]. Furthermore, as pharmaceuticals products are frequently and mostly detected in waters, they are considered as emerging pollutants [34].

Thus, the presence of drugs in aquatic environment represents one of the main concerns that must have a great attention and monitoring.

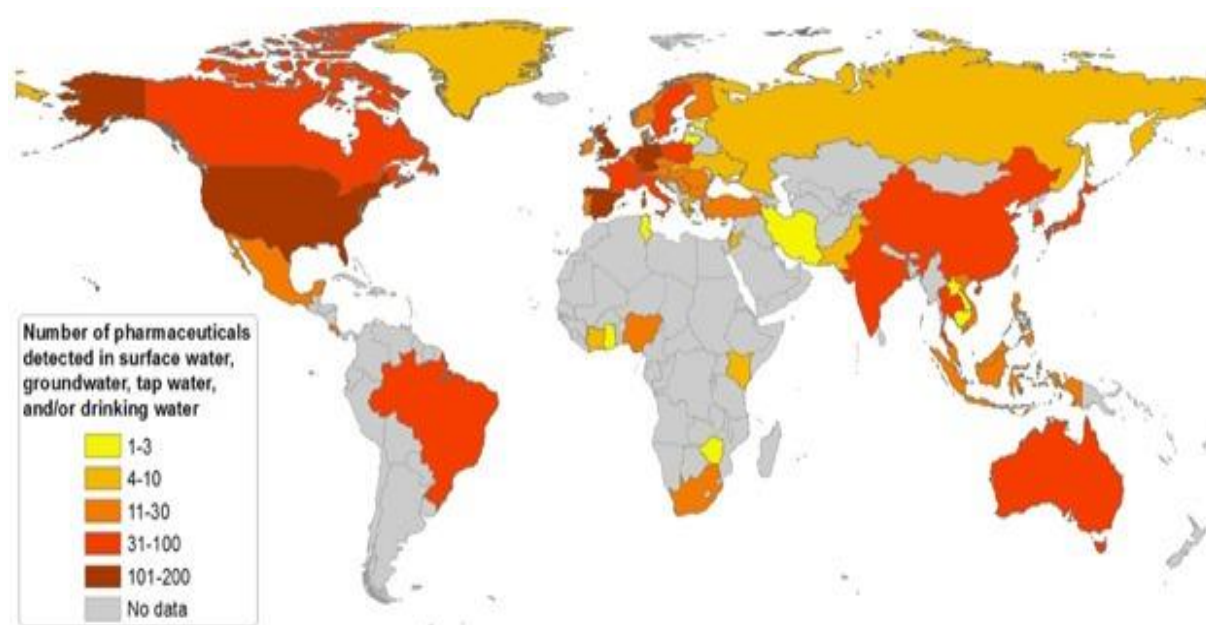


Figure IV.2. Country survey on the number of pharmaceutical substances detected in surface waters, groundwater, or tap/drinking water [33].

IV.1.5. Risk of the presence of pharmaceuticals in environment

The presence of pharmaceutical products in surface and drinking water leads to several adverse effects on humans and ecosystems. In surface waters, these compounds behave as pseudo-persistent organic pollutants that exhibit toxic effects on aquatic organisms, consequently, are a risk to humans [28]. Moreover, as most of these products are not biodegradable, their accumulation leads to their moving through the food chains to lead finally to human body. Contamination of drinking water or food with pharmaceuticals leads to the emergence of antibiotic resistant strains of bacteria, reproductive disorders in various animals with the appearance of unnatural physiological processes, increased cases of cancer and increased levels of toxicity due to the mixing of various metabolites are other potential problems associated with pharmaceutical contaminants [19]. Ingestion of PAR overdose leads to paracetamol poisoning, if a patient has ingested less than 75 mg/kg, the dose should be non-toxic, whereas if a patient has ingested more than 150 mg/kg, the overdose is potentially serious [35], and the patient may develop an hepatic toxicity, kidney and/or liver damages [36] that can lead to oxidative stress, self-poisoning and hepatocyte death [35].

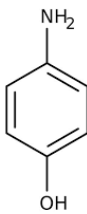
For to the above-mentioned reasons, it is almost important and necessary to develop monitoring and control devices for even trace amounts of pharmaceuticals in the environment.

IV.1.6. Aminophenol

IV.1.6.1. Generality

4-Aminophenol (or p-aminophenol) is chemically 4-Hydroxyaniline, a white chemical powder. An organic compound with an aromatic ring substituted by two oxidizable groups (NH_2 and OH), is one of the three isomers of aminophenol, which has the amino substituent in para position to the phenolic $-\text{OH}$ group [37]. The Table IV.1 show physicochemical proprieties of 4-aminophenol at ambient temperature.

Table IV.1. Main physicochemical properties of 4-aminophenol [37].

4-Aminophenol		
N° CAS	123-30-8	<i>Molecular formula</i> 
Molecular weight	109.13 g.mol ⁻¹	
Solubility in water (at 25 °C)	1.6 x 10 ⁺³ mg.L ⁻¹	
pKa	5.48 ; 10.46	
Log Kow	0.04	
Boiling Point	284 °C	
Melting Point	187.5 °C	

IV.1.6.2. Uses

4-Aminophenol has been widely used for different purposes. It involved as the drug intermediates in several pharmaceutical preparations, such as the paracetamol production where it is used like a basis pharmaceutical intermediate in the reaction of acetylation of aminophenol with acetic anhydride [38]. The p-aminophenol is also extensively used in the photography industry, preparation of thermal dyes, development of antioxidants, the manufacture of stabilizers of polymeric materials, and the preparation of certain types of pesticides [39].

Furthermore, this organic compound serves as intermediate in the production of sulfur and azo-dyes which have useful applicability in the textile, leather and alimentary industries [40].

IV.1.6.3. Side effects

P-Aminophenol is a toxic organic compound that can contaminate environment as well as pharmaceuticals. It is usually used as drug intermediate in various pharmaceutical productions; it is therefore considered to be the main impurity that can affect the medicine products, this impurity can result from the degradation of drugs (like paracetamol) or from the presence of this drug intermediate in the final product [41]. The excessive ingestion or exposition to aminophenol can cause serious problems to human body, such as dermatitis, allergic reactions, nephrotoxicity and teratogenic effects [42, 43]. This organic compound is considered to be an environmental pollutant having a toxic effect on the aquatic environment [44]. Due to all these negative effects associated with the use of this intermediate drug, monitoring its amount is necessary to ensure the quality of the final product, human health and environment protection.

IV.1.6.4. Norms

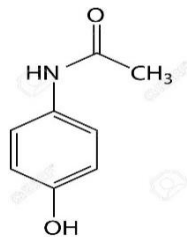
The European, United States and Chinese Pharmacopoeias authorities stipule that the tolerance level of AMP in drugs formulations substances do not excited 50 ppm (limit of detection of 23 μM) [45]. In addition, the detection of AMP in urine sample should be a useful indicator to monitor the health of individual exposed to aniline, because once it is absorbed, it will extensively oxidized to p-aminophenol. Thus, the urine p-aminophenol concentration serves as a biological marker for evaluate the exposures to aniline. It should be noted that the 4-aminophenol acceptable level found in individuals should be less than 10 mg.L^{-1} ($9 \times 10^{-5} \text{ mol.L}^{-1}$) [46].

IV.1.7. Paracetamol

IV.1.7.1. Generality

Paracetamol (Acetaminophen), chemically called N-(4-Hydroxyphenyl) acetamide, an odorless white crystalline solid with bitter taste [47]. It is a benzene nucleus substituted by an hydroxyl group and the nitrogen atom of the amide group in the para-position [48]. Acetaminophen is synthesized by multiple routes, the mostly and effective used route is by the acetylation of 4-aminophenol [49]. Their main physicochemical properties are summarized in Table IV.2. It is an analgesic and antipyretic drug, included in the Non-Steroidal Anti-Inflammatory Drugs (NSAIDs) therapeutic group, even if it does not it proper anti-inflammatory action but their mechanism action is similar to that of NSAIDs [21].

Table IV.2. Main physicochemical properties of paracetamol [47].

Paracetamol (Acetaminophen)		
<i>N° CAS</i>	103-90-2	
<i>Molecular weight</i>	151.16 g.mol ⁻¹	
<i>Solubility in water (at 25 °C)</i>	14 mg.L ⁻¹	
<i>pKa</i>	9.38	
<i>Log Kow</i>	0.46	
<i>Boiling Point</i>	> 500 °C	
<i>Melting Point</i>	170 °C	

IV.1.7.2. Uses

Paracetamol, a drug widely prescribed and administered in daily life to treat headache, fever, postoperative pain [50], and to suppress various inflammation-related substances in animals and in inflamed dental tissue [51]. Acetaminophen is recommended as the first-line remedies for cold, flu and coronavirus (COVID-19) [52]. When paracetamol is used in a conventional oral dose, it is considered like the most efficacious, safe and cost-effective drugs needed in a health system and is included on the World Health Organization's List of Essential Medicines [53].

IV.1.7.3. Side effects

Paracetamol represents one of most emerging pollutants that is frequently detected in environmental water and represent a risk for aquatic environment [30]. These target drugs were found in both raw (effluent), treated (effluent) wastewater and tap water samples with an average concentration of 3.61–99.6 ng.mL⁻¹, < 90.5 ng.mL⁻¹ and 230 µg.L⁻¹, respectively [33,

54] In addition, when paracetamol is taken on an overindulge quantities of 4 g/ daily, it leads to serious negative effects for the human health **[55]**. Its high consumption produces an accumulation of toxic metabolites, which can lead to hepatic toxicity, kidney and liver damages **[36]**. When paracetamol becomes hepatotoxic, it leads to oxidative stress, self-poisoning and hepatocyte death **[35]**. Furthermore, acetaminophen toxicity is the second most common cause of liver transplantation worldwide and the most common in the US **[56]**.

IV.1.7.1. Norms

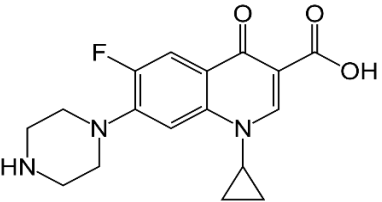
To reduce the risk of acetaminophen toxicity, the U.S. Food and Drug Administration (FDA) is asking drug manufacturers to limit the prescription of paracetamol to 325 mg per tablet, capsule, or other dosage unit, making these products safer for patient **[57]**. The recommended dose of acetaminophen for adults is 650 mg to 1000 mg every 4 to 6 hours, not to exceed 4 grams/day **[58]**. In addition, the National Medicines Safety Agency (ANSM) calls for vigilance in the use of paracetamol and stipulates their no free accessibility in pharmacies since January 2020, and strengthening the role of pharmacist advice for patients who wish to dispose of it in particular without a prescription. In order to promote the proper use of these commonly used drug **[59]**. The median paracetamol concentration in urine is around 60 mg.L⁻¹ and a high concentration mean possible adverse effects **[60]**.

IV.1.8. Ciprofloxacin

IV.1.8.1. Generality

Ciprofloxacin called chemically 1-cyclopropyl-6-fluoro-1, 4-dihydro-4-oxo-7-(piperazinyl) quinolone-3-carboxylic acid, is a faint to light yellow crystalline powder with an unpleasant taste **[61]**. Its main physicochemical proprieties are summarized in **Table IV.3**. It is a fluoroquinolone antibiotic consisted of a quinolone ring structure substituted by fluorine atom at the C-6 position and a synthetic broad spectrum antibiotic that present enhanced activity against both Gram positive and Gram negative bacteria **[62]**. Moreover, ciprofloxacin is characterized with a wide antibacterial range, low toxicity and poor antibacterial resistance **[63]**.

Table IV.3. Main physicochemical properties of ciprofloxacin [61].

Ciprofloxacin		
<i>N° CAS</i>	85721-33-1	
<i>Molecular weight</i>	331.34 g.mol ⁻¹	
<i>Solubility in water (at 25 °C)</i>	30 mg.L ⁻¹	
<i>pKa</i>	6.09; 8.74	
<i>Log Kow</i>	0.28	
<i>Melting Point</i>	255-257 °C	

IV.1.8.2. Uses

Ciprofloxacin is one of the most prescribed antibacterial medicine for humans and animals [64], approved by the FDA as one of the antibiotics for patients who have been exposed to an inhaled form of anthrax [65]. Used for treating several infections such as urinary, skin, digestive and respiratory infections [66]. In livestock, this drug is widespread not only for the therapeutic treatment, but also used for treating animals in order to increase their productivity, to the prevention and etiology of microbial diseases [67, 68]. In addition, in animal husbandry, it is also widely used to prevent and control diseases [69].

IV.1.8.3. Side effects

An overdose of ciprofloxacin can cause in addition to their common side effects, serious problems to the human health such as internal organ damage, digestive system bleeding and leukopenia in the blood system [66, 70]. In addition, it has been observed that this antibacterial compound can be hepatotoxic and genotoxic for the human body [71]. As this antibiotic is also prescribed for animals, it can be transferred into the food chain [72]. Moreover, this widely used drug is considered a pollutant mostly founded in waters in relatively high concentrations ranging from 1 g/L to ng/L [73]. The accumulation of ciprofloxacin, even at low concentrations, leads not only to the environmental contamination but also produces antibiotic-resistant bacteria in human body, which decreases considerably the efficacy of drugs and increase risks to human health [71]. There is therefore a need to develop sensitive and rapid devices for industrial quality control and clinical and environmental monitoring of ciprofloxacin.

IV.1.8.4. Norms

The use of ciprofloxacin antibiotic was strictly regulated, the recommended dose for adults is 400 mg to 500 mg every 8 hours, not to exceed 1 grams/day [74]. The European Union limits the maximum residue for ciprofloxacin in the milk, chicken and pig muscle at 100 $\mu\text{g.kg}^{-1}$ [75]. CIP is largely excreted unchanged in the urine, knowing that after a 250 mg oral dose, urine concentrations of CIP usually exceed 200 $\mu\text{g/mL}$ during the first two hours and are approximately 30 $\mu\text{g/mL}$ at 8 to 12 hours after dosing [76].

IV.1.9. Pharmaceuticals interactions

Each medicine has its specific and effective uses. However, sometimes the use of more than two drugs at the same time can cause a drug interaction, a situation in which the activities of drugs have been affected by increasing, decreasing their own effects or producing new effects. However, it should also be noted that drug-food interactions can also be established between pharmaceuticals and foods [77]. For example, ciprofloxacin interacts with dairy products because calcium and casein present in these products decrease the absorption of ciprofloxacin and can therefore make the medication less effective [78]. Contrariwise, paracetamol can be hepatotoxic for the individuals who regularly drink moderate to large quantities of alcohol [79]. In the study of pharmacokinetic drug interactions between ciprofloxacin and paracetamol, an increase in the concentration-time profile of ciprofloxacin was observed when co-administered with paracetamol [80]. Therefore, even if there are not many studies on CIP-PAR interactions, it is to believe that a pharmacokinetic interaction may have occurred.

Part IV.2: Electrochemical detection of ciprofloxacin, paracetamol and 4-aminophenol at cavity microelectrode modified with carbon black and activated carbon

The second part of this chapter presents the optimization of the different operating conditions for the design of a new electrochemical micro-sensor for the determination of 4-aminophenol, paracetamol and ciprofloxacin. The so-designed microelectrode was characterized by scanning electron microscopy technique and electrochemical impedance spectroscopy method. A study of the performances of the proposed microelectrode was carried out by SWV for the individual detections of 4-aminophenol, paracetamol and ciprofloxacin separately and then for their simultaneous detection. The feasibility of the developed micro-sensor for the real analysis was evaluated for the simultaneous detection in wastewater and artificial urine samples.

IV.2.1. Introduction

Carbon nanomaterials with their physicochemical, electronic, thermal and structural properties have received a great deal of attention in recent years [81]. In our study, we chose to investigate the performances of two carbon nanomaterials (activated carbon and black carbon) in the electrochemical area and exceptionally in the development of a sensitive and selective sensor.

As it is mentioned in the literature, the activated carbon (AC) is a group of carbonaceous materials synthesized by functionalization or carbonization of carbonaceous materials such as graphite [81]. AC is a porous amphoteric carbon material, used for its high adsorption capacity of mineral and organic substances [82]. In recent time, AC is considered as an interesting material in electrochemical sensing due to its remarkable properties such as porosity, high surface area, high conductivity, good stability and tenability of both surface and structure [83].

Moreover, the carbon black (CB) is an amorphous quasi structured carbon material, produced from the combustion or thermal decomposition of petroleum products [84]. It represents a novel outlook for the development of the sensitive electrochemical sensors, due to its diverse proprieties. The Carbon black nanomaterial is characterized by an abundant pore size, large surface area and high conductivity, which will allow enhancing the analytical signal and electron transfer kinetics [85]. The use of CB as modifier of electrode improves considerably the analytical performances of the electrochemical devices such as higher sensitivity, lower limits of detection and quantification, better stability, reproducibility and repeatability. This performances can be observed when CB is used in modified working electrodes, alone or in a combination with other nanostructured materials [86].

Therefore, both carbon black and activated carbon are important adsorbing agent materials, which represent both high surface areas with a higher one for the carbon black. This two carbon nanomaterials were introduced in the cavity of a microelectrode to have a CBf-AC/ CME as a micro-sensor for the simultaneous analysis of AMP, PAR and CIP.

IV.2.2. Characterization of the CBf-AC/ CME

a. Characterization of the modified electrode by scanning electron microscopy (SEM)

SEM technique was carried out in order to study the morphologies of the electrode matrix compounds and its final nanostructuration. For this purpose, we have first investigated the impact of the pretreatment of the used carbon materials. The Fig.IV.3-A show the graphite structure without any pretreatment, which is in the form of dispersed platelets composed of stacked sheets of less than 4 μm length. After activation (Fig.IV.3-B) the platelets structure was bursting, which promote a larger surface area. Otherwise, the carbon black appears as aggregates and agglomerates composed of spherical particles with diameter at around 100 nm (Fig.IV.3-C). For the functionalized CB, the global morphology of the aggregates was not significantly affected, with more compact agglomerates which could be attribute to the grafted function group on the surface of CB particles, (Fig.IV.3-D). For the CME, on the Fig. IV.3-E & F, it can be seen the nanostructured materials introduced in the CME and that in the mixture, AC (25 %) and CBf (75 %) are linked together with an uniform dispersion, given a nanostructured surface with a large surface area, which promote the accessibility of the analytes in their surface, improve the charge surface and enhance the performances of the developed micro-sensor.

b. Characterization of the modified electrode by Fourier transform infrared (FTIR) spectroscopy

FTIR analysis was employed to investigate the change in the carbon black caused by the functionalization treatment and to characterize the surface functional groups after and before modification (shown in Fig. IV.4). The both FTIR spectrums of the CB before and after functionalization presented adsorption bands between 2090 to 2330 cm^{-1} that was related to $\text{C}\equiv\text{C}$ elongation vibrations, the band peak in 1000-1200 cm^{-1} may be attributed to different function groups containing single bonded oxygen atoms such as phenols, ethers, and lactones. The bands at 1114 and 1118 cm^{-1} observed, respectively, for CB and oxidized CB can be attributed to C–O stretching. The modification of the CB was confirmed in the Fig. IV.4-B, which show a broad adsorption band at approximately 3430 cm^{-1} that could be attributed to the O–H stretching of the hydroxyl groups, band at 1635 cm^{-1} corresponding to conjugated $\text{C}=\text{O}$ elongation vibration. The presence of the hydroxyl and oxygen groups confirm the functionalization treatment and show clearly the difference between CB and CBf.

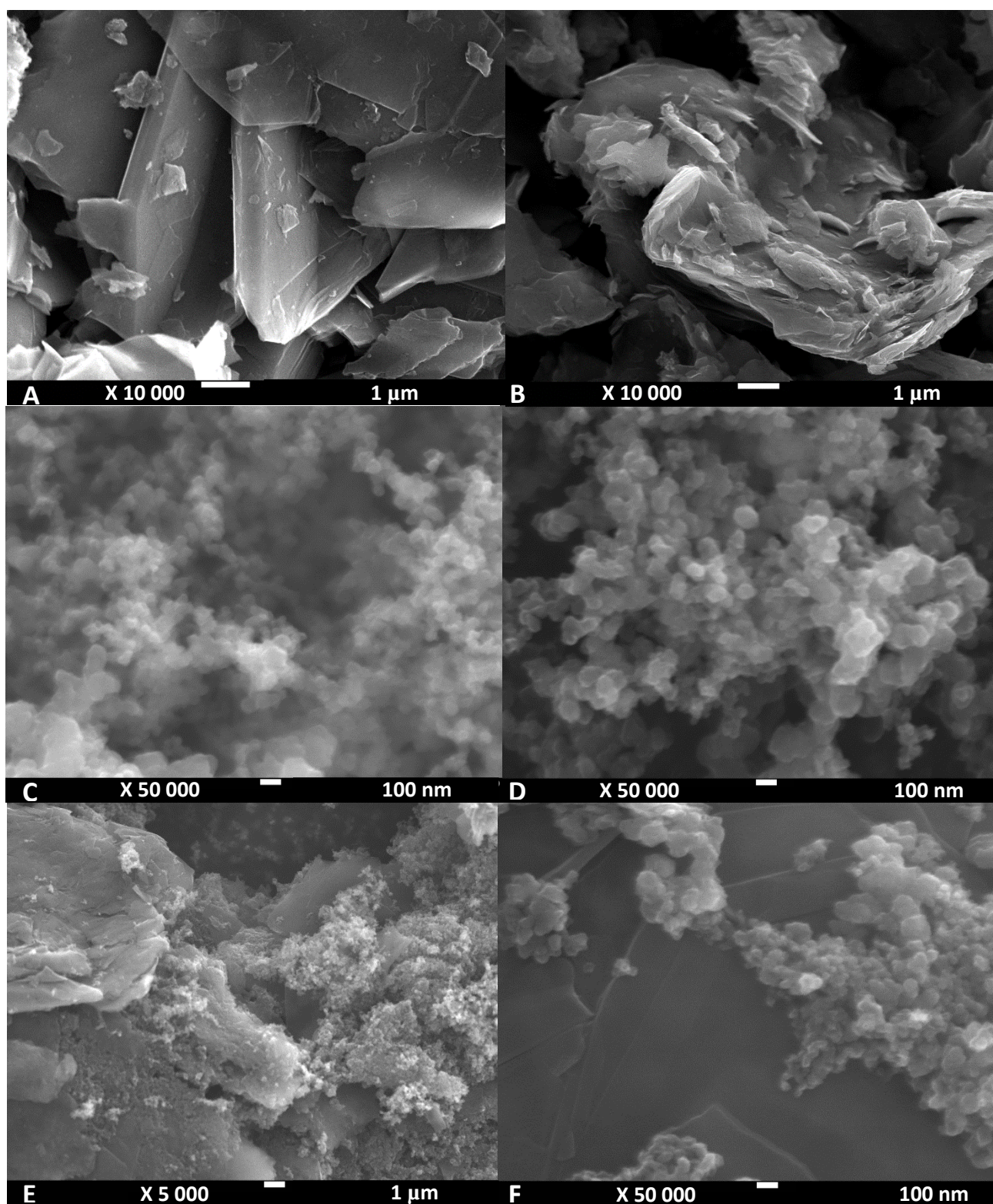


Figure IV.3. SEM images for (A) graphite (x10.000), (B) AC (x10.000), (C) CB (x50.000), (D) CBf (x50.000), (E) CBf-AC (x5.000) and (F) the mixture CBf-AC (75/25%, respectively) (x50.000).

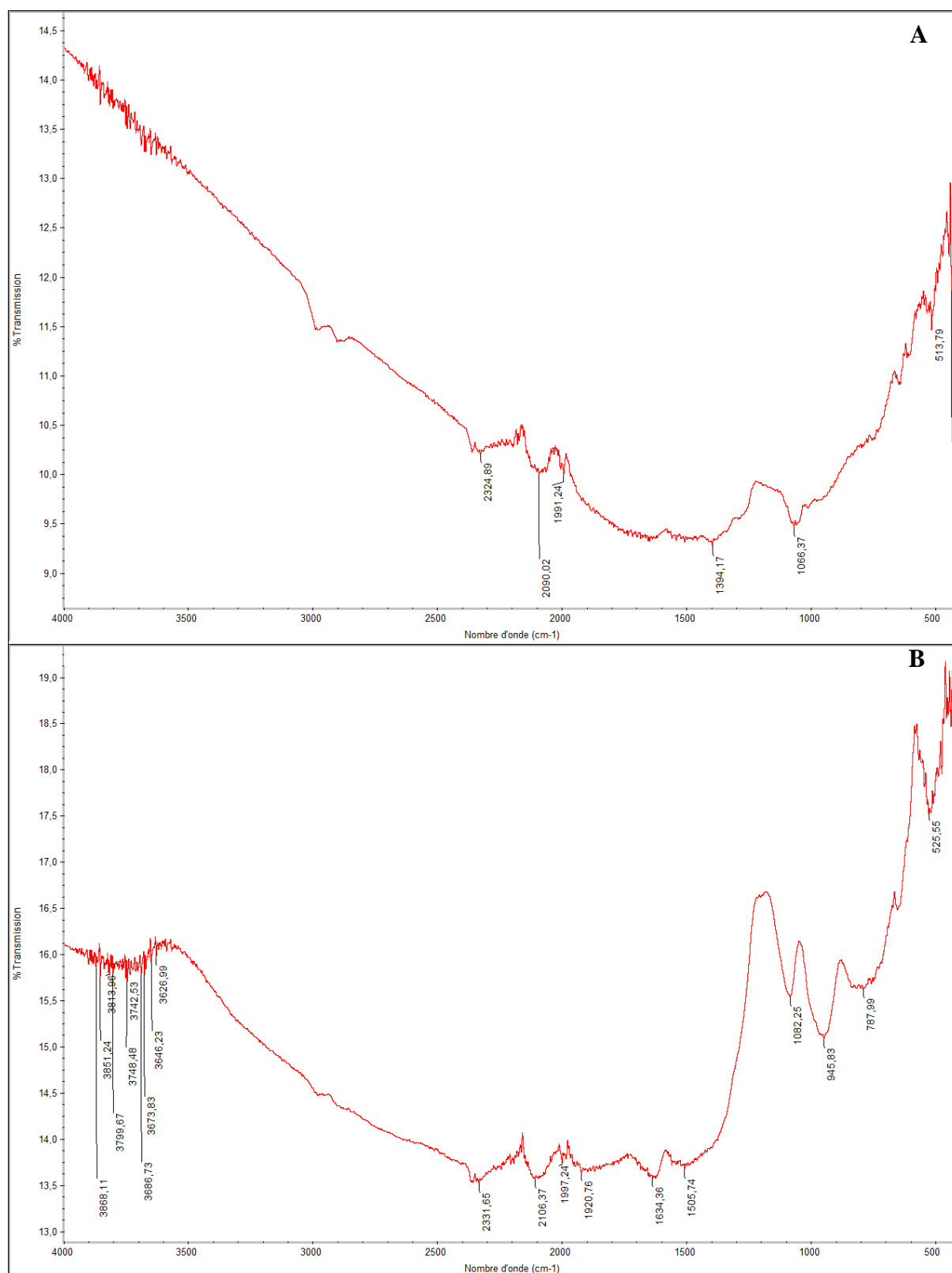


Figure IV.4. Fourier transform infrared spectrograms of (A) CB and (B) CBf.

c. Characterization of the modified electrode by electrochemical impedance spectroscopy (EIS)

In order to show the interest of the mixing of CBf and AC in improving the surface characteristics of the developed microelectrode, we also compared the final sensor so-designed with those of their constituents (CBf and AC). The impedance spectra were plotted in BR solution 0.04 M at pH = 5 containing 1 mM of $[\text{Fe}(\text{CN})_6]^{3-/4-}$ as electroactive probe, in the frequency range of 10^{-3} to 10^5 Hz by using a sinusoidal excitation signal (sine signal) with amplitude of 10 mV (Fig. IV.5).

The Nyquist plots of AC and CBf cavity microelectrodes alone, showed large incomplete semicircles with a charge transfer resistance of 5.92×10^8 and 2.16×10^9 Ω , respectively. Mixing the two materials in CBf-AC/ CME results in a smaller clear semicircle, indicating lower charge transfer resistance of 5.56×10^7 Ω . This decrease in the resistance of charge transfer is due to the nanostructuration of the CME that lead consequently to an increase in the kinetics of electron transfer. Generally a Nyquist plot, presents in addition to a semi-circle a linear part, which is attributed to the diffusional process. However, no linear part has been observed in the results of this study, this mean that the electrical impedance at the interface electrode / electrolyte is limited by an electron transfer process and not a diffusional one.

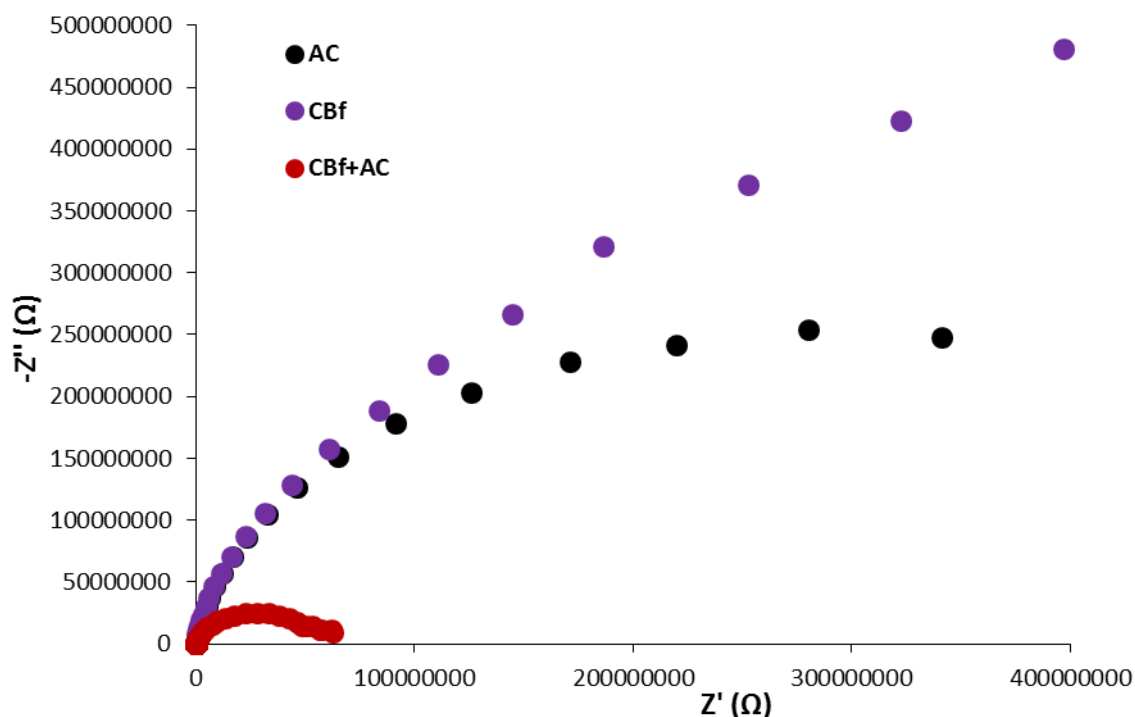


Figure IV.5. Nyquist diagrams for EIS of AC/CME (●), CBf/CME (●) and CBf-AC/CME (●) in 1 mM $\text{Fe}(\text{CN})_6^{3-/4-}$ at BRS 0.04 M (pH=5).

IV.2.3. Electrochemical behavior of the CBf-AC/ CME

The performance and the sensitivity of the developed sensor were evaluated by studying the responses of the cavity microelectrode toward AMP, PAR and CIP at different compositions, by CV measurements from 0 to 1.3 V at scan rate of 20 mV.s^{-1} . The study was carried out for AC, CBf and for a mixture of AC and CBf with two different proportion (25/75)% and (75/25)% for CBf and AC, respectively, in a presence of $5 \text{ }\mu\text{M}$ of each analyte AMP, PAR and CIP, in Britton-Robinson buffer at $\text{pH}=5$ as supporting electrolyte. From the Fig. IV.6-A, it can be seen that the three analytes show three well defined and separated oxidant peaks at around 0.20 V, 0.53 V and 1.00 V corresponding to the oxidation of AMP, PAR and CIP, respectively. Moreover, in the reverse scan, a reduction peak is observed for PAR and AMP at the same oxidation potential, respectively, it characterizes a reversible charge transfer processes. However, the absence of the reduction peak current for CIP indicates irreversible oxidation step. It is also observed that the mixture of 75 % CBf and 25 % AC enhances considerably the current peaks for all compounds, improves the charge transfer at the modified surface and enhances the sensitivity. This higher sensitivity was observed with the CBf-AC/ CME at (75/25; CBf/AC) proportion (Fig. IV.6-B). These results are due to the combination of AC and CBf leading to a heterogeneous nanostructured surface of the CME. This improves the structuring and the contact surface developed between the matrix of the designed micro-sensor and the compounds thus improving the sensitivity and the potential of the CBf-AC / CME for the simultaneous determination of the three analytes.

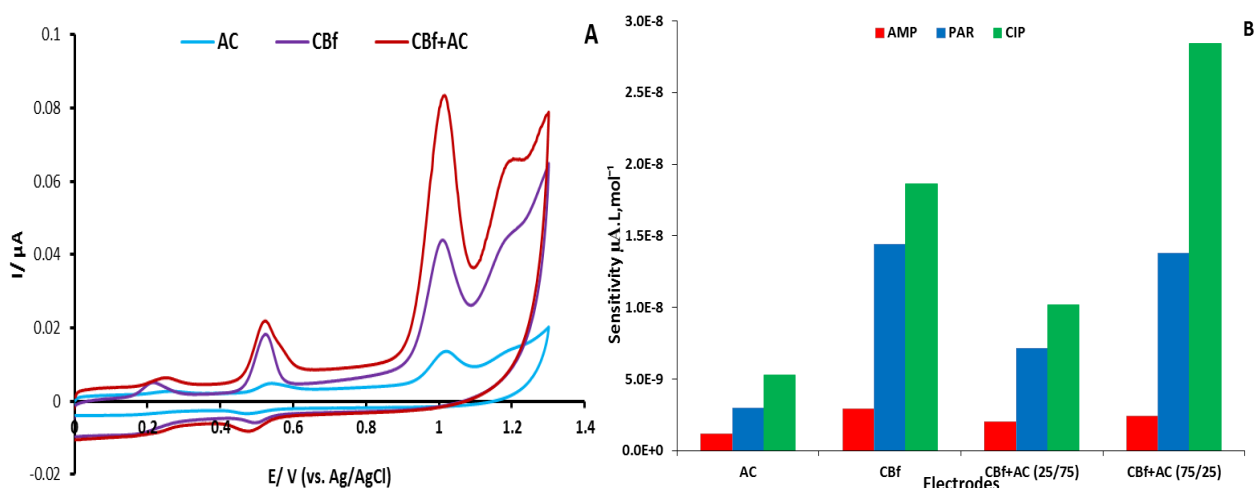


Figure IV.6. (A) Cyclic voltammograms of the AC/CME, CBf/CME and CBf-AC/ CME in the presence of $5 \text{ }\mu\text{M}$ AMP, PAR and CIP in BRS 0.04 M ($\text{pH} = 5$); 20 mV.s^{-1} (B) The corresponding sensitivity of the CMEs.

IV.2.4. Effect of pH

The pH effect of the supporting electrolyte on the electrochemical behavior of the AMP, PAR and CIP at the CBF-AC/ CME was investigated in the presence of 5 μM of each cited analytes in BRS (0.04 M) at the pH range of 3 to 6 at 25 $^{\circ}\text{C}$. Analyzes were carried out by CV method in the range from 0 to 1.3 V at 20 mV.s^{-1} . The obtained cyclic voltammograms are illustrated on Fig. IV.7.

As can be seen in Fig. IV.8 (A, B & C), the current peaks of AMP, PAR and CIP increased with increasing pH values, reach the maximum peak current intensity at pH = 5, then decreased with a further increase of pH value. This may be due to the fact that at higher pH levels, the difference between pKa and pH leads to different form of adsorption and a change in the affinity of the analytes with the electrode surface. However, pH = 5 seems to be an ideal pH value where an equilibrium between protons and electrons that participate in the reactions.

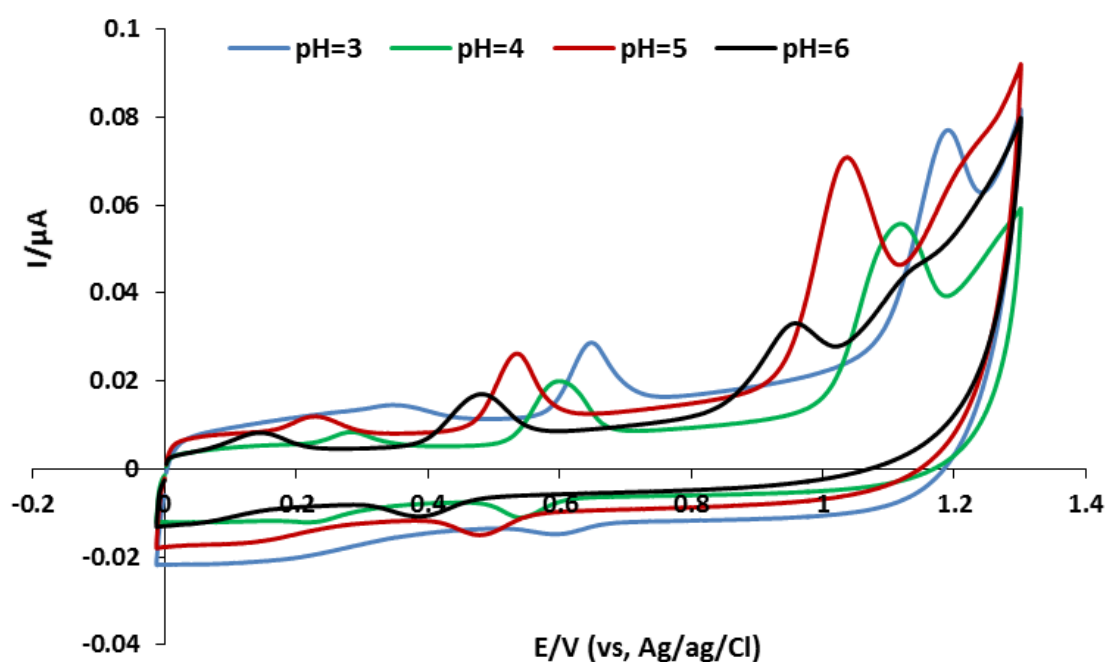


Figure IV.7. Cyclic voltammograms of 5 μM AMP, PAR and CIP in BRS 0.04 M at different pH value (3 to 6) at the CBF-AC/CME

Furthermore, as shown in the Fig. IV.8 (D, E & F), the potential peaks of these three molecules are shifted into the negative side with the increasing of the pH values. This reveals that protons involve in the reaction of AMP, PAR and CIP at CBf-AC/ CME. Their linear relationships are expressed as follow:

$$E_{p(AMP)} = -6.62 \times 10^{-2} \text{pH} + 0.550, (R^2=0.993) \quad \text{Eq. 4.1}$$

$$E_{p(PAR)} = -7.67 \times 10^{-2} \text{pH} + 1.42, (R^2=0.994) \quad \text{Eq. 4.2}$$

$$E_{p(CIP)} = -5.79 \times 10^{-2} \text{pH} + 0.862, (R^2=0.997) \quad \text{Eq. 4.3}$$

The above results indicate that pH = 5 gives a fast electron transfer reactions (well defined peaks) with a higher peak currents. This can be explained by the fact that at this pH value, good electrostatic interactions were established between each studied analytes with the modified nanostructured surface of the CME. Consequently, the BR solution at pH = 5 is selected as an appropriate electrolyte for further studies.

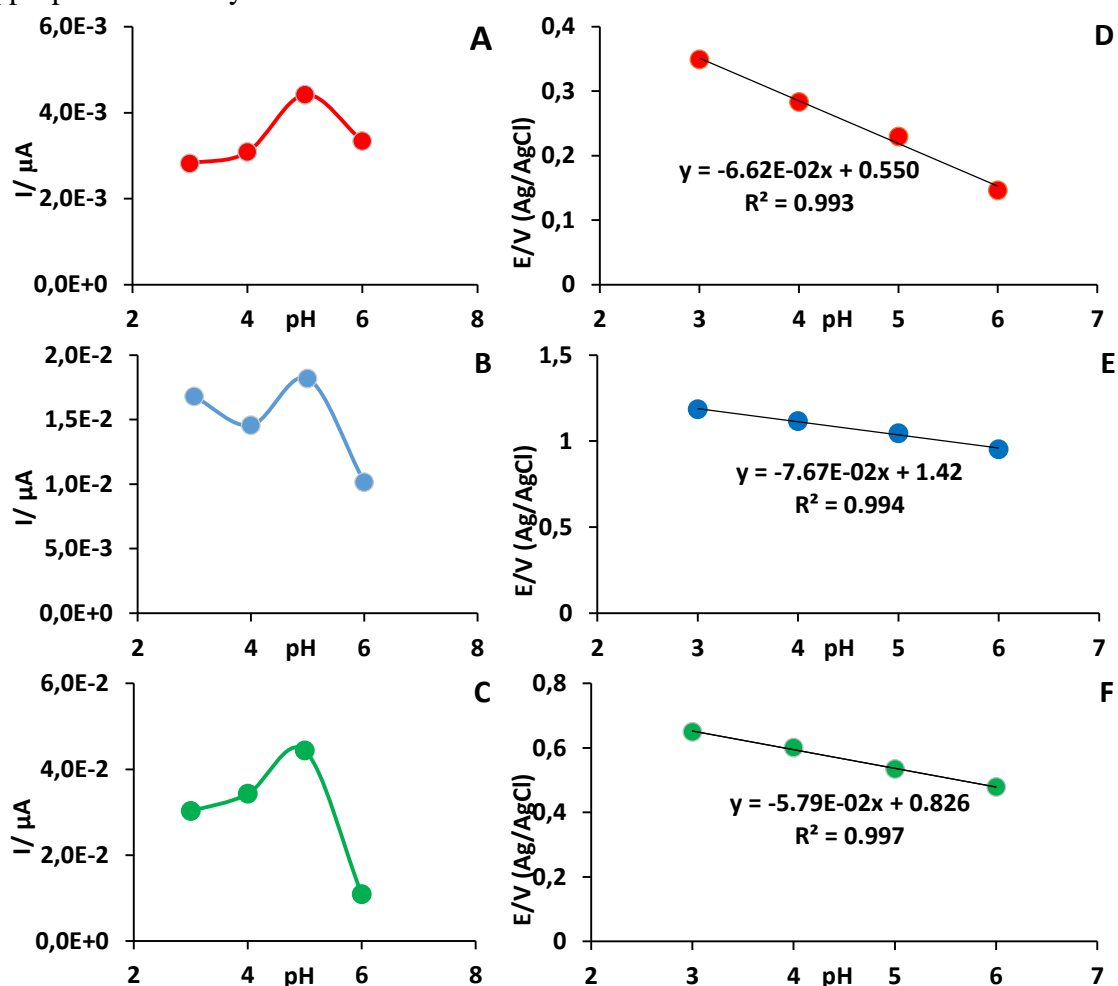


Figure IV.8. A, B and C: Effect of pH on the peaks current oxidation of AMP, PAR and CIP, respectively. E, F and G: Corresponding plots of the oxidation peaks potential of AMP, PAR and CIP versus pH, respectively at the CBf-AC/CME

IV.2.5. Effect of scan rate

In order to determinate the type of process that control the electrochemical reaction of AMP, PAR and CIP into Cbf-AC /CME, we study the effect of scan rate on the currents peaks intensity. For this 5 μM AMP, PAR and CIP was introduced in the electrochemical cell containing the conventional three electrode with Cbf-AC /CME as working electrode in BR solution at pH = 5. The measurement was recorded by cyclic voltammetry method in the range scan rate of 25 to 275 mV.s^{-1} . The resulting voltammograms are presented in Fig. IV.9.

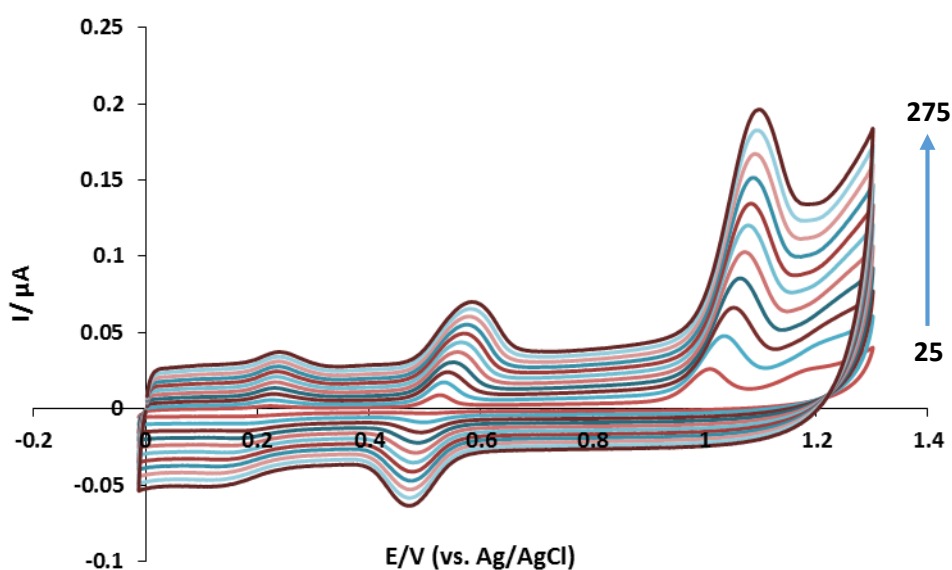


Figure IV.9. Cyclic voltammograms of 5 μM AMP, PAR and CIP in BRS 0.04 M (pH=5) with different scan rate values (25 to 275 mV.s^{-1}) at the Cbf-AC/CME

The dependence of the currents peaks on the variation of the scan rate in the range between 25 and 275 mV.s^{-1} at Cbf-AC/ CME is presented in the Fig. IV.10. For all three analytes, the redox currents peaks increase linearly with the increasing of the scan rate, their linear regression equations are as follow:

$$I_{p(\text{AMP})} = 3.716 \times 10^{-5} \vartheta + 2.334 \times 10^{-3}, (R^2 = 0.996) \quad \text{Eq. 4.4}$$

$$I_{p(\text{PAR})} = 1.294 \times 10^{-4} \vartheta + 1.264 \times 10^{-2}, (R^2 = 0.992) \quad \text{Eq. 4.5}$$

$$I_{p(\text{CIP})} = 3.946 \times 10^{-4} \vartheta + 1.338 \times 10^{-2}, (R^2 = 0.998) \quad \text{Eq. 4.6}$$

This indicates that an adsorption step controls the oxidation reaction of the studied drugs at Cbf-AC/ CME surface.

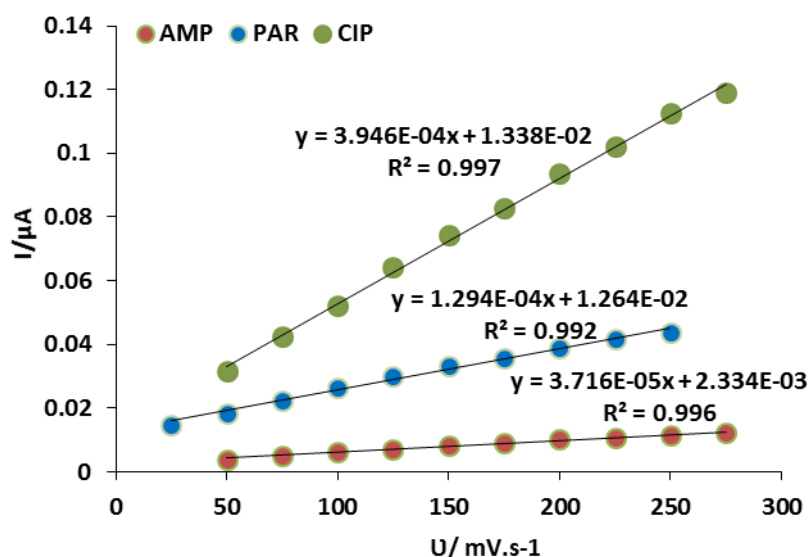


Figure IV.10. Plot of the peaks current oxidation of 5 μM of AMP, PAR and CIP versus scan rates at the CBf-AC/CME in BRS 0.04 M (pH = 5)

IV.2.6. Effect of accumulation time

In the [section IV.2.5](#), we demonstrated that the electrochemical reactions of the studied analytes are controlled by an adsorption step. Thus, the study of the accumulation time effect on the current responses is necessary. The electrochemical measurements were carried out by CV method in the presence of 5 μM AMP, PAR and CIP in BRS pH = 5 at CBf-AC/CME. As shown in [Fig. IV.11](#), the oxidation peak currents of the three molecules increase gradually with increasing of accumulation time from 1 to 5 min, reach the maximum current response at 5 min, and then remain almost constant or decrease at longer accumulation times. For practical reasons, we have chosen to set the accumulation time at 5 min for all subsequent analyzes.

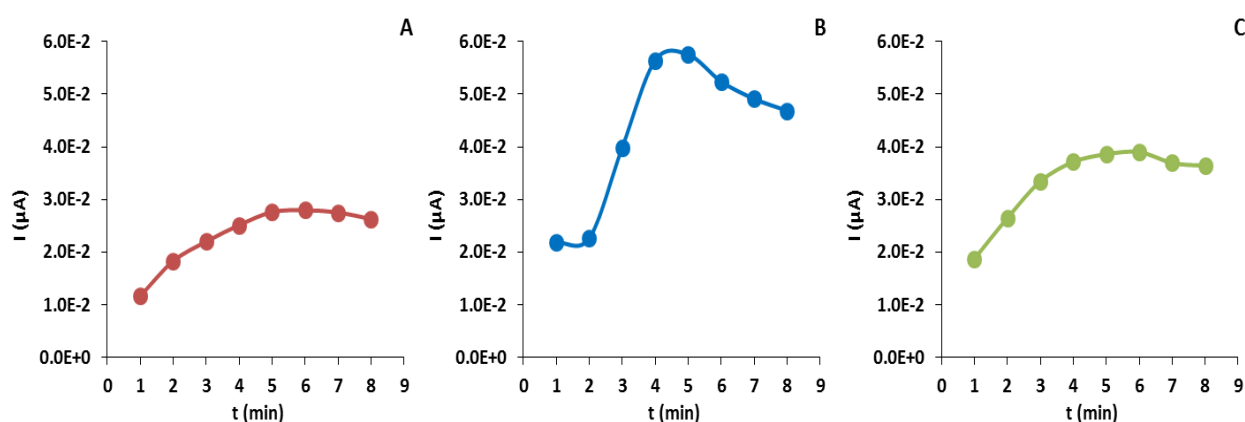


Figure IV.11. A, B and C: The effect of accumulation time on the oxidation peak current of 5 μM AMP, PAR and CIP, respectively at the CBf-AC/CME in BRS 0.04 M (pH = 5).

IV.2.7. Individual analysis of 4-aminophenol

The individual analysis of AMP for different concentrations was performed by square wave voltammetry at CBf-AC/ CME in BRS (0.04 M) at pH = 5, 20 mV.s⁻¹ scan rate, modulation amplitude of 25 mV and frequency of 10 Hz. Fig. IV.12-A shows the obtained voltammograms. The intensity of the oxidation peak current of AMP increases with the AMP concentrations from 3×10⁻⁷ to 5×10⁻⁶ mol.L⁻¹. The calibration curve for peak current (I_p) versus [AMP] (Fig. IV.12-B) indicates a clearly linear line with the following regression equation:

$$I_{p(\text{AMP})} = 3.471 \times 10^3 [\text{AMP}] - 6.076 \times 10^{-4}, R^2 = 0.999 \quad \text{Eq. 4.7}$$

The detection limit of the proposed method is estimated to be 6.6 × 10⁻⁸ mol.L⁻¹, calculated from the formula: LOD = 3.3 × SD/b

$$\text{Eq. 4.8}$$

where SD is the standard deviation of the linear regression solution and b is the slope of the linear regression [87].

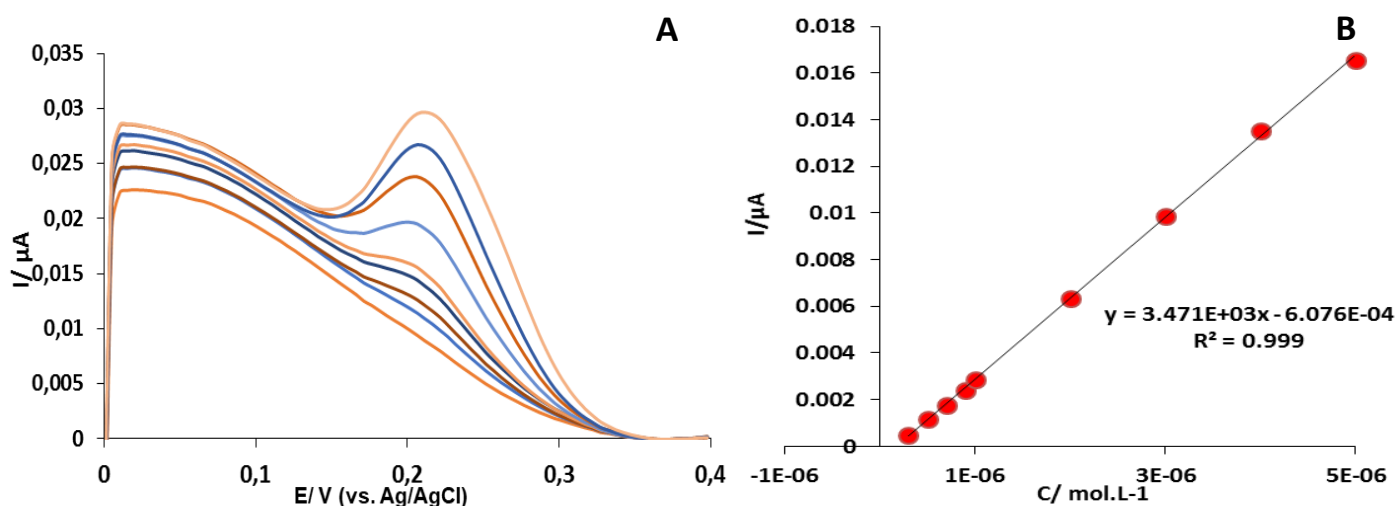


Figure IV.12. (A) Square wave voltammograms of the determination of AMP from 0.1 to 3 μM at CBf-AC/CME in BRS 0.04M (pH = 5). (B) Calibration curves of AMP concentrations against peak current.

Generally, the 4-aminophenol undergoes oxidation reaction to form quinoneimine, according to the following reaction [41, 44, 45]:

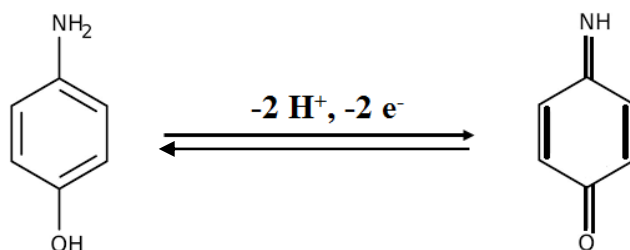


Figure IV.13. Mechanism of the electrochemical reaction of 4-aminophenol

IV.2.8. Individual analysis of paracetamol

The individual analysis of PAR concentrations was performed by square wave voltammetry at CBf-AC/ CME in BRS (0.04 M) at pH = 5, 20 mV.s⁻¹ scan rate, modulation amplitude of 25 mV and frequency of 10 Hz. The Fig. IV.14-A shows the obtained voltammograms. The intensity of the oxidation peak current of PAR increases with the PAR concentrations from 5×10⁻⁸ to 2×10⁻⁶ mol.L⁻¹. The calibration curve for peak current (I_p) versus [PAR] (Fig. IV.14-B) indicates a clearly linear line with a following regression equation:

$$I_p(\text{PAR}) = 6.787 \times 10^2 [\text{PAR}] + 7.173 \times 10^{-5}, R^2 = 0.999 \quad \text{Eq. 4.9}$$

The detection limit of the proposed method is estimated to be 2.6 × 10⁻⁸ mol.L⁻¹.

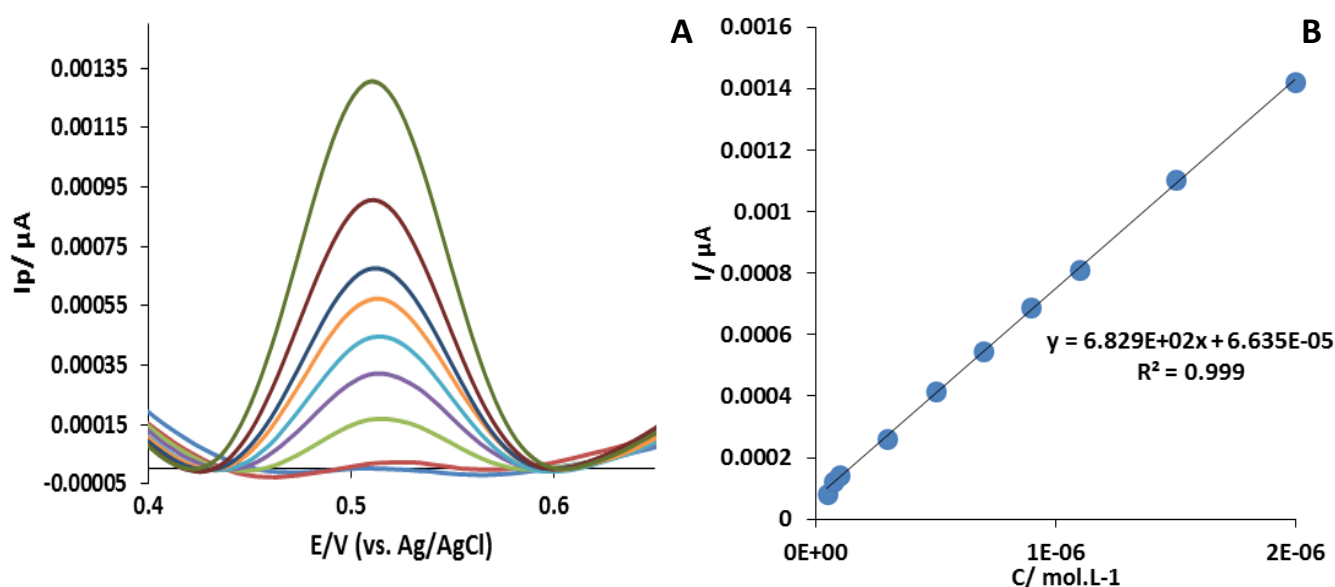


Figure IV.14. (A) Square wave voltammograms of the determination of PAR from 0.05 to 2 μM at CBf-AC/CME in BRS 0.04M (pH = 5). (B) Calibration curves of PAR concentrations against peak current.

Generally, the paracetamol undergoes oxidation reaction, according to the following reaction [88, 89]:

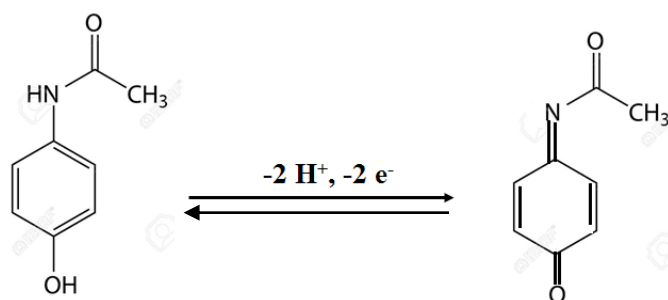


Figure IV.15. Mechanism of the electrochemical reaction of paracetamol

IV.2.9. Individual analysis of ciprofloxacin

The individual analysis of CIP concentrations was performed by square wave voltammetry at CBf-AC/ CME in BRS (0.04 M) at pH = 5 and 20 mV.s⁻¹ scan rate. The Fig. IV.16-A shows the obtained voltammograms. The intensity of the oxidation peak current of CIP increases with the CIP concentrations from 1×10⁻⁷ to 3×10⁻⁶ mol.L⁻¹. The calibration curve for peak current (I_p) versus [CIP] (Fig.IV.16-B) indicates a clearly linear line with the following regression equation:

$$I_{p(\text{CIP})} = 1.181 \times 10^3 [\text{CIP}] + 7.542 \times 10^{-5}, R^2 = 0.998. \quad \text{Eq. 4.10}$$

The detection limit of the proposed method is estimated to be 7.2 × 10⁻⁸ mol.L⁻¹.

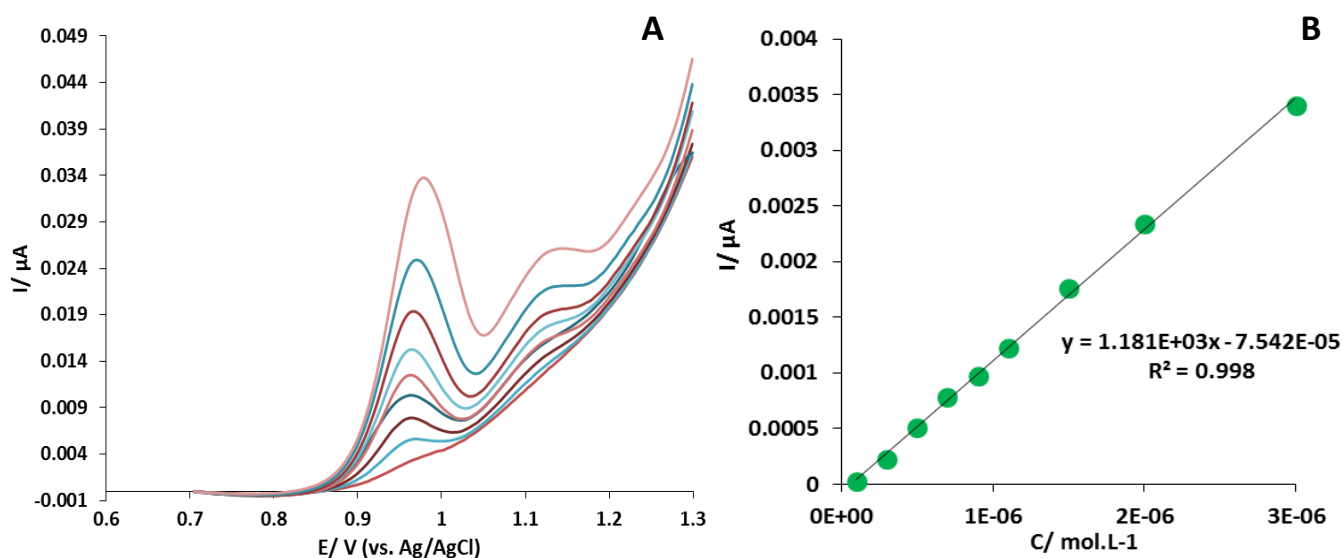


Figure IV.16. (A) Square wave voltammograms of the determination of CIP from 0.1 to 3 μM at CBf-AC/CME in BRS 0.04M (pH = 5). (B) Calibration curves of CIP concentrations against peak current.

Generally, the ciprofloxacin oxidation reaction is as follow [90, 91]:

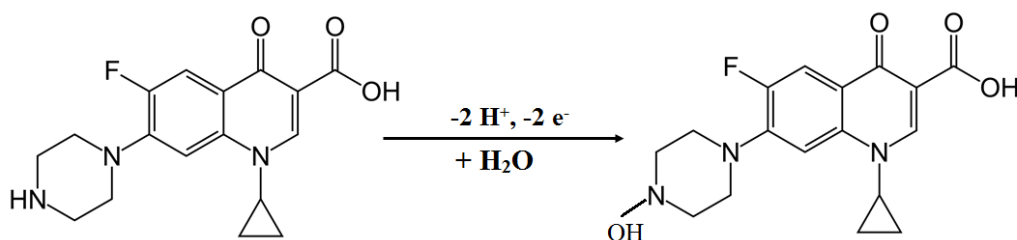


Figure IV.17. Mechanism of the electrochemical reaction of ciprofloxacin

IV.2.10. Simultaneous analysis of 4-aminophenol, paracetamol and ciprofloxacin

The electrochemical sensing performances of CBf-AC/ CME towards simultaneous detection of AMP, PAR and CIP was investigated by SWV method in BRS (0.04 M, pH=5). As shown in the Fig. IV.18, three oxidation peaks are well separated, and their current intensities increase gradually with increasing of their concentrations.

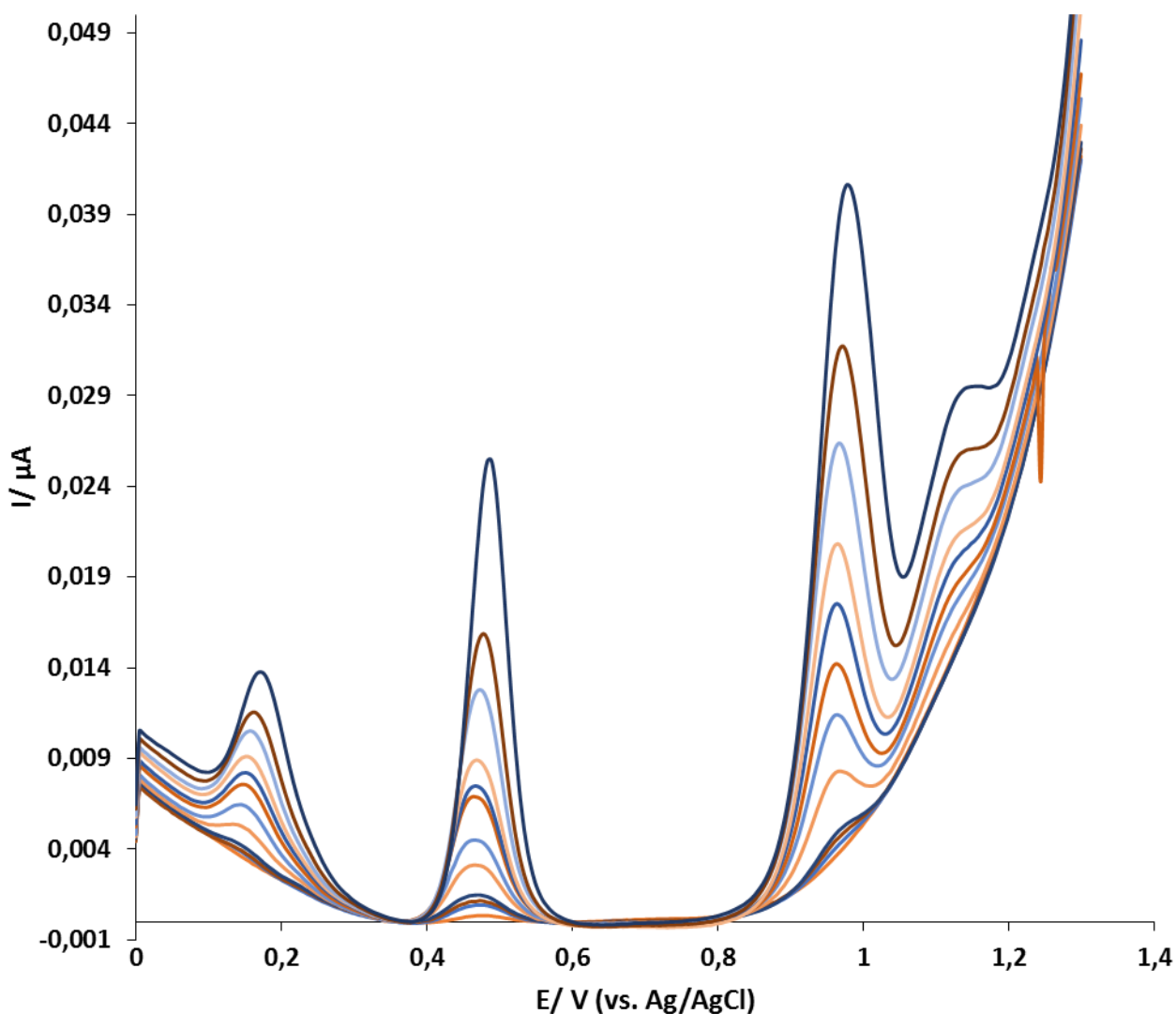


Figure IV.18. Square wave voltammograms of the simultaneous determination of AMP, PAR and CIP from 0.1 to 3 μM ; 0.025 to 3 μM and 0.05 to 3 μM , respectively, at CBf-AC/CME in BRS 0.04 M (pH = 5).

Examination of the calibration curves of each analytes Fig. IV.19 (A, B & C), exhibits good linear relationships between the AMP, PAR and CIP current peaks and their concentrations.

The linear equations and their corresponding concentration ranges are as follows:

AMP: from 1×10^{-7} to 3×10^{-6} M:

$$I_{p(\text{AMP})} = 4.486 \times 10^2 [\text{AMP}] + 1.744 \times 10^{-5}, (R^2=0.999) \quad \text{Eq. 4.11}$$

PAR: from 2.5×10^{-8} to 3×10^{-6} M:

$$I_{p(\text{PAR})} = 8.180 \times 10^2 [\text{PAR}] + 5.811 \times 10^{-5}, (R^2=0.999) \quad \text{Eq. 4.12}$$

CIP: from: 5×10^{-8} to 3×10^{-6} M:

$$I_{p(\text{CIP})} = 1.234 \times 10^3 [\text{CIP}] + 2.666 \times 10^{-5}, (R^2=0.999) \quad \text{Eq. 4.13}$$

The comparison of these last result with those obtained with individuals detection, leads to conclude that the sensitivities of PAR and CIP are a little higher in the simultaneous detection than in the individual one, and in the contrast, the sensitivity of AMP is remarkably weakened. This can probably be attributed to the fact that AMP and PAR have an almost similar molecular structure with biggest structure for PAR. Thus, competition in the adsorption of these two molecules at the surface of the cavity microelectrode leads to the adsorption of PAR preferentially to that of AMP.

The detection limits of AMP, PAR and CIP were 63, 23 and 39 nM, respectively.

Overall, it should be noted that there is compatibility in the results obtained from the individual and simultaneous determination with good sensitivities and a better detection limits for the all analyzed drugs. These results showed that the modified cavity microelectrode is able to detect simultaneously AMP, PAR and CIP with high sensitivity.

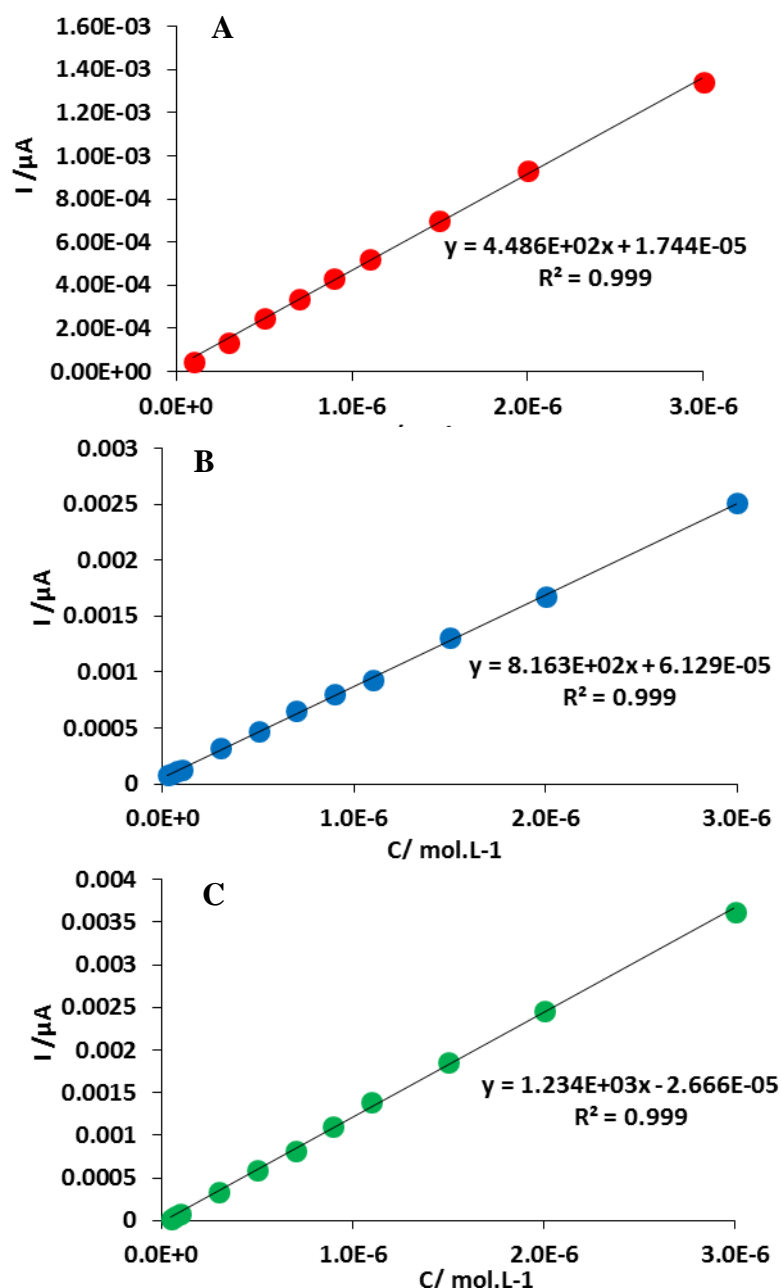


Figure IV.19. A, B and C: Calibration curves of AMP, PAR and CIP concentrations against peak current, respectively in the simultaneous determination at CBf-AC/CME in BRS 0.04 M (pH = 5).

The analytical performance of the proposed micro-sensor compared to some latest reported devices on the AMP, PAR and CIP detection are presented in the [Table IV.4](#). According to the literature it is clear that the previous modified cavity microelectrode is the first one used for the simultaneous detection of the three drugs together. In addition, this modified CME offer wider linear ranges and lower detection limits.

Moreover, the proposed electrochemical sensor shows very good performance by just following very simple steps in the preparation of the sensor using few cost electrodes materials in comparison with some reports, which give practically similar analytical characteristics. Therefore, this new, simple and economical CBf-AC/CME micro-sensor could be a good alternative for the simultaneous analysis of AMP, PAR and CIP.

Table IV.4. Comparison of this work with those previously reported for the simultaneous analysis of AMP, PAR and CIP with electrochemical sensor.

Electrode	Analytes	LR (μM)	DL (nM)	Ref.
CS/Ag-Pd@rGO/GCE	AMP PAR	1 to 300 0.5 to 300	13 23	[92]
Bis-schiff Base Cobalt Complexes/GCE	AMP PAR	5 to 30 5 to 30	2080 1860	[93]
NiONPs-GO-CTS: EPH/GCE	PAR CIP	0.1 to 2.9 0.04 to 0.97	6.7 6	[94]
Sm ₂ O ₃ /GPE	PAR CIP	0.001 to 300 0.05 to 170	0.1 5	[95]
copper zinc ferrite nanoparticle-CPE	PAR CIP	0.18 to 47.6 0.9 to 4700	2.5 88.5	[96]
CBf-AC/ CME	AMP PAR CIP	0.1 to 3 0.025 to 3 0.025 to 3	63 23 39	This work

IV.2.11. Repeatability and reproducibility of CBf-AC/ CME

The repeatability and the reproducibility of the CBf-AC/CME sensor toward the simultaneous detection of AMP, PAR and CIP were studied for three different concentrations (0.3, 0.6 and 0.9 μM) for each reagent with square wave voltammetry in the BR solution (0.04 M, pH = 5) at 20 mV.s⁻¹ (Table IV.5). The repeatability of the sensor was investigated with three successive measurements by using the same modified CME. The relative standard deviation (RSD) for consecutive determination of AMP, PAR and CIP were less than 3 %, which confirms an acceptable repeatability of the sensor. In addition, the reproducibility was evaluated for three different modified CMEs with the same composition of AC and CBf, the obtained values of RSD were less than 8 %, indicating good reproducibility of the sensor.

Table IV.5. Study of the repeatability and reproducibility of the simultaneous detection for different concentrations at CBf-AC/CME in BRS 0.04 M (pH = 5). *n = 3

Concentration (μM)	Analytes	Repeatability of I_p RSD%*	Reproducibility of I_p RSD%*
0.3	AMP	0.5	1.8
	PAR	1.6	2.8
	CIP	3.0	4.3
0.6	AMP	2.8	1.8
	PAR	2.1	5.8
	CIP	2.1	6.1
0.9	AMP	1.6	5.0
	PAR	0.8	7.8
	CIP	2.0	5.9

IV.2.12. Selectivity of CBf-AC/ CME

The selectivity of the CBf-AC/CME was investigated using the SWV technique for a solution containing 0.5 μM of AMP, PAR and CIP in the presence of some potential interfering substances at similar concentrations.

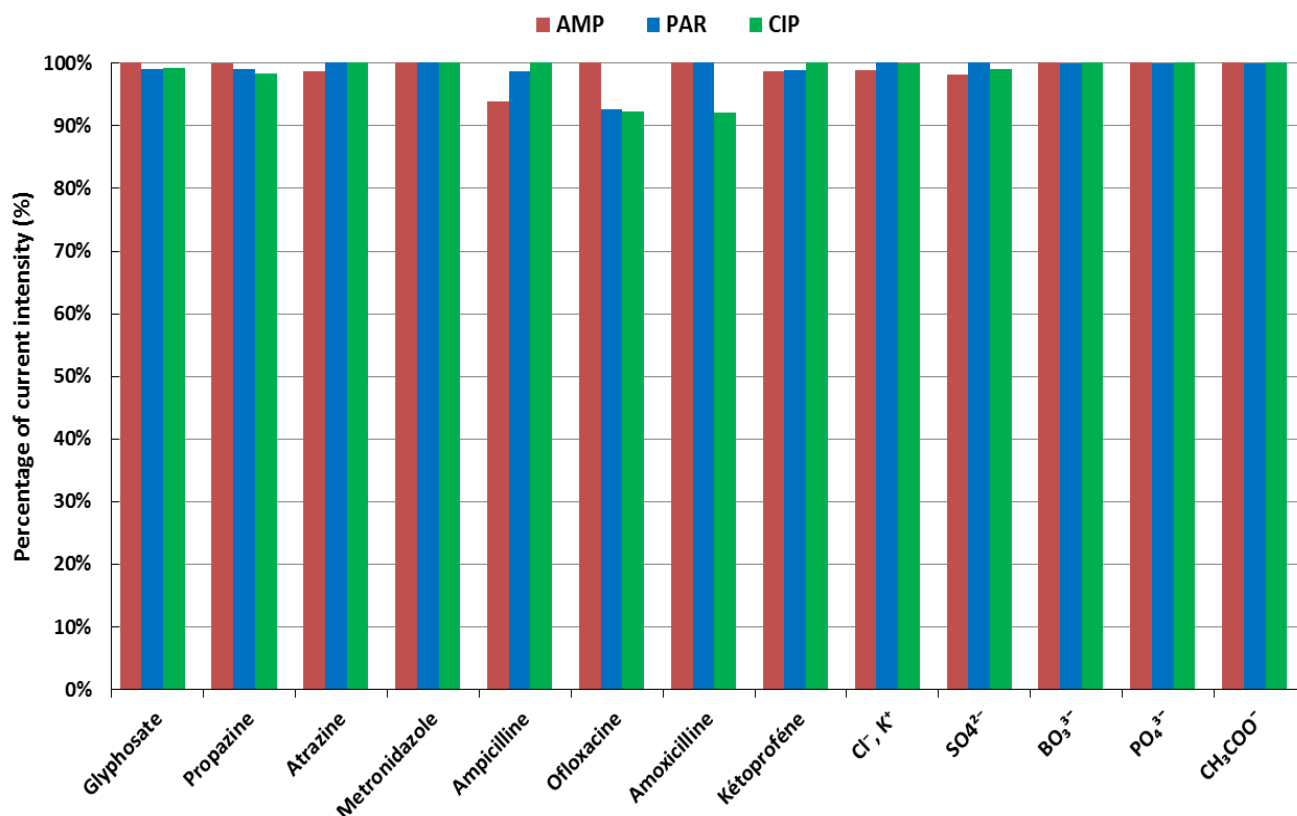


Figure IV.20. The relative peak current response of AMP, PAR and CIP in the presence of some potential interfering substances at the CBf-AC/CME in BRS 0.04 M (pH = 5).

According to the results summarized in Fig. IV.20, the presence of some pesticides such as glyphosate, propazine, atrazine and metronidazole have no effect on peak intensity (variation less than 2 %, for all the three molecules). This indicates that the proposed micro-sensor do not have matrix effects for the analysis of effluents. In addition, the response of the CME toward the detection of the AMP, PAR and CIP was studied in the presence of some pharmaceutical products. Ketoprofen have no influence on the response of the micro-sensor toward the three reagents (variation < 2 %). However, ofloxacin and amoxicillin affect the CIP and PAR response with a variation of no more than 8%, ampicillin effect weakly the detection of AMP (variation less than 7%). These low variations in the oxidation current responses of the target were likely due to the presence of a similar electroactive functional group. But, it remains a negligible variation and the proposed CME can be used for the determination of the AMP, PAR

and CIP in biological fluid. Moreover, in order to eliminate all possibility of interference, it is preferable to dilute samples to minimize their concentrations and to analyze low concentrations of AMP, PAR and CIP with an adsorption step to guarantee the specificity of the response. Other interferents such sulfate, chloride, Fe^{3+} , oxalate and acetate ions have negligible impact on current responses. Therefore, it can be concluded that CBf-AC/CME can be used for the simultaneous determination of AMP, PAR and CIP with acceptable selectivity and include their feasibility for real sample analysis.

IV.2.13. Validation of the proposed sensor in water samples

The validation of the CBf-AC/CME sensor for the simultaneous detection of the three analytes (AMP, PAR and CIP) was applied in wastewater collected from the wastewater treatment plant in Betton (Rennes), France. The sample was simply filtered through syringe filter (0.45 μm) to remove any impurities, then diluted twice with a supporting electrolyte (10 mL of SBR 0.04 M at pH = 5 with 10 mL filtered wastewater). The prepared samples were transferred into the electrochemical cell for the validation of the proposed CB/ CME. No pics were detected with the modified microelectrode in voltammetric analysis, indicating that the concentration of the studied drugs is lower than LOD or the target molecules are not present in the analyzed wastewater samples. After that, the solution was spiked with known AMP, PAR and CIP amounts (0.30 μM). Therefore, to find the spiked previously known three drugs amounts, the standard addition method was used, with successive addition of known AMP, PAR and CIP amounts (0.10; 0.20 and 0.30 μM) in the electrochemical cell containing the diluted wastewater sample. The recovery values are between 104-107 % and the RSD values are less than 5 % for the different reagents (Table IV.6), indicating no interference effects of the water matrix. Therefore, the proposed method could be applied for the simultaneous detection of AMP, PAR and CIP drugs with a simple dilution of the water samples by the SBR solution (pH=5). This proposed electroanalytical method demonstrates a performance of the proposed micro-sensor and its feasibility in environmental waters analysis with high accuracy.

Table IV.6. Validation of the CBf-AC/CME in the determination of AMP, PAR and CIP in wastewater sample. (*n=3)

Analytes	Concentration added (μM)	Concentration found (μM)	RSD* (%)	Recovery (%)
AMP	0.30	0.33	3.1	107.3
PAR	0.30	0.32	3.9	107.1
CIP	0.30	0.31	4.4	104.1

IV.2.13. Validation of the proposed sensor in urine samples

The validation of the CBf-AC/CME sensor was evaluated for the simultaneous detection of the three analytes (AMP, PAR and CIP) in the synthetic urine samples. Their preparation steps are presented in the [section II.8.2](#). For this analysis 10 mL of urine sample was add to 10 mL of BR electrolyte (0.04 M, pH = 5). After stirring, the solution was spiked with known AMP, PAR and CIP amounts, two concentrations were analyzed (1 and 3 μM). After that, to find the spiked previously known three drugs amounts, the standard addition method was used, with successive addition of known AMP, PAR and CIP amounts (1; 2 and 3 μM) in the electrochemical cell containing the diluted urine sample. The average recovery of the proposed method was from 102.0 % to 107.3 % and the RSD values (n=3) are below 4.1 % for the different reagents ([Table IV.7](#)). Therefore, the developed nanostructured modified cavity microelectrode (CBf-AC/CME) is able to detect simultaneously AMP, PAR and CIP drugs with a simple dilution of the urine by the SBR solution (pH=5). This proposed electroanalytical method demonstrates a performance of the proposed micro-sensor and its feasibility in urine sample analysis with high accuracy.

Table IV.7. Validation of the CBf-AC/CME in the determination of AMP, PAR and CIP in inartificial urine. (*n=3)

Analytes	Concentration added (μM)	Concentration found (μM)	RSD* (%)	Recovery (%)
AMP	1.00	1.07	3.1	107.2
	3.00	3.16	3.2	105.5
PAR	1.00	1.12	3.5	106.6
	3.00	3.22	4.1	107.3
CIP	1.00	1.06	3.4	106.5
	3.00	3.06	0.8	102.0

Conclusion

In this chapter, we developed a cavity microelectrode nanostructured with activated carbon and functionalized carbon black for the simultaneous determination of 4-aminophenol, paracetamol and ciprofloxacin. The excellent proprieties of the carbon materials used in the design of this micro-sensor improve considerably their electrochemical and analytical performance, by enhancing the surface area and accelerating the electrons transfer that lead to higher conductivity with lower electrochemical interferences. The so-designed microelectrode was used for the simultaneous detection of the drugs in BR solution (0.04 M) at pH= 7 after a previous stirring step of 5 minutes with square wave voltammetry. The results show wide linear responses in the range of 0.1 to 3 μ M, 0.025 to 3 μ M and 0.05 to 3 μ M for 4-aminophenol, paracetamol and ciprofloxacin, respectively and with their detection limits of 63, 23 and 39 nM, respectively. In addition, the CBf-AC/ CME show a high selectivity, good repeatability and reproducibility.

The originality of this work is the use of the cavity microelectrode as device for the design of the sensor, known that in the literature; they are a few researches that use the CMEs for the electrochemical sensing. In addition, the use of this microelectrode in the simultaneous detection that can be considered as a first study realized in this purpose.

This micro-sensor has solved issues such as overlapping of the potential peaks, interferent effects, and it has been successfully applied for the analysis of wastewater and artificial urine samples with a satisfactory recovery without any specific procedure, just by diluting the sample in the BR electrolyte.

Hence, the proposed modified cavity microelectrode could be a promising and suitable device for the simultaneous analysis of 4-aminophenol, paracetamol and ciprofloxacin in biological or environmental samples. It offers advantages in their capability to detect three drugs simultaneously with any overlapping in the potential peaks or interfering effects between them by just using a simple, economical and rapid procedure. Moreover, this developed device offers the possibility to follow the degradation of paracetamol to 4-aminophenol in real samples. A study that can be investigated and developed in the future research.

References

- [1] Yessoufou, A., Mama, D., Suanon, F., Alamou, E. A., Fayomi, B., Degbey, C. & Dedjiho, C. A. (2016). Pharmaceuticals and Personal Care Products (PPSPS) in the Aquatic Environment: Status and Issues in the Republic of Benin, *Research Journal of Pharmaceutical Sciences*, 5 (3), 1.
- [2] World Drug Report. (2020). Drug use and health consequences, Booklet 2 (United Nations publication, Sales No. E.20.XI.6).
- [3] Hedegaard, H., Miniño, A.M. & Warner, M. (2020). Drug overdose deaths in the United States, 1999–2018. NCHS Data Brief, no 356. Hyattsville, MD: National Center for Health Statistics.
- [4] Sharma, P., Kumar, D., & Mutnuri, S. (2020). Probing the degradation of pharmaceuticals in urine using MFC and studying their removal efficiency by UPLC-MS/MS, *Journal of Pharmaceutical Analysis*.
- [5] Santos, L.H.M.L.M., Paíga, P., Araújo, A.N., Pena, A., Delerue-Matos, C. & Montenegro, M.C.B.S.M. (2013). Development of a simple analytical method for the simultaneous determination of paracetamol, paracetamol-glucuronide and p-aminophenol in river water, *Journal of Chromatography B*, 930, 75.
- [6] Nief, R. A. (2019). HPLC Method for Determination of Paracetamol in Pharmaceutical Formulations and Environmental Water Samples, *Chemical Science Transactions*, 8(2), 237.
- [7] Emami, J. & Rezazadeh, M. (2016). A simple and sensitive high-performance liquid chromatography method for determination of ciprofloxacin in bioavailability studies of conventional and gastroretentive prolonged-release formulations, *Advanced Biomedical Research*, 5, 163.
- [8] Lu, X., Wei, F., Xu, G., Wu, Y., Yang, W. & Hu, Q. (2017). Surface Molecular Imprinting on Silica-Coated CdTe Quantum Dots for Selective and Sensitive Fluorescence Detection of p-aminophenol in Water, *Journal of Fluorescence*, 27, 181.
- [9] Montaseri, H. & Forbes, P. B. C. (2017). Fluorescence sensor probe for the detection of acetaminophen using L-cysteine CdSe/ZnS quantum dots and molecular imprinted polymer@quantum dots, *2017 IEEE SENSORS, Glasgow*, 1.
- [10] El Kojok, H., El Darra, N., Khalil, M., Capo, A., Pennacchio, A., Staiano, M., Camarca, A., D'Auria, S., & Varriale, A. (2020). Fluorescence polarization assay to detect the presence of traces of ciprofloxacin. *Scientific reports*, 10(1), 4550.

- [11] Chen, C. & Hahn J. H. (2011). Enhanced aminophenols monitoring using in-channel amperometric detection with dual-channel microchip capillary electrophoresis, *Environmental Chemistry Letter*, 9, 491.
- [12] Hložek, T., Křížek, T., Tůma, P., Bursová, M., Coufal, P. & Čabala, R. (2017). Quantification of paracetamol and 5-oxoproline in serum by capillary electrophoresis: Implication for clinical toxicology, *Journal of Pharmaceutical and Biomedical Analysis*, 145, 616.
- [13] Díaz-Quiroz, C. A., Hernández-Chávez, J. F., Ulloa-Mercado, G., Gortáres-Moroyoqui, P., Martínez-Macías, R., Meza-Escalante, E. & Serrano-Palacios, D. (2018). Simultaneous quantification of antibiotics in wastewater from pig farms by capillary electrophoresis, *Journal of Chromatography B*, 1092, 386.
- [14] Chen, S., Huang, R., Zou, J., Liao, D., Yu, J. & Jiang, X. (2020). A sensitive sensor based on MOFs derived nanoporous carbons for electrochemical detection of 4-aminophenol, *Ecotoxicology and Environmental Safety*, 191, 110194.
- [15] Mangaiyarkarasi, R., Premalatha, S., Khan, R., Pratibha, R. & Umadevi, S. (2020). Electrochemical performance of a new imidazolium ionic liquid crystal and carbon paste composite electrode for the sensitive detection of paracetamol, *Journal of Molecular Liquids*, 319, 114255.
- [16] Matsunaga, T., Kondo, T., Osasa, T., Kotsugai, A., Shitanda, I., Hoshi, Y., Itagaki, M., Aikawa, T., Tojo, T. & Yuasa, M. (2020). Sensitive electrochemical detection of ciprofloxacin at screen-printed diamond electrodes, *Carbon*, 159, 247.
- [17] Guo, H., Fan, T., Yao, W., Yang, W., Wu, N., Liu, H., Wang, M. & Yang, W. (2020). Simultaneous determination of 4-aminophenol and acetaminophen based on high electrochemical performance of ZIF-67/MWCNT-COOH/Nafion composite, *Microchemical Journal*, 158, 105262.
- [18] Pollap, A., Baran, K., Kuszewska, N. & Kochana, J. (2020). Electrochemical sensing of ciprofloxacin and paracetamol in environmental water using titanium sol based sensor, *Journal of Electroanalytical Chemistry*, 878, 114574.
- [19] Dhar, D., Roy, S. & Nigam, V.K. (2019). Chapter 10 - Advances in protein/enzyme-based biosensors for the detection of pharmaceutical contaminants in the environment, Editor(s): Brar, S.K., Hegde, K. & Pachapur, V.L. *Tools, Techniques and Protocols for Monitoring Environmental Contaminants*, Elsevier, 207.
- [20] Daly, C., Griffin, E., Corcoran, P., Webb, R.T., Ashcroft, D.M., Perry, I.J. & Arensman, E. (2020). A national case fatality study of drugs taken in intentional overdose, *International Journal of Drug Policy*, 76, 102609.

- [21] Parolini, M. (2020). Toxicity of the Non-Steroidal Anti-Inflammatory Drugs (NSAIDs) acetylsalicylic acid, paracetamol, diclofenac, ibuprofen and naproxen towards freshwater invertebrates: A review, *Science of the Total Environment*, 740, 140043.
- [22] Valdez-Carrillo, M., Abrell, L., Ramírez-Hernández, J., Reyes-López, J. A., & Carreón-Díazconti, C. (2020). Pharmaceuticals as emerging contaminants in the aquatic environment of Latin America: a review. *Environmental science and pollution research international*, 27 (36), 44863.
- [23] Rex Reklaitis, G.V. (2017). Prospects and Challenges for Process Systems Engineering in Healthcare, Editor(s): Espuña, A., Graells, M. & Puigjaner, L. *Computer Aided Chemical Engineering*, Elsevier, 40, 3.
- [24] Munteanu, F. D., Titoiu, A. M., Marty, J. L., & Vasilescu, A. (2018). Detection of Antibiotics and Evaluation of Antibacterial Activity with Screen-Printed Electrodes. *Sensors (Basel, Switzerland)*, 18(3), 901.
- [25] Boxall, A.B., Rudd, M.A., Brooks, B.W., Caldwell, D.J., Choi, K., Hickmann, S., Innes, E., Ostapyk, K., Staveley, J.P., Verslycke, T. & Ankley, G.T. (2012). Pharmaceuticals and personal care products in the environment: what are the big questions?. *Environmental Health Perspectives* 120 (9), 1221.
- [26] Food and Drug Administration. (2009). Determining Established Pharmacologic Class for Use in the Highlights of Prescribing Information guidance. From <https://www.fda.gov/media/77834/download>. Accessed on 20 February 2021.
- [27] United States Pharmacopoeia. USP Medicare model guidelines v. 7.0.
- [28] Feier, B., Florea, A., Cristea, C. & Săndulescu, R. (2018). Electrochemical detection and removal of pharmaceuticals in waste waters, *Current Opinion in Electrochemistry*, 11, 1.
- [29] Pemberthy, M. D., Padilla, Y., Echeverri, A. & Peñuela, G. A. (2020). Monitoring pharmaceuticals and personal care products in water and fish from the Gulf of Urabá, Colombia, *Heliyon*, 6 (6), e04215
- [30] Żur, J., Piński, A., Marchlewicz, A., Hupert-Kocurek, K., Wojcieszynska, D., & Guzik, U. (2018). Organic micropollutants paracetamol and ibuprofen-toxicity, biodegradation, and genetic background of their utilization by bacteria. *Environmental science and pollution research international*, 25(22), 21498.
- [31] Velásquez Arias, J. A. (2019). Pharmaceutical and Personal Hygiene Products (PPcPs): A Threat Little Studied in Colombian Waters. *Agriculture Research and Technology: Open Access Journal*, 22 (3), 556201.

- [32] Szymonik, A., Lach, J. & Malińska, K. (2017). Fate and Removal of Pharmaceuticals and Illegal Drugs Present in Drinking Water and Wastewater, *Ecological Chemistry and Engineering S*, 24(1), 65.
- [33] Aus der Beek, T., Weber, F.-A., Bergmann, A., Hickmann, S., Ebert, I., Hein, A. & Küster, A. (2016). Pharmaceuticals in the environment—Global occurrences and perspectives. *Environmental Toxicology and Chemistry*, 35, 823.
- [34] Henrique, J.M.M., Monteiro, M.K.S., Cardozo, J.C., Martínez-Huitle, C.A., da Silva, D.R. & dos Santos, E.V. (2020). Integrated-electrochemical approaches powered by photovoltaic energy for detecting and treating paracetamol in water, *Journal of Electroanalytical Chemistry*, 876, 114734.
- [35] Dear, J.W. & Bateman, D.N. (2020). Paracetamol poisoning, *Medicine*, 48(3), 208.
- [36] Smilkstein, M. J., Knapp, G. L., Kulig, K. W. & Rumack, B. H. (1988). Efficacy of oral N-acetylcysteine in the treatment of acetaminophen overdose. Analysis of the national multicenter study (1976 to 1985), *The New England Journal of Medicine*, 319, 1557.
- [37] National Center for Biotechnology Information (2021). PubChem Compound Summary for CID 403, 4-Aminophenol. From <https://pubchem.ncbi.nlm.nih.gov/compound/4-Aminophenol>. Accessed on 22 February 2021.
- [38] Németh, T., Jankovics, P., Németh-Palotás, J. & Kőszegi-Szalai, H. (2008). Determination of paracetamol and its main impurity 4-aminophenol in analgesic preparations by micellar electrokinetic chromatography, *Journal of Pharmaceutical and Biomedical Analysis*, 47, 746.
- [39] Rahman, M.M. (2020). Selective and sensitive 4-Aminophenol chemical sensor development based on low-dimensional Ge-doped ZnO nanocomposites by electrochemical method, *Microchemical Journal*, 157, 104945.
- [40] Tranchant, M., Serrà, A., Gunderson, C., Bertero, E., García-Amorós, J., Gómez, E., Michler, J. & Philippe, L. (2020). Efficient and green electrochemical synthesis of 4-aminophenol using porous Au micropillars, *Applied Catalysis A: General*, 602, 117698.
- [41] Fiaschi, G., Cosentino, S., Pandey, R., Mirabella, S., Strano, V., Maiolo, L., Grandjean, D., Lievens, P., Shacham-Diaman, Y. (2018). A novel gas-phase mono and bimetallic clusters decorated ZnO nanorods electrochemical sensor for 4-aminophenol detection, *Journal of Electroanalytical Chemistry*, 811, 89.
- [42] Klos, C., Koob, M., Kramer, C. & Dekant, W. (1992). p-Aminophenol nephrotoxicity: Biosynthesis of toxic glutathione conjugates, *Toxicology and Applied Pharmacology*, 115, 98.

- [43] Harmon, R.C., Kiningham, K.K. & Valentovic, M.A. (2006). Pyruvate reduces 4-aminophenol in vitro toxicity, *Toxicology and Applied Pharmacology*, 213, 179.
- [44] Scandurra, G., Antonella, A., Ciofi, C., Saitta, G., & Lanza, M. (2014). Electrochemical detection of p-aminophenol by flexible devices based on multi-wall carbon nanotubes dispersed in electrochemically modified Nafion. *Sensors (Basel, Switzerland)*, 14(5), 8926.
- [45] Liu, X., Li, H., Zhou, H., Liu, J., Li, L., Liu, J., Yan, F. & Luo, T. (2020). Direct electrochemical detection of 4-aminophenol in pharmaceuticals using ITO electrodes modified with vertically-ordered mesoporous silica-nanochannel films, *Journal of Electroanalytical Chemistry*, 878, 114568.
- [46] Chen, C.F., Tseng, Y.T., Tseng, H.K. & Liu, T.Z. (2004). Automated spectrophotometric assay for urine p-aminophenol by an oxidative coupling reaction, *Annals of clinical and laboratory science*, 34, 336.
- [47] National Center for Biotechnology Information. (2021). PubChem Compound Summary for CID 1983, Acetaminophen. From <https://pubchem.ncbi.nlm.nih.gov/compound/Acetaminophen>. Accessed on 18 February 2021
- [48] Srabovic, M., Huremovic, M., Catovic, B., Muratovic, S. & Taletović, A. (2017). Design synthesis and crystallization of acetaminophen, *Journal of Chemical, Biological and Physical Sciences Section A*, 7(1), 218.
- [49] Vanden Eynde J. J. (2016). How Efficient Is My (Medicinal) Chemistry?. *Pharmaceuticals (Basel, Switzerland)*, 9(2), 26. <https://doi.org/10.3390/ph9020026> Accessed on 20 January 2021.
- [50] Goscianska, J., Olejnik, A., Ejsmont, A., Galarda, A. & Wuttke, S. (2021). Overcoming the paracetamol dose challenge with wrinkled mesoporous carbon spheres, *Journal of Colloid and Interface Science*, 586, 673.
- [51] Kingsley Ogemdi, I. (2019). A Review on the Properties and Uses of Paracetamol. *International Journal of Pharmacy and Chemistry*. 5(3), 31.
- [52] Razi Zaidi, S. T. & Hasan, S. S. (2021). Personal protective practices and pharmacy services delivery by community pharmacists during COVID-19 pandemic: Results from a national survey, *Research in Social and Administrative Pharmacy*, 17 (1), 1832.
- [53] World Health Organization. (2019). World Health Organization Model List of Essential Medicines, 21st list, 1-65. <https://www.who.int/publications/i/item/WHOMVPEMPIAU2019.06> Accessed 23 January 2021.

- [54] Shraim, A., Diab, A., Alsuhaime, A., Niazy, E., Metwally, M., Amad, M., Sioud, S. & Dawoud, A. (2017). Analysis of some pharmaceuticals in municipal wastewater of Almadinah Almunawarah, *Arabian Journal of Chemistry*, 10 (1), S719.
- [55] Mutharani, B., Ranganathan, P., Chen, SM. & Karuppiyah. C. (2019). Simultaneous voltammetric determination of acetaminophen, naproxen, and theophylline using an in-situ polymerized poly(acrylic acid) nanogel covalently grafted onto a carbon black/La₂O₃ composite. *Microchimical Acta*, 186, 651.
- [56] Agrawal S, Khazaeni B. Acetaminophen Toxicity. [Updated 2020 Nov 20]. In: StatPearls [Internet]. Treasure Island (FL): StatPearls Publishing; 2021 Jan-. Available from: <https://www.ncbi.nlm.nih.gov/books/NBK441917/>. . Accessed on 19 January 2021.
- [57] U.S. Food & Drug Administration. (2018). Drug Safety and Availability, FDA Drug Safety Communication. <https://www.fda.gov/drugs/drug-safety-and-availability/fda-drug-safety-communication-prescription-acetaminophen-products-be-limited-325-mg-dosage-unit>. Accessed on 23 January 2021.
- [58] Acetaminophen Dosage. Medically reviewed by Drugs.com. Last updated on Aug 7, 2020. <https://www.drugs.com/dosage/acetaminophen.html>. Accessed on 23 February 2021.
- [59] ANSM. (2019). Bon usage du paracétamol et des anti-inflammatoires non stéroïdiens (AINS) : l'ANSM veut renforcer le rôle de conseil du pharmacien - Point d'Information.
- [60] Modick, H., Weiss, T., Dierkes, G., Brüning, T., & Koch, H. M. (2014). Ubiquitous presence of paracetamol in human urine: sources and implications. *Reproduction (Cambridge, England)*, 147(4), R105.
- [61] National Center for Biotechnology Information (2021). PubChem Compound Summary for CID 2764, Ciprofloxacin. From <https://pubchem.ncbi.nlm.nih.gov/compound/Ciprofloxacin>. Accessed on 18 February 2021.
- [62] H. Bagheri, H. Khoshshafar, S. Amidic and Ardakani, Y. H. (2016). Fabrication of an electrochemical sensor based on magnetic multi-walled carbon nanotubes for the determination of ciprofloxacin, *Analytical Methods*, 8, 3383.
- [63] Jalal, N.R., Madrakian, T., Afkhami, A. & Ghamsari, M. (2019). Polyethylenimine@Fe₃O₄@carbon nanotubes nanocomposite as a modifier in glassy carbon electrode for sensitive determination of ciprofloxacin in biological samples, *Journal of Electroanalytical Chemistry*, 833, 281.

- [64] Trevino, N., Montes, W. & Ganta, D. (2019). Disposable chronoamperometric sensor for detecting ciprofloxacin, *Engineering Research Express*, 1 (1), 15.
- [65] Ensafi, A. A., Allafchian, A. R., & Mohammadzadeh, R. (2012). Characterization of MgFe_2O_4 nanoparticles as a novel electrochemical sensor: application for the voltammetric determination of ciprofloxacin. *Analytical sciences: the international journal of the Japan Society for Analytical Chemistry*, 28(7), 705.
- [66] Cinková, K., Andrejčáková, D. & Švorc L. (2016). Electrochemical method for point-of-care determination of ciprofloxacin using boron-doped diamond electrode, *Acta Chimica Slovaca* 9(2), 146.
- [67] Yuphintharakun, N., Nurerk, P., Chullasat, K., Kanatharana, P., Davis, F., Sooksawat, D. & Bunkoed, O. (2018). A nanocomposite optosensor containing carboxylic functionalized multiwall carbon nanotubes and quantum dots incorporated into a molecularly imprinted polymer for highly selective and sensitive detection of ciprofloxacin, *Spectrochimica Acta Part A: Molecular and Biomolecular Spectroscopy*, 201, 382.
- [68] Faria, L.V., Pereira, J.F.S., Azevedo, G.C., Matos, M.A.C., Munoz, R.A.A., & Matos, R.C.. (2019). Square-Wave Voltammetry Determination of Ciprofloxacin in Pharmaceutical Formulations and Milk Using a Reduced Graphene Oxide Sensor. *Journal of the Brazilian Chemical Society*, 30(9), 1947.
- [69] Carvalho, S.W.M.M., Santana, T.B.S., Matos, C.R.S., Costa, L.P., Sussuchi, E.M., & Gimenez, I.F. (2019). Synthesis of Hydrotalcite-Supported CdTe Semiconductor Nanocrystals for Electrochemical Detection of Ciprofloxacin. *Journal of the Brazilian Chemical Society*, 30(6), 1266.
- [70] Shen, R., Yu, Y., Lan, R., Yu R., Yuan, Z. & Xia, Z. (2019). The cardiovascular toxicity induced by high doses of gatifloxacin and ciprofloxacin in zebrafish, *Environmental Pollution*, 254 (B), 112861.
- [71] Song, T., Pham, H., Mahon, P.J., Lai, G. & Yu, A. (2018). Reduced Graphene Oxide Nanocomposite Modified Electrodes for Sensitive Detection of Ciprofloxacin, *Electroanalysis*, 30 (9), 2185.
- [72] Bai, F.-Y., Ni, S., Tang, Y.-Z., Pan, X.-M. & Zhao, Z. (2019). Ciprofloxacin transformation in aqueous environments: Mechanism, kinetics, and toxicity assessment during $\bullet\text{OH}$ -mediated oxidation, *Science of the Total Environment*, 699, 134190.
- [73] Wang, Y., Shen, C., Zhang, M., Zhang, B.-T. & Yu, Y.-G. (2016). The electrochemical degradation of ciprofloxacin using a $\text{SnO}_2\text{-Sb/Ti}$ anode: Influencing factors, reaction pathways and energy demand, *Chemical Engineering Journal*, 296, 79.

- [74] Drugs.com. (2020). Ciprofloxacin Dosage. From <https://www.drugs.com/dosage/ciprofloxacin.html>, Accessed 01 February 2021.
- [75] Gendrel, D., Chalumeau, M., Moulin, F. & Raymond, J. (2003). Fluoroquinolones in paediatrics: a risk for the patient or for the community?, *The Lancet Infectious Diseases*, 3, 537.
- [76] FDA US Food & Drug Administration. (2013). CIPRO® (ciprofloxacin hydrochloride) TABLETS CIPRO® (ciprofloxacin*) ORAL SUSPENSION, Manufactured for: Bayer HealthCare Pharmaceuticals Inc. Wayne, NJ 07470.
- [77] Bushra, R., Aslam, N., & Khan, A. Y. (2011). Food-drug interactions. *Oman medical journal*, 26(2), 77.
- [78] Pápai, K., Budai, M., Ludányi, K., Antal, I., & Klebovich, I. (2010). In vitro food-drug interaction study: Which milk component has a decreasing effect on the bioavailability of ciprofloxacin?. *Journal of pharmaceutical and biomedical analysis*, 52(1), 37.
- [79] Graham, G.G., Scott, K.F. & Day, R.O. (2004). Alcohol and paracetamol. *Australian Prescriber*, 27, 14.
- [80] Issa, M. M., Nejem, R. M., El-Abadla, N. S., El-Naby, M. K., Roshdy, A. A., & Kheiralla, Z. A. (2007). Effects of paracetamol on the pharmacokinetics of ciprofloxacin in plasma using a microbiological assay. *Clinical drug investigation*, 27(7), 463.
- [81] Bagheri, S., Julkapli, N.M. & Abd Hamid S.B. (2015). Functionalized Activated Carbon Derived from Biomass for Photocatalysis Applications Perspective, *International Journal of Photoenergy*, Article ID 218743, 30.
- [82] Tehrani-Bagha, A.R. & Balchi, T. (2018). Chapter 12 - Catalytic Wet Peroxide Oxidation, Editor(s): Ameta, S.C. & Ameta, R. Advanced Oxidation Processes for Waste Water Treatment, *Academic Press*, 375.
- [83] Ayyalusamy, S., Mishra, S. & Suryanarayanan, V. (2018). Promising post-consumer PET-derived activated carbon electrode material for non-enzymatic electrochemical determination of carbofuran hydrolysate. *Scientific Reports*, 8, 13151.
- [84] Ibáñez-Redín, G., Silva, T.A., Vicentini, F.C. & Fatibello-Filho, O. (2018). Effect of carbon black functionalization on the analytical performance of a tyrosinase biosensor based on glassy carbon electrode modified with dihexadecylphosphate film, *Enzyme and Microbial Technology*, 116, 41.
- [85] Kutty, M., Settu, R., Chen, S.-M., Chen, T.-W., Tseng, T.-W., Hatamleh, A. A., Yu, J., Yu, R. & Huang, C.-C. (2019). An Electrochemical Detection of Vanillin Based on

Carbon Black Nanoparticles Modified Screen Printed Carbon Electrode, *International Journal of Electrochemistry Science*, 14, 5972.

- [86] Jebril, S., Cubillana-Aguilera, L., Palacios-Santander, J. M. & Dridi, C. (2021). A novel electrochemical sensor modified with green gold sononanoparticles and carbon black nanocomposite for bisphenol A detection, *Materials Science and Engineering: B* 264, 114951.
- [87] Shrivastava, A. & Gupta, V. B. (2011). Method for the determination of limit of detection and limit of quantification of the analytical methods, *Chronicles of Young Scientists*, 2 (1), 21.
- [88] Keerthi, M. (2019). An Efficient Electrochemical Sensor Based on Ag Nanoparticle Decorated MnO₂/reduced Graphene Oxide Ternary Nanocomposite for Detection of Acetaminophen in Human Urine Sample. *International Journal of Electrochemical Science*, 346.
- [89] Purohit, B., Kumar, A., Mahato, K. & Chandra, P. (2020). Novel Sensing Assembly Comprising Engineered Gold Dendrites and MWCNT-AuNPs Nanohybrid for Acetaminophen Detection in Human Urine. *Electroanalysis*, 32 (3), 561.
- [90] Ensafi, A. A., Allafchian, A. R., & Mohammadzadeh, R. (2012). Characterization of MgFe₂O₄ nanoparticles as a novel electrochemical sensor: application for the voltammetric determination of ciprofloxacin. *Analytical sciences: the international journal of the Japan Society for Analytical Chemistry*, 28(7), 705.
- [91] Reddy, K.R., Brahman, P.K. & Suresh, L. (2018). Fabrication of high performance disposable screen printed electrochemical sensor for ciprofloxacin sensing in biological samples, *Measurement*, 127, 175.
- [92] Dou, N., Zhanga, S & Qu, J. (2019). Simultaneous detection of acetaminophen and 4-aminophenol with an electrochemical sensor based on silver–palladium bimetal nanoparticles and reduced graphene oxide, *Royal Society of Chemistry Advances*, 9, 31440.
- [93] Liang, Q., Liu, Z., Liang, C., Han, G.-C., Zhang, S. & Feng, X.-Z. (2019). Electrochemical Simultaneous Detection of Paracetamol and 4-aminophenol Based on bis-Schiff Base Cobalt Complex, *International Journal of Electrochemical Science*, 14, 7178.
- [94] Santos, A. M., Wong, A., Almeida, A. A. & Fatibello-Filho, O. (2017). Simultaneous determination of paracetamol and ciprofloxacin in biological fluid samples using a glassy carbon electrode modified with graphene oxide and nickel oxide nanoparticles, *Talanta*, 174, 610.

- [95] Biswas, S., Naskar, H., Pradhan, S., Chen, Y., Wang, Y., Bandyopadhyay, R. & Pramanik, P. (2020). Sm₂O₃ nanorod modified graphite paste electrode for trace level voltammetric determination of acetaminophen and ciprofloxacin, *New Journal of Chemistry*, 44, 1921.
- [96] Kingsley, M. P., Kalambate, P. & Srivastava, A. K. (2016). Simultaneous determination of ciprofloxacin and paracetamol by adsorptive stripping voltammetry using copper zinc ferrite nanoparticles modified carbon paste electrode, *Royal Society of Chemistry Advances*, 6, 15101.

Chapter V

**Ultra-traces analysis of paracetamol in water by electrochemical
preconcentration on a carbon black cavity microelectrode**

Introduction

Paracetamol is the most widely prescribed and administered drug and is widely used for the treatment of headaches, fever and temporary pain [1]. It is on the World Health Organization's list of essential medicines [2]. However, when PAR is ingested in overdose, it becomes hepatotoxic, causing acute liver failure and generating metabolites that lead to oxidative stress, self-poisoning and hepatocyte death [3]. The FDA is calling for the restriction of the prescription of PAR in order to make it safer for patients [4]. Currently, PAR is one of the most emerging pollutants that is frequently detected in environmental waters [5]. This target drug was found in raw (influent), treated (effluent) and tap water samples with an average concentration of $3.61\text{--}99.6\text{ ng.mL}^{-1}$, $< 90.5\text{ ng.mL}^{-1}$ and $230\text{ }\mu\text{g.L}^{-1}$, respectively [6, 7].

In this context, various electrochemical sensors have been reported for the determination of PAR, such as carbon paste, glassy carbon or screen-printed electrodes modified with polymers [8, 9], ionic liquid [10, 11] carbonaceous materials [12-15] and/or metal nanoparticles [16-18]. But most of them require a complex surface modification procedure and/or use large amounts of material. However, the use of cavity microelectrode (CME), having a very small size microcavity, has several advantages over other electrodes (see Chapter I.4.2) [19]. Furthermore, to the best of our knowledge, no work has been reported in the literature on the detection of PAR with a cavity microelectrode. Moreover, the use of carbon black (CB), which has abundant pores, large surface area and high conductivity, to modify the electrodes will improve the analytical signal, electron transfer kinetics and significantly improve their analytical performance, such as sensitivity, detection and quantification limits, stability, reproducibility and repeatability [20, 21]. In addition, electrochemical preconcentration (EP) at a controlled potential is one of the most frequently applied techniques for traces analysis, in order to preconcentrate the analyte at electrode surface. It offers various advantages like simplicity, high and efficient preconcentration of the target analyte on the sensor surface without any risk of contamination [22].

In this chapter, we present the design, optimisation and validation of the electrochemical preconcentration method for paracetamol on a carbon black modified cavity microelectrode. We also demonstrate the utility of combining the cavity microelectrode, carbon black and the electrochemical preconcentration method to improve the electroanalytical properties and performance of the designed micro-sensor.

V.1. Characterization of electrode

V.1.1. Characterization of the electrode material by scanning electron microscopy (SEM)

As can be seen in Fig. V.1, carbon black consists of extremely fine particles forming an infrastructure in the form of three-dimensional networks of random orientation. In fact, carbon black is made up of spherical particles with an average diameter at around 100 nm that gather in the form of aggregates. These aggregates accumulate to form massive groups called agglomerates of different sizes and shapes. The nanostructure carbon black provides a large, coherent and homogeneous surface, which leads to improved properties of the designed sensor.

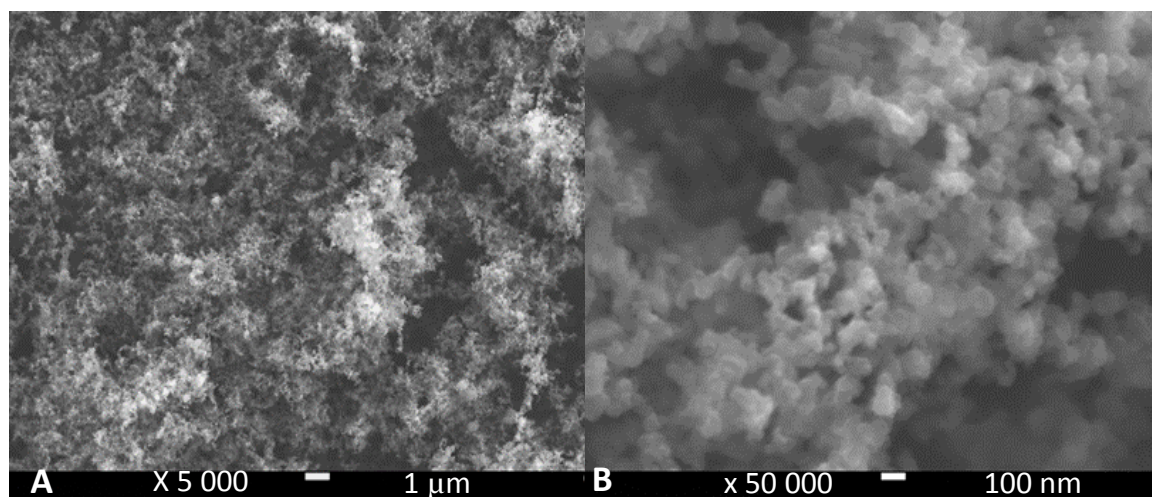


Figure V.1. SEM images for CB (A) (x 5.000), (B) (x 50.000)

V.1.2. Characterization of the modified electrode CB/CME by electrochemical impedance spectroscopy (EIS)

Electrochemical impedance spectroscopy (EIS) is an effective method for characterizing the electron transfer at the surface of the micro-sensor. The diameter of the semicircle in the impedance spectrum is equal to the charge transfer resistance (R_{ct}). Therefore, the charge transfer resistance (R_{ct}) can be used to describe the interface properties of the electrode, and to characterize the adsorption on its surface.

Impedance spectra were plotted in an electrolyte solution containing 1 mM of $[\text{Fe}(\text{CN})_6]^{3-/4-}$ as redox probe, in the frequency range 10^{-3} to 10^{+5} Hz using a sinusoidal excitation signal (sine signal) with amplitude of 10 mV at CB/ CME with and without EP (Fig. V.2). Both Nyquist plots showed a large semicircle with no linear part, indicating that an electron transfer

process limits the reaction process at the CME / electrolyte interface. The charge transfer resistance of the CB / MCE without EP is 10.7 MΩ; it decreases to 6.69 MΩ with EP at 0V. This decrease of charge transfer resistance can be attributed to the ability of the EP in the adsorption of the analyte in the electrode surface, which promote electron transfer and increase their transfer kinetic.

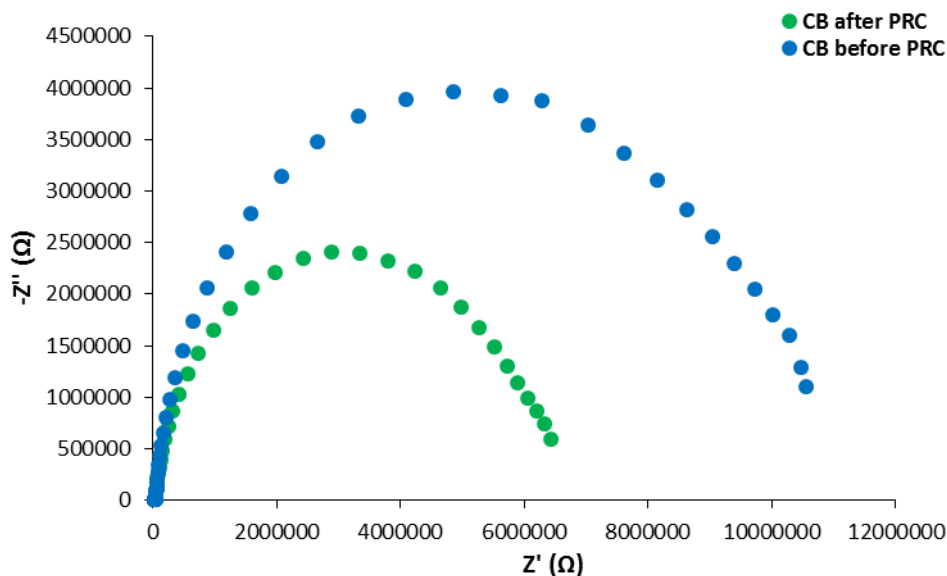


Figure V.2. Nyquist diagram of CB/CME of 1 mM $\text{Fe}(\text{CN})_6^{3-/4-}$ in BRS 0.04 M (pH=7) with and without EP at 0V

V.1.3. Determination of the electrochemical active area

The effective surface of the proposed microelectrode was estimated by the CV technique, using potassium ferrocyanide (II) as a redox probe with a completely reversible system and fast electron transfer kinetics at different potential scan rates. For this reversible process, the surface area was determinate by the following Randles-Sevcik equation, which shows the relation between peak current and scan rate [23]:

$$I_{Pa} = (2.69 \times 10^5) n^{3/2} A D^{1/2} C_0 U^{1/2} \quad \text{Eq. 5.1}$$

Where I_{Pa} is the anodic peak current, n number of electrons transferred during the reaction, A is the active area of the microelectrode, C_0 is the initial concentration of ferrocyanide, U is the scan rate and D the diffusion coefficient of ferrocyanide which is well known to be $7.6 \times 10^{-6} \text{ cm}^2 \cdot \text{s}^{-1}$ [24] in aqueous electrolyte at 25 °C. Voltaamperogram of 1 mM of $\text{K}_4\text{Fe}(\text{CN})_6$ in BRS electrolyte at different scan rates (5 to 300 $\text{mV} \cdot \text{s}^{-1}$) are represented in the Fig.V.3-A, $n = 1$. Thus, from the slope of the linear regression line of the current density versus the square root

of the scan rate ($I_{pa} = 1.81 \times 10^{-3} U^{1/2} - 1.02 \times 10^{-3}$ with $R^2 = 0.999$), the electrochemical active area of the sensor was estimated to be $2.44 \times 10^{-3} \text{ cm}^2$. While the geometric surface of the unmodified CME was calculated to be $7.06 \times 10^{-6} \text{ cm}^2$ considering the cross section of the cavity. Therefore, modification of the CME by incorporation of CB significantly enhances the surface area of about 345 times. This demonstrates the role of CB in improving the electrode surface area.

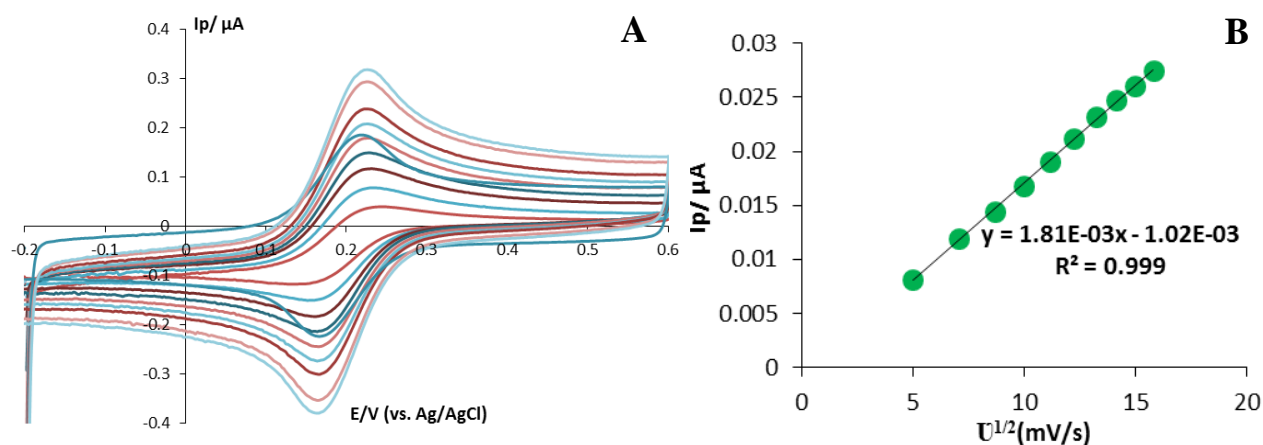


Figure V.3. (A) Cyclic voltammograms of 1 mM of $K_3Fe(CN)_6$ in BRS 0.04 M (pH = 7) at different scan rate values (5 to 300 mV.s^{-1}) at the CB/CME (B) Plot of the peaks current oxidation of PAR versus scan rate

V.2. Optimization of the electrochemical detection method

V.2.1. Effect of scan rate

The EP/CV of $1 \mu\text{M}$ PAR on the CB/ CME at different scan rates was investigated measurements in BRS at pH = 7. The resulting voltammograms are shown in the Fig. V.4-A. A linear relationship is observed between the anodic peak current and the scan rate in the range of 25 to 250 mV.s^{-1} (Fig. V.4-B) indicating adsorption-controlled process for PAR oxidation:

$$I_{pa} = 3.61 \times 10^{-5} U - 8.68 \times 10^{-4} \quad (R^2 = 0.999) \quad \text{Eq. 5.2}$$

In order to confirm the adsorption behavior control, the dependence of the peak current on the scan rate was also studied for a lower concentration of $0.05 \mu\text{M}$ PAR on the CB/ CME at the same scan rate range. As seen in the Fig. V.4-C, a linear relationship was also observed:

$$I_{pa} = 3.31 \times 10^{-6} U - 8.97 \times 10^{-5} \quad (R^2 = 0.998)$$

Eq. 5.3

This result can be probably due to the deposition of infinite quantity of PAR on the surface of the electrode, which allows to largely adsorption controlled nature of the microelectrode process. This adsorption step leads to higher sensibility and lower detection limit.

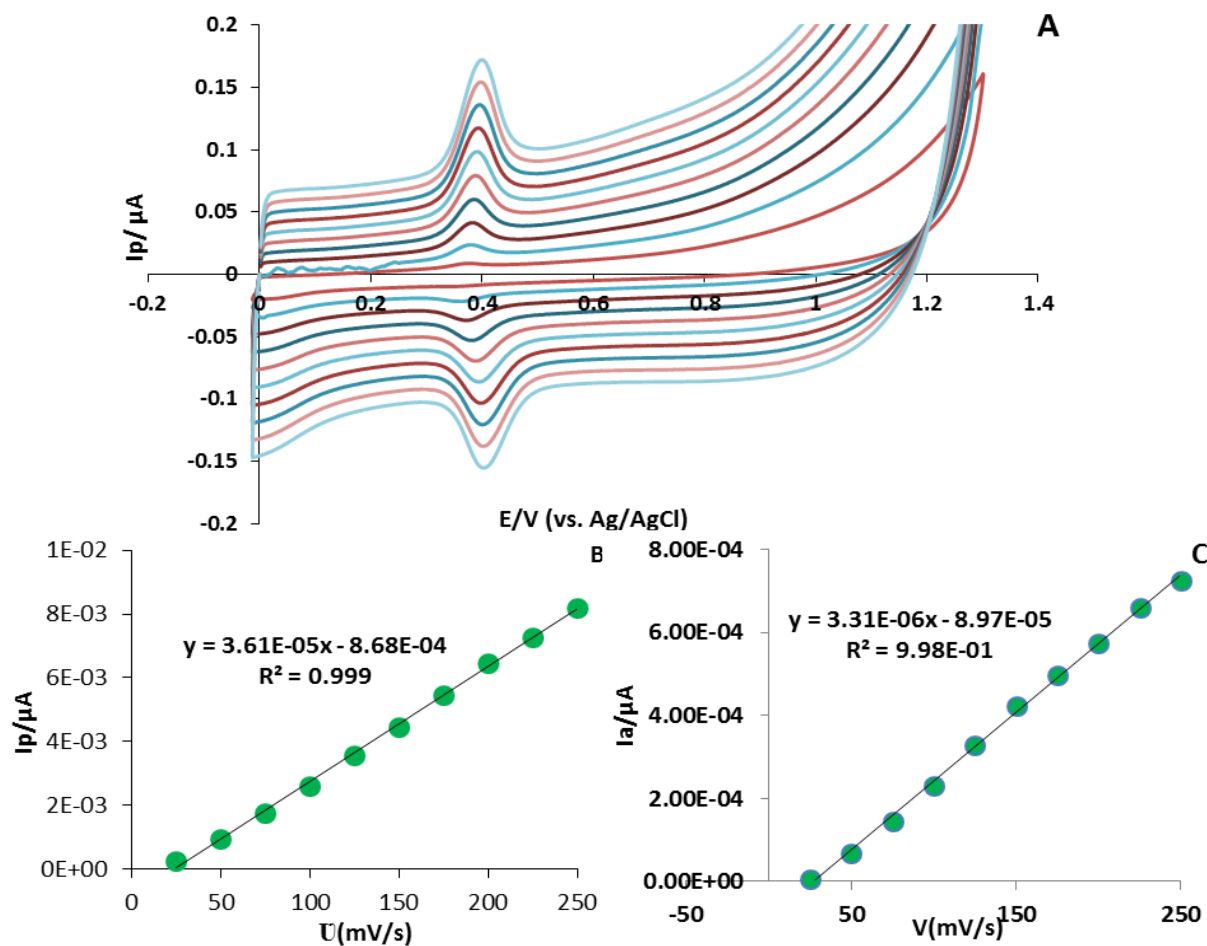


Figure V.4. (A) Cyclic voltammograms of 1 μM PAR in BRS 0.04 M (pH = 7) at different scan rate values (25 to 250 mV.s⁻¹) at the CB/CME (B) Plot of the peaks current oxidation of PAR versus scan rate for 1 μM PAR (C) Plot of the peaks current oxidation of PAR versus scan rate for 0.05 μM PAR.

V.2.1. Effect of pH

Examination of the dependence of the electrochemical response of CB/ CME on the pH value of the solution (Fig. V.5-A) was done in 0.04 M BR solutions at various pH values in the range of 3 to 9 by CV in the presence of 1 μ M PAR. As shown in the Fig. V.5-B, the anodic peak intensity of PAR increases with increasing pH until reaching the maximum at pH=7. A further increase in pH results in a decrease of the oxidation current peak intensity. These results indicate that protons are involved in the PAR oxidation reaction. Thus, the electrochemical response of the CB/ CME toward PAR detection depends on the pH of the solution. In addition, as the pKa of PAR is equal to 9.38 at 25°C, this result indicates that the analyte was preferentially adsorbed in the natural form. Therefore, the BR solution at pH = 7 was chosen as the optimal electrolyte.

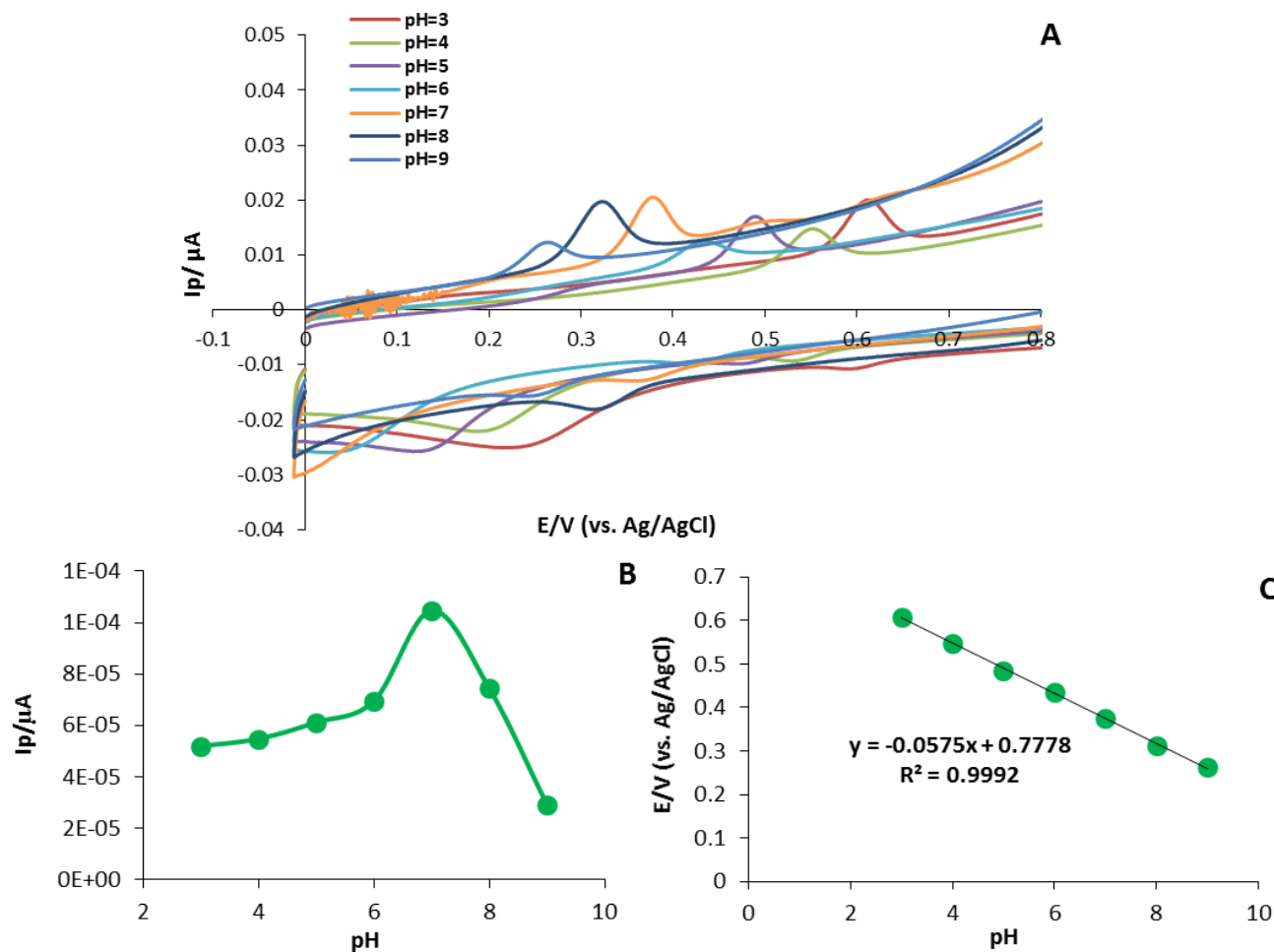


Figure V.5. (A) Cyclic voltammograms of 1 μ M PAR in BRS 0.04 M at different pH value (3 to 9) at the CB/CME (B) Effect of pH on the peaks current oxidation of PAR in BRS 0.04 M with different pH value (3 to 9) at the CB/CME. (C) Corresponding plots of the oxidation peaks potential of PAR versus pH

The peak potential values shift to lower values with increasing pH, as shown in Fig. V.5-C. Therefore, the oxidation peak potential depends linearly on pH according to the following equation:

$$E_{pa}(V) = -0.0575 \text{ pH} + 0.778 \quad (R^2 = 0.999) \quad \text{Eq. 5.4}$$

The slope obtained is nearly close to the theoretical value of 57.6 mV per pH unit at the room temperature [23]; and it indicates that an equal number of protons and electrons are involved in the oxidation process of adsorbed PAR compound.

V.2.2. Effect of preconcentration potential in EP/SWV

The preconcentration potential has a significant impact on the EP process for the detection of PAR. The study of this parameter was investigated with SWV by scanning the potential from -0.7 to 0.8 V, in the presence of 0.1 μM PAR in BRS at pH=7. As shown in Fig V.6, the intensity of the anodic peak increases gradually with the increasing potential from -0.7 V and reaches the highest intensity value at 0 V potential. Subsequently, the peak intensity decreases at more positive potentials and the signal intensity drops rapidly, tending to stabilize from $E = 0.4$ V, in this potential, the surface of the electrode is certainly positively charged, which does not favor the adsorption of neutral PAR, however, around 0V, the surface is not charged. The results allow the 0 V potential to be chosen as the pre-concentration potential in the determination of the RAP using CB/ CME.

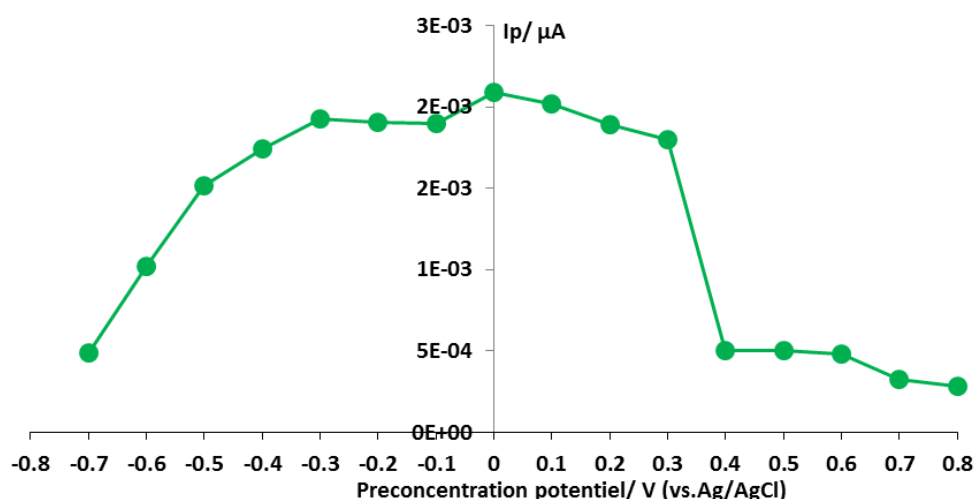


Figure V.6. Effect of the preconcentration potential on the oxidation peak current of 0.1 μM PAR at the CB/CME in BRS 0.04 M (pH = 7).

V.2.3. Effect of preconcentration time

The preconcentration time is another factor that considerably influences the micro-sensor response. The effect of this factor was evaluated by SWV for 0.1 μM PAR in BRS pH=7 at 0 V. As shown in Fig. V.7, the anodic peak current of PAR increased gradually with accumulation time from 0 to 900 s due to the preconcentration of PAR on the surface of the modified CME. It reached the maximum current response at 900 s then remained nearly constant due to saturation of active sites on the electrode surface. Consequently, 900 s was selected as the optimal accumulation time.

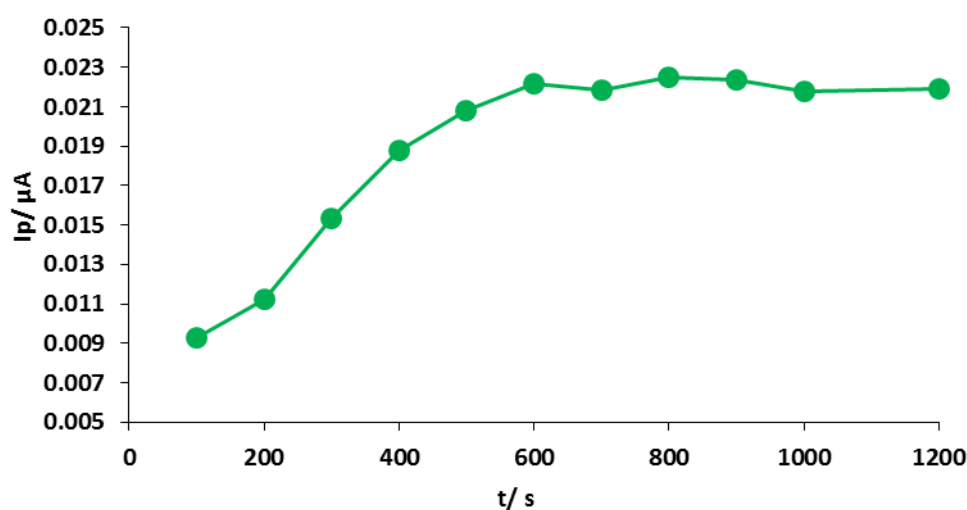


Figure V.7. Effect of the preconcentration time on the oxidation peak current of 0.1 μM PAR at the CB/CME in BRS 0.04 M (pH = 7).

V.3. Electrochemical behavior of PAR on the CB/ CME

The electrochemical behavior of PAR on CB/ CME was investigated by CV in the presence of $10^{-6} \text{ mol.L}^{-1}$ of PAR at a scan rate of 25 mV.s^{-1} in BR buffer at pH=7 as the supporting electrolyte. As can be seen in Fig. V.8-A, the CV voltammogram shows an electrochemical system characterized by an oxidation peak at 0.371 V and a reduction peak at 0.354 V. The potential difference between the two peaks is $\Delta E=0.017 \text{ V}$ for the modified micro-sensor indicating a rapid electrochemical system.

In order to demonstrate the impact of EP on the performance of the proposed sensor, 3×10^{-7} mol.L⁻¹ of PAR was analyzed by SWV on the CB/ CME before and after electrochemical preconcentration (EP) (Fig. V.8-B). The result shows that the peak oxidation current intensity of PAR increases from 7.12×10^{-4} to 2.34×10^{-3} μ A with application of an EP at 0 V for 900 s, the current response is increased by about 3.3 times. Consequently, the association of the use of carbon black as modifier material of the CME with the application of EP allows to accumulate more PAR, leads to high sensitivity, enhances the analytical signal.

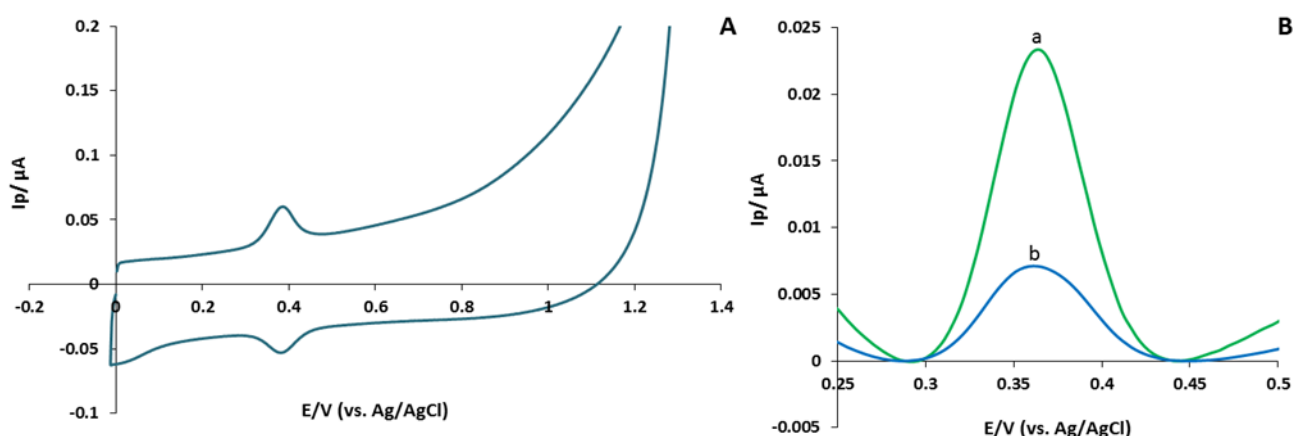


Figure V.8. (A) Cyclic voltammogram of CB/CME in a presence of 1 μ M PAR in BRS 0.04 M (pH = 7) at 25 mV.s⁻¹ (B) SW voltammograms of 30 μ M PAR (a) before and (b) after EP at 0 V for 900 s on CB/ CME.

V.4. Determination of PAR on the CB/ CME

The SWV was performed to evaluate the detection of PAR without and with EP on CB/ CME in BRS at pH = 7 (Fig. V.9-A & B). PAR analysis, both without and with EP, was carried out after stirring the electrolyte solution spiked with the appropriate concentration of PAR for 900 s. The EP was applied by imposing a potential 0 V in addition to the stirring. The calibration curves (Fig. 9-C & D) for peak current (I_{pa}) versus [PAR] for both case (with and without EP) show linear relationships.

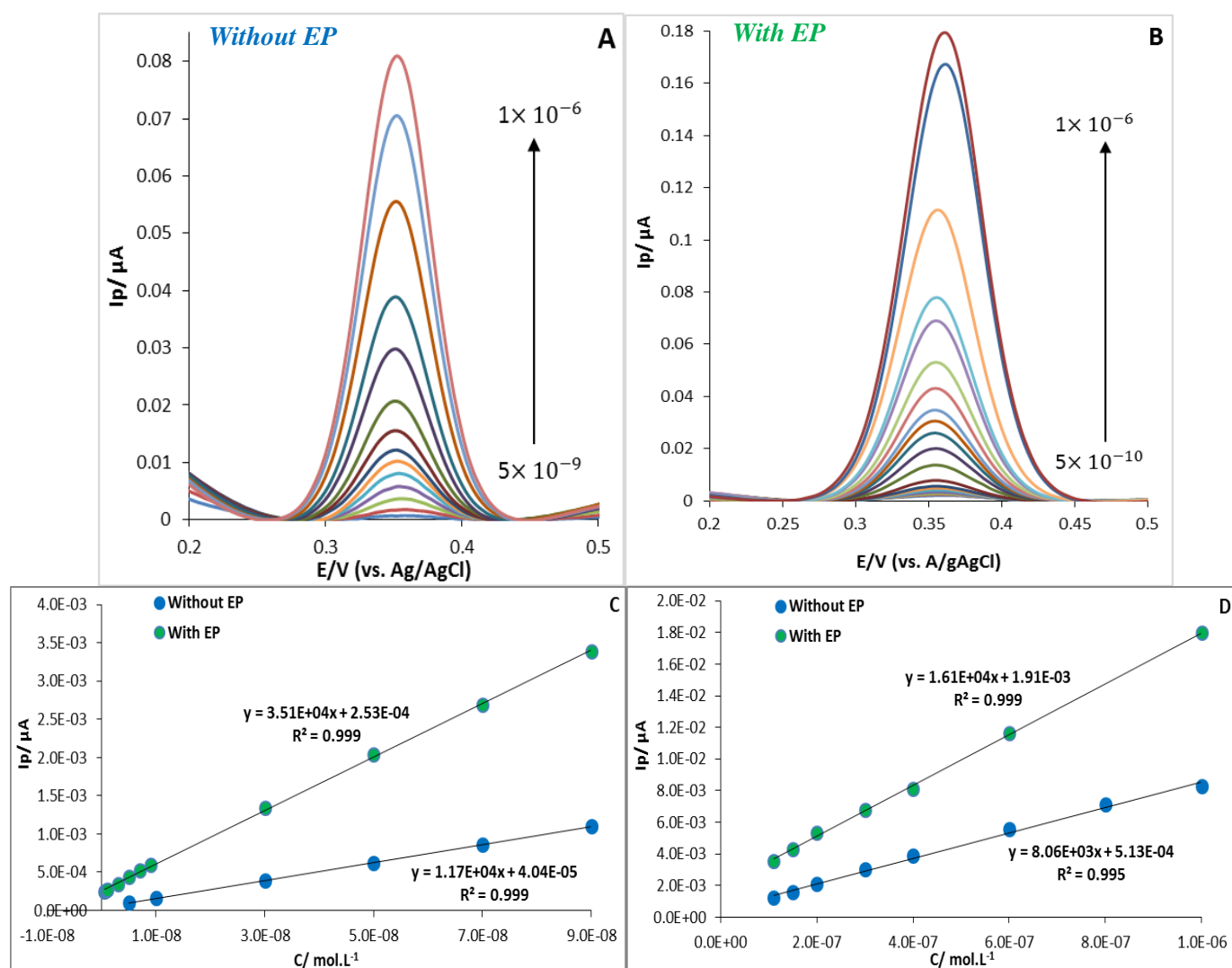


Figure V.9. (A) SW voltammograms of PAR from 5×10^{-9} to 1×10^{-6} without EP (B) SW voltammograms of PAR from 5×10^{-10} to 1×10^{-6} with EP at 0 V for 900 s on CB/ CME in BRS 0.04 M (pH = 7). (C& D) Calibration curves of [PAR] vs peak currents from 5×10^{-9} to 9×10^{-8} and from 1×10^{-7} to 1×10^{-6} , respectively.

The parameters of these curves are summarized in Table V.1. It should be noted that for both analyses there are two clearly defined linear ranges, which do not indicate two different processes, but are simply due to the fact that for higher concentration ($>10^{-7}$ M), the adsorption does not take place only on the external surface of the electrode material but in all the materials. However, for low concentrations, the adsorption takes place just on the external surface of the materials.

This last conclusion was verified by studying the impact of preconcentration time of one higher concentration of PAR localized in the second linear range which was 10^{-7} M. This verification was carried out by SWV for 10^{-7} M PAR in BRS pH=7 at 0 V. The results shown in Fig. V.10 demonstrate that the anodic peak current of PAR increases rapidly with accumulation time without reaching saturation even after 2600 s. This observation can be attributed to higher concentration of PAR that had not yet saturated the active sites present on the electrode surface and confirms the hypothesis that for higher concentration ($>10^{-7}$ M) the EP needs more time for the adsorption or the preconcentration of the PAR on CB/ CME.

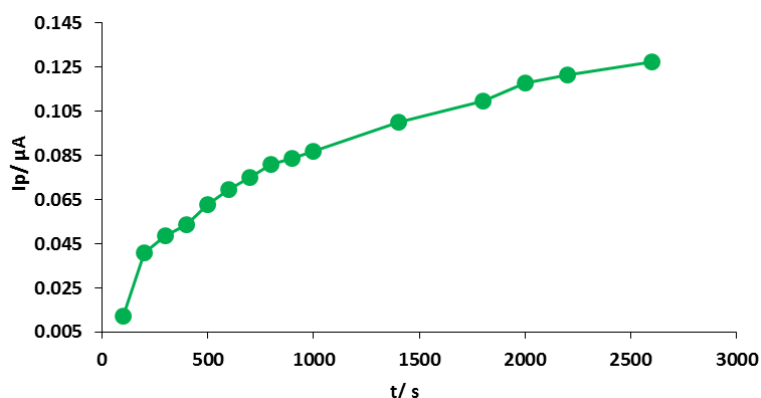


Figure V.10. Effect of the preconcentration time on the oxidation peak current of 0.1 μ M PAR at the CB/CME in BRS 0.04 M (pH =7).

Table V.1. Parameters and characteristics of the calibration curves for the analysis of PAR without and with electrochemical preconcentration at 0 V for 900 s in CB/ CME in BRS 0.04 M (pH = 7).

	Linear range (mol.L ⁻¹)	Slope	Intercept	R ²	LOD (mol.L ⁻¹)	LOQ (mol.L ⁻¹)
Without EP	5×10^{-9} to 9×10^{-8}	$1.17 \times 10^{+4}$	4.04×10^{-5}	0.999	1.42×10^{-9}	4.30×10^{-9}
	1×10^{-7} to 1×10^{-6}	$8.06 \times 10^{+3}$	5.13×10^{-4}	0.995		
With EP	5×10^{-10} to 9×10^{-8}	$3.5 \times 10^{+4}$	2.53×10^{-4}	0.999	1.40×10^{-10}	4.26×10^{-10}
	1×10^{-7} to 1×10^{-6}	$1.61 \times 10^{+4}$	1.91×10^{-3}	0.999		

The limits of detection and quantification of the micro-sensor are calculated from the formulae: $LOD = 3.3 \times SD/b$ and $LOQ = 10 \times SD/b$, respectively. Where, *SD* is the standard deviation of the linear regression solution and *b* is the slope of the linear regression [25]. It is found that the analysis without EP leads to a LOD of 1.42×10^{-9} M and LOQ of 4.30×10^{-9} M. However, the analysis with EP leads to an LOD of 1.40×10^{-10} M and an LOQ of 4.26×10^{-10} M.

M. Thus, EP enhances clearly the sensitivity of the micro-sensor and significantly improves the detection and quantification limits.

The comparison of the CB/ CME efficiency with previous works for PAR detection (Table V.2) shows that the proposed micro-sensor is among the most sensitive with a lower detection limit and a wider linear concentration range. The use of nanostructured carbon black as the electrode material in the microcavity makes the micro-sensor a high-performance, low-cost device with a very simple design, requiring only a rapid modification step. Hence, the so-designed device could be an interesting micro-sensor for the monitoring and trace analysis of PAR in environmental waters.

Table V.2. Comparison of the results of this study with those recently reported for the PAR analysis

Electrode	Linear range (mol.L ⁻¹)	LOD (mol.L ⁻¹)	Ref.
ILC-CPE	0 to 120 × 10 ⁻⁴	2.8 × 10 ⁻⁶	[10]
AgNP-xGnP/GCE	4.98 × 10 ⁻⁶ to 3.38 × 10 ⁻⁵	8.5 × 10 ⁻⁸	[26]
N,S-doped C@Pd nanorods/GCE	3.3 × 10 ⁻⁸ to 1.2 × 10 ⁻⁴	1.1 × 10 ⁻⁸	[27]
Sm ₂ O ₃ @ZrO ₂ /CNTs/GCE	3.7 × 10 ⁻⁹ to 2.2 × 10 ⁻⁶	3.4 × 10 ⁻¹⁰	[28]
GrNF/GCE	1.0 × 10 ⁻⁹ to 1.5 × 10 ⁻⁴	4.3 × 10 ⁻¹⁰	[29]
CB/ CME	5 × 10 ⁻¹⁰ to 9 × 10 ⁻⁸ 1 × 10 ⁻⁷ to 1 × 10 ⁻⁶	1.4 × 10 ⁻¹⁰	This work

V.5. Repeatability and reproducibility

Under the optimized conditions, the repeatability of PAR detection by EP/SWV on CB/ CME was evaluated for the same micro-sensor by performing 3 consecutive SW voltammograms of three different concentrations (1, 10 and 50 nmol.L⁻¹). The relative standard deviation values presented in Table V.3 are less than 2 %, indicating good repeatability. Furthermore, three different CB/ CMEs prepared with the same procedure were used to determine independently the three concentrations. As can be seen in Table V.3, the obtained RSD values are less than 4 %, suggesting that the proposed modified CME has a high reproducibility.

Table V.3. Study of the repeatability and reproducibility of detection of PAR concentrations at CB/CME in BRS 0.04 M (pH = 7).

Concentration (mol.L ⁻¹)	Repeatability of I_p RSD%*	Reproducibility of I_p RSD%*
1 × 10 ⁻⁹	0.3	2.0
1 × 10 ⁻⁸	1.0	3.9
5 × 10 ⁻⁸	1.6	2.2

V.6. Selectivity of the modified cavity microelectrode

Selectivity is an important factor that represents the performance of the micro-sensor. This factor was investigated for the EP of 10^{-7} M PAR by SWV at the proposed CB/ CME in BRS at pH = 7 in the presence of some potential interfering substances at similar concentrations (Fig. V.11). The presence of pharmaceutical residues such as carbamazepine and 4-aminophenol has a negligible effect on peak intensity (variation < 7 %). The greatest variation, not exceeding 10 %, was noted for bisphenol A. This is probably due to the presence of a similar electroactive functional group and the large structure of the molecule, which hinders the accessibility of the PAR. However, the presence of pesticides such as atrazine, propazine and glyphosate had no effect on the microsensor response (variation < 5 %).

Other interferents such sulfate, chloride, Fe^{3+} , oxalate and acetate ions have a negligible impact on the current response. Consequently, the CB/ CME can be used for the EP of PAR with acceptable selectivity and allows their feasibility for real sample analysis.

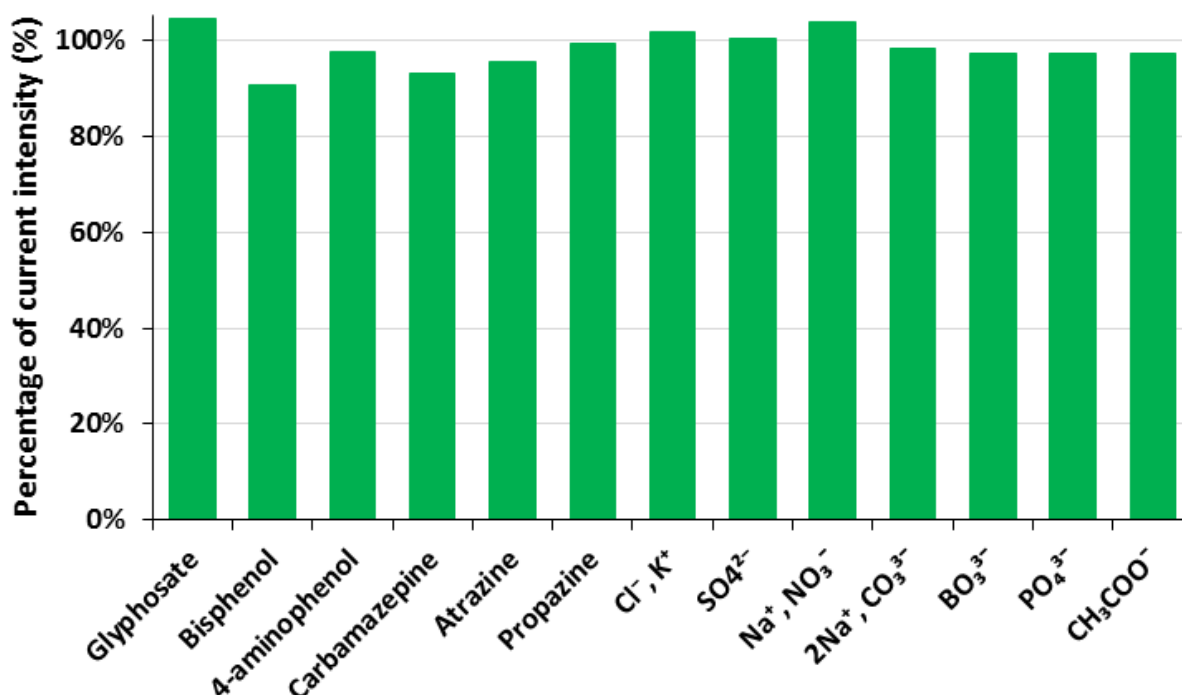


Figure V.11. The relative peak current response of PAR in the presence of some potential interfering substances at the CB/CME in BRS 0.04 M (pH = 7).

V.7. Real simple analysis

In order to evaluate the potential applicability of the proposed electrochemical micro-sensor, the detection of trace amounts of PAR by EP/SWV on CB/ CME was applied in local tap water and wastewater collected from the wastewater treatment plant in Betton (Rennes), France. Both samples were just filtered through syringe filter (0.45 μm) to remove any particles impurities, without prior dilution or use of a supporting electrolyte. The prepared samples were transferred directly into the electrochemical cell for the validation of the proposed CB/ CME. No traces of PAR were detected with the modified microelectrode in voltammetric analysis, indicating that the concentration of PAR residues is lower than LOD (0.02 $\mu\text{g.L}^{-1}$) in the analyzed tap and waste water samples. Therefore, the water samples were spiked with traces concentration of PAR (1 and 10 nmol.L^{-1}) to validate the analytical method with micro-sensor by the standard addition method under optimized conditions. The results obtained are compiled in Table V.4. The recovery values are between 101-104 % and the RSD values are less than 5 % for the different samples, indicating no interference effects of the water matrix on the accuracy of PAR concentration values. Therefore, the proposed method could be applied for the direct analysis of the environmental samples without any specific procedures.

Table V.4. Validation of the CB/CME in the determination of PAR directly in tap and wastewater samples by EP/SWV.

Samples	C(mol.L ⁻¹) added	C(mol.L ⁻¹) found	RSD %*	Recovery (%)	Accorancy (%)
Waste water	1 \times 10 ⁻⁹	1.1 \times 10 ⁻⁹	4.8	101.7	98.3
	1 \times 10 ⁻⁸	1.3 \times 10 ⁻⁸	4.4	103.3	96.7
Tap water	1 \times 10 ⁻⁹	1.6 \times 10 ⁻⁹	3.6	101.8	98.2
	1 \times 10 ⁻⁸	1.1 \times 10 ⁻⁸	3.1	103.9	96.1

*n=3

Conclusion

In this chapter, we have described how to fabricate an efficient electrochemical micro-sensor for the direct detection of paracetamol in water, using the electrochemical preconcentration technique on a cavity microelectrode modified with carbon black nanomaterial. The optimisation of the operating conditions was studied by CV and SWV, and the sensor performance study was evaluated by SWV. The results demonstrate that with an EP of PAR on CB/ CME at 0 V for 900 s in BRS 0.04 M at pH = 7, the new proposed micro-sensor exhibits a large linear response in ranges of 5×10^{-10} to 9×10^{-8} mol.L⁻¹ for the ultra-traces concentrations and 1×10^{-7} to 1×10^{-6} mol.L⁻¹ for medium concentrations. The detection and quantification limits are estimated to be 1.40×10^{-10} and 4.26×10^{-10} mol.L⁻¹, respectively. The use of the nanostructured carbon black improves the surface area and conductivity of the CB/ CME. In addition, the application of EP significantly enhances electrons transfer and leads to excellent electrochemical and analytical properties.

The so-designed micro-sensor has been successfully applied to the analysis of paracetamol traces in tap water and waste water samples with a satisfactory result without any specific preparation of the samples, simply by dropping the micro-sensor in the samples. Hence, the developed CB modified CME is suitable and promising sensor to paracetamol trace analysis and for environmental monitoring applications.

The originality of this work is firstly the use of the cavity microelectrode as tool for the design of the micro-sensor. Secondly, the application of EP which improves considerably the electrochemical characteristics. In addition to the simplicity, low cost and various advantages in improving the analytical characteristics of the modified MCE such as selectivity, low detection limit, high sensitivity and, most importantly, the feasibility of performing a real in situ PAR analysis following a simple procedure.

References

- [1] Goscianska, J., Olejnik, A., Ejsmont, A., Galarda, A. & Wuttke, S. (2021). Overcoming the paracetamol dose challenge with wrinkled mesoporous carbon spheres, *Journal of Colloid and Interface Science*, 586, 673.
- [2] World Health Organization. (2019). World Health Organization Model List of Essential Medicines, 21st list, 1.
<https://www.who.int/publications/i/item/WHOMVPEMPIAU2019.06>. Accessed 23 January 2021.
- [3] Dear, JW. & Bateman, D. N. (2020). Paracetamol poisoning, *Medicine*, 48 (3), 208.
- [4] U.S. Food & Drug Administration. (2018). Drug Safety and Availability, FDA Drug Safety Communication. <https://www.fda.gov/drugs/drug-safety-and-availability/fda-drug-safety-communication-prescription-acetaminophen-products-be-limited-325-mg-dosage-unit> Accessed 23 January 2021.
- [5] Żur, J., Piński, A., Marchlewicz, A., Hupert-Kocurek, K., Wojcieszynska, D. & Guzik, U. (2018). Organic micropollutants paracetamol and ibuprofen—toxicity, biodegradation, and genetic background of their utilization by bacteria, *Environmental Science and Pollution Research*, 25, 21498.
- [6] Shraim, A., Diab, Alsuhaime, A., Niazy, E., Metwally, M., Amad, M., Sioud, S. & Dawoud, A. (2017). Analysis of some pharmaceuticals in municipal wastewater of Almadinah Almunawarah, *Arabian Journal of Chemistry*, 10 (1), S719.
- [7] Aus der Beek, T., Weber, F. A., Bergmann, A., Hickmann, S., Ebert, I., Hein, A. & Küster, A. (2016). Pharmaceuticals in the environment—Global occurrences and perspectives, *Environmental Toxicology and Chemistry* 35(4), 823.
- [8] Sunil Kumar Naik, T.S., Kumara Swamy, B.E., Ramamurthy, Praveen C. & Chetankumar, K. (2020). Poly (L-leucine) modified carbon paste electrode as an electrochemical sensor for the detection of paracetamol in presence of folic acid, *Materials Science for Energy Technologies*, 3, 626.
- [9] Mulyasuryani, A., Triandi Tjahjanto, R., & Andawiyah, R. (2019). Simultaneous Voltammetric Detection of Acetaminophen and Caffeine Base on Cassava Starch—Fe₃O₄ Nanoparticles Modified Glassy Carbon Electrode, *Chemosensors*, 7 (4), 49.
- [10] Mangaiyarkarasi, R., Premlatha, S., Khan, R., Pratibha, R. & Umadevi, S. (2020). Electrochemical performance of a new imidazolium ionic liquid crystal and carbon paste composite electrode for the sensitive detection of paracetamol, *Journal of Molecular Liquids*, 319, 114255.

- [11] Atta, N. F., Ibrahim A. H. & Gala A. (2016). Nickel oxide nanoparticles/ionic liquid crystal modified carbon composite electrode for determination of neurotransmitters and paracetamol, *New Journal of Chemistry*, 40, 662.
- [12] Serrano, N., Castilla, Ò., Ariño, C., Diaz-Cruz, M.S. & Díaz-Cruz, J.M. (2019). Commercial Screen-Printed Electrodes Based on Carbon Nanomaterials for a Fast and Cost-Effective Voltammetric Determination of Paracetamol, Ibuprofen and Caffeine in Water Samples. *Sensors*, 19, 4039.
- [13] Ibáñez-Redín, G., Wilson, D., Gonçalves, D. & Oliveira, O.N. (2018). Low-cost screen-printed electrodes based on electrochemically reduced graphene oxide-carbon black nanocomposites for dopamine, epinephrine and paracetamol detection, *Journal of Colloid and Interface Science*, 515, 101.
- [14] Patil, M. M., Shetti, N. P., Malode, S. J., Nayak, D. S. & Chakklabbi, T. R. (2019). Electroanalysis of paracetamol at nanoclay modified graphite electrode, *Materials Today: Proceedings*, 18, (3), 986.
- [15] Fu, L., Wang, A., Lai, G., Lin, C., Yu, J., Yu, A., Liu, Z., Xie, K & Su, W. (2018). A glassy carbon electrode modified with N-doped carbon dots for improved detection of hydrogen peroxide and paracetamol, *Microchimical Acta* 185, 87.
- [16] Matt, S.B., Raghavendra, S., Shivanna, M. Sidlinganahalli, M. & Sidlinganahalli, D. M. (2020). Electrochemical Detection of Paracetamol by Voltammetry Techniques Using Pure Zirconium Oxide Nanoparticle Based Modified Carbon Paste Electrode, *Journal of Inorganic and Organometallic Polymers and Materials*, 64.
- [17] Amare, M. (2019). Voltammetric determination of paracetamol in tablet formulation using Fe (III) doped zeolite-graphite composite modified GCE, *Heliyon*, 5 (5), e01663.
- [18] Beitollahi, H., Garkani-Nejad, F., Tajik, S. & Ganjali, MR. (2019). Voltammetric Determination of Acetaminophen and Tryptophan Using a Graphite Screen Printed Electrode Modified with Functionalized Graphene Oxide Nanosheets Within a Fe₃O₄@SiO₂ Nanocomposite, *Iranian Journal of Pharmaceutical Research*, 18 (1), 80.
- [19] Vivier, V., Cachet-Vivier, C., Mezaille, S., Wu, B. L., Cha, C. S., Nedelec, J-Y., Fedoroff, M., Michel, D. & Y, L. T. (2000). Electrochemical Study of Bi₂O₃ and Bi₂O₂CO₃ by Means of a Cavity Microelectrode. I. Observed Phenomena and Direct Analysis of Results, *Journal of The Electrochemical Society*, 147 (11), 4252.
- [20] Kutty, M., Settu, R., Chen, S.-M., Chen, T.-W., Tseng, T.-W., Hatamleh, A. A., Yu, J., Yu, R. & Huang, C.-C. (2019). An Electrochemical Detection of Vanillin Based on Carbon Black Nanoparticles Modified Screen Printed Carbon Electrode, *International Journal of Electrochemistry Science*, 14, 5972.

- [21] Jebril, S., Cubillana-Aguilera, L., Palacios-Santander, J. M. & Dridi, C. (2021). A novel electrochemical sensor modified with green gold sononanoparticles and carbon black nanocomposite for bisphenol A detection, *Materials Science and Engineering: B* 264, 114951.
- [22] Samandari, L., Bahrami, A., Shamsipur, M., Farzin, L. & Hashemi, B. (2019): Electrochemical preconcentration of ultra-trace Cd^{2+} from environmental and biological samples prior to its determination using carbon paste electrode impregnated with ion imprinted polymer nanoparticles, *International Journal of Environmental Analytical Chemistry*, 99 (2), 172.
- [23] Bard, A. J. & Faulkner, L. R. (2001). *Electrochemical Methods: Fundamentals Applications*, (2nd Eds), New York: Wiley, 87.
- [24] Denuault, G., Mirkin, M. V. & Brad, A. J. (1991). Direct determination of diffusion coefficients by chronoamperometry at microdisk electrodes, *Journal of Electroanalytical Chemistry* 308, 27.
- [25] Shrivastava, A. & Gupta, V. B. (2011). Method for the determination of limit of detection and limit of quantification of the analytical methods, *Chronicles of Young Scientists*, 2 (1), 21.
- [26] Zamarchi, F. & Vieira, I.C. (2021). Determination of paracetamol using a sensor based on green synthesis of silver nanoparticles in plant extract, *Journal of Pharmaceutical and Biomedical Analysis*, 113912.
- [27] Wang, L., Yang, Y., Liang, H., Wu, N., Peng, X., Wang L. & Song, Y. (2020). A Novel N,S-Rich COF and Its Derived Hollow N,S-doped Carbon@Pd Nanorods for Electrochemical Detection of Hg^{2+} and Paracetamol, *Journal of Hazardous Materials*, 124528
- [28] Teker, T. & Aslanoglu, M. (2020). Sensitive and selective determination of paracetamol using a composite of carbon nanotubes and nanoparticles of samarium oxide and zirconium oxide, *Microchemical Journal*, 158, 105234.
- [29] Fu, R., Shen, M., Ding, Y., Li, M., Li, L., Ren, Z. & Wu, Q. (2020). Electrocatalytic Oxidation and Sensitive Determination of Paracetamol based on Nanosheets Self-assembled Lindgrenite Microflowers, *Electroanalysis*, 32 (5), 978.

***General Conclusion, perspectives and
originality of the thesis***

General Conclusion

The overall aim of this thesis was to develop new electrochemical sensors based on carbon nanomaterials with practical applicability in environmental and food monitoring to ensure human health safety. The veritable goals were, first of all, to design simple, miniaturized and economical devices with a lower detection limit and a higher sensitivity for the selective analysis of target molecules in food and water. In addition to demonstrate the interest of using of nanostructured carbon nanomaterials in electrochemical sensing. For this purpose, three electrochemical sensors were manufactured for the detection of vanillin (VAN) as food additive in commercial sugar vanilla (*Chapter III*); simultaneous determination of ciprofloxacin (CIP), paracetamol (PAR) and 4-aminophenol (AMP) in urine and water (*Chapter IV*); and for the electrochemical preconcentration of trace amounts of PAR in waters (*Chapter V*). The general conclusions of this study include:

The conception of a sensitive sensor for VAN quality control: the sensor elaborated was based on modified carbon paste electrode with a nanostructured mixture of fullerene and functionalized multi-walled carbon nanotubes (f-MWCNTs-FNTs/CPE). The excellent proprieties of the nanostructured carbon paste enhance surface area and significantly improve electron transfer. This leads to a remarkable electrochemical and analytical performances when operated by cyclic voltammetry in BR solution (0.04 M) at pH= 7 after a preliminary stirring step (300 s). Indeed, the responses are linear and extended in the range of 5×10^{-8} to 9×10^{-6} mol.L⁻¹, for VAN trace levels, and from 10^{-5} to 10^{-4} mol.L⁻¹ for higher concentrations with a low detection limit of 3.4×10^{-8} mol.L⁻¹. The f-MWCNTs-FNTs/CPE sensor showed good stability, repeatability and reproducibility (< 7 %). This nanostructured sensor was successfully applied to determine VAN concentration as additive in commercial vanilla sugar samples with satisfactory recovery and good accuracy (< 6.5 %) compared to the UPLC/UV control method and without any specific preparation of the samples, just by dissolving the sample in the BR electrolyte.

We also designed a nanostructured cavity microelectrode with activated carbon and functionalized carbon black for the simultaneous determination of AMP, PAR and CIP. The nanostructuration of the material in the microcavity leads to fast charge transfer, high current and displays excellent responses towards simultaneous oxidation of commonly used drugs in BR solution (0.04 M) at pH= 7 after a previous stirring step of 5 minutes when operated by square wave voltammetry. The results show wide linear responses in the range of 1×10^{-7} to 3

$\times 10^{-6}$ mol.L⁻¹, 2.5×10^{-8} to 3×10^{-6} mol.L⁻¹ and 5×10^{-8} to 3×10^{-6} mol.L⁻¹ for AMP, PAR and CIP, respectively, with their detection limits of 63, 23 and 39 nM, respectively. In addition, the CBf-AC/ CME show high selectivity, good repeatability and reproducibility (< 8 %). This micro-sensor has been successfully applied for the analysis of wastewater and artificial urine samples with a satisfactory recovery (< 4 %) without any specific procedure, simply by diluting the sample in the BR electrolyte.

It offers advantages in their capability to detect three drugs simultaneously without any overlap in potential peaks or interfering effects between them by just using a simple, economical and rapid procedure.

Finally, we have successfully developed a cavity microelectrode modified with carbon black (CB/ CME). This is a simple and economical electrode for electrochemical preconcentration (EP) and trace detection of PAR directly in water. The EP of PAR on CB/ CME at 0 V for 900 s show a large linear response in ranges from 5×10^{-10} to 9×10^{-8} mol.L⁻¹ for the ultra-traces concentrations and from 1×10^{-7} to 9×10^{-6} mol.L⁻¹ for medium concentrations with a detection and quantification limits of 1.40×10^{-10} and 4.26×10^{-10} mol.L⁻¹, respectively. The performance of the new proposed CB/ CME has been successfully applied to the analysis of local tap water and waste water samples with a satisfactory recovery (< 7%) and relation standard deviation less than 4%. This indicates that the electrochemical micro-sensor is an effective device for monitoring PAR concentration directly in environmental applications without any pretreatment.

Our work has demonstrated the feasibility of the use of nanostructured carbon electrodes for the electrochemical detection in various fields (food, drugs and environment). Performance and selectivity depends on the nanostructuration of carbon nanomaterials used in the electrode matrix, the pH of the electrolyte and the sensing target. The creation of a high performance sensor depends on the judicious choice of a combination of these three parameters in order to obtain a relative adsorption of the analytes.

Perspectives

In the future, we plan to study other combinations of carbon nanomaterials and to use carbon dots and graphene oxide in the nanostructuring of new electrochemical detection devices. In addition, we think to integrate the cavity microelectrode into the electrochemical cell to create a specific miniaturised microsystem capable of performing the analysis by anyone, anywhere, at any time. Moreover, we plan to use imposed potential electrochemical preconcentration for other potential electrochemical detection applications such as pharmaceuticals, foods, pesticides, etc. In addition, the designed Cbf-AC/ CME offers the possibility to follow the degradation of paracetamol to 4-aminophenol in real samples, a study that can be investigated and developed in future research.

Originality of the thesis

Overall, the originality of the thesis consists in the development of new sensitive and selective sensors and micro-sensors based on nanostructured carbon materials for quality control of food additives, monitoring of pharmaceutical products, biological diagnostics and in the environment. In order to improve quality of industrial products, prevent disease, protect the environment and ensure the safety of human health, the use of carbon nanomaterials ensures high sensitivity and fast adsorption of the analytes. The different combinations of carbon nanomaterials investigated in our work (f-MWCNTs, FNTs, graphite and f-CB, AC) allow us to obtain uniform and nanostructured carbon paste with excellent properties. This nanostructuring has improved the surface area, reduced charge transfer resistance and increased considerably the electron transfer kinetics, leading to remarkable electrochemical and analytical performance. The selectivity of each combination toward selective targets was ensured by its affinity to be selectively absorbed on the surface of the nanostructured electrode and its molecular charge in relation with pKa value and pH of electrolyte. The so-designed sensors and micro-sensors are economical, simple, use small amount of reagents, are fast and applicable for the in-situ analysis.

Another element of novelty is that, to our knowledge, the use of cavity microelectrode as device for electrochemical sensing has not been widely reported in the literature. The combination of this miniaturized electrode with carbon nanomaterials offers the advantages of higher surface area, higher sensitivity and lower limit of detection.



Contents lists available at ScienceDirect

Journal of Food Composition and Analysis

journal homepage: www.elsevier.com/locate/jfca

Original Research Article

Fullerene-MWCNT nanostructured-based electrochemical sensor for the detection of Vanillin as food additive

Lydia Taouri^{a,b}, Mustapha Bourouina^a, Saliha Bourouina-Bacha^c, Didier Hauchard^{b,*}^a Département de Chimie, Faculté de Science Exacte, Université de Bejaia, 06000 Bejaia, Algeria^b Université Rennes, Ecole Nationale Supérieure de Chimie de Rennes, CNRS, ISCR (Institut des Sciences Chimiques de Rennes), UMR 6226, F-35000 Rennes, France^c Laboratoire de génie de l'environnement, Faculté de Technologie, Université de Bejaia, 06000 Bejaia, Algeria

ARTICLE INFO

Keywords:

Vanillin

Vanilla sugar

Fullerene-MWCNT

Electrochemical sensors

Food samples

ABSTRACT

In this paper, a simple, economical, selective and sensitive electrochemical sensor is proposed for the quantification of vanillin (VAN) in real food samples. It consists of a carbon paste electrode (CPE) nanostructured with Fullerene (FNTs) and functionalized multi-walled carbon nanotubes (f-MWCNTs). The developed electroanalytical method was performed with cyclic voltammetry after optimization of operating conditions, such as supporting electrolytes, pH values and accumulation time. After optimization, the nanostructured sensor showed wide linear responses in the range from 5×10^{-8} to 9×10^{-6} mol.L⁻¹ for VAN trace levels and from 10^{-5} to 10^{-4} mol.L⁻¹ for higher concentrations, with a low detection limit of 3.4×10^{-8} mol.L⁻¹. For concentrations lower than 10^{-5} mol.L⁻¹, VAN was stripped after a previous quick adsorption step (300 s). The f-MWCNTs-FNTs/CPE sensor showed a good stability, repeatability and reproducibility (less than 7 %). This nanostructured sensor was successfully applied to determine VAN concentration as additive in commercial vanilla sugar samples with a satisfactory recovery and a good accuracy (< 6.5 %) in comparison with UPLC/UV control method.

1. Introduction

Vanillin (4-hydroxy-3-methoxybenzaldehyde) is a polyfunctional compound with an aromatic ring bonded to an aldehyde group, -OH phenolic, and a methoxy group (Isac-García et al., 2016). It is the flavor component of vanilla bean, one of the most popular flavors in the world. According to vanilla and vanillin market report done in 2019, the global VAN demand was 37.286 Tons in 2018 and it is estimate to reach 59.458 Tons by 2024. This growing demand is due to its wide use in foods, beverages, fragrance, and pharmaceutical products (Research And Markets, 2019).

Apart from its flavor properties, this widespread application of VAN is due to their beneficial proprieties, when it is used in low concentrations, offered by their biological and therapeutic activities such as antioxidant, antimicrobial, antimutagenic, hypolipidemic, antisickling and others activities, when it is used in low concentrations (Sinha et al., 2008).

However, excessive ingestion of VAN have a side effects toward the human health, it can cause potential health problems and aggravate the

condition of migraine sufferers, headaches, insomnia, nausea, vomiting, and even liver and kidney problems, apart from the fact that the enticing smell of VAN may cause addiction to such food or beverages (Sivakumar et al., 2017). Also, skin contact can cause irritation and swelling (inflammation) (Ahmad et al., 2020). In addition, VAN in high concentrations (mM range) has been described as a cytotoxic agent against many cell lines, including mouse fibroblast 3T3 cells, human ovarian carcinoma A2780-SC1 cells, human colorectal carcinoma HT-29 cells, HepG2 cells, human cervical carcinoma HeLa cells, and human colorectal carcinoma SW480 cells (Bezerra et al., 2016).

An acceptable daily intake (ADI) of 10 mg/Kg for VAN has been set by the Joint FAO/WHO Expert Committee on Food Additive (JECFA) in 1967 and later confirmed in its 2001 re-evolution as flavoring. This value of ADI has been also agreed by the European Union (Younes et al., 2018). Toxic effects are observed when the intake exceeds 75 mg/Kg (Ramesh and Muthuraman, 2018).

Therefore, the monitoring of the level of VAN is necessary not only to control the quality of the product but also to ensure the protection of the human health.

* Corresponding author at: Université Rennes, Ecole Nationale Supérieure de Chimie de Rennes, CNRS, ISCR (Institut des Sciences Chimiques de Rennes), UMR 6226, F-35000 Rennes, France.

E-mail addresses: nassimalydia35@gmail.com (L. Taouri), bouryas@yahoo.fr (M. Bourouina), 1gebej@yahoo.fr (S. Bourouina-Bacha), didier.hauchard@ensc-rennes.fr (D. Hauchard).

<https://doi.org/10.1016/j.jfca.2021.103811>

Received 20 October 2020; Received in revised form 22 December 2020; Accepted 16 January 2021

Available online 21 January 2021

0889-1575/© 2021 Published by Elsevier Inc.

Several analytical techniques have been proposed for the quantitative determination of VAN such as high performance liquid chromatography with a fluorescence detector (Nasuno et al., 2020), capillary electrophoresis (Shu et al., 2016), optical fluorescence (Durán et al., 2015) and colorimetric assay (Zhao et al., 2018). However, these techniques are often complicated, expensive, require qualified personnel and often very long analysis time.

However, electrochemical techniques constitute a promising alternative because of their simplicity, sensitivity, inexpensiveness, fast response time and their capacity to miniaturize (Manasa et al., 2019; Karimi-Maleh et al., 2020). Especially, the use of carbon paste electrode (CPE) has received the highest attention due to its simple preparation procedure, homogeneity, low background current, cost-effectiveness and adaptability to modifications (Bojdi et al., 2016).

In the literature, various types of electrodes and modified electrodes have been reported recently for the detection of VAN based on carbon materials as graphite (Dilgin, 2019), carbon black (Kutty et al., 2019), carbon nanotubes modified with gold nanoparticles (Ceylan Koçak and Ulubay Karabiberoglu, 2018), graphene (including reduced graphene oxide and graphene oxide) containing metal nanoparticles (Gao et al., 2018; Ning et al., 2018; Mohan et al., 2019). Moreover, others sensors involve surface modification by metal oxide or metal nanoparticles or by using other material such as cetyltrimethylammonium bromide (CTAB) (Durán et al., 2018; Murtada et al., 2018; Erady et al., 2020). However, the most of them need a complicated procedure of surface functionalization and/or do not aim the determination of the real VAN concentration in food samples.

Recent work revealed that the Fullerene, the third allotropes of carbon which were discovered in 1985 (Kroto, 1987), attracted enormous attention from physicists, chemists and material designers due to its unique tree-dimensional nanostructure, remarkable electrochemical, electrocatalysis and photocatalysis proprieties. Especially, Fullerene possess high electroactive surface area, good electronic conductivity, high chemical stability. These new discovered carbon allotropes have multiple redox states and an ability to accept and transport easily electrons, which leads to the possibility of functionalization, signal mediation and others remarkable characteristics (Sherigara et al., 2003; Pan et al., 2020; Pilehvar and Wael, 2015). The use of Fullerene as electrode modifier material is still recent and considered as new and attractive element in the development of sensors and biosensors.

In the recent years and with the emergence of nanotechnology, the scientists are focusing on arranging atoms and molecules in different shapes and patterns by self-assembly in order to recognize their properties (Rao et al., 2016). In this context, novel various form of fullerene have been investigated such as fullerene nanowhiskers (C₆₀NWs), fullerene nanofibers (FNFs) and fullerene nanotubes (FNTs). In our study, we have interested to the use of FNTs as material in the conception of a nanostructured sensor. The fullerene nanotubes (FNTs) are fullerene that grow spontaneously into the form of tubes with a single crystalline, polycrystalline or amorphous structures (Miyazawa, 2009).

Carbon nanotubes are considered as graphite sheets that are rolled up into cylindrical shapes, which has received a great attention due to its exceptional optical, mechanical, electronic and thermal properties. Their electrocatalytic properties have driven the researchers to explore these nanomaterials in electrochemical sensing (D'Souza et al., 2017).

In addition, fullerene and multi-walled carbon nanotube composite was used for the first time by H. Zhang and his team to modify a glassy carbon electrode and studied the direct electrochemical behavior of hemoglobin (Hb) in aqueous solutions. Their study demonstrated that MWCNTs-FNTs films nanocomposite were more effective in facilitating the direct electron transfer of hemoglobin (Hb) than MWCNTs films. Furthermore, the heterogeneous electron transfer rate constant *k*s of Hb calculated on MWCNTs-FNTs composite film was almost an order of magnitude larger than that on MWCNTs film (Zhang et al., 2006). In the same case of application of MWCNTs-FNTs composite like electrochemical sensor, H. Zhu et al. have developed a MWCNTs-FNTs

electrode for the sensitive detection of dopamine in presence of ascorbic acid (Zhu et al., 2009). M. Mazloun-Ardakani et al. have fabricated an electrochemical sensor based on fullerene-functionalized carbon nanotubes composite for the sensitive and simultaneous determination of the levodopa and acetaminophen (Mazloun-Ardakani et al., 2016). Both works investigated the performance of FNTs and multi-walled carbon nanotubes on the responses of the sensor. But, as our knowledge, no sensor based on fullerene is available for the quantification of VAN.

In the present work, we describes the simple design and the performance of a nanostructured and sensitive f-MWCNTs-FNTs modified carbon paste electrode as a new electrochemical sensor for the quantification of VAN in real samples of commercial vanilla sugar and our method was validated in comparison to UPLC/UV control method. The newly fabricated electrode offers several advantages over other techniques used for the determination of VAN, including the simplicity of the sensor preparation, low cost, rapidity with very good analytical characteristics as selectivity, high sensitivity and low detection limits. Moreover, the most important advantage is the feasibility to the determination of the real VAN concentration in real matrices, with any pretreatment by following a simple procedure.

2. Experimental

2.1. Reagents

Graphite powder (4 µm) (995%) were purchased from Prographite GmbH; Multi-walled carbon nanotubes (1.5 µm) (90 %) from Good-Fellow (NC006090); Fullerene nanotube multi-walled (20 nm, 5–20 µm) (95 %), Paraffin oil and VAN (≥ 98 %) and acetic acid (≥ 99 %) from Fulka Chemika; phosphoric acid (85 %) and Boric acid (99.5 %) from Acros Organics. Nitric acid (70 %), sulfuric acid (98 %), sodium hydroxide (≥ 98) and potassium hexacyanoferrate (III) (≥ 99) were purchased from Sigma-Aldrich. All aqueous solutions were prepared by deionized water 10–15 MΩ.cm at 25 °C.

2.2. Apparatus

The voltammetric measurements were carried out with an Autolab PGSTAT20 Metrohm potentiostat / galvanostat, controlled by a computer equipped with NOVA 2.1.2 software for controlling analysis and data processing. A conventional three electrodes system was used throughout this study. The working electrode was f-MWCNTs-FNTs/CPE (diameter 1.6 mm), the auxiliary and reference electrode were respectively a platinum wire and a Ag/AgCl (3 M KCl) as reference electrode. All measurements were performed at room temperature. The surface morphology was characterized by scanning electron microscopy (SEM) (JEOL JSM-7100 F, Detector EDS Oxford Instrument 50 mm²) from CMEBA center of ISCR-CNRS6226 at Rennes, France. The analytical measurements were performed with Ultra performance Liquid Chromatography (UPLC) which was conducted on ACQUITY HClass Waters model including Acquity UPLC R BEH C18 1.7 µm, 2.1 × 100 mm column thermostated at 30 °C and equipped with PDA eλ detector. An elution gradient was used by using two mobile phases, A: ultra-pure water, 10 % Acetonitrile and 0.1 % formic acid and B: acetonitrile with 0.1 % in a flow rate of 0.4 mL.min⁻¹. The injected volum was 10 µL and the chromatograms were registred at 230 nm.

2.3. Preparation of the functionalized multi-walled carbon nanotubes (f-MWCNTs)

The preparation of f-MWCNTs was inspired by the method followed by (Baykal et al., 2013) with some modification in the procedure: 0.5 g of MWCNTs was added in 15 mL concentrated sulfuric acid and 5 mL concentrated nitric acid. The mixture was stirring vigorously for 24 h. Then, 100 mL of distilled water was added to the previous solution and

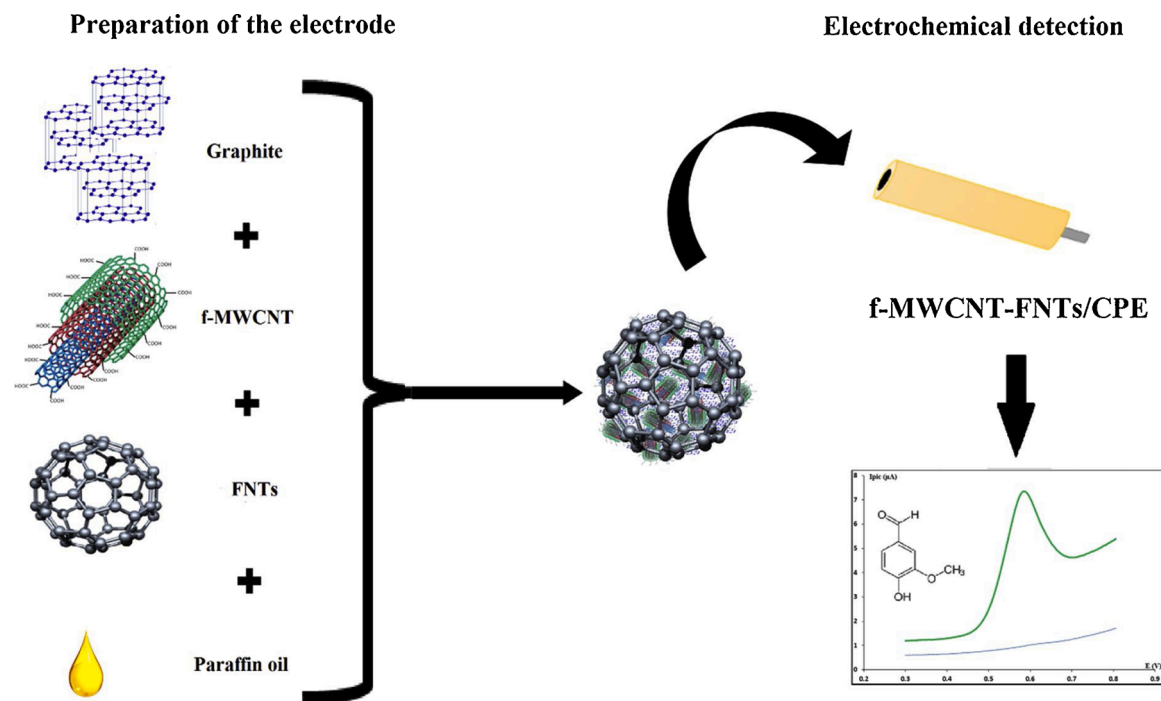


Fig. 1. Graphical presentation of f-MWCNTs-FNTs/ CPE sensor fabrication.

stirring for another hour. After that, the suspension was filtered and washed 2 times with distilled water and dried at room temperature for a night. Afterwards, the product was washed again with distilled water for 3 times. At the end, the f-MWCNTs were dried at 70 °C for 18 h.

2.4. Fabrication of the proposed sensor

The functionalized multi-walled carbon nanotubes/FNTs/serene composite modified carbon paste electrodes (f-MWCNTs-FNTs/ CPE) was prepared by thoroughly mixing of graphite, f-MWCNTs, FNTs with paraffin oil at ration (55 %; 20 %; 10 %; 15 %), respectively, in agate mortar with pestle. All the components were homogenized to obtain a paste. The latter was introduced and compacted into the cylindrical cavity (1.6 mm diameter and 3 mm depth) at the extremity of the electrode body and smoothed on a clean paper until it had a uniform surface. A wire of copper passing through the electrode support ensured the electrical contact with the paste.

In order to compare the performance of the developed sensor and to improve the impact of the introducing of FNTs in the matrix of the electrode, we have also prepared CPE (85 % of graphite) and f-MWCNTs/ CPE, were the composition of the graphite and f-MWCNTs was 55 % and 30 %, respectively. The portion of the binder (paraffin oil) was been maintaining at 15 %. This percentage was chosen to have a paste with good mechanical strength, consistent, which does not crumble and with sufficient conductivity. The steps of the preparation of f-MWCNTs-FNTs/ CPE are illustrated in Fig. 1.

2.5. Electrochemical measurements

The electrochemical behavior of different electrodes was investigated in an electrochemical cell containing a platinum wire as auxiliary electrode and an Ag/AgCl (3 M KCl) electrode as reference electrode. The three electrodes were immersed in 20 mL BR solution (0.04 mol.L⁻¹) at pH = 7. Then, an appropriate micro-volume of VAN concentrated solution was added into the cell. The *i*~*E* curves were recorded by cyclic voltammetry, in the potential range of -0.2 to 1.2 V at a scan rate of 20 mV.s⁻¹, after 5 min of constant stirring at room temperature. All electrochemical measurements were performed inside a

Faraday cage in order to minimize the contribution of background noise to the analytical signal.

2.6. Preparation of the commercial food samples

Sugar vanilla samples of four different commercial brands were purchased from a local supermarket. Their packaging indicated just the ingredients without indications of quantities: sugar, cornstarch, VAN and exhausted vanilla pods. The sample solutions were prepared by the following procedure. About 5 mg of each samples was dispersed in 100 mL of ultra-pure water. Then, sonicated for 30 min in ultrasonic bath. After filtration with syringe filter (0.45 µm), 1 mL of each sample was transferred in the voltammetric cell containing 19 mL of the supporting electrolyte (BR Solution, pH = 7), for voltammetric analysis. Each solution was analyzed in the day of preparation according to the same procedure developed for the synthetic solution. In parallel, the filtrated solutions of sugar samples were analyzed by UPLC/UV as control method after the realization of a calibration curve (0.2 – 15 mg. L⁻¹) by integrating the peak chromatogram at *t_r* = 2.03 min (230 nm).

3. Results and discussions

3.1. Characterization of the materials of electrode

The morphology and particle size analysis of the components of the f-MWCNTs-FNTs modified electrode were studied by SEM technique. The graphite appears as particles with flake shaped structure ranging in size from lower than 4 µm diameter and lower than 1 µm thick. (Fig. 2-A). While fullerene wires showed their nanometrical size in diameter (estimated from 15 to 20 nm) they have a tube shaped structure and are wound into a ball and appear as balls of wood with a diameter lower than 50 µm (Fig. 2C, D). The multi-walled carbon nanotubes (MWCNTs) appear with a spaghetti shaped structure less compacted than FNTs and with a diameter slightly weaker 10–15 nm (Fig. 2E). The functionalization of MWCNTs as proposed in section 2.3 provided a more disperse structure with lower length of the nanotubes in comparison with the non-functionalized one (Fig. 2F). For the CPE modified electrode, in the (Fig. 2B), it can be seen that in the mixture of f-MWCNTs, FNTs and

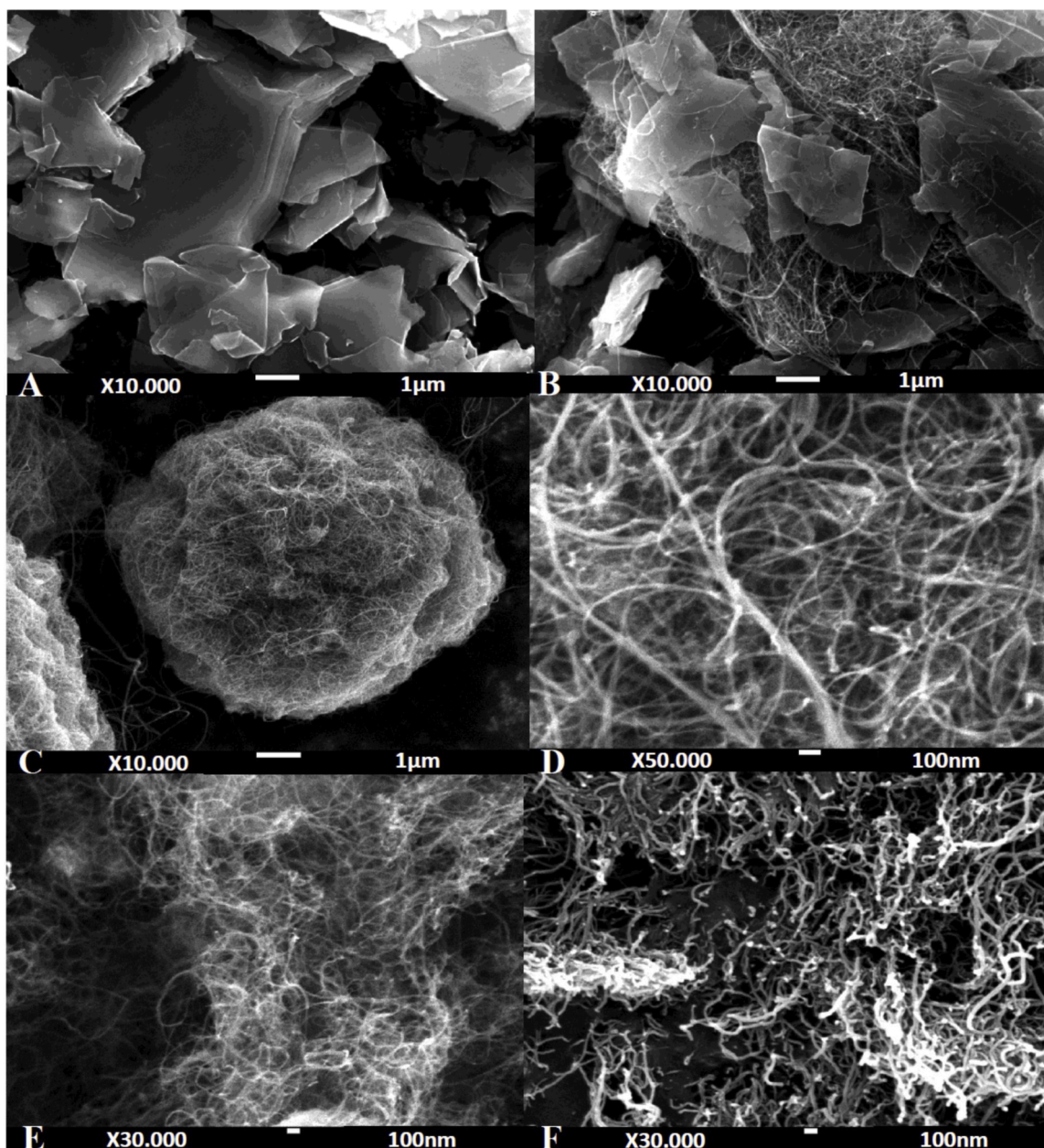


Fig. 2. SEM images for (A) graphite (x10.000), (B) f-MWCNTs-FNTs/ CPE (x10.000), (C) FNTs (x10.000), (D) FNTs (x50.000), (E) MWCNT (x30.000) and (F) f-MWCNT (x30.000).

graphite are linked in a way to avoid the stacking of graphite platelet and to promote the accessibility to the analyte in their surfaces and improve the charge transfer in the paste. Globally, the f-MWCNTs-FNTs electrode showed a uniform and nanostructured surface which could yield to large surface area and improve the characteristics of the pervious fabricated sensor.

3.2. Chronoamperometry (CA) studies

Chronoamperometric measurement was performed to determine active surface area of the prepared electrode. This study was recorded in the presence of $1 \times 10^{-3} \text{ mol.L}^{-1}$ of potassium hexacyanoferrate (III) as the redox probe in the condition of diffusion control for the current obtained in CA. In this case, the current-time response is described by the Cottrell equation (Bard and Faulkner, 2001):

$$i = \frac{nFAD^{1/2}C^*}{\pi^{1/2}t^{1/2}}$$

Where A is the active area of the electrode, C^* is the initial concentration of ferrocyanide, D the diffusion coefficient of ferrocyanide which is well known to be $6.22 \times 10^{-6} \text{ cm}^2 \cdot \text{s}^{-1}$ (Denuault et al., 1991) in aqueous electrolyte and the other parameters have their typical significances.

The electrochemical active area of the sensor was estimate to be 0.14 cm^2 from the slope of the linear regression line of current density versus square root of time. While, the geometric surface of the 2 mm diameter electrode was calculated to be 0.02 cm^2 considering the cross section of the cavity. Thus, the nanostructuration of the carbon paste sensor gives a greater specific surface than the geometric one and enables the access of the cell solution to a larger surface of graphite particles by avoiding their stacking.

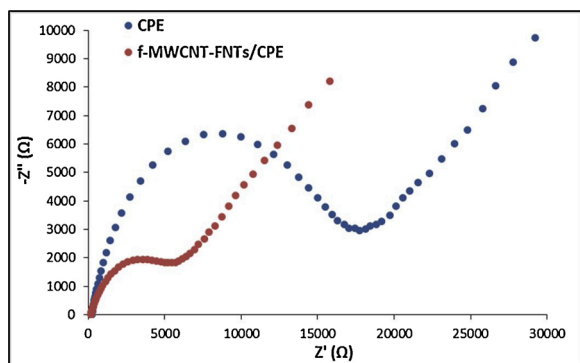


Fig. 3. Nyquist diagrams for EIS of CPE (■) and f-MWCNT-FNTs/CPE (●) in 1 mM $\text{Fe}(\text{CN})_6^{3-}$ $\text{Fe}(\text{CN})_6^{3-/4-}$ and BRS 0.04 M at pH = 7; frequency range 0.001–10 000 Hz, potential amplitude 10 mV.

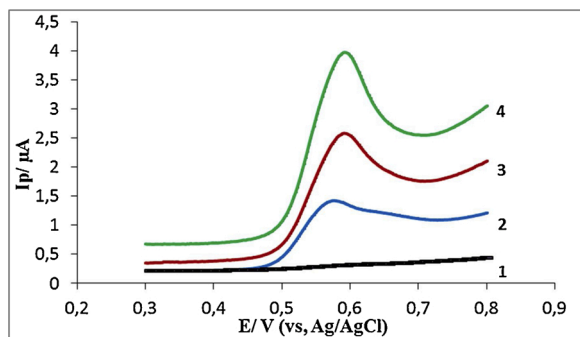


Fig. 4. Cyclic voltammograms at (1) CPE without VAN, and with $10^{-5} \text{ mol.L}^{-1}$ VAN at (2) CPE, (3) f-MWCNTs/CPE and (4) f-MWCNTs-FNTs/CPE in BRS 0.04 M (pH = 7); 20 mV.s^{-1} .

3.3. Electrochemical impedance spectroscopy (EIS) studies

EIS is a sensitive electrochemical technique to characterize the electrical impedance of the interface between electrode and electrolyte. This procedure also give information about the change in conductance or impedance of an electrode/electrolyte interface during its modifications. EIS diagram named Nyquist plot have a semicircle part at higher frequencies corresponding to the limiting by electron transfer process and a linear part at lower frequencies correlating with the diffusional controlled region (Randviir and Banks, 2013; Pajkossy and Jurczakowski, 2017).

The impedance spectra were recorded for the electrodes of CPE and f-MWCNTs-FNTs/CPE in electrolyte solution containing $10^{-3} \text{ mol.L}^{-1}$ of

potassium hexacyanoferrate (III) in the frequency range from 10^{-3} to 10^5 Hz by using a sinusoidal excitation signal (sine signal) with amplitude of 0.01 V (Fig. 3).

The CPE showed a semicircle with a large diameter and charge transfer resistance of 16.7 KΩ. The nanostructuration of CPE leads to the decrease of the semicircle diameter at 6.81 KΩ, which indicated a lower charge transfer resistance (reduction by a factor of 2.5). This is ascribed to the nanostructuration by f-MWCNT and FNTs, which reduce charge transfer resistance and therefore increase the electron transfer kinetic. The linear parts for the lowest frequencies are not depending on the composition of the carbon paste electrode (same slope). This is consistent with the diffusional controlled process identical in the two cases.

3.4. Voltammetric Behavior of VAN at f-MWCNTs-FNTs/CPE

In order to evaluate the performance and the sensitivity of developed f-MWCNTs-FNTs/CPE sensor toward the detection of VAN, voltammetric curves (CV) were recorded for CPE, f-MWCNTs and f-MWCNTs-FNTs nanostructured modified CPE in presence of $10^{-5} \text{ mol.L}^{-1}$ VAN at the scan rate of 20 mV.s^{-1} in BR buffer at pH = 7 as the supporting electrolyte (Fig. 4). The CV of CPE, in the presence of VAN shows a not well defined anodic peak (2.3 μA) at around +0.6 V. The incorporation of f-MWCNTs in the paste (30 %) leads to enhance the peak current of VAN oxidation (6.3 μA). The addition of FNTs (10 %, by replacing a part of MWCNTs and maintaining all the carbon nanotubes to 30 %), improves notably the peak intensity. Therefore, the anodic peak current obtained with the nanostructured modified electrode (9.2 μA) is 4 times higher than with CPE. The combination of FNTs and f-MWCNTs facilitate the accessibility of VAN to graphite particles and the electron transfer at the electrode material.

3.5. Effect of pH

The effect of the electrolyte pH on the oxidation of $10^{-6} \text{ mol.L}^{-1}$ VAN was investigated using CV measurements in the BR solution in the pH range from 5 to 9 at 18 °C.

As can be seen in Fig. 5A, the oxidation peak current of VAN is depending on the pH value and increases with increasing pH until it reaches the maximum at pH = 7, and then decreases with higher pH values. The optimized pH corresponding to the higher peak current was 7, indicating that protons are involved in the reaction of VAN oxidation. Moreover, as the pKa of VAN was equal to 7.4 at 25 °C (Serjeant and Dempsey, 1979), this result indicated that the analyte was preferentially adsorbed in the neutral form.

In addition, it is found that the values of peak potential shift to lower values with the increase of pH, as shown in Fig. 5B. Thus, the peak potential is linearly depended on the pH according to the following equation:

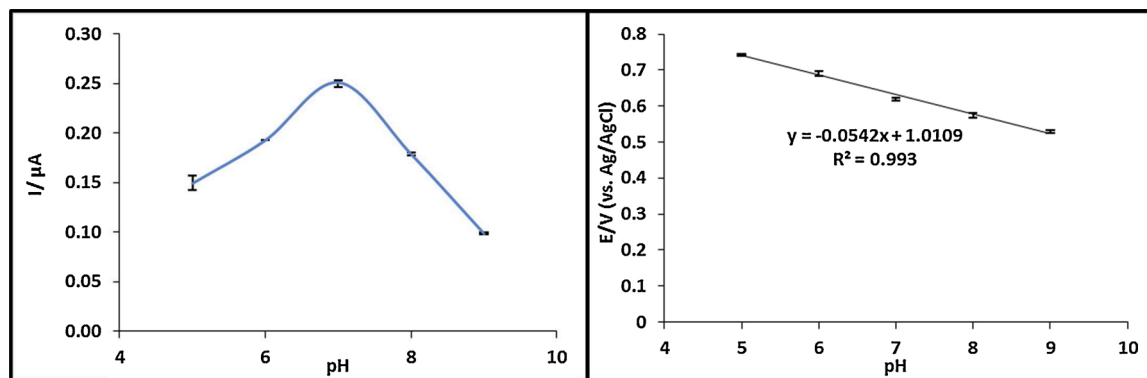


Fig. 5. (A) Effect of pH on the peak current oxidation of VAN with different pH value (5 to 9) at the f-MWCNTs-FNTs/CPE in BRS 0.04 M (pH = 7) at 20 mV.s^{-1} . (B) Corresponding plot of the oxidation peak potential of VAN versus pH.

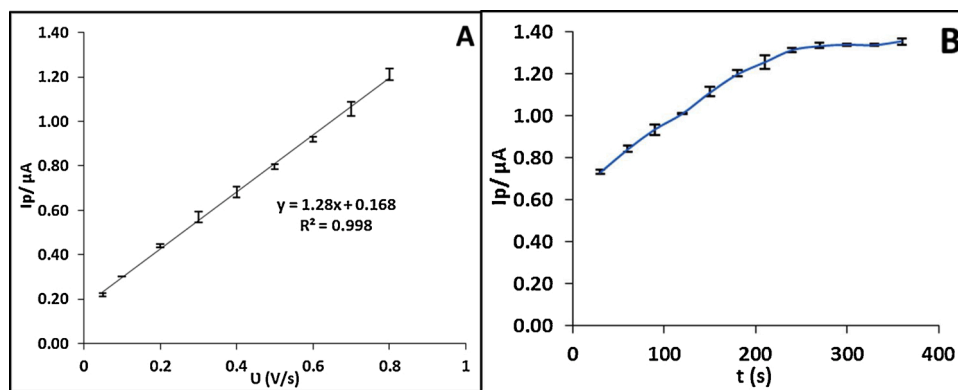


Fig. 6. (A) The effect of different scan rates (10 to 80 $mV.s^{-1}$) and (B) the effect of accumulation time on the oxidation peak current of $10^{-6} mol.L^{-1}$ VAN at the f-MWCNTs-FNTs/ CPE in BRS 0.04 M (pH = 7).

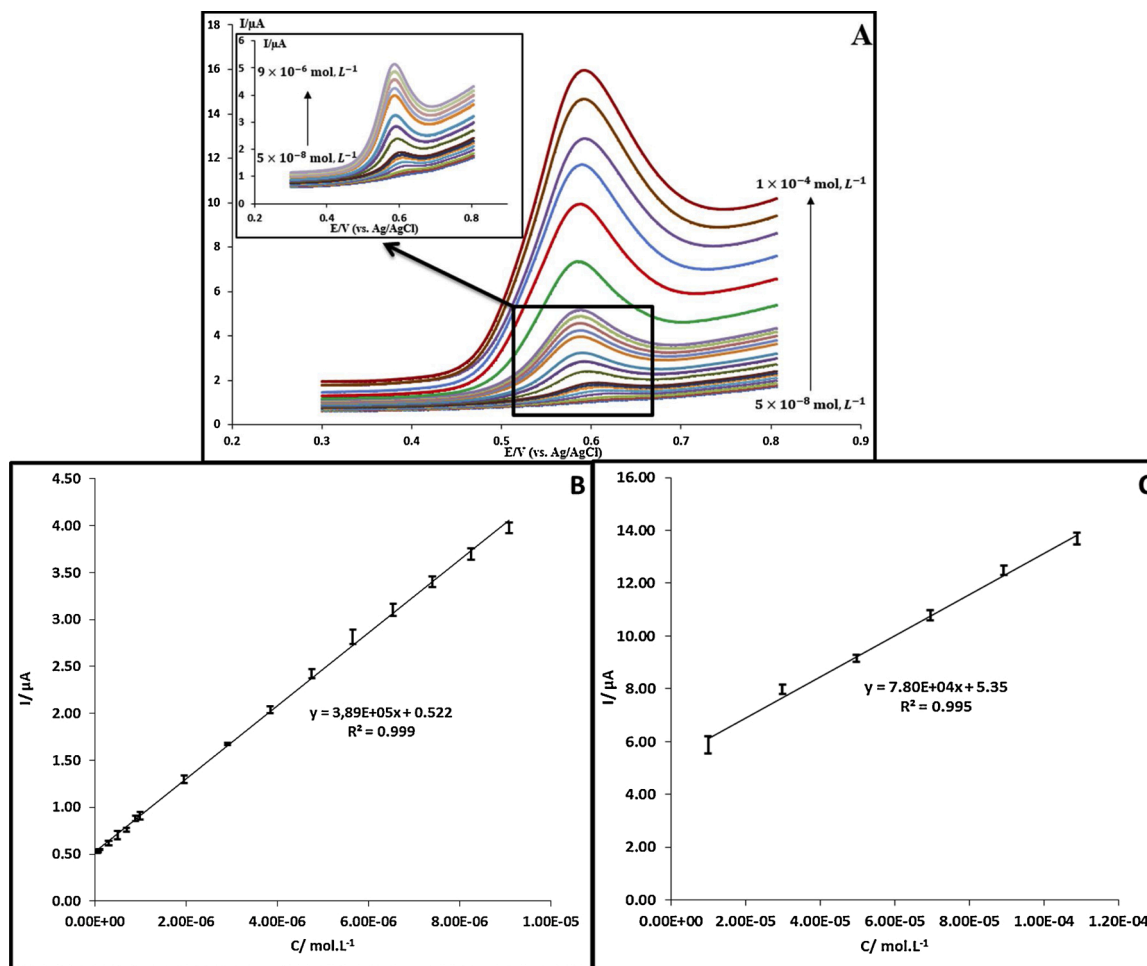


Fig. 7. (A) Cyclic voltammograms of VAN from 5×10^{-8} to $1 \times 10^{-4} mol.L^{-1}$ at f-MWCNTs-FNTs/ CPE in BRS 0.04 M (pH = 7), Insert: from 5×10^{-8} to $9 \times 10^{-6} mol.L^{-1}$. (B, C) Calibration curves of VAN concentrations against peak current from 5×10^{-8} to $9 \times 10^{-6} mol.L^{-1}$ and from 1×10^{-5} to $1 \times 10^{-4} mol.L^{-1}$, respectively.

$E_p(V) = -0.0542 \text{ pH} + 1.01$ ($R = 0.993$). A shift of typically 54.2 mV per pH unit is approximately close to the theoretical value of 57.6 mV per pH unit at 18 °C (Bard and Faulkner, 2001), and it demonstrates that the electron-transfer process during the oxidation of VAN, involved an equal number of protons and electrons (two electrons and two protons take part in the oxidation process), which is in agreement with that obtained before by different authors (Ceylan Koçak and Ulubay Karabiberoğlu, 2018; Abbasghorbani, 2017; Kalaiyarasi et al.,

2017).

3.6. Effect of potential scan rate

Cyclic voltammograms of $10^{-6} mol.L^{-1}$ VAN at f-MWCNTs-FNTs modified paste electrode were recorded for different potential scan rates and the variation of the peak current in function of the scan rate are presented in Fig. 6A. It can be seen that, in presence of a low VAN

Table 1

Comparison with this work of previously reported VAN analysis with electrochemical sensor.

Electrode	Linear range (mol.L ⁻¹)	Detection limit (mol.L ⁻¹)	Ref.
Au-MWCNTs/GCE ^a	7 × 10 ⁻⁸ to 6.5 × 10 ⁻⁶ and 7 × 10 ⁻⁶ to 7.5 × 10 ⁻⁵	3.8 × 10 ⁻⁸	Ceylan Koçak et al., 2018
p-PGE ^b	5 × 10 ⁻⁷ to 1 × 10 ⁻⁵	1.6 × 10 ⁻⁷	Dilgin, 2019
CPE/NiO-SWCNTs/BPrPF ₆ ^c	1 × 10 ⁻⁸ to 3.5 × 10 ⁻⁴	4 × 10 ⁻⁹	Gupta et al., 2018
CB/SPCE ^d	5 × 10 ⁻⁵ to 4.5 × 10 ⁻⁴	3.9 × 10 ⁻⁸	Kutty et al., 2019
CNT-SPE ^e	2.5 × 10 ⁻⁶ to 7.5 × 10 ⁻⁴	1.03 × 10 ⁻⁶	Chen et al., 2019
CaN ₄ /GCE ^f	2 × 10 ⁻⁸ to 1 × 10 ⁻⁵ and 1.5 × 10 ⁻⁵ to 2 × 10 ⁻⁴	7 × 10 ⁻⁹	Fu et al., 2020
BGPE ^g	4 × 10 ⁻⁶ to 1.5 × 10 ⁻⁵ and 2 × 10 ⁻⁵ to 7 × 10 ⁻⁵	1.29 × 10 ⁻⁶	Raril and Manjunatha, 2020
T3T-Au electrode ^h	1 × 10 ⁻⁷ to 1.13 × 10 ⁻⁵	4 × 10 ⁻⁸	Tabanlıgil Calam, 2020
f-MWCNTs-FNTs/ CPE	5 × 10 ⁻⁸ to 9 × 10 ⁻⁶ and 1 × 10 ⁻⁵ to 1 × 10 ⁻⁴	3.5 × 10 ⁻⁸	This work

^a Gold nanoparticles modified multi-walled carbon nanotubes glassy carbon electrode.

^b Pre-oxidized Pencil Graphite Electrode.

^c Carbon Paste Electrode modified with NiO decorated single wall carbon nanotubes and 1-butylpyridinium hexafluorophosphate.

^d Carbon Black Nanoparticles Modified Screen Printed Carbon Electrode.

^e Multi-walled carbon nanotube screen-printed electrode.

^f Pyrolyzed graphitic carbon nitride electrode.

^g Bare graphene paste electrode.

^h 1H-1,2,4-triazole-3-thiol polymer film modified gold electrode.

concentration, the oxidation peak current of VAN increases linearly with the scan rate in the range from 0.005 to 0.08 V.s⁻¹, with a linear relationship $I_{\text{pic}} = 7.80 \times 10^{-4} \nu + 5.35$ and a correlation coefficient of $R^2 = 0.995$. This indicates that the oxidation of VAN is not controlled by the diffusion of VAN but by an adsorption-controlled process for this low VAN concentration. This adsorption step will provide sensibility for the developed sensor and lead to a low detection limit.

3.7. Effect of accumulation time

Accumulation time for the electrochemical measurements is an important parameter that affects the current response of 10⁻⁶ mol.L⁻¹ VAN at f-MWCNTs-FNTs/ CPE. As shown in Fig. 6B, the oxidation peak current of VAN gradually increased with increasing accumulation time from 30 to 360 s, and reached the maximum current response at 300 s then remains almost constant at longer accumulation times. For practical purposes, a 300 s accumulation time is sufficient and used for a determination of VAN.

3.8. Calibration curves and detection limit

In order to evaluate the linear range and detection limit of the f-MWCNTs-FNTs/CPE, the quantitative analysis of VAN concentration using the developed sensor was performed by cyclic voltammetry under the optimized conditions (Fig. 7A).

The intensity of the oxidation peak current of VAN increases with the VAN concentration. The calibration curve for peak current (I_p) versus [VAN] (Fig. 7B & C) indicates that there are two clearly defined linear ranges:

Table 2

Validation of the electrochemical method: (A) Study of repeatability and reproducibility of detection for different VAN concentrations at f-MWCNTs-FNTs/ CPE in BRS 0.04 M (pH = 7); preconcentration time under stirring 300 s; 20 mV.s⁻¹. (B) Determination of VAN mass fraction in different real commercial sugar vanilla samples with electrochemical and UPLC/UV methods.

Table 2-A

VAN concentration (μM)	Determination of repeatability & reproducibility	
	Repeatability of I_p RSD% *	Reproducibility of I_p RSD% **
0.1	2.1%	2.1%
1	6.7%	5.8%
10	2.9%	1.1%

Table 2-B

Sugar samples	Determination of VAN mass fraction mg.g ⁻¹				Recovery (%)	Relative error (%)
	Electrochemical method (n=3)		UPLC Analytical method (n=3)			
	Mean ± confidence interval ***	RSD %	Mean ± confidence interval ***	RSD %		
E1	3.91 ± 0.22	3.0	3.67 ± 0.02	0.3	106.5	6.5
E2	4.79 ± 0.92	10.4	4.61 ± 0.02	0.2	103.9	3.9
E3	3.64 ± 0.23	3.3	3.61 ± 0.01	0.1	100.8	0.8
E4	2.88 ± 0.34	6.5	2.76 ± 0.02	0.7	104.3	4.3

* n = 3.

** n = 2.

*** Confidence interval for $\alpha = 0.5$.

- from 5 × 10⁻⁸ to 9 × 10⁻⁶ mol.L⁻¹ with a linear regression equation of $I_p = 3.89 \times 10^{-5}[\text{VAN}] + 0.522$, $R^2 = 0.999$

- from 1 × 10⁻⁵ to 1 × 10⁻⁴ mol.L⁻¹ with a linear regression equation of $I_{\text{pic}} = 7.80 \times 10^{-4}[\text{VAN}] + 5.35$, $R^2 = 0.995$

These two concentration ranges indicate that the VAN oxidation is not controlled by the same process. For the lowest concentrations (below 10⁻⁵ mol.L⁻¹), the peak current is controlled by an adsorption step of VAN at the electrode surface (as seen in 3.6 section) which provides an interesting sensibility. For highest concentration (>10⁻⁵ mol.L⁻¹) the peak current is controlled by the diffusion of VAN.

The detection limit of the proposed method is found to be 3.4 × 10⁻⁸ mol.L⁻¹, calculated from the formula:

$$LD = 3.3 \times \frac{SD}{b}$$

Where SD the standard deviation of the linear regression solution and b is the slope of the linear regression (Shrivastava and Gupta, 2011).

As can be seen on Table 1, the f-MWCNTs-FNTs/CPE prepared sensor shows a low detection limit and a large linear concentration range compared to those reported in the literature (Ceylan Koçak et al., 2018; Dilgin, 2019; Chen et al., 2019; Fu et al., 2020; Raril and Manjunatha, 2020, 2020; Tabanlıgil Calam, 2020).

Thus, the proposed electrochemical sensor show very good performances by just using a few cost electrodes materials in comparison with some reports that give practically similar analytical characteristics. It is also distinguished by the simplicity and the quick modification step of the electrode, which make it an attractive sensor for the monitoring of the quality analysis of food products containing VAN as additive.

3.9. Repeatability and reproducibility of f-MWCNTs-FNTs/ CPE

The repeatability of the nanostructured carbon paste electrode is carried for three different concentrations (10⁻⁷, 10⁻⁶ and 10⁻⁵ mol.L⁻¹), in order to cover the two adsorption and diffusion control processes. Three successive measurements were carried out for each

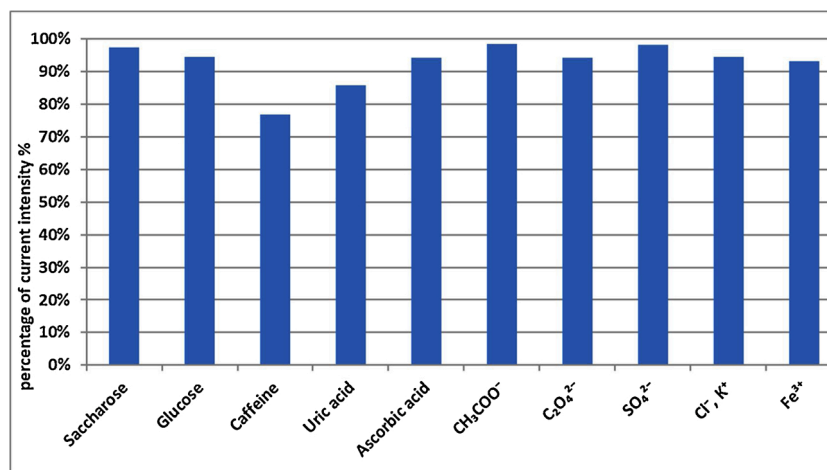


Fig. 8. The relative peak current response of 1 μ M VAN in the presence of some potential interfering substances at the f-MWCNTs-FNTs/ CPE in BRS 0.04 M (pH = 7).

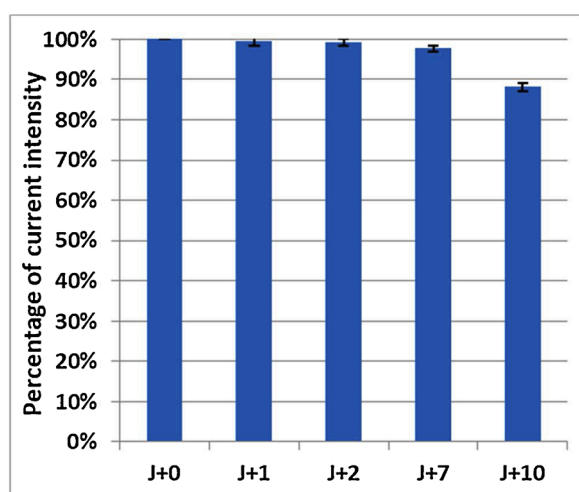


Fig. 9. The study of stability of the f-MWCNTs-FNTs/ CPE for the relative peak current response of 1 μ M VAN in ten days of storage.

concentration by using the same sensor. The resulted values of relative standard deviation (RSD) are presented in Table 2A indicating an acceptable repeatability (less than 7%). Furthermore, reproducibility is checked by recording the current response of three concentrations at two independent sensor prepared with the same procedure and paste composition. As one can see from Table 2A, the obtained values of RSD are lower than 6% and good accuracy could be achieved especially for the lowest concentration (10^{-7} mol.L⁻¹) with RSD value of 2.1 %.

3.10. Selectivity and stability of f-MWCNTs-FNTs/ CPE

The selectivity of the f-MWCNTs-FNTs/CPE is tested using the CV technique in adsorption control process by performing the response of 10^{-6} mol.L⁻¹ of VAN in the presence of some potential interfering substances at similar concentrations.

The presence of sugars such as glucose and saccharose have no noticeable effect on peak intensity (variation < 5 %; Fig. 8). This indicates that it is unlikely to have matrix effects for the analysis of vanilla sugars. The greater effects were observed for caffeine and uric acid with a variation not exceeding 22 %. These low variations in the oxidation current response of VAN were likely due to the presence of a similar electroactive functional group. In order to preserve the selectivity for VAN for samples containing these interferents, it is preferable to dilute samples to minimize their concentrations and to analyze low

concentrations of VAN with an adsorption step to guarantee the specificity of the response. Indeed, for any target molecules to be adsorbed on the surface of the electrode, they must have sufficient affinity for the sensor material to adsorb selectively in order to be detected. Vanillin has a hydrophobic character ($\log K_{ow} = 1.37$) in comparison with the hydrophilic tested interferents ($\log K_{ow} < 0$). This is probably not the own reason that could explain this selectivity. In fact, the possibility of charge on molecule, in relation with pKa value and pH of electrolyte could influence molecule adsorption on carbon paste. For vanillin (pKa = 7.4), it adsorbed preferentially in neutral form while others studied molecules such uric acid and ascorbic acid (pKa < 5.5) are charged negatively in PBS electrolyte (pH = 7), and this could be unfavorable to their adsorption. Other interferents such sulfate and chloride anion, Fe³⁺ ion, oxalate and acetate, show negligible impact on current responses. Therefore, the results demonstrate the possibility to obtain a high selectivity of f-MWCNTs-FNTs/CPE toward VAN and permit feasibility for real food sample analysis of VAN.

Moreover, the stability of f-MWCNTs-FNTs/ CPE sensor is evaluated using CV for VAN (10^{-5} mol.L⁻¹) in BRS (pH = 7.0) at 20 mV.s⁻¹. Then, the CV current responses were tested before and after storage at 25 °C during 10 days without following a specific procedure and the results are shown in Fig. 9. It appears that the electrode remains stable during 7 days storage, with a slight decreasing of peak current lower than 5%. The variation doesn't exceed 10 % after 10 days indicating a good stability of the sensor.

3.11. Vanilla sugar analysis

The performance and the feasibility of the developed sensor to quantify VAN are evaluated by using the f-MWCNTs-FNTs/ CPE in four real sugar vanilla samples from different commercial brands for which the manufacturers don't indicate the VAN proportion in composition. The concentration of VAN in the samples was determinate by standard addition method by successive addition of known VAN amounts (2×10^{-6} ; 4×10^{-6} and 6×10^{-6} mol.L⁻¹) in the electrochemical cell containing the electrolyte in which the sugar sample was dissolved (as described in Section 2.6). This operation was achieved in triplicate for each sugar sample. In order to validate the results, high performance liquid chromatography (UPLC/UV) was used as a control method to determine the content of VAN in these samples. The results obtained with the proposed method and the control analytical method are compiled in Table 2B. The contents of VAN for the different samples were between 2.9 and 4.8 mg of VAN per g of sugar (lower than 0.5 %) with repeatability comparable to that observed previously in synthetic solutions (see section 3.9). The results obtained with the developed sensor were in accordance with those obtained by the UPLC/UV control

method (recovery values between 100–107 % for the different samples). We can conclude that the constituents of vanilla sugar do not interfere in the VAN analysis.

Therefore, the proposed nanostructured composite modified carbon paste electrode (f-MWCNTs-FNTs/CPE) is able to control VAN as ingredient after simple dissolution of vanilla sugar samples without extraction procedure. This proposed electroanalytical method demonstrates a good accuracy of the proposed sensor and its feasibility in food sample analysis.

4. Conclusion

The proposed sensor for the detection of vanillin was fabricated using a carbon paste electrode modified with fullerene and functionalized multi-walled carbon nanotubes. The excellent properties of the nanostructured carbon paste enhance surface area and improve considerably the electrons transfer that lead to a remarkable electrochemical and analytical performances with a wide linear range, lower detection limit, excellent sensitivity, good stability and satisfactory repeatability and reproducibility. The proposed modified electrode was successfully applied to the determination of vanillin in commercial sugar vanilla samples with a satisfactory recovery in comparison of the control UPLC/UV analytical method and without any specific preparation of the samples, just by dissolving the sample in the BRS electrolyte. Hence, the so-designed sensor could be a promising and suitable device to quantify and monitor vanillin as ingredient in commercial food.

Authorship statement

Conception and design of study: D. Hauchard, M. Bourouina
acquisition of data: L. Taouri
analysis and/or interpretation of data: D. Hauchard, M. Bourouina,
S. Bourouina-Bacha, L. Taouri
Drafting the manuscript: D. Hauchard, Taouri, M. Bourouina
revising the manuscript critically for important intellectual content:
D. Hauchard, L. Taouri, M. Bourouina
Approval of the version of the manuscript to be published (the names
of all authors must be listed):
D. Hauchard, L. Taouri, M. Bourouina, S. Bourouina-Bacha

CRediT authorship contribution statement

Lydia Taouri: Conceptualization, Methodology, Validation, Formal analysis, Investigation, Writing - original draft, Visualization. **Mustapha Bourouina:** Conceptualization, Methodology, Resources, Writing - review & editing, Supervision. **Saliha Bourouina-Bacha:** Writing - review & editing. **Didier Hauchard:** Conceptualization, Methodology, Validation, Resources, Writing - review & editing, Supervision.

Declaration of Competing Interest

The authors declare no conflict of interest.

Acknowledgements

The authors acknowledge the financial support of the Algerian Ministry of Education and Scientific Research and Campus France program under grant agreement PROFAS B+, and express their grateful acknowledgements to F. Gouttefangeas from the CMEBA center of ISCR-CNRS 6226 for the MEB analysis and to C. Gardin from CIP team of ISCR-CNRS 6226 for chromatographic analysis.

References

- Abbasghorbani, M., 2017. Electrochemical determination of vanillin in food samples using MgO/SWCNTs-ionic liquid modified electrode. *Int. J. Electrochem. Sci.* 12 (12), 11656–11665.
- Ahmad, H., Khera, R.A., Hanif, M.A., Ayub, M.A., Jilani, M.I., 2020. Chapter 48: Vanilla. In: Hanif, M.A., Khun, M.M., Nawaz, H., Byrne, H.J. (Eds.), *Medicinal Plants of South Asia. Novel sources for drug discovery*, pp. 657–669.
- Bard, A.J., Faulkner, L.R., 2001. *Electrochemical Methods: Fundamentals Applications*, 2nd eds. Wiley, New York, p. 87.
- Baykal, A., Senel, M., Unal, B., Karaoglu, E., Sözeri, H., Toprak, M.S., 2013. Acid functionalized multiwall carbon Nanotube/Magnetite (MWCNT)-COOH/ Fe₃ O₄ hybrid: synthesis, characterization and conductivity evaluation. *J. Inorg. Organomet. Polym.* 23, 726–735.
- Bezerra, D.P., Soares, A.K.N., De Sousa, D.P., 2016. Overview of the Role of Vanillin on Redox Status and Cancer Development. *Oxidative Medicine and Cellular Longevity*, p. 9.
- Bojdi, M.K., Behbahani, M., Omidi, F., Hesam, G., 2016. Application of a novel electrochemical sensor based on modified siliceous mesocellular foam for electrochemical detection of ultra-trace amounts of mercury ions. *New J. Chem.* 40, 4519–4527.
- Ceylan Koçak, Ç., Ulubay Karabiberoglu, Ş., 2018. Electrochemical vanillin determination on gold nanoparticles modified multiwalled carbon nanotube electrode. *J. Sci. Eng.* 20 (59), 461–470.
- Chen, L., Chaisiwamongkhol, K., Chen, Y., Compton, R.G., 2019. Rapid electrochemical detection of vanillin in natural Vanilla. *Electroanalysis* 31 (6), 1067–1074.
- D'Souza, O.J., Mascarenhas, R.J., Satpati, A.K., Mane, V., Mekhalif, Z., 2017. Application of a Nanosensor Based on MWCNT-Sodium Dodecyl Sulphate Modified Electrode for the Analysis of a Novel Drug, Alpha-Hydrazinonitroalkene in Human Blood Serum. *Electroanalysis* 29 (7), 1794–1804.
- Denuault, G., Mirkin, M.V., Brad, A.J., 1991. Direct determination of diffusion coefficients by chronoamperometry at microdisk electrodes. *J. Electroanal. Chem.* 308, 27–38.
- Dilgin, D.G., 2019. Voltammetric determination of vanillin using a pretreated pencil graphite electrode. *Akademik Gıda* 17 (1), 1–8.
- Durán, G.M., Contento, A.M., Ríos, A., 2015. β -Cyclodextrin coated CdSe/ZnS quantum dots for vanillin sensing in food samples. *Talanta* 131, 286–291.
- Durán, G.M., Llorent-Martínez, E.J., Contento, A.M., Ríos, A., 2018. Determination of vanillin by using gold nanoparticle-modified screen-printed carbon electrode modified with graphene quantum dots and Nafion. *Microchim. Acta* 185, 204.
- Erady, V., Mascarenhas, R.J., Satpati, A.K., 2020. Highly efficient and selective quantification of vanillin in food, beverages and pharmaceuticals using surfactant modified carbon paste sensor. *Proc. IEEE Sens.* 1, 100023.
- Fu, L., Xie, K., Wu, D., Wang, A., Zhang, H., Ji, Z., 2020. Electrochemical determination of vanillin in food samples by using pyrolyzed graphitic carbon nitride. *Mater. Chem. Phys.* 242, 122462.
- Gao, J., Yuan, Q., Ye, C., Guo, P., Du, S., Lai, G., Yu, A., Jiang, N., Fu, L., Lin, C.T., Chee, K.W.A., 2018. Label-free electrochemical detection of vanillin through low-defect graphene electrodes modified with Au nanoparticles. *Materials* 11 (4), 489.
- Gupta, V.K., Karimi-Maleh, H., Agarwal, S., Karimi, F., Bijad, M., Farsi, M., Shahidi, S.A., 2018. Fabrication of a food nano-platform sensor for determination of vanillin in food samples. *Sensors* 18, 2817.
- Isac-García, J., Dobado, J.A., Calvo-Flores, F.G., Martínez-García, H., 2016. Chapter 11 - microscale experiments. In: Isac-García, J., Dobado, J.A., Calvo-Flores, F.G., Martínez-García, H. (Eds.), *Experimental Organic Chemistry*, 1st eds. Academic press, pp. 371–408.
- Kalaiyarasi, J., Meenakshi, S., Pandian, K., Gopinath, Subash, C.B., 2017. Simultaneous voltammetric determination of vanillin and guaiacol in food products on defect free graphene nanoflakes modified glassy carbon electrode. *Microchim Acta* 184, 2131–2140.
- Karimi-Maleh, H., Karimi, F., Alizadeh, M., Sanati, A.L., 2020. Electrochemical Sensors, a bright future in the fabrication of portable kits in analytical systems. *Chem. Rec.* 20, 682–69.
- Kroto, H.W., 1987. The stability of the fullerenes C_n, with n = 24, 28, 32, 36, 50, 60 and 70. *Nature* 329, 529–531.
- Kutty, M., Settu, R.L., Chen, S.M., Chen, T.W., Tseng, T.W., Hatamleh, A.A., Yu, J., Yu, R., Huang, C.C., 2019. An electrochemical detection of vanillin based on carbon black nanoparticles modified screen printed carbon electrode. *Int. J. Electrochem. Sci.* 14, 5972–5983.
- Manasa, G., Ronald, J.M., Basavanakote, M.B., 2019. Sensitively-selective determination of Propyl Paraben preservative based on synergistic effects of polyaniline-zinc-oxide nano-composite incorporated into graphite paste electrode. *Colloids Surf. B Biointerfaces* 184, 110529.
- Mazloum-Ardakani, M., Ahmadi, S.H., Safaei Mahmoudabadi, Z., Khoshroo, A., 2016. Nano composite system based on fullerene-functionalized carbon nanotubes for simultaneous determination of levodopa and acetaminophen. *Measurement* 91, 162–167.
- Miyazawa, K., 2009. Synthesis and properties of fullerene nanowhiskers and fullerene nanotubes. *J. Nanosci. Nanotechnol.* 9 (1), 41–50.
- Mohan, H.K.S.V., Chee, W.K., Li, Y., Nayak, S., Poh, C.L., Thean, A.V.Y., 2019. A highly sensitive graphene oxide based label-free capacitive aptasensor for vanillin detection. *Mater. Des.* 186, 108208.
- Murtada, K., Jodeh, S., Zougagh, M., Ríos, A., 2018. Development of an Aluminium Doped TiO₂ Nanoparticles-modified Screen Printed Carbon Electrode for Electrochemical Sensing of Vanillin in Food Samples. *Electroanalysis* 30, 969.

- Nasuno, R., Shino, S., Yoshikawa, Y., Yoshioka, N., Sato, Y., Kamiya, K., Takag, H., 2020. Detection system of the intracellular nitric oxide in yeast by HPLC with a fluorescence detector. *Anal. Biochem.* 598, 113707.
- Ning, J., He, Q., Luo, X., Wang, M., Liu, D., Wang, J., Liu, J., Li, G., 2018. Rapid and sensitive determination of vanillin based on a glassy carbon electrode modified with Cu₂O-Electrochemically reduced graphene oxide nanocomposite film. *Sensors* 18 (9), 2762.
- Pajkossy, T., Jurczakowski, R., 2017. Electrochemical impedance spectroscopy in interfacial studies. *Curr. Opin. Electrochem.* 1 (1), 53–58.
- Pan, Y., Liu, X., Zhang, W., Liu, Z., Zeng, G., Shao, B., Liang, Q., He, Q., Yuan, X., Huang, D., Chen, M., 2020. Advances in photocatalysis based on fullerene C60 and its derivatives: properties, mechanism, synthesis, and applications. *Appl. Catal. B* 265, 118579.
- Pilehvar, S., Wael, K.D., 2015. Recent advances in electrochemical biosensors based on FNTserene-C60 nano-structured platforms. *Biosensors* 5 (4), 712–735.
- Ramesh, M., Muthuraman, A., 2018. Flavoring and Coloring Agents: Health Risks and Potential Problems, Natural and Artificial Flavoring Agents and Food Dyes, *Handbook of Food Bioengineering*, pp. 1–28.
- Randviir, E.P., Banks, C.E., 2013. Electrochemical impedance spectroscopy: an overview of bioanalytical applications. *Anal. Methods* 5, 1098–1115.
- Rao, R.V.K., Karthik, P.S., Abhinav, V.K., Lin, Z., Myint, M.T.Z., Nishikawa, T., Hada, M., Yamashita, Y., Hayashi, Y., Singh, S.P., 2016. Self-assembled C60 fullerene cylindrical nanotubes by LLIP method. 16th International Conference on Nanotechnology - IEEE NANO, Institute of Electrical and Electronics Engineers, [7751386] 303–306.
- Raril, C., Manjunatha, J.G., 2020. A simple approach for the electrochemical determination of vanillin at ionic surfactant modified graphene paste electrode. *Microchem. J.* 154, 104575.
- Research And Markets, The World's Largest Market Research Store, 2019. Vanilla and Vanillin Market: Global Industry Trends, Share, Size, Growth, Opportunity and Forecast 2019-2024, IMARC Group, Report ID: 4752325.
- Serjeant, E.P., Dempsey, B., 1979. Ionisation constants of organic acids in aqueous solution, International union of pure and applied chemistry. IUPAC Chem. Data Serie 23, 989.
- Sherigara, B.S., Kutner, W., Souza, F.D., 2003. Electrocatalytic properties and sensor applications of fullerenes and carbon nanotubes. *Electroanalysis* 15 (9), 753–772.
- Shrivastava, A., Gupta, V.B., 2011. Method for the determination of limit of detection and limit of quantification of the analytical methods. *Chron. Young Sci.* 2 (1), 21–25.
- Shu, M., Man, Y., Ma, H., Luan, F., Liu, H., Gao, Y., 2016. Determination of vanillin in milk powder by capillary electrophoresis combined with Dispersive liquid-Liquid microextraction. *Food Anal. Methods* 9, 1706–1712.
- Sinha, A.K., Sharma, U.K., Sharma, N., 2008. A comprehensive review on vanilla flavor: extraction, isolation and quantification of vanillin and others constituents. *Int. J. Food Sci. Nutr.* 59 (4), 299–326.
- Sivakumar, M., Sakthivel, M., Chen, S.-M., 2017. Simple synthesis of cobalt sulfide nanorods for efficient electrocatalytic oxidation of vanillin in food samples. *J. Colloid Interface Sci.* 490, 719–726.
- Tabanlıgil Calam, T., 2020. Voltammetric determination and electrochemical behavior of vanillin based on 1H-1,2,4-triazole-3-thiol polymer film modified gold electrode. *Food Chem.* 328, 127098.
- Younes, M., Aggett, P., Aguilar, F., Crebelli, R., Dusemund, B., Filipic, M., Jose Frutos, M., Galtier, P., Gundert-Remy, U., Georg Kuhnle, G., Lambre, C., Leblanc, J. C., Therese Lillegaard, I., Moldeus, P., Mortensen, A., Oskarsson, A., Stankovic, I., Waalkens-Berendsen, I., Woutersen, R.A., Wright, M., Tobback, P., Smeraldi, C., Gott, D., 2018. Safety of orthosilicic acid-vanillin complex (OSA-VC) as a novel food ingredient to be used in food supplements as a source of silicon and bioavailability of silicon from the source. *Efsa J.* 16 (1), 5086.
- Zhang, H., Fan, L., Yang, S., 2006. Significantly accelerated direct electron-transfer kinetics of hemoglobin in a C60-MWCNT nanocomposite film. *Chem. Eur. J.* 12 (27), 7161–7166.
- Zhao, J., Xia, H., Yu, T., Jin, L., Li, X., Zhang, Y., Shu, L., Zeng, L., He, Z., 2018. A colorimetric assay for vanillin detection by determination of the luminescence of o-toluidine condensates. *PLoS One* 13 (4), e0194010.
- Zhu, H., Wu, W., Zhang, H., Fan, L., Yang, S., 2009. Highly selective and sensitive detection of dopamine in the presence of excessive ascorbic acid using electrodes modified with C60-Functionalized multiwalled carbon nanotube films. *Electroanalysis* 21 (24), 2660–2666.

Abstract

This thesis focuses on the development of electrochemical sensors and micro-sensors based on carbon nanomaterials with practical applicability in environmental and food monitoring to ensure human health safety. The originality of this project resides in the nanostructuration of the developed sensors with different combinations of carbon nanomaterials, which leads to remarkable electrochemical and analytical performance. In addition, the use of the cavity microelectrode and its combination with carbon nanomaterials offers the advantages of higher surface area, higher sensitivity and lower limit of detection. Three electrochemical sensors were manufactured for the detection of vanillin as food additive in commercial sugar vanilla, the simultaneous determination of ciprofloxacin, paracetamol and 4-aminophenol in artificial urine, and for the electrochemical preconcentration of traces of paracetamol in tap water and wastewater. The proposed simple and economical micro-sensors show high sensitivity and selectivity, low detection limits (in order of nM), good repeatability and reproducibility with the feasibility of the real analysis in-situ without any specific preparation of the samples.

Résumé

Cette thèse se concentre sur le développement de capteurs et micro-capteurs électrochimiques basés sur des nanomatériaux de carbone avec une applicabilité pratique dans la surveillance environnementale et alimentaire pour assurer la sécurité de la santé humaine. L'originalité de ce projet réside dans la nanostructuration des capteurs développés avec différentes combinaisons de nanomatériaux de carbone, ce qui conduit à des performances électrochimiques et analytiques remarquables. En plus de l'utilisation de la microélectrode à cavité et sa combinaison avec des nanomatériaux de carbone offre les avantages d'une plus grande surface, d'une sensibilité plus élevée et des limites de détection plus faibles. Trois capteurs électrochimiques ont été réalisés pour la détection de la vanilline comme additif alimentaire dans le sucre commercial de vanille, la détermination simultanée de la ciprofloxacine, du paracétamol et du 4-aminophénol dans l'urine artificielle, et pour la préconcentration électrochimique de traces de paracétamol dans l'eau du robinet et les eaux usées. Les micro-capteurs simples et économiques proposés présentent une sensibilité et une sélectivité élevée, des limites de détection faibles (de l'ordre du nM), une bonne répétabilité et reproductibilité avec la faisabilité de l'analyse réelle in-situ sans préparation spécifique des échantillons.

ملخص

تركز هذه الأطروحة على تطوير أجهزة الاستشعار الكهروكيميائية القائمة على المواد النانوية الكربونية مع إمكانية التطبيق العملي في مراقبة البيئة والغذاء لضمان سلامة صحة الإنسان. تكمن أصالة هذا المشروع في البنية النانوية لأجهزة الاستشعار المطورة بمجموعات مختلفة من المواد النانوية الكربونية، مما يؤدي إلى أداء كهروكيميائي وتحليلي رائع بالإضافة إلى استخدام الألكتروود المجهرية وتوليفه مع المواد النانوية الكربونية، فإنه يوفر مزايا مثل مساحة سطح أكبر، حساسية أعلى وحدود كشف أقل. تم تطوير ثلاثة أجهزة استشعار كهروكيميائية من أجل الكشف عن الفانيلين كمضاف غذائي في سكر الفانيليا التجاري. التحديد المتزامن للسيبروفلووكساسين، الباراسيتامول و4-أمينوفينول في البول الاصطناعي. وللتركيز الكهروكيميائي المسبق لآثار الباراسيتامول في مياه الصنبور ومياه الصرف. تتميز المستشعرات الدقيقة البسيطة والاقتصادية المقدمة بحساسية وانتقائية عالية، وحدود كشف منخفضة (بترتيب نانومتر)، وقابلية جيدة للتكرار واستنساخ القياسات مع إمكانية إجراء تحليل حقيقي في الموقع دون إعداد محدد للعينات.